



HAL
open science

New Functional Architectures for Molecular Recognition, Low Band Gap Conjugated Systems and Advanced Electrode Materials

Flavia-Florina Pop-Piron,

► **To cite this version:**

Flavia-Florina Pop-Piron,. New Functional Architectures for Molecular Recognition, Low Band Gap Conjugated Systems and Advanced Electrode Materials. Organic chemistry. Université d'Angers, 2009. English. NNT: . tel-01016464

HAL Id: tel-01016464

<https://theses.hal.science/tel-01016464>

Submitted on 30 Jun 2014

HAL is a multi-disciplinary open access archive for the deposit and dissemination of scientific research documents, whether they are published or not. The documents may come from teaching and research institutions in France or abroad, or from public or private research centers.

L'archive ouverte pluridisciplinaire **HAL**, est destinée au dépôt et à la diffusion de documents scientifiques de niveau recherche, publiés ou non, émanant des établissements d'enseignement et de recherche français ou étrangers, des laboratoires publics ou privés.

New Functional Architectures for Molecular Recognition, Low Band Gap Conjugated Systems and Advanced Electrode Materials

Ph.D. THESIS
in Organic chemistry

Doctoral school "Matière, Molécules, Matériaux en Pays de la Loire" (3MPL)
Doctoral school of Faculty of Chemistry and Chemical Engineering, Cluj-Napoca

Public defense
December, 8th 2009
at Cluj-Napoca

by **Flavia-Florina PIRON (POP)**

Jury:

Muriel HISSLER	reviewer	Professor at University of Rennes 1
Marius ANDRUH	reviewer	Professor at University of Bucharest Member of the Romanian Academy

Scientific advisors:

Jean RONCALI	Directeur de recherche CNRS, University of Angers
Ion GROSU	Professor at "Babeș-Bolyai" University, Cluj-Napoca
Philippe LERICHE	member Professor at University of Angers
Cristian SILVESTRU	member Professor at "Babeș-Bolyai" University, Cluj-Napoca, Corresponding member of the Romanian Academy

Laboratory of "Chimie et Ingénierie Moléculaire d'Angers" (CIMA)
UMR CNRS 6200 – University of Angers
2, boulevard Lavoisier – 49045 ANGERS
Laboratory of Center of Organic and Computational Chemistry with Applications in
Nanotechnologies (COCCAN)
11, Arany Janos - RO-400028, CLUJ-NAPOCA



Organic Chemistry Department & CCOCCAN,
"BABEŞ- BOLYAI" UNIVERSITY
CLUJ-NAPOCA
ROMANIA



Group Linear Conjugated Systems CIMA, CNRS
UNIVERSITY OF ANGERS
ANGERS
FRANCE

**New Functional Architectures for Molecular Recognition, Low
Band Gap Conjugated Systems and
Advanced Electrode Materials**

Flavia-Florina PIRON (POP)

**Scientific advisors:
D.R. Jean RONCALI
Prof. Dr. Ion GROSU**

**Cluj-Napoca
2009**

Acknowledgments

I would like to offer special thanks to the members of the jury for accepting to participate at the thesis and for the patience to read it.

This co-joint PhD thesis was made between the University “Babeş-Bolyai” from Cluj-Napoca, Faculty of Chemistry and Chemical Engineering, COCCAN (Center of Organic and Computational Chemistry with Applications in Nanotechnologies) and University of Angers, CIMA (Chimie, Ingénierie Moléculaire d'Angers) Laboratory, Group Linear Conjugated Systems. I thank Prof. Dr. Ion Grosu and D.R. Jean Roncali for accepting me as a co-joint PhD student in their laboratories.

I am thanking Dr. Ion Grosu, Professor at “Babeş-Bolyai” University, for the guidance offered during all these years: License, Master and now PhD diplomas, for giving me the opportunity to develop this research work, for guidance, support and encouragement during my formation.

I am most grateful to Dr. Jean Roncali, Directeur de Recherche at University of Angers, for receiving me in his laboratory in a co-joint thesis and for accepting me to work in his team. I also want to thank him for giving me the opportunity to spend a second research stage in Angers and for the help he provided me. Special thanks also for his generous support, helpful discussions and patience for manuscript revision.

I would like to express my special thanks to Dr. Philippe Leriche, Professor at University of Angers, for the guidance and support that he offered me during my stays in Angers, for his helpful discussions, suggestions and advices during the work in the lab. I thank him also for his availability (in person, via e-mail or Skype chat) each time I needed and for manuscript revision.

I thank to Dr. Crina Cismaş, researcher at “Babeş-Bolyai” University and to Dr. Anamaria Terec and Dr. Elena Bogdan, Lecturers at “Babeş-Bolyai” University, for fruitful discussions, help, support, guidance and collaboration in the lab work.

I express grateful thanks to Mr. Christian Roussel, Professor at “Paul Cézanne-Aix-Marseille” University, and the members of his group (Dr. Nicolas Vanthuylne, Bérangère Joulin, Ingénieur de recherche CNRS Jean-Valère Naubron) for DHPLC analysis, VCD and IR spectra and absolute configuration determinations for the chiral butadienes.

Thanks also to Dr. Magali Allain from CIMA Laboratory in Angers and Dr. Richard Atilla Varga from Faculty of Chemistry in Cluj-Napoca for X-Ray Crystallographic determinations.

Thanks to Mihaela Țițaș for some NMR, ESI-MS spectra and numerous drafts of the thesis and also to Raluca Turdean for some NMR spectra that I needed in the last months of my thesis.

I would also want to thank my former colleagues: Dr. Radu Gropeanu, Dr. Niculina Bogdan, Dr. Carmen Florian, Dr. Emilia Paunescu, Dr. Roiban Doru, Dr. Nicoleta Tosa for the help they provided me during the work for my Master and PhD theses, for their advice, suggestions and support with the work in the lab.

Thanks to my friends and colleagues from Cluj-Napoca and from Angers: Mihaela Țițaș, Monica Cîrcu, Raluca Turdean, Anca Petran, Claudia Lar, Andrei Gâz, Adrian Woiczehowski-Pop, Ioana Dobra, Ilișca Mihalca, Cornelia Oprea, Emilie Ripaud, Laurent Pouchain, David Canevet, Charlotte Mallet, Quentin Bricaud, Ali Yassin, Theodulf Rousseau.

Last but not the least I have to thank my family: my parents, my husband and my brothers for all the support they offered me during all these years, for their understanding and encouragements.

Funding from Romanian Government, CNCSIS AT – 64/2006, PNCDI II program (UEFISCSU; projects: TD 82/2007, ID 2358/2009), “Babeș-Bolyai” University through Erasmus scholarship are gratefully acknowledged. Thanks also to World Federation of Scientists for supporting this research through WFS scholarship program and CNRS for supporting the research stage in Angers (October-December 2008).

List of abbreviations

A	Acceptor (electron deficient)
APCI-MS	Atmospheric Pressure Chemical Ionization- Mass Spectrometry
B ₄ NPF ₆	Tetrabutylammonium hexafluorophosphate
BHJ	Bulk Heterojunction
BLA	Bond Length Alternation
BT	Bithiophene
CDCl ₃	Chloroform- <i>d</i>
CD ₂ Cl ₂	Dichloromethane- <i>d</i> ₂
C ₆ D ₆	Benzene- <i>d</i> ₆
CHCl ₃	Chloroform
CH ₂ Cl ₂	Dichloromethane
CMP	Conjugated Microporous Polymers
C ₄ T ₂	3,3',5,5'-tetra[9-(2-ethylhexyl)carbazole]-2,2'-bithiophene
CV	Cyclic Voltammogram
D	Donor (electron rich)
DCINQ	2,3-Dichloronaphthoquinone
DHPLC	Dynamic High Performance Liquid Chromatography
DNMR	Dynamic Nuclear Magnetic Resonance
DFT	Density Functional Theory
ΔG^\ddagger	Free activation energy
EE	EDOT-EDOT
EDOT	3,4-Ethylenedioxythiophene
ETE	EDOT-Thiophene-EDOT
E ₄ T ₂	3,3',5,5'-tetra(3,4-ethylenedioxythiophene)-2,2'-bithiophene
E ₄ T ₄	2,2',5,5'-tetra(3,4-ethylenedioxythiophene)-3,3'-dithienyl-2,2'- bithiophene
E ₈ T ₂	3,3',5,5'-tetra[bis(3,4-ethylenedioxythiophene)]-2,2'-bithiophene
E ₈ T ₄	2,2',5,5'-tetra[bis(3,4-ethylenedioxythiophene)]-3,3'-dithienyl- 2,2'-bithiophene
EtOH	Ethanol
ESI	ElectroSpray Ionization
EI	Electron Impact
E _g	Bandgap energy

E_{pa}	Anodic peak potential
HOMO	Highest Occupied Molecular Orbital
HPLC	High Performance liquid Chromatography
HRMS	High Resolution Mass Spectrometry
ITO	Indium Tin Oxide
J	Coupling constant
LUMO	Lowest Unoccupied Molecular Orbital
IR	Infrared
MALDI-TOF	Matrix Assisted Laser Desorption Ionization (Time of Flight)
Me	Methyl
MOF	Metal Organic Framework
m.p.	Melting point
MS	Mass spectrometry
m/z	Mass-to-charge ratio
NBS	N-Bromosuccinimide
NMR	Nuclear Magnetic Resonance
OLED	Organic Light Emitting Diodes
PCBM	[6,6]-Phenyl-C ₆₁ -butyric acid methyl ester
PEDOT	Polyethylenedioxythiophene
Qd	Electrodeposition charge
Q_r	Charge reversibly exchanged
R_f	Retention factor
rt	Room temperature
SCE	Saturated Calomel Electrode
TETE	Thiophene-EDOT-Thiophene-EDOT
TLC	Thin Layer Chromatography
TMS	Tetramethylsilane
UV	Ultra-Violet
UV-Vis	Ultra-Violet-Visible
UV-Vis-NIR	Ultra-Violet-Visible-Near-Infrared
vdW	Van der Waals
VCD	Vibrational Circular Dichroism

Table of contents

Chapter 1

One-pot homoacetylenic Cu-catalyzed coupling of some podands with cyanurate / isocyanurate units	1
---	----------

Chapter 2

Synthesis, structural analysis and chiral investigations of new atropisomers with <i>EE</i>- tetrahalogeno-1,3-butadiene core	66
--	-----------

Chapter 3

New building blocks for the synthesis of low band gap conjugated polymers as active materials for organic solar cells	124
--	------------

Chapter 4

Three-dimensional π-conjugated architectures based on a twisted bithiophene core	149
--	------------

General conclusions	209
----------------------------	------------

List of compounds	211
--------------------------	------------

List of publications	220
-----------------------------	------------

Chapter 1

**One-pot homoacetylenic Cu-catalyzed coupling of some podands with
cyanurate / isocyanurate units**

Table of contents

1.1.	Introduction	01
1.1.1.	General remarks on Cu-catalyzed acetylenic coupling	01
1.1.2.	Cryptands by one-pot homoacetylenic coupling	01
1.1.2.1.	Synthesis, structure and properties of cryptands with aromatic units	01
1.1.2.2.	Synthesis, structure and properties of cryptands with triphenylphosphine units	08
1.1.2.3.	Synthesis, structure and properties of some fullerene precursors	10
1.2.	Podands with heterocyclic units – Synthesis and reactivity	15
1.2.1.	Synthesis of the podands precursors	17
1.2.2.	Synthesis and analysis of podands with aromatic 1,3,5-triazine units	19
1.2.3.	Synthesis and analysis of podands with isocyanurate units	23
1.3.	Macrocycles by Cu-catalyzed homoacetylenic coupling reactions	28
1.3.1.	Synthesis and analysis of macrocycles with cyanurate units	29
1.3.2.	Synthesis and analysis of macrocycles with isocyanurate units	37
1.3.3.	Solid state structural investigation for bis-macrocycle 36	42
1.4.	Conclusions	44
1.5.	Experimental part	45
1.5.1.	General remarks	45
1.5.2.	Synthesis and characterization of compounds	46
	Annexes	65

1.1. Introduction

1.1.1. General Remarks on Cu-catalyzed Acetylenic Coupling

Acetylenic homocoupling represents an interesting tool for molecular construction and has been extensively used and diversified since Glaser's discovery of oxidative coupling of copper alkynylbenzene.¹ The most important and successful modifications of the initial Glaser coupling technique were reported by Eglinton² (the Eglinton-Galbraith method: excess Cu(OAc)₂ in pyridine, 20–40% yield) and Hay³ [the Glaser-Hay coupling: CuCl, *N,N,N',N'*-tetramethylethylenediamine (TMEDA), solvent, up to 97% yield]. Despite the wide range of applications of alkyne coupling,⁴ from natural products to pharmaceuticals and macrocyclic derivatives,⁵ the mechanism of this reaction has not yet been elucidated. This introduction is resuming the modified coupling procedures that have been used to afford cage compounds by one-pot cyclization reactions.

1.1.2. Cryptands by one-pot homoacetylenic coupling

1.1.2.1. Synthesis, structure and properties of cryptands with aromatic units

The formation of three-dimensional macrobicyclic receptors with triphenylmethane units containing three buta-1,3-diyne diyl spacers, by a one-pot triple-coupling reaction of two tris-ethynyl substituted half cages, has been first reported by Breslow and co-workers.⁶ They have obtained the 1,1,1-triphenylethane derivative **IIa** by performing the triple oxidative dimerization in *dry oxygen-free pyridine* in the presence of both anhydrous Cu(I) and Cu(II) salts (Scheme 1, Table 1). Despite their report on complete failure when employing standard coupling conditions [Cu(II)-pyridine or Cu(I)-TMEDA-O₂], Voegtle and co-workers have later obtained compound **IIa** in similar yields, by using Cu(OAc)₂ in pyridine or acetonitrile.⁷

¹ Glaser, C. *Ber. Dtsch. Chem. Ges.* **1869**, *2*, 422-424

² Eglinton, G.; Galbraith, A. R. *Chem. Ind. (London)* **1956**, 737-738

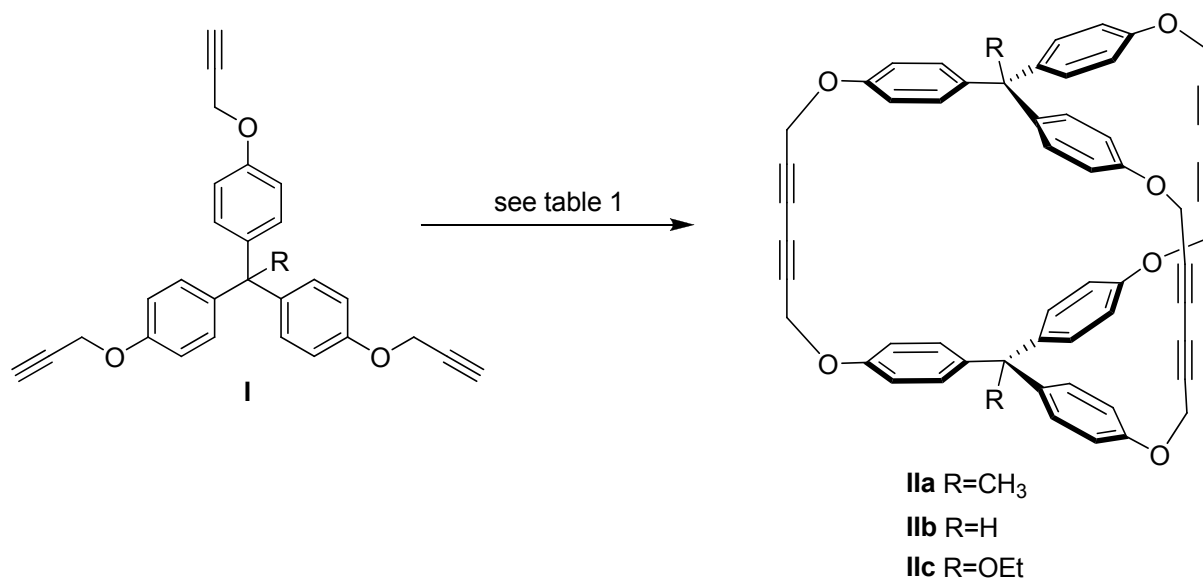
³ Hay, A. S. *J. Org. Chem.* **1962**, *27*, 3320-3321

⁴ Siemsen, P.; Livingston, R. C.; Diedrich, F. *Angew. Chem., Int. Ed.* **2000**, *39*, 2634-2657

⁵ (a) Breitenbach, J.; Boosfeld, J.; Voegtle, F. *Comprehensive Supramolecular Chemistry vol. 2* (Ed. F. Voegtle), Pergamon, Oxford, **1996**, pp. 29-67; (b) Whitlock, B. J.; Whitlock, H. W. *ibid*, pp. 309-324

⁶ O'Krongly, D.; Denmeade, S. R.; Chiand, M. Y.; Breslow, R. *J. Am. Chem. Soc.* **1985**, *107*, 5544-5545

⁷ Berscheid, R.; Nieger, M.; Voegtle, F. *Chem. Ber.* **1992**, *125*, 2539-2552



Scheme 1. Synthesis of derivatives **I** and **II**

Breslow's macrocyclization reaction was also employed for the synthesis of macrobicyclic compound **IIb**⁸ in 35% yield (Scheme, Table). The dimeric cage molecule **IIb** has also been synthesized following Eglinton coupling procedure with copper(II) acetate monohydrate in pyridine or acetonitrile.^{5b}

Table 1. The reaction conditions for Cu-catalyzed acetylenic coupling for the formation of derivatives **I** and **II**

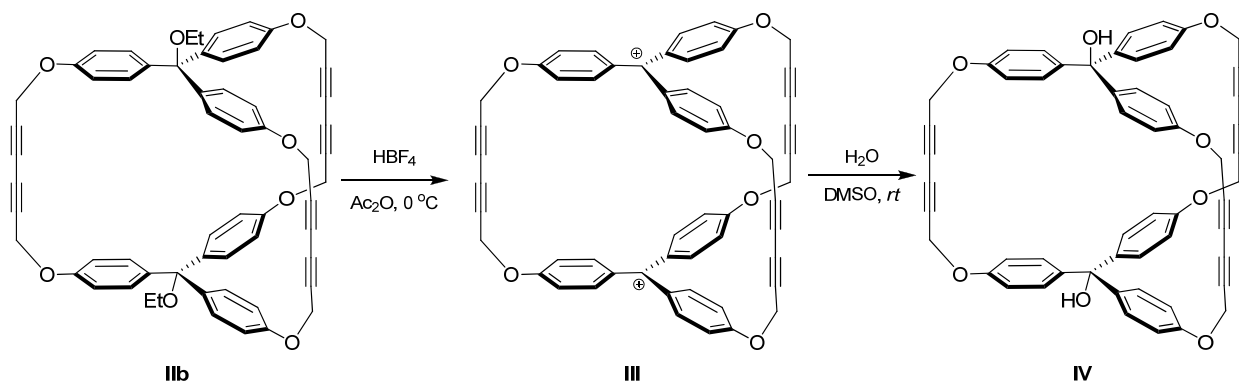
Compd.	Reaction conditions	Yield (%)	Ref.
IIa	100 equiv. 100 mM anh. CuCl/ 12.2 equiv. 12.2 mM anh. CuCl ₂ , dry O ₂ -free Py, 48 h, 0 °C	35	6
	Cu(OAc) ₂ in Py or AcCN	17 – 21	5b
IIb	100 equiv. 200 mM anh. CuCl/ 12 equiv. 24 mM anh. CuCl ₂ , dry O ₂ -free Py, 7 d, <i>rt</i>	35	8
IIc	10 equiv. 112 mM Cu(OAc) ₂ in AcCN, 1 h, 60 °C	32	9

Voegtle and co-workers have reported on the first synthesis of a new type of concave dyestuff,⁹ bearing a relatively large cavity formed from two tritylium cation units (**III**, Scheme 2). The precursor is the diethoxy protected derivative **IIc**, obtained by oxidative

⁸ (a) Voegtle, F.; Berscheid, R.; Schnick, W. *J. Chem. Soc., Chem. Commun.* **1991**, 414-416; (b) Berscheid, R.; Nieger, M. and Voegtle, F. *Chem. Ber.* **1992**, 125, 1687-1695

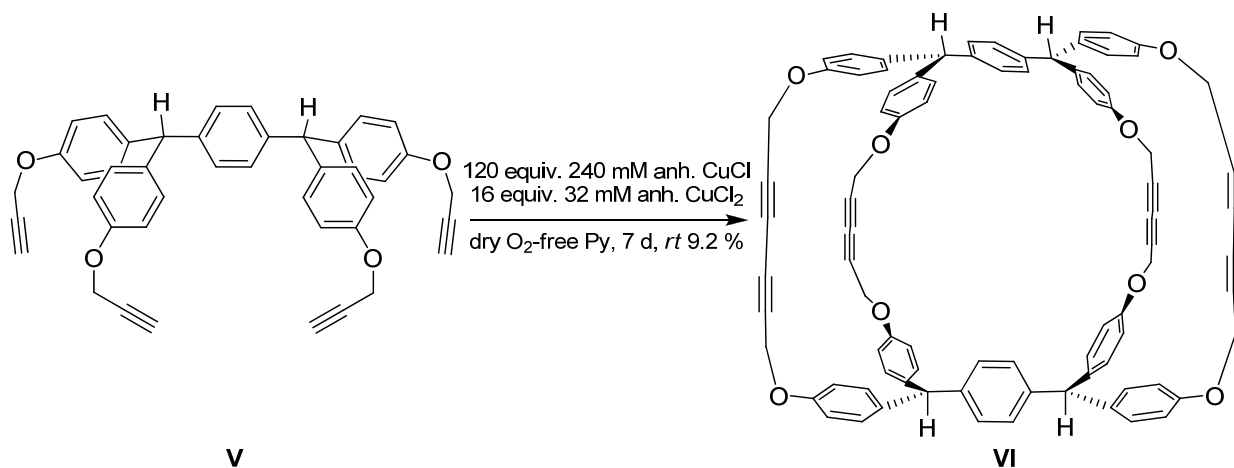
⁹ Berscheid, R.; Voegtle, F. *Synthesis* **1992**, 58-61

cyclodimerization with Cu(II) in acetonitrile. The usage of acetonitrile instead of pyridine had lead to a considerable yield improvement, from 18 % to 32 %, probably due to a template effect of the first.



Scheme 2. Synthesis of derivatives III and IV

An interesting example is compound VI (Scheme 3), an analogue of derivative IIb, with a larger cavity formed by triphenylmethane units. Performing the four-fold oxidative Cu(I)/Cu(II)-catalyzed acetylenic coupling, a significant decrease in yield was observed when compared to the three-fold bridging (IIb) (9.2 % vs. 35 %).

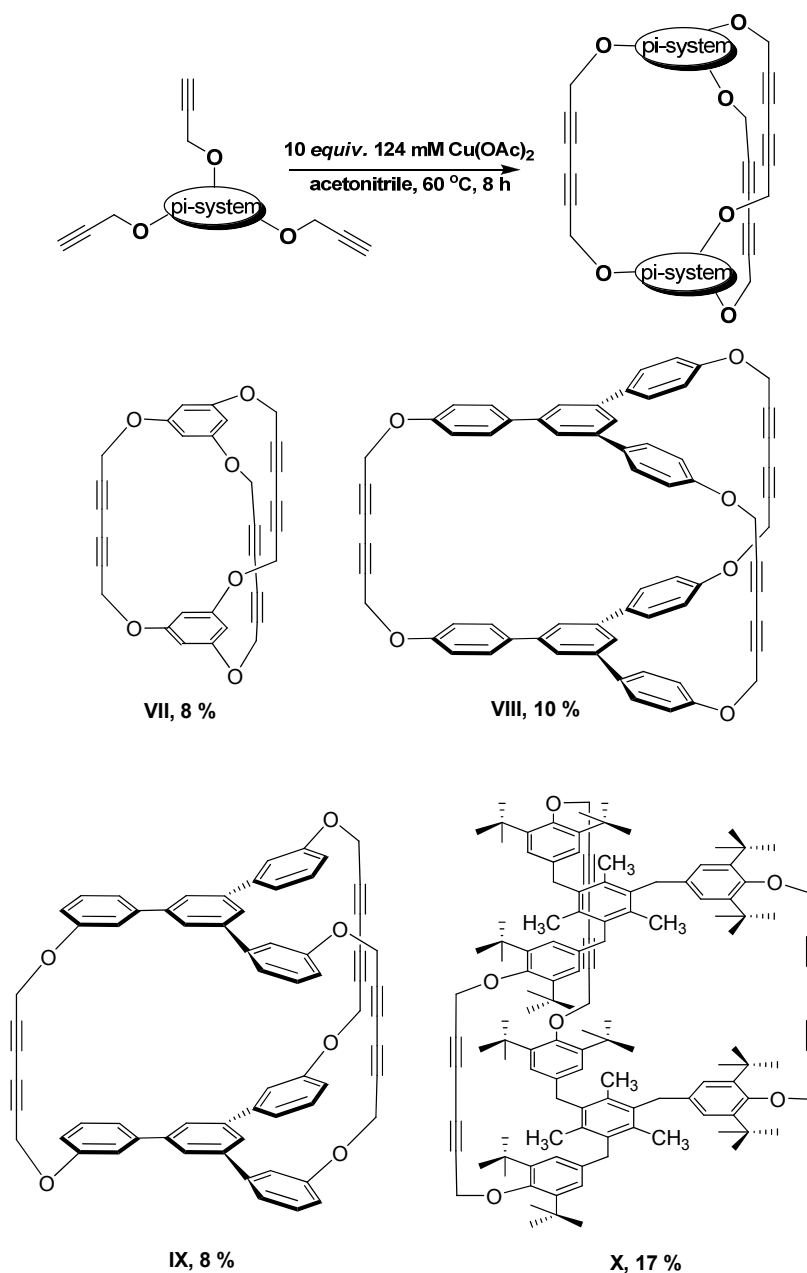


Scheme 3. Synthesis of derivative VI

An example of a smaller macrobicyclic cavity for the inclusion of acetonitrile was described by the same authors.¹⁰ Derivative VII (Scheme 4) was synthesized in 8 % yield using Cu(OAc)₂·H₂O in pyridine under normal atmosphere. The larger cage compounds VIII – X were

¹⁰ Berscheid, R.; Nieger, M.; Voegtle, F. *J. Chem. Soc., Chem. Commun.* **1991**, 1364-1366

obtained in low yields by performing the mild, modified Eglinton acetylenic coupling in acetonitrile.¹¹



Scheme 4. Synthesis of derivatives VII – X

The multiple hexa-2,4-diyne bridges in combination with the aromatic units described above are forming concave cavities able to include neutral organic guests, mainly solvent molecules. The conjugated alkyne units do not show interactions for the inclusion process with the guest molecules.

¹¹ Voegtle, F.; Michel, I.; Berscheid, R.; Nieger, M.; Rissanen, K.; Kotila, S.; Airola, K.; Armarolli, N.; Maestri, M.; Balzani, V. *Liebigs Ann.* **1996**, 1697-1704

The macrobicyclic host **IIb** was crystallized from acetonitrile as a 1:1 adduct and from phenylacetonitrile as a 1:3 adduct (Fig. 1).

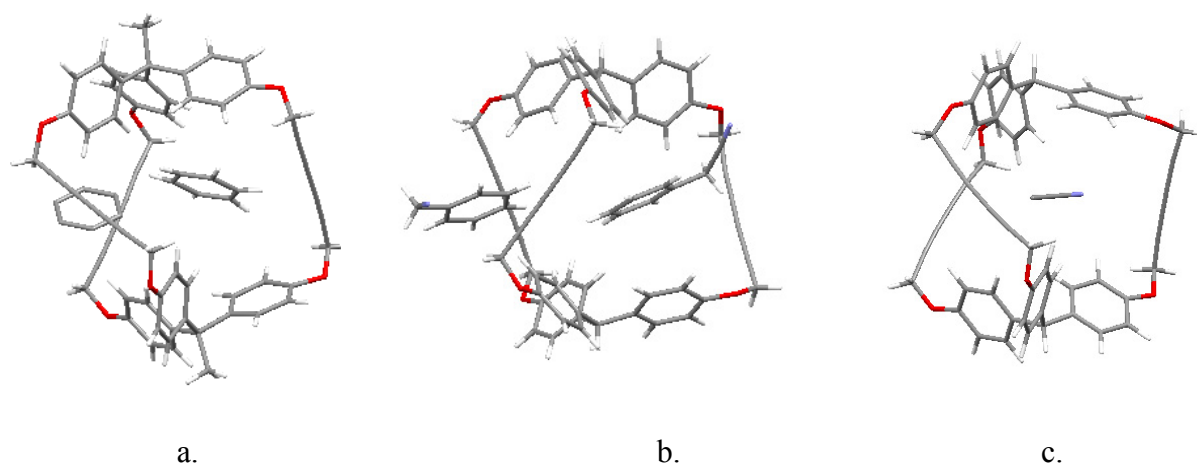


Fig. 1. X-ray structures for inclusion complexes a. **IIa**x5 C₆H₆, b. **IIb**x3BnCN and c. **IIc**x6MeCN

A comparison with the complex of **IIa** with benzene (**IIa**x5C₆H₆) did show that hosts **IIa** and **IIb** have similar torsion angles along their *pseudo* C₃ axis (26 – 36°) and similar cavity sizes (Fig. 1). These guests are not located in the center of the cavity and it was assumed that flat aromatic compounds are not sterically suitable for a spherical shaped host. This assumption has been proved later by the single-crystal X-ray structure of the inclusion complex of **IIa** with acetone (Fig. 2, a). Acetone was located in the center of the cavity and held by multiple σ - π interactions between the methyl groups of the guest and the aromatic rings of the host.

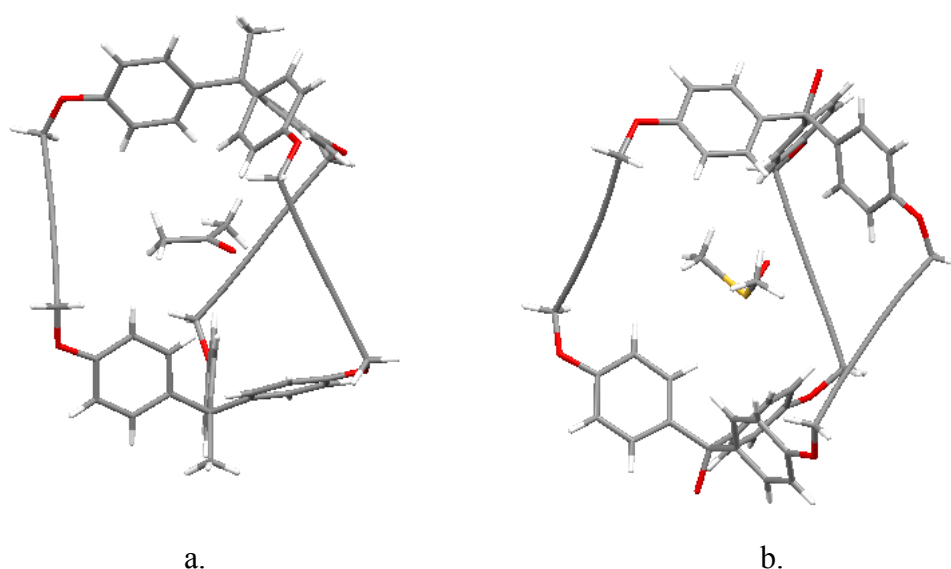


Fig. 2. X-ray structures for inclusion complexes a. **IIa**xacetone and b. **IV**xDMSO

Further evidence of the importance of topological complementarities between the shape of the host and the bonded guest has been provided by the inclusion complex of DMSO in the cavity of compound **IV** (Scheme 2). The guest molecule is situated, as acetone in **IIa**, in the middle of the cavity (Fig. 2, b).

The geometry of the complex formed by the smaller host **VII** with acetonitrile turned out to be completely different from **IIb** with respect to the orientation of acetonitrile (Fig. 3). The host phenylene rings in **IIb**xMeCN (Fig.) interact with the nitrile group, while in **VII**xMeCN there is an interaction between the methyl group of acetonitrile and the host phenyl rings. The two aromatic rings approach each other to 7.12 Å and a torsion angle along its *pseudo* C₃ axis of 13° was measured.

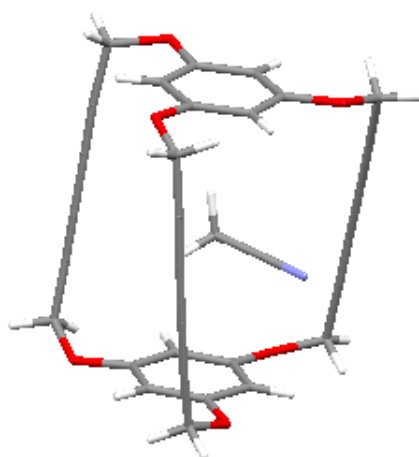


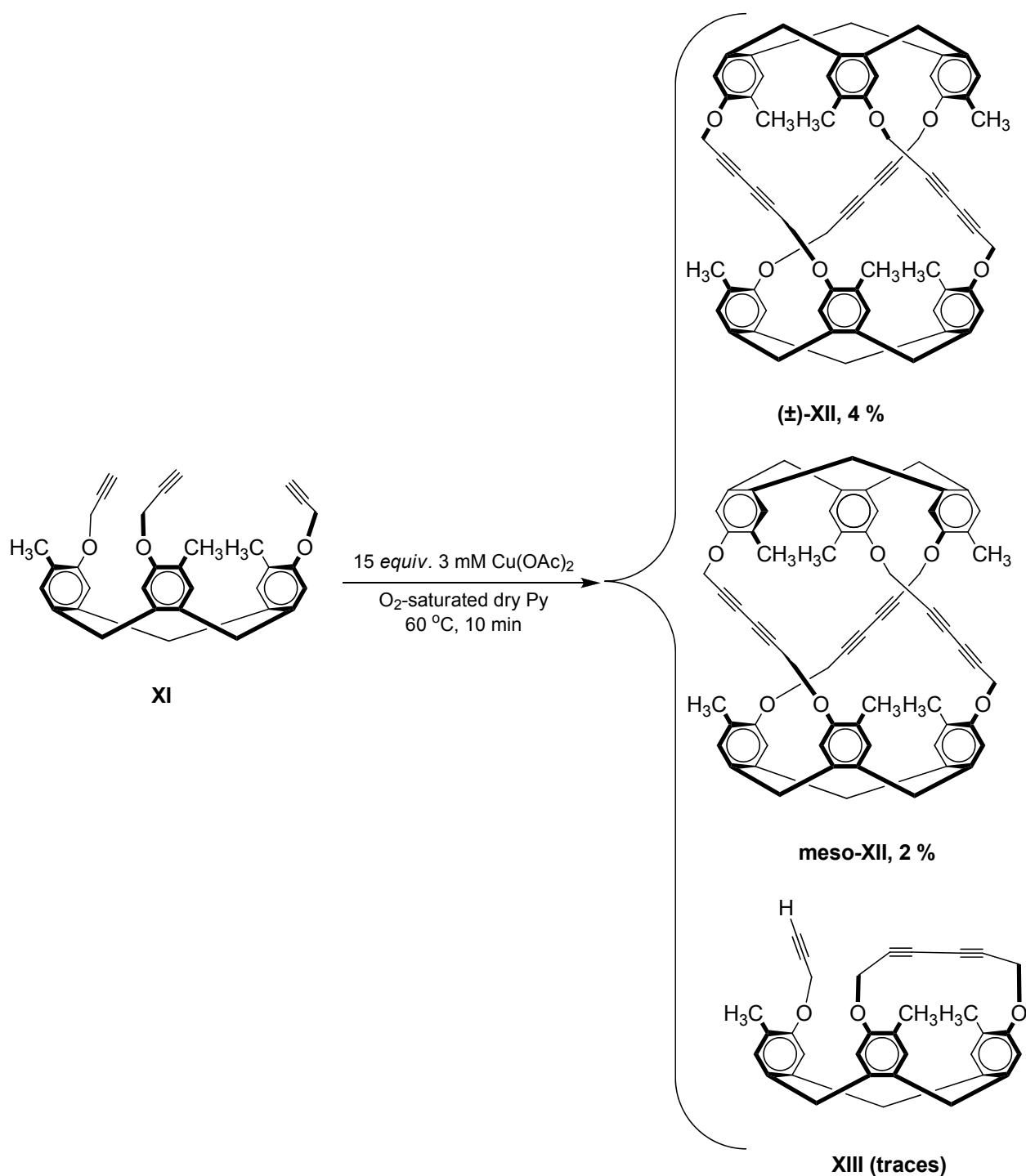
Fig. 3. X-ray structures for inclusion complex **VII**xMeCN

The larger host **VIII** did not show any endocavitational complexation with flat aromatic guests, possibly because the distance between the aromatic units (8.09 Å) is far from the ideal distance for the inclusion of aromatic guests by $\pi - \pi$ interactions (6.84 Å).¹²

Cram and co-workers¹³ have reported the synthesis of chiral [1.1.1]orthocyclophane carcerand **XII** by oxidative Eglinton coupling of acetylene **XI** (Scheme 5). They performed the most detailed study published so far on the employed conditions and concluded that *anaerobic conditions, even with excess Cu(II) salt gave no desired product*, while increasing the reaction temperature to 85°C led to the exclusive formation of a trace of intramolecularly coupled product **XIII**.

¹² Whitlock, B. J.; Whitlock, H. W. *J. Am. Chem. Soc.* **1994**, *116*, 2301

¹³ Cram, D. J.; Tanner, M. E.; Keipert, S. J.; Knobler, C. B. *J. Am. Chem. Soc.* **1991**, *113*, 8909-8916



Scheme 5. Synthesis of derivative **XII**

The configurations of the two diastereoisomers have been assigned by single crystal X-ray structure determinations. The crystal structure of (±)-**XII** (from CH₂Cl₂) shows a compact structure with an almost spherical cavity and D₃ symmetry (Fig. 4, a). In contrast, *meso*-**XII** presents a larger cavity with an approximately ellipsoidal shape (Fig. 4, b).

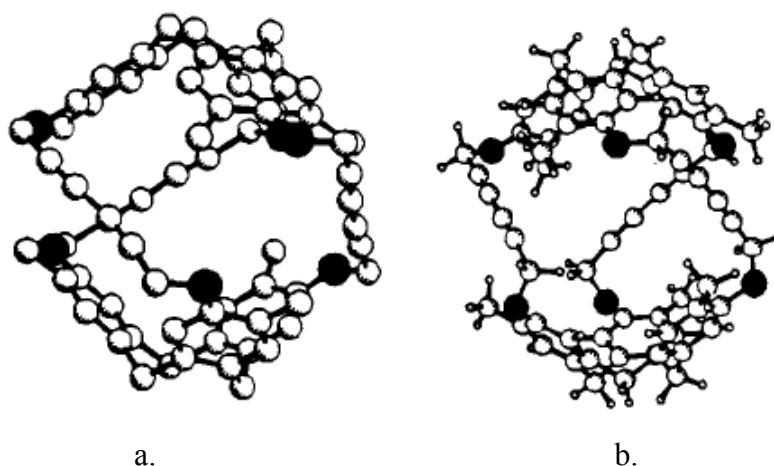


Fig. 4. X-ray structures for the free diastereoisomeric carcerands a. (±)-XII and b. *meso*-XII

In order to assess the complexation properties of the diastereoisomeric carcerands XII, ^1H NMR studies in hexachloroacetone were performed. The results demonstrated that (±)-XII is strongly binding small neutral organic molecules with complementary shape and appropriate size. The association constants for complexing CHCl_3 , $(\text{CH}_3)_3\text{COH}$, CH_2Cl_2 , cubane, propylene oxide and benzene were determined in $(\text{CCl}_3)_2\text{CO}$ at $-20\text{ }^\circ\text{C}$.

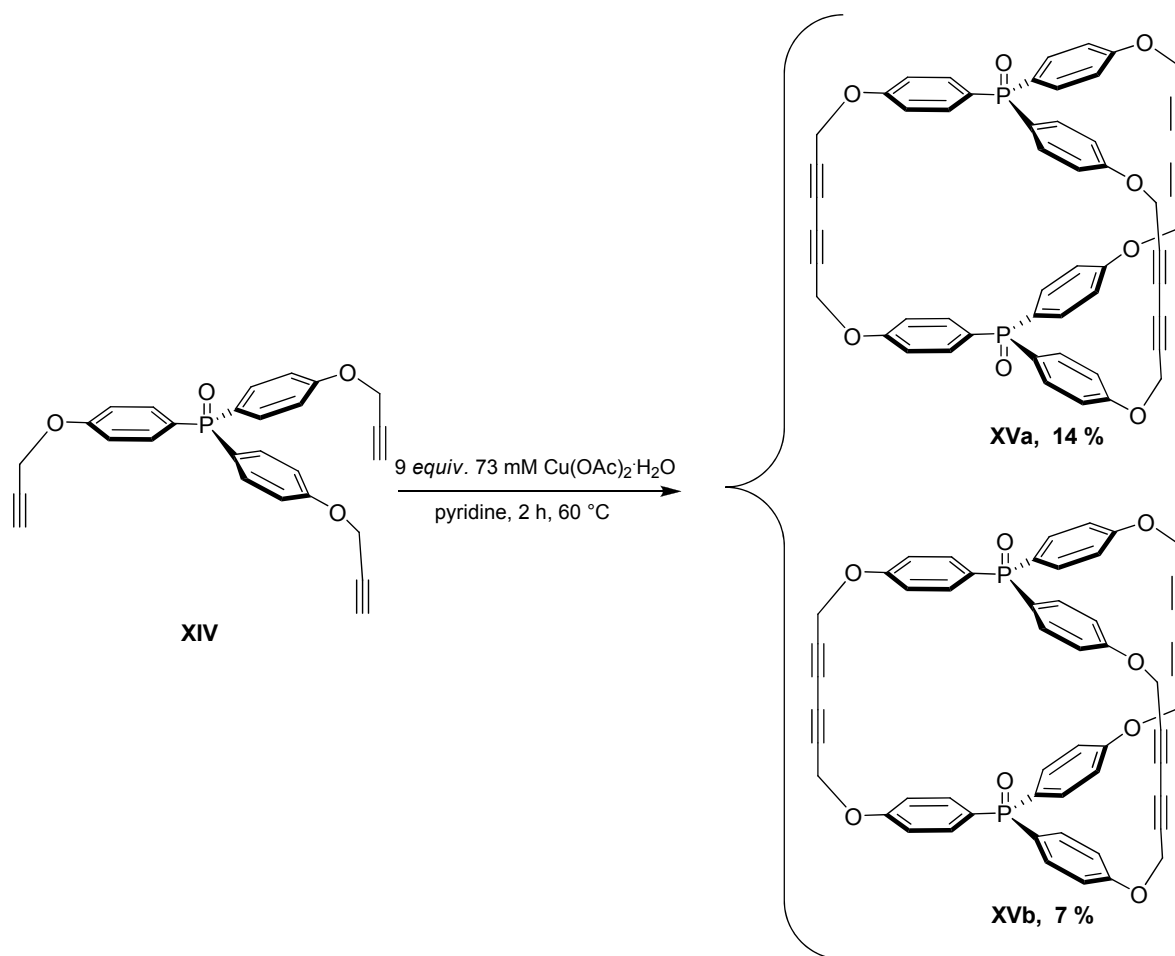
The ^1H NMR spectra of *meso*-XII in $(\text{CCl}_3)_2\text{CO}$ showed no signs of complexation with any of the guests, from -20 to $-40\text{ }^\circ\text{C}$. It was assumed to be due to the fact that solvent binds better to the *meso* diastereoisomer than it binds to the (±) one.

1.1.2.2. Synthesis, structure and properties of cryptands with triphenylphosphine units

As phosphine oxides can serve as hydrogen-bond acceptors, Whitlock and Friedrichsen^{14,15} have considered this moiety for the synthesis of this type of well defined three-dimensional host molecules. Treatment of XIV in pyridine at $60\text{ }^\circ\text{C}$ with $\text{Cu}(\text{OAc})_2\cdot\text{H}_2\text{O}$ provided a mixture of isomeric diyne-bridged bis-phosphoryl macrocycles XVa (*exo-exo*) and XVb (*endo-exo*) in 14 % and 7 % yield, respectively (Scheme 6).

¹⁴ Friedrichsen, B. P.; Whitlock, H. W. *J. Am. Chem. Soc.* **1989**, *111*, 9132-9134

¹⁵ Friedrichsen, B. P.; Powell, D. R.; Whitlock, H. W. *J. Am. Chem. Soc.* **1990**, *112*, 8931-89



Scheme 6. Synthesis of derivatives **XVa** and **XVb**

The X-ray structures of compound **XVa** (from chloroform, Fig. 5, a) and **XVb** (from anisole, Fig. 5, b) showed the orientation of the phosphoryl groups and the helical nature of both species. Complete ^1H and ^{31}P NMR studies were undertaken and proved that *exo-exo* host **XVa** forms only extracavity complexes, while *endo-exo* host **XVb** allows also intracavity complexation.

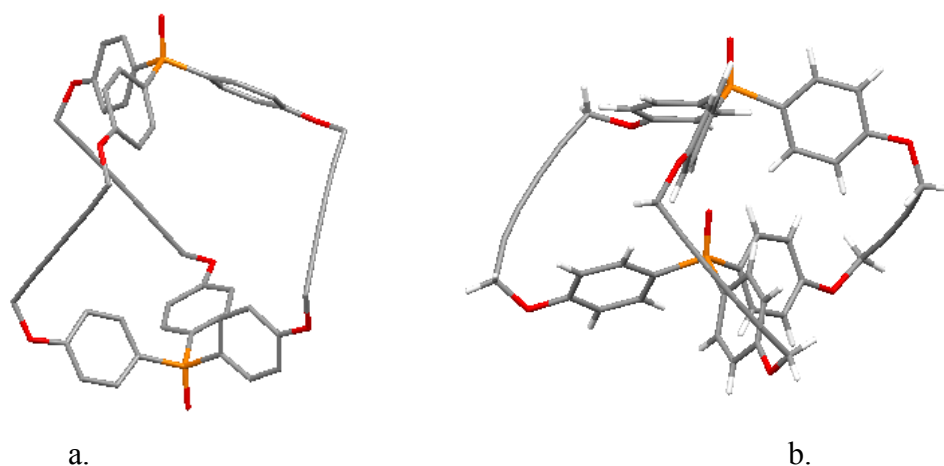


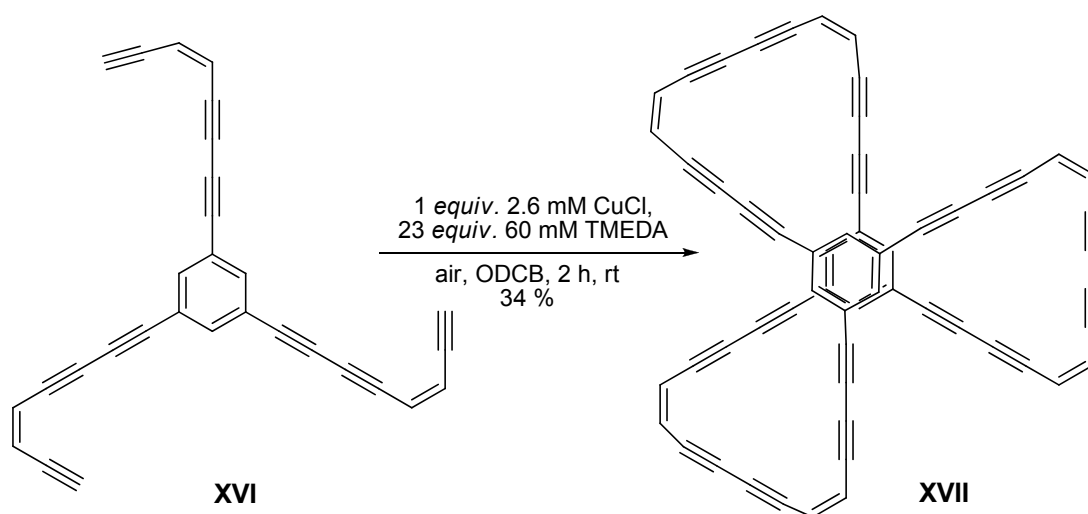
Fig. 5. X-ray structures for the free cryptands a. **XVa** and b. **XVb**

The 1:2 complexation mechanisms of **XVb** with a variety of guests has been studied by ^1H NMR spectroscopy. The calculated chemical shifts for the 1:1 and 1:2 complexes have evidenced the initial *endo* complexation of most of the guests. The association constants were modest and range from 18 M^{-1} (for phenol) to 354 M^{-1} (for *p*-nitrophenol) for the formation of the 1:1 complex with mono- and unsubstituted phenols, while the association constants for 1:2 complexes range from 1 M^{-1} to 320 M^{-1} . Surprisingly, even larger hosts such as 4-[(*p*-nitrophenyl)-azo]phenol and 6-nitro-2-naphtol showed preference for the initial *endo* complexation. The exception from this mechanism was proved for pentafluorophenol, which prefers to complex with **XVb** by initial *exo* pathway. No complexation was observed for 2,4-dinitrophenol, 4-nitrothiophenol, benzoic acid and pyridine hydrochloride.

The ^{31}P NMR studies allowed calculation of the association constants for the *exocavit*al complexes of **XVa** and brought further information regarding the complexation of **XVb**. It has been shown that 2,6-dimethyl-4-nitrophenol, acetic acid and pentafluorophenol prefer initial *exo* complexation with the *endo-exo* phosphine oxide moieties.

1.1.2.3. Synthesis, structure and properties of some fullerene precursors

The first approach to the unconventional synthesis of buckminsterfullerene (C_{60}) and heterofullerenes from polyalkynyl precursors was reported by Rubin.¹⁶ Cyclization of **XVI** under Hay conditions, in *o*-dichlorobenzene at 25°C , afforded the corresponding macrocyclic cyclophane **XVII** in 34% yield (Scheme 7).



Scheme 7. Synthesis of derivative **XVII**

¹⁶ Rubin, Y.; Parker, T. C.; Khan, S. I.; Holliman, C. L.; McElvany, S. W. *J. Am. Chem. Soc.* **1996**, *118*, 5308-5309

The single crystal X-ray structure of macrobicyclic compound **XVII**, together with the partial packing diagram is showing the helical chirality of the structure (Fig. 6). The only solvent that resulted in well defined crystals was *o*-dichlorobenzene, forming co-crystals with the cyclophane by separating the right handed helices from the opposite-handed partner.

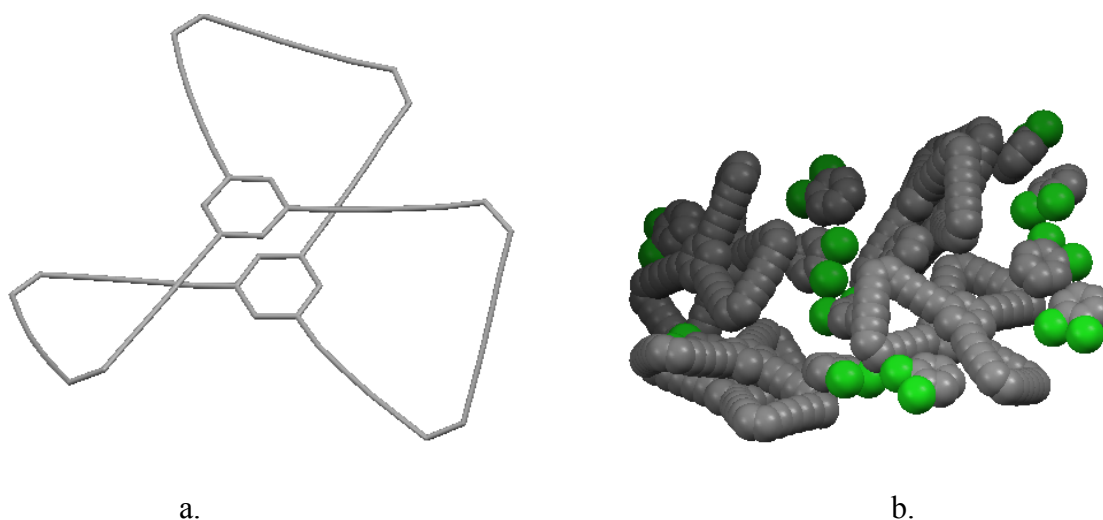
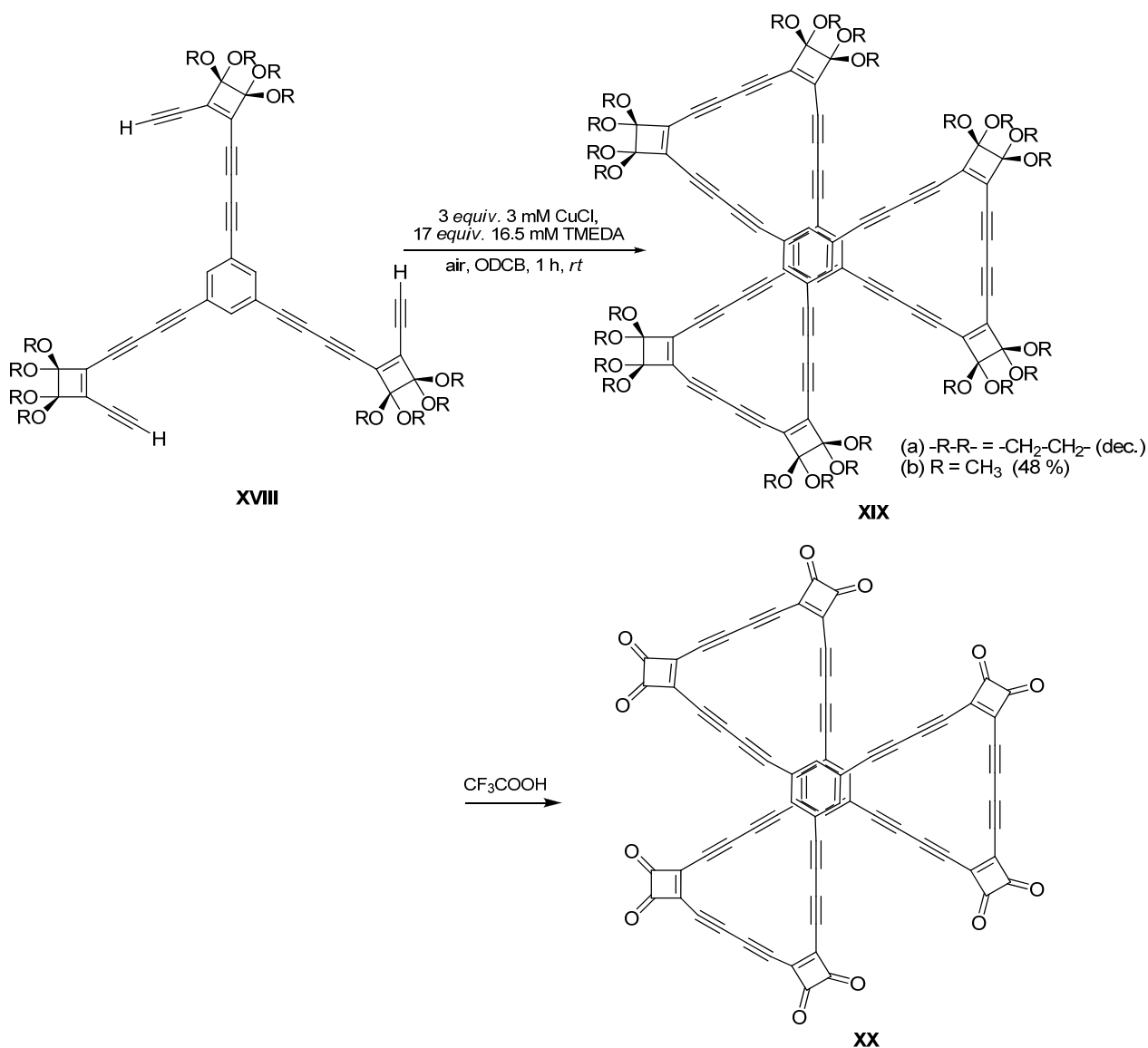


Fig. 6. X-ray structure (a) and crystal packing (b) for the free cage **XVII**

Thermochemical studies on macrocycle **XVII** have shown an unexpected stability of the parent molecular ion ($C_{60}H_{18}$). Therefore, Rubin and co-workers have synthesized the cyclobutanedione **XX** (Scheme 8) that would rearrange to the more highly unsaturated precursor $C_{60}H_6$ and generates C_{60} ions in mass spectrometric experiments. Cyclization of dimethoxyacetal alkyne **XVIII**¹⁷ ($R = CH_3$) by a modified Hay procedure (Scheme 8) has led to the formation of macrocycle **XIX** as a solid in a very good yield (48%).

¹⁷ Rubin, Y.; Parker, T. C.; Pastor, S. J.; Jalisatgi, S.; Boule, C.; Wilkins, C. L. *Angew. Chemie. Int. Ed.* **1998**, *37*, 1226-1229



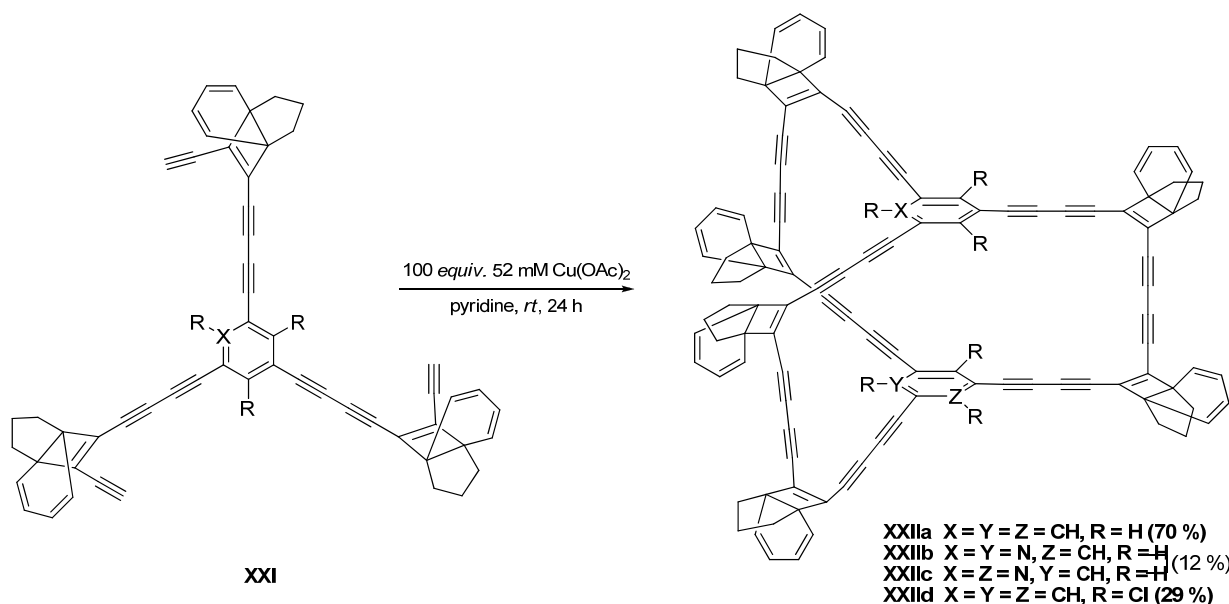
Scheme 8. Synthesis of derivatives XIX and XX

A different approach in the formation of fullerenes was reported by Tobe and co-workers.^{18,19,20} Cage molecules **XXIIa** was synthesized in an impressive 70% yield by oxidative homoacetylenic coupling under high dilution modified Eglinton conditions (Scheme 9). The analogue tris(propellane)trichloro-substituted benzene macrocyclic derivative **XXIIb** was obtained in only 29% yield, probably due to its increased instability.

¹⁸ Tobe, Y.; Nakagawa, N.; Naemura, K.; Wakabayashi, T.; Shida, T.; Achiba, Y. *J. Am. Chem. Soc.* **1998**, *120*, 4544-4545

¹⁹ Tobe, Y.; Nakagawa, N.; Kishi, J.; Sonoda, M.; Naemura, K.; Wakabayashi, T.; Shida, T.; Achiba, Y. *Tetrahedron* **2001**, *57*, 3629-3636

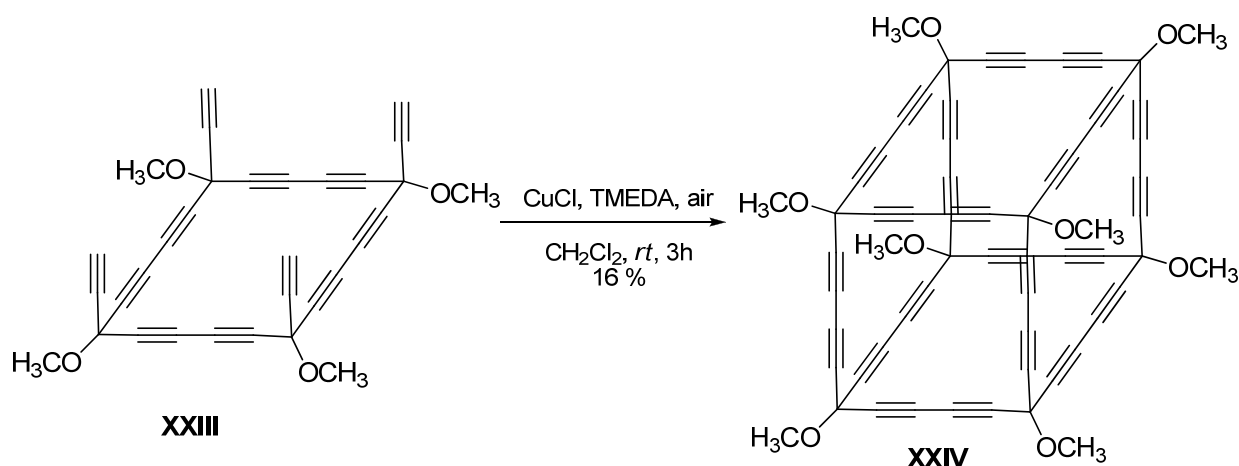
²⁰ Tobe, Y.; Umeda, R.; Sonoda, M.; Wakabayashi, T. *Chem. Eur. J.* **2005**, *11*, 1603-1609



Scheme 9. Synthesis of derivatives **XXII a - b**

The same dimerization conditions were followed for the synthesis of macrocyclic polyynes C₅₈H₄N₂ (**XXIIb** and **XXIIc**) as precursors to diazafullerene.²¹ The nitrogen substitution of one carbon atom in the benzene ring has led to the formation of a mixture of both regioisomers in a rather low yield (12%).

Diedrich and co-workers²² have successfully applied Hay's acetylenic homocoupling conditions for the synthesis of expanded cubane **XXIV** (Scheme 10). The four-fold oxidative coupling cyclization afforded **XXIV** in a quite low yield (16%), reasonable when considering its instability.



Scheme 10. Synthesis of derivative **XXIV**

²¹ Tobe, Y.; Nakanishi, H.; Sonoda, M.; Wakabayashi, T; Achiba, Y. *Chem. Commun.* **1999**, 1625-1626

²² Manini, P.; Amrein, W.; Gramlich, V.; Diederich, F. *Angew. Chem. Int. Ed.* **2002**, 41, 4339-434

The procedures for the one pot formation of cage molecules by Cu-catalyzed acetylenic coupling uses both Cu (I) and Cu (II) catalysts and acetonitrile, dichlorobenzene, pyridine or dichloromethane as solvents. The yields of these reactions vary from fair to good in agreement with the pre-organization and the steric complementarities of the reacting molecules, but the mechanism of this coupling reaction is not yet elucidated. The target cryptands successfully bind neutral molecules as solvents and aromatic compounds. The host guest interactions are insured by the participation of the aromatic core of the cryptands and no evidence of the participation of the diyne bridges to this process was revealed. Some of the target molecules were used for the synthesis of fullerenes and heterofullerenes.

1.2. Podands with heterocyclic units – Synthesis and reactivity

Supramolecular chemistry²³ is one of the most dynamic areas in the chemical research of the last decades and its development requires the rapid access to large molecules with well defined structures.

The design of a variety of host molecules having intramolecular cavities that can act as host systems for cationic, anionic or neutral organic molecules is also an area of considerable interest. Tripodal architectures represent a targeted intermediate step between small molecules and macromolecular and supramolecular structures. Substrates with C₃ symmetry are of high interest and many works are focused on the synthesis of derivatives with 1,3,5-trisubstituted benzene,²⁴ tertiary amines²⁵ or phosphines,²⁶ cyclotrimeratrylene²⁷ and 1,3,5-triazine²⁸ units. The transformation of C₃ symmetry tripodal molecules in efficient hosts requires reactive functional groups at the ends of the pending arms. These groups can participate to the facile enclosure of the macrocycles and to the formation of the corresponding cryptands or/and can facilitate the attachment of various units with high ability to interact with many guests and to allow the construction of supramolecular entities with acyclic hosts. The recent developments in organic synthesis (e.g. coupling reactions,²⁹ click chemistry,³⁰ three components coupling of alkynes, aldehydes and amines³¹) suggest triple bonds as efficient candidate for the terminal groups of the arms of versatile tripodal intermediates.

For this purpose we investigated the synthesis of tripodands corresponding to esters of both cyanuric (**A**) and isocyanuric acids (**B**) bearing terminal triple bonds, extremely useful intermediates for the synthesis of macromolecular or supramolecular compounds (Fig. 7). As main core we have used 1,3,5-triazine unit which is an electron poor heteroaromatic system and

²³ Atwood, J. L., Steed, J. W. *Encyclopedia of Supramolecular Chemistry*, by Marcel Dekker, Inc., **2004**

²⁴ a) Gomez-Lor, B.; Hennrich, G.; Alonso, B.; Monge, A.; Gutierrez-Puebla, E.; Echavarren, A.M. *Angew. Chem. Int. Ed.* **2006**, *45*, 4491-4494; b) Kumazawa, K.; Yamanoi, Y.; Yoshizawa, M.; Kusukawa, T.; Fujita, M. *Angew. Chem. Int. Ed.* **2004**, *43*, 5936-5940; c) Kotha, S.; Kashinath, D.; Lahiri, K.; Sunoj, R.B. *Eur. J. Org. Chem.* **2004**, 4003-4013

²⁵ Seel, C.; Vogtle, F. *Angew. Chem. Int. Ed.* **1992**, *31*, 528-549

²⁶ Lee, K.H.; Lee, D.H.; Hwang, S.; Lee, O.S.; Chung, D.S.; Hong, J.I. *Org. Lett.* **2003**, *5*(9), 1431-1433

²⁷ a) Carruthers, C., Ronson, T. K., Sumbly, C., Westcott, A., Harding, L. P., Prior, T. J., Rizkallah, P., Hardie, M. L. *Chem. Eur. J.* **2008**, *14*, 10286-10296. b) Ahmad, R., Hardie M.J. *Supramolecular Chemistry* **2006**, *18*, 29-38.

²⁸ a) Anelli, P.L., Lunazzi, L., Montanari, F., Quici, S. *J. Org. Chem.* **1984**, *49*, 4197-4203; b) Sandford, G. *Chem. Eur. J.* **2003**, *9*, 1465-1469.

²⁹ Chinchilla R., Nájera, C. *Chem. Rev.* **2007**, *107*, 874-922

³⁰ Kolb, H.C., Finn M.G., Sharpless, K.B. *Angew. Chem. Int. Ed.* **2001**, *40*, 2004-2021.

³¹ Li, P., Zhang, Y., Wang, L. *Chem. Eur. J.* **2009**, *15*, 2045-2049

its isomeric isocyanurate structure which can participate via the oxygen atoms as donors to the formation of hydrogen bonds.³²

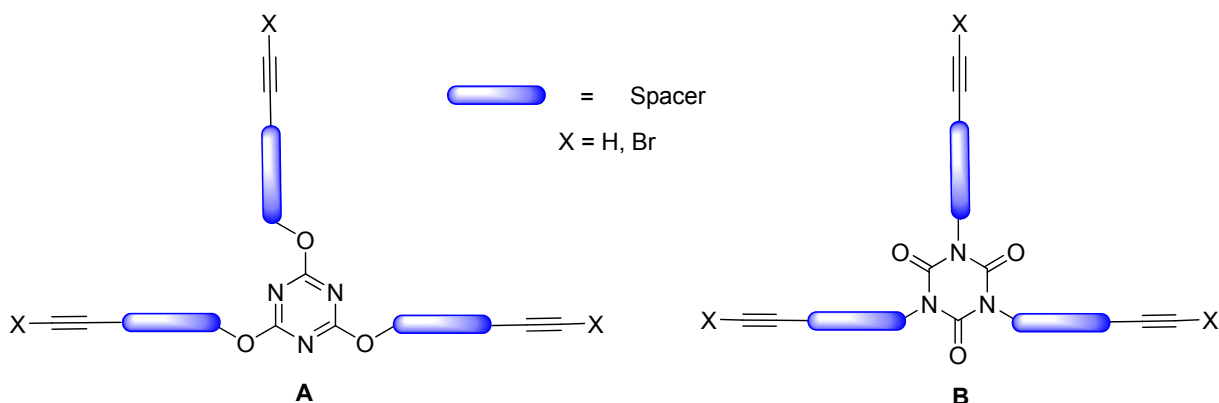
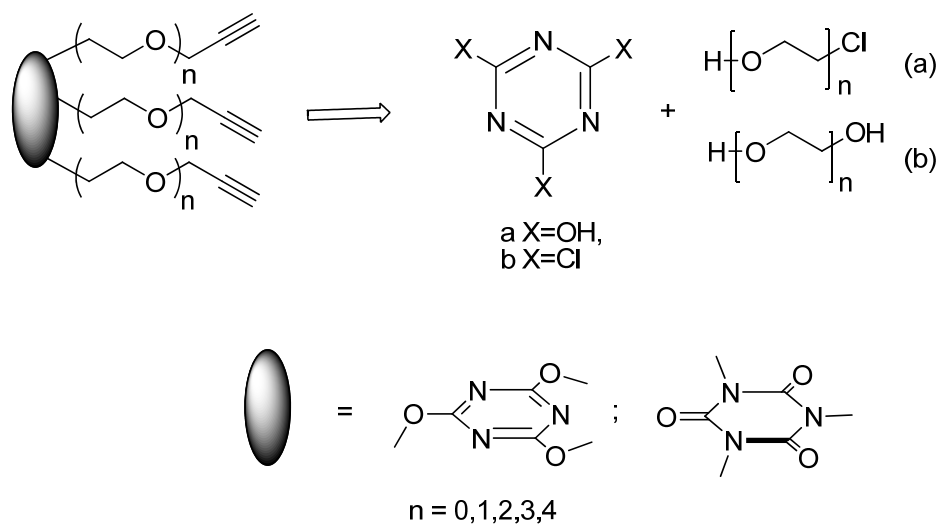


Fig.7. Target molecules

Several synthetic routes were considered in order to obtain the targeted tripodands. Heteroaromatic 1,3,5-triazine-2,4,6-trisubstituted podands were prepared starting from the commercially available cyanuril chloride and polyethyleneglycols while the access to 1,3,5-trisubstituted-2,4,6-trione derivatives was achieved from cyanuric acid and chloroethanols (Scheme 11).



Scheme 11. Retrosynthetic scheme envisaged for podand synthesis

These types of compounds raise special interest by reason of terminal alkyne units and also because of their high degree of pre-organization. Presence of terminal alkyne units opens

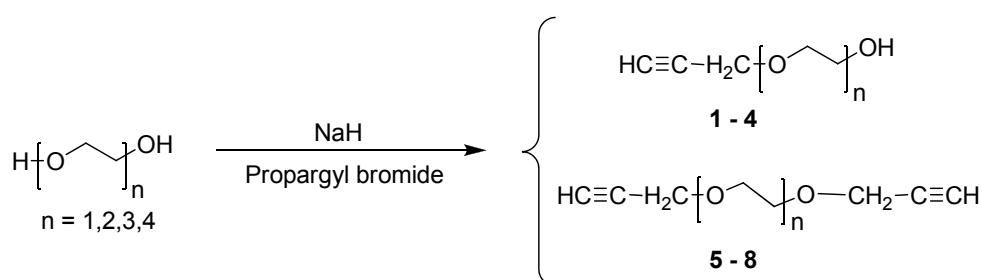
³² Blotny, G. *Tetrahedron* **2006**, 62, 9507-9522

opportunities for different reaction affording the synthesis of a large number of macrocyclic derivatives. Thus acetylenic coupling,³³ alkynes metathesis,³⁴ [2+2+2] cycloadditions³⁵ reactions, intensively studied and with good yields in classic organic chemistry, could be performed with this podands. Alkyne units can also be used for aromatic cycle formation using cyclotrimerization reactions as well as other cycloadditions, conducting in this way to the formation of some pyridine³⁶ or thiophene derivatives.³⁷

The attachment of functional groups (X = Br, Fig. 7) to the terminal triple bonds increases the possible synthetic approaches and invest these compounds as important precursors for host molecules (cage molecules, cryptands, cyclophanes), hyperbranched macromolecules and dendrimers with C₃ symmetry.

1.2.1. Synthesis of the podands precursors

Alcohol precursors with terminal alkyne units have been synthesized using a procedure described in the literature³⁸ for one of the terms of the series. We used as starting compounds several polyethylene glycols to which alkynes units were attached. Terminal alkynes were introduced by a nucleophilic substitution reaction based on the high reactivity of propargylbromide. Thus using a high excess of polyethyleneglycols, compounds **1 – 4** were obtained in moderate yields $\eta = 21\text{-}27\%$ (Scheme 12). The di-substitution products of polyethyleneglycols **5 - 8** were also separated and fully characterized as side products of the main reaction.



Scheme 12. Synthesis of mono- and di- substituted polyethylene glycols

³³ a) Siemsen, P.; Livingston, C.P.; Diederich, F. *Angew. Chem. Int. Ed.*, **2000**, *39*, 2632-2657; b) Rubin, Y.; Parker, T.C.; Khan, S.I.; Holliman, C.L.; McElvany, S.W. *J. Am. Chem. Soc.*, **1996**, *118*, 5308-5309; c) Heuft, M. A.; Collins, S. K.; Yap, G. P. A.; Fallis, A. G. *Org. Lett.*, **2001**, *3*, 2883-2886

³⁴ Granier, T.; Cardenas, D.J. si Echavarren, A.M. *Tetrahedron Lett.*, **2000**, *41*, 6775

³⁵ Shibata, T.; Yamashita, K.; Takagi, K.; Otha, T. Si Soai, K. *Tetrahedron Lett.*, **2000**, *56*, 9259-9267; b) Crvalho, M.F.; Almeida, F.; Galvao, A.; Pombeiro, A. *Journal of Organometallic Chemistry*, **2003**, *679*, 143; c) Galan, B.R.; Rovis, T. *Angew. Chem. Int. Ed.* **2009**, *48*, 2-8

³⁶ Varela, J. A.; Saa, C.; *Chem. Rev.* **2003**, *103*, 3787-3801

³⁷ Kromer, J.; Bauerle, P.; *Tetrahedron* **2001**, *57*, 3785-3794

³⁸ a) Black, D. K.; Landor, S. R.; Patel, A. N. and Whiter, P. F. *J. Chem. Soc. (C)* **1967**, 2260-2262; b) Auricchio, S.; Bruckner, S.; Malpezzi, L.; Vajna de Pava, O. *J. Chem. Research (M)* **1983**, 1201-1209

Proton NMR spectra of compound **2** ($n = 2$) is in agreement with the proposed structure displaying a triplet signal for alkyne proton, a doublet signal for protons in propargylic position, a multiplet for ethylene protons and a broadened signal for hydroxyl groups (Fig. 8).

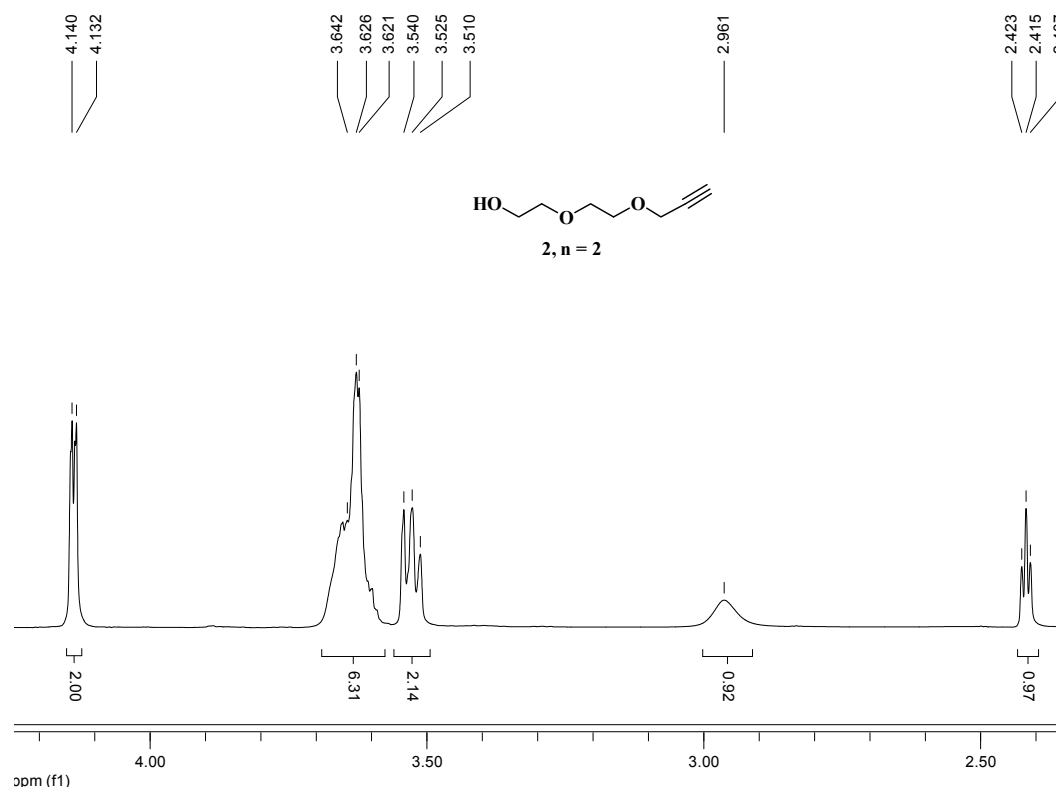
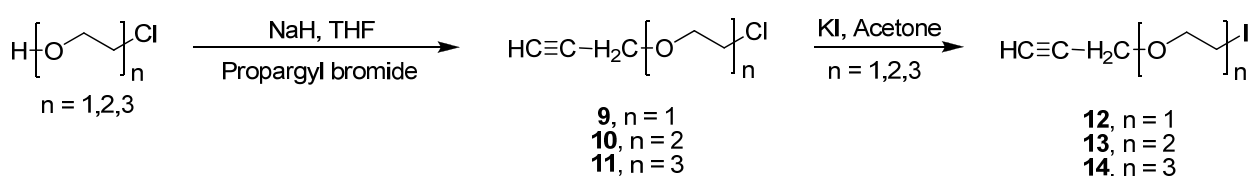


Fig. 8. Fragment of ^1H -RMN spectra of 2-(prop-2-ynyloxy)ethanol (**2**, $n = 2$) (CDCl_3 , 300 MHz)

Chloro-alkyne derivatives **9** - **11** were synthesized starting from the corresponding chloroethanols and propargylbromide in a reaction with sodium hydride in THF.³⁹ Next a halogen exchange reaction was performed with the synthesis of iodo-alkynes **12** - **14** (Scheme 13). We have chosen a halogen exchange reaction in order to improve the reactivity of the compounds toward the nucleophilic substitution reactions.



Scheme 13. Synthesis of halo-alkynes **9** - **14**

³⁹ a) Scobie, M.; Mahon, M. F. and Threadgill, M. D. *J. Chem. Soc. Perkin Trans 1* **1994**, 203-210; b) Scobie, M. and Threadgill, M.D. *J. Org. Chem.* **1994**, 59, 7008-7013

1.2.2. Synthesis and analysis of podands with aromatic 1,3,5-triazine units

Trialkoxycyanurates have long been known⁴⁰ their synthesis involving the reaction of silver cyanurates with alkyl halides, trimerization of imidates and, mostly used, the nucleophilic substitution of the chloride atoms from cyanuric chloride with alkoxides.

Given the availability of cyanuric chloride, our attempts to obtain compounds **15** - **19** (Scheme 14) were based on the nucleophilic substitution of the chlorine atoms from cyanuric chloride with alkoxides of the polyethylene chains with terminal triple bond.

Derivative **15** has been previously synthesized⁴¹ from cyanuric chloride and commercially available propargyl alcohol, in acetone using sodium hydroxide as base. Compound **15** was later used as intermediate for the construction of dendrimers.⁴² Our attempts to obtain **15** and the compounds of the series using this procedure gave poor yields. The other procedures reported for the synthesis of trialkoxycyanurates starting from cyanuric chloride with alcohols propose sodium hydride,⁴³ sodium hydroxide, DIPEA⁴⁴ or *t*Bu-OK⁴⁵ as bases and request a high excess of alcohol and thus were considered not appropriate for the obtainment of compounds **15-19**.

The synthesis of trialkoxycyanurates starting from cyanuric chloride with alcohols using BuLi as a base was recently reported.⁴⁶ For this procedure no excess of alcohol was required. We considered of interest this alternative procedure and using an adapted procedure for our target compounds **15-19** were obtained, in THF, without excess of alcohol (ratio cyanuric chloride / alcohol = 1 / 3).

⁴⁰ a) Dudley, J.R., Thurston, J.T., Schaeffer, F.C., Holm-Hansen, D., Hull C.J., Adams, P. *J. Am. Chem. Soc.* **1951**, *73*, 2986-2990; b) Schaeffer, F.C., Thurston, J.T., Dudley, J.R. *J. Am. Chem. Soc.* **1951**, *73*, 2990-2992

⁴¹ a) Danilov, S.N.; Yastrebova, L.N.; Galka, A.L.; Sanina, A.S. *Zh. Org. Khim.* **1979**, *70*, 3726-3728; b) Azev, Y.A.; Duclks, T.; Gabel, D. *Tetrahedron Letters* **2004**, *44*, 8689-8691

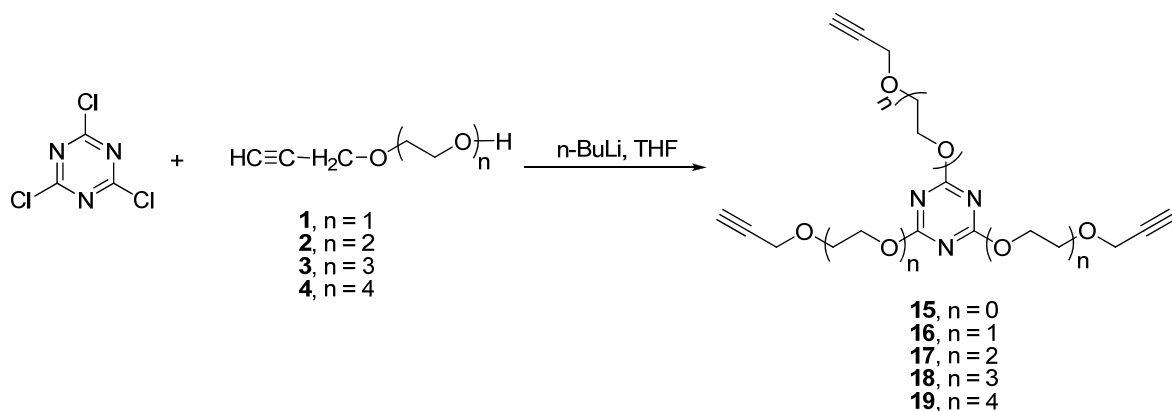
⁴² Wu, P., Feldman, A.K., Nugent, A.K., Hawker, C.J., Scheel, A., Voit, B., Pyun, J., Frechet, J.M.J., Sharpless, B., Fokin, V.V. *Angew. Chem. Int. Ed.* **2004**, *43*, 3928-3932.

⁴³ a) Spielman, M.A., Close, W.J., Wilk, I.J. *J. Am. Chem. Soc.* **1951**, *73*, 1775-1777; b) Horrom, B.W. *J. Am. Chem. Soc.* **1954**, *76*, 3032-3033; c) Kogan, T.P., Dupre, B., Bui, H., McAbee, K.L., Kassir, J.M., Scott, I.L., Hu, X., Vanderslice, P., Beck, P.J., Dixon, R.A.F. *J. Med. Chem.* **1998**, *41*, 1099-1111.

⁴⁴ Perez-Balderas, F., Ortega-Munoz, M., Morales-Sanfrutos, J., Hernandez-Mateo, F., Calvo-Flores, F.G., Calvo-Asin, J.A., Isac-Garcia, J., Santoyo-Gonzalez, F. *Org. Lett.* **2003**, *5*, 1951-1954.

⁴⁵ Fornasier, R., Montanari, F. *Tetrahedron Lett.* **1976**, *17*, 1381-1384

⁴⁶ Afonso, C.A.M.; Lourenco, N.M.T.; de Rosatella, A.A. *Molecules* **2006**, *11*, 81-102



Scheme 14. Synthesis of podands with 1,3,5-triazine units

The proposed route using *n*-BuLi as base and the corresponding alkyne derivatives gave considerably increased yields (55 – 65 %) starting with the most reactive propargyl alcohol and finishing with the less reactive longer chain alcohol **4** (Table 2).

Table 2. Yields of 2,4,6-trisubstituted-1,3,5-triazine podands

Compound	Yield
<p>15</p>	65
<p>16</p>	63
<p>17</p>	63
<p>18</p>	57
<p>19</p>	55

Structure determination of cyanurate podands is based on NMR spectroscopy and ESI-MS spectrometry analyses. ^1H -RMN spectra of compound **17** ($n = 2$) displays multiplet signal for the protons close to the aromatic ring at 4.50 ppm, a doublet signal for the propargylic protons at 4.15 ppm and a triplet signal for the alkyne protons at 2.40 ppm (Fig. 9).

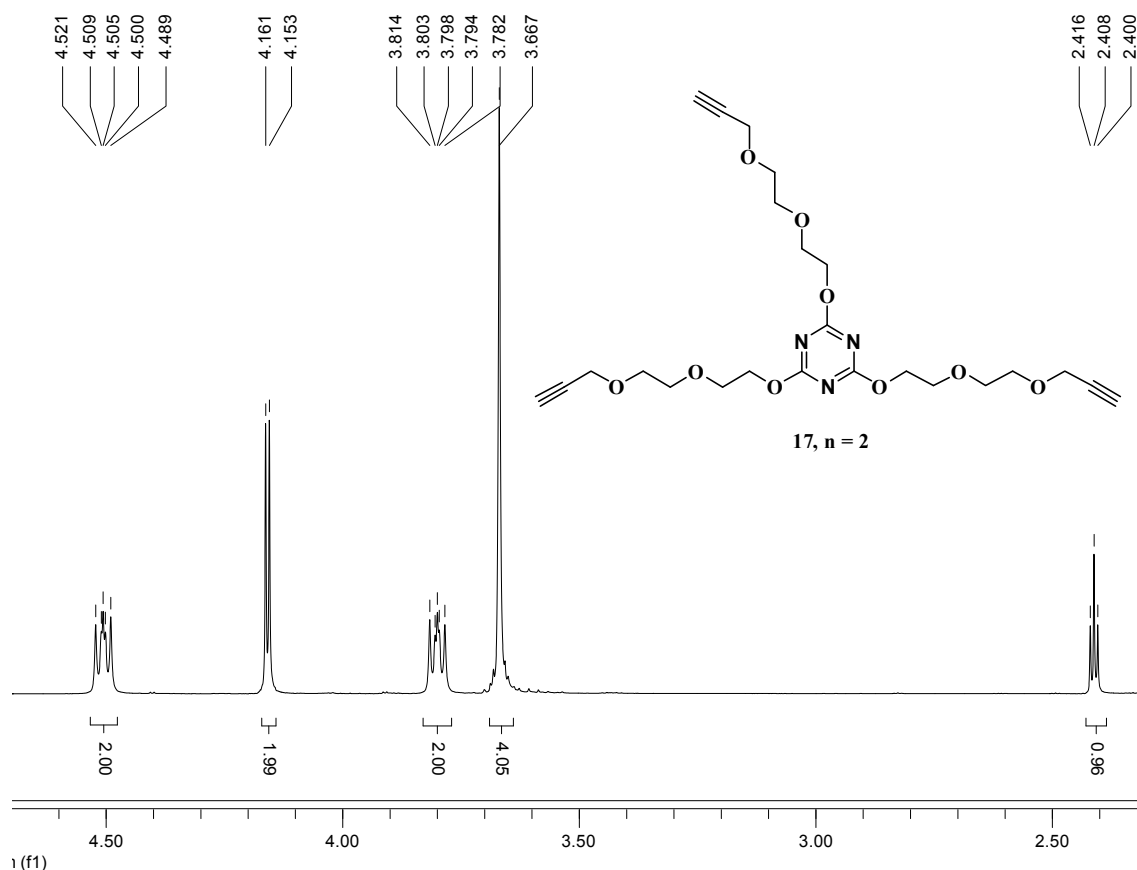


Fig. 9. Fragment of ^1H -RMN spectra of compound **17** ($n = 2$) (CDCl_3 , 300 MHz)

The carbon spectrum of the same compound shows eight signals corresponding to the eight types of carbon atoms of the molecule. The most shifted signal corresponds to carbon atoms of the 1,3,5-triazine ring at 172.8 ppm, and the most shielded is for the carbon atoms in propargylic position at 58.3 ppm (Fig. 10).

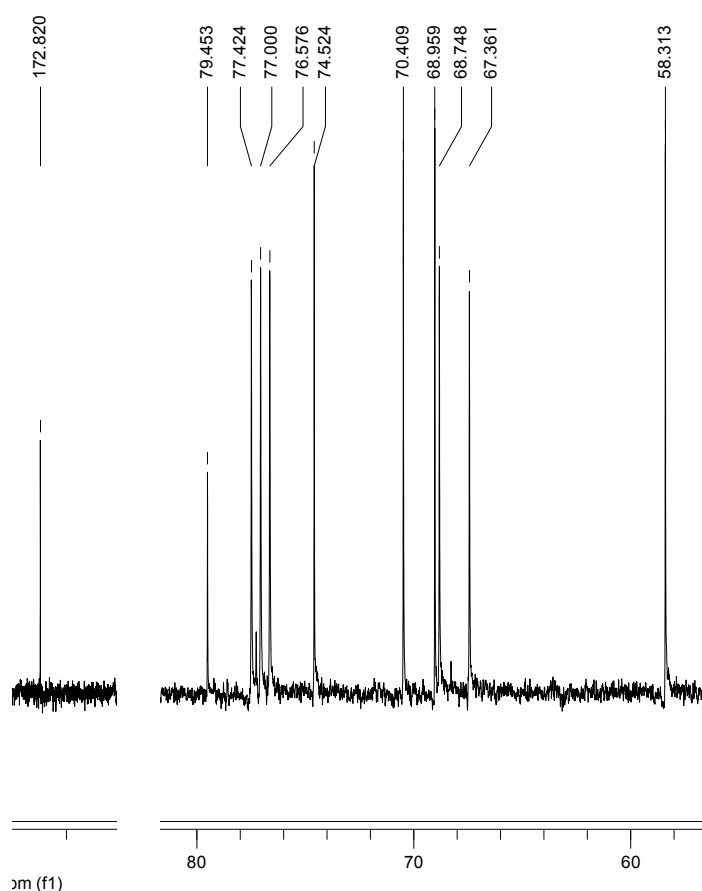
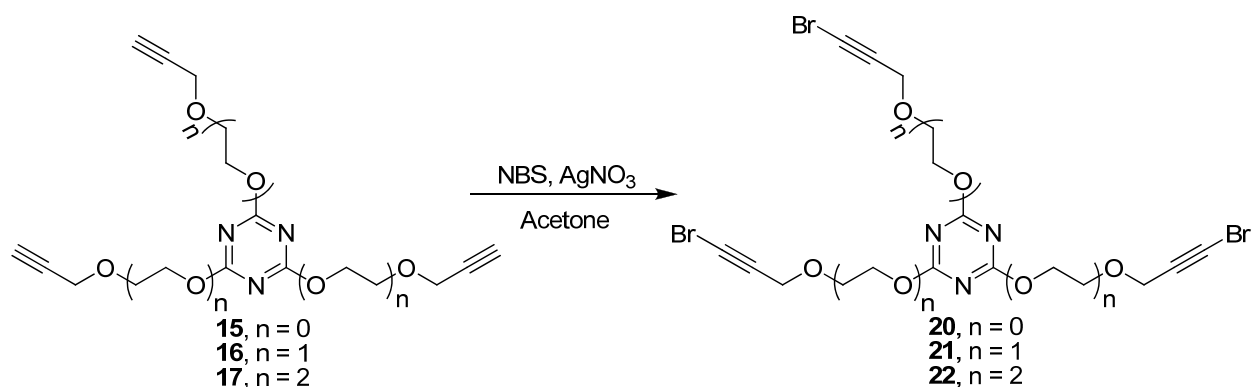


Fig. 10. Fragment of ^{13}C -RMN spectra of podand **17** ($n = 2$) (CDCl_3 , 75 MHz)

In order to extend the synthetic possible applications of these podands, from homocoupling to heterocoupling reactions, we have synthesized the corresponding tris-bromo-derivatives. The bromination reaction of terminal triple bonds was performed using N-bromo-succinimide (NBS) and AgNO_3 in acetone, at room temperature⁴⁷ (Scheme 15). C_3 - symmetry bromine functionalized podands **20** - **22** were obtained in moderate yields, analyzed and characterized by NMR spectroscopy and mass spectrometry.

⁴⁷ Bandyopadhyay, A.; Varghese, B.; Sankararaman, S. *J. Org. Chem.* **2006**, *71*, 4544-4548



Scheme 15. Synthesis of bromo-derivatives 20 - 22

These compounds represent interesting tools raising the number of their possible utilities to obtain podands with increased size of pendant branches or for the unsymmetrical synthesis of the three-dimensional macrobicycles by heterocoupling reactions.

1.2.3. Synthesis and analysis of podands with isocyanurate units

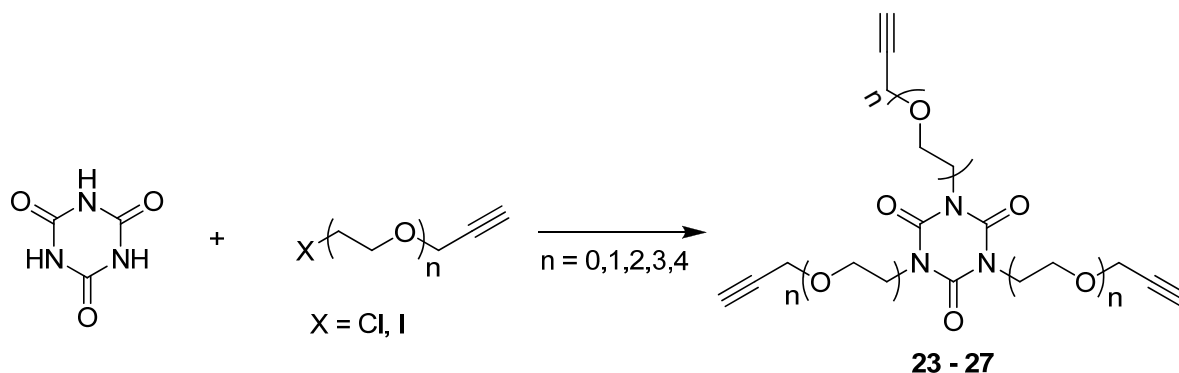
In the series of isocyanuric acid derivatives, the literature shows that they can be formed by trimerization of the corresponding isocyanates,⁴⁸ by substitution under harsh conditions of cyanuric acid,⁴⁹ or by rearrangement from the corresponding cyanurates.

Several synthetic routes were investigated for the synthesis of the targeted podands with isocyanurate unit. These routes propose the use of commercially available cyanuric acid, 1,3,5-tris(2-hydroxyethyl)cyanuric acid or the cyanurate podands (**15** - **19**) previously described.

The first attempts to obtain the isocyanurated derivatives (Scheme 16) were carried out using the reaction of cyanuric acid with halogenated (poly)ethyleneoxy-alkynes **9** - **14**.

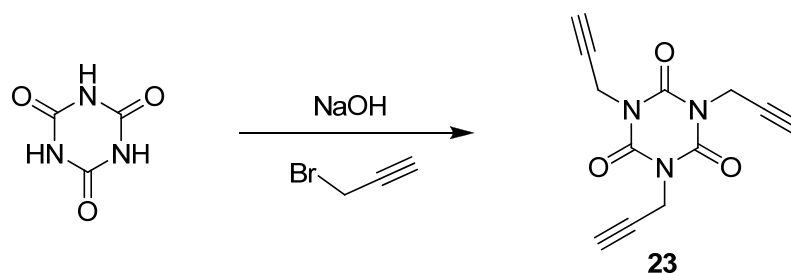
⁴⁸ a) Bortnick, N.; Luskin, L.S.; Hunvitz, M.D.; Rytina, A.W. *J. Am. Chem. Soc.* **1956**, 78(17), 4358-4361; Kaiser, D.W.; Greenwich, O. *Us Pat* 2,536,849, 2 Jan. **1951**; b) Etienne, A.; Bonte, B.; Druet, B., *Bull. SOC. Chim. Fr.*, **1972**, 251-257

⁴⁹ Smolin, E.M.; Rapoport, L., *The Chemistry of Heterocyclic Compounds*, vol. 13, A. Weissberger, ed., Interscience Publishers, a division of John Wiley & Sons, Inc., New York, **1967**, 17-146



Scheme 16. Synthesis of 1,3,5-triazine-2,4,6-trione derivatives

The proposed procedure was employed for the already described compound **23** ($n = 0$).⁵⁰ Thus 1,3,5-tris(propargyl)triazinan-2,4,6-trione was synthesized from cyanuric acid with propargylbromide in the presence of sodium hydroxide (Scheme 17).

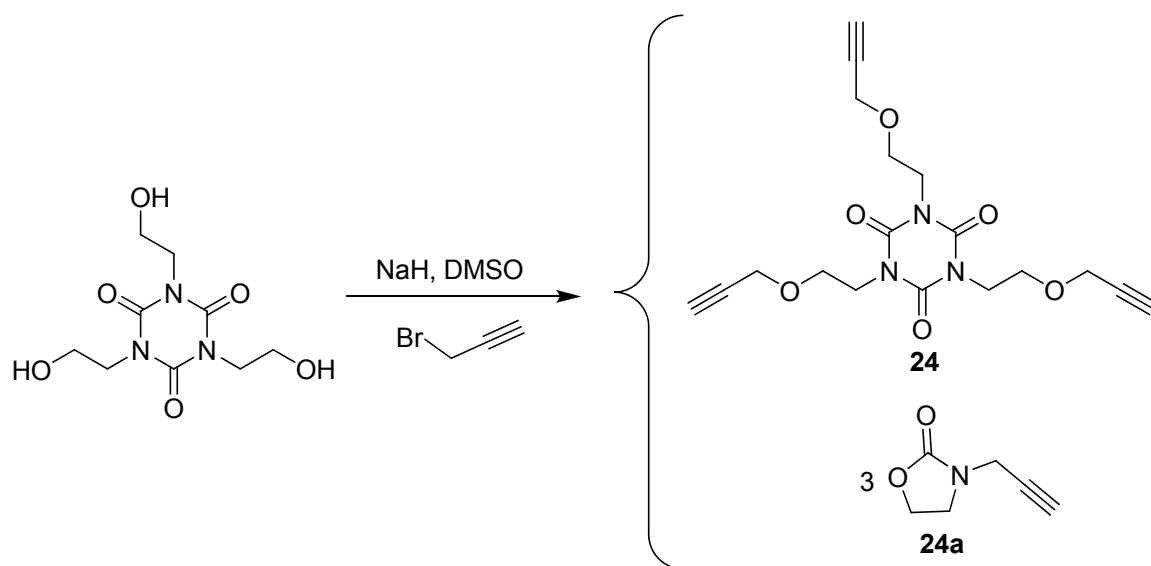


Scheme 17. Synthesis of 1,3,5-tris(prop-2-ynyl)-[1,3,5]-triazinan-2,4,6-trione **23**

Attempts to use the same synthetic strategy for the larger terms of the series failed, probably due to the low reactivity of the halogenated alkynes compared to propargyl bromide.

Another procedure, involving the nucleophilic substitution using propargyl bromide or iodo derivatives **12 - 14** and the commercially available 1,3,5-tris(2-hydroxyethyl)cyanuric acid was taken into consideration. The reaction with highly reactive propargyl bromide in the presence of sodium hydride afforded the isocyanurate **24**, together with 2-oxazolidone **24a** (Scheme 18).

⁵⁰ a) Grigoryan, S. G.; Avetisyan, K. G.; Arzumanyan, A. M.; Mardoyan, M. K.; Matnishyan, A.; Yerevan A. USSR. *Khimicheskaya Promyshlennost, Seriya: Reaktivy i Osobo Chistye Veshchestva* **1981**, 3, 34; b) Tugcu, N.; Park, S.K.; Moore, J.A., Cramer, S.M. *Ind. Eng. Chem. Res.* **2002**, 41, 6482-6492



Scheme 18. Synthesis of compounds **24** and **24a**

Cleavage of tris(2-hydroxyethyl)isocyanurate heterocycle is due to the attack of the formed sodium alkoxide to the carbonyl site with *in situ* formation of the unsubstituted 2-oxazolidone which further reacts with propargyl bromide to afford compound **24a**. Similar behavior has been previously observed for 2-hydroxyethyl isocyanurates on vacuum pyrolysis⁵¹ and on heating it in dimethylformamide solution at high temperatures.⁵²

During the reaction thin layer chromatography (TLC) revealed the presence of two products, the tris-functionalized derivative and the N-propargyl-1,3-oxazolidin-2-one. By controlling the reaction temperature we could obtain as major product either the isocyanurate derivative **24** or the 1,3-oxazolidin-2-one **24a** (Table 3). Thus at 35-40 °C we obtain as major product with 31% yields compound **24a** and running out the reaction at 20-25 °C compound **24** in 20% yield.

The two compounds were purified and isolated by column chromatography, analyzed and characterized by NMR spectroscopy and mass spectrometry. Proton spectra of the two compounds display similar patterns. Differences were found in the chemical shifts and are in accordance with the structure of the two species (Fig. 11).

⁵¹ Frazier, T. C., Little, E. D., Lloyd, B. E. *J. Org. Chem.* **1960**, *25*, 1944-1946

⁵² Cummins, R. W. *J. Org. Chem.* **1963**, *28*, 85-89

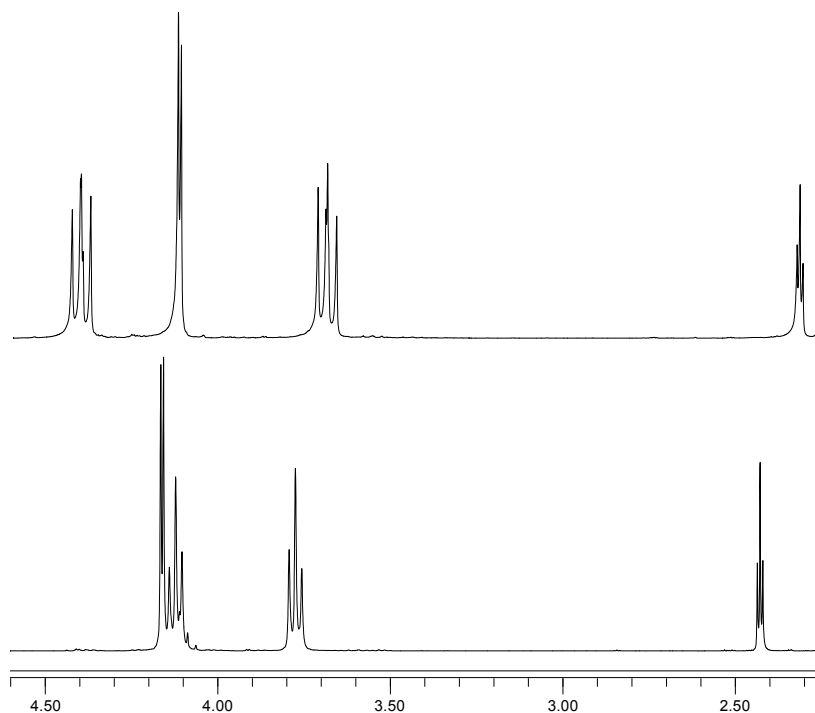


Fig. 11. ^1H -RMN spectra of 3-(prop-2-ynyl)oxazolidin-2-one **24a** (top) and 1,3,5-tris(2-(prop-2-yn-1-yloxy)ethyl)-1,3,5-triazinan-2,4,6-trione **24** (bottom)

Attempts to synthesize the other terms of the series using the same conditions and iodo-(poly)ethoxy-alkynes (**11** - **14**) instead of propargylbromide failed, probably due to their lower reactivity.

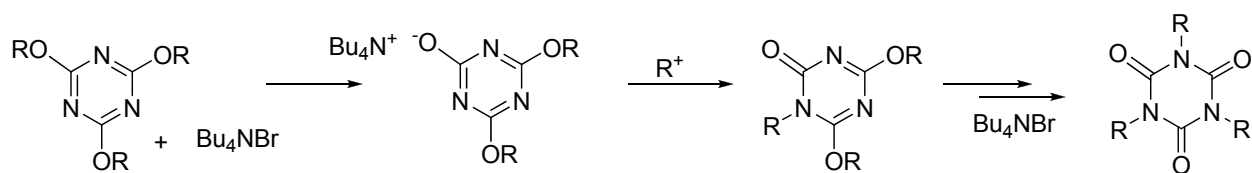
For the synthesis of the last terms of this series we followed a third strategy starting from cyanuric podands (1,3,5-triazine units) **17** and **18** via a cyanurate-isocyanurate isomerization reaction. This reaction is based on the alkyl group migration from oxygen to nitrogen by a cyanurate-isocyanurate rearrangement reaction.^{53,54} The rearrangement is catalyzed by tetrabutylammonium bromide or tetrabutylphosphonium bromide and the mechanism is presented in Scheme 19.

Even though there are reports that this is a thermal isomerisation that occurs at temperatures higher than 100 °C,⁵⁵ working with toluene or xylene under reflux conditions we obtained no isocyanurates.

⁵³ Harrington, P.J. and Sanchez, I.H. *Synthetic Communications*, **1993**, 23(9), 1307-1314

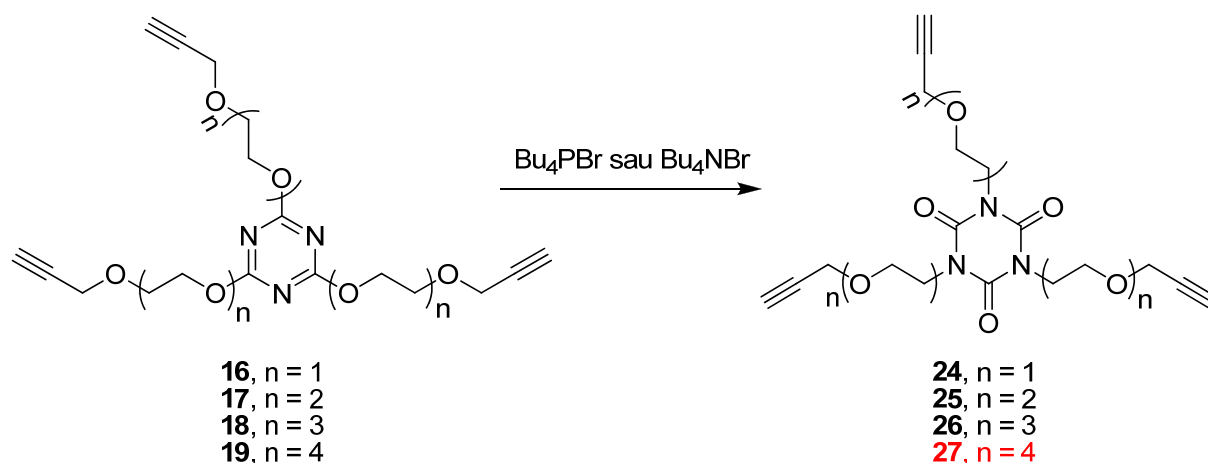
⁵⁴ Likhterov, V.R.; Klenovich, S.V.; Etlis, V.S.; Tsareva, L.A.; Pomerantseva, E.G., Shmuilovich, S.M. *Chem. Heterocycl. Compd. (Engl. Transl.)*, **1988**, 308-311

⁵⁵ Martynov, I. V., Kruglyak, Y. L., Gruzdeva, V. L., Dobryanskii, V. S., Kashnikova, I. I. *Pharmaceutical Chemistry Journal*, **1990**, 24, 885 - 889



Scheme 19. Cyanurate-isocyanurate isomerization mechanism

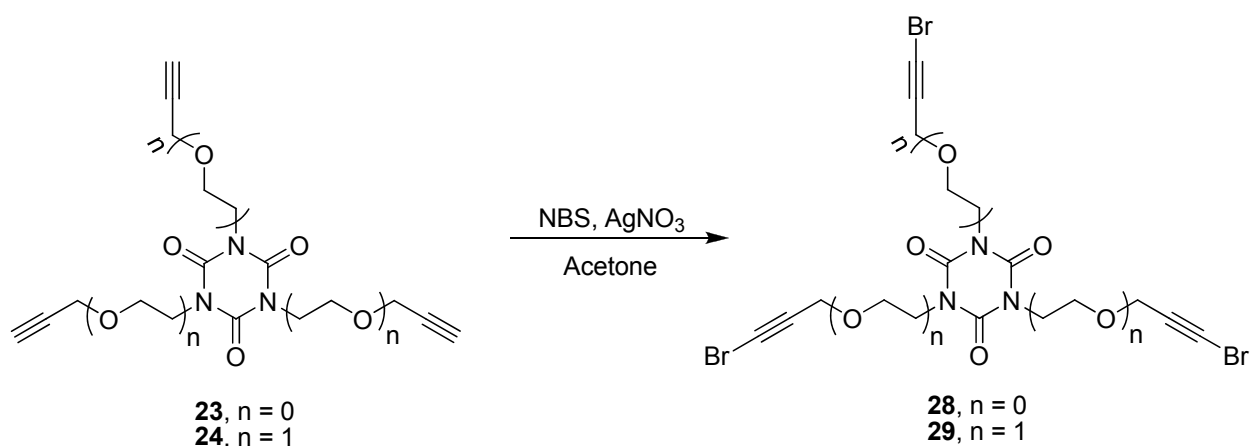
Thus we have synthesized with moderate yields compounds **24- 26** (Scheme 20), but in the case of compound **27** ($n = 4$) the reaction failed.



Scheme 20. Synthesis of isocyanuric derivatives

The structure of new isocyanurates **24 – 26** has been revealed by the NMR investigations which show different chemical shifts in comparison with the corresponding cyanurates - for the quaternary carbon of the main cycle C=O (148-149 ppm) compared with C-O (172-173 ppm), for the CH₂-N carbon atoms (41-42 ppm) and protons (4.1-4.15 ppm) as for CH₂-O the similar atoms are giving signals at 67-70 ppm and 4.51-4.55 ppm.

As for cyanurate podands presented above, bromination of terminal triple bonds of the isocyanurate derivatives was achieved with NBS and AgNO₃ in acetone at room temperature (Scheme 21), with the moderate yields obtaining of compounds **28** and **29**.

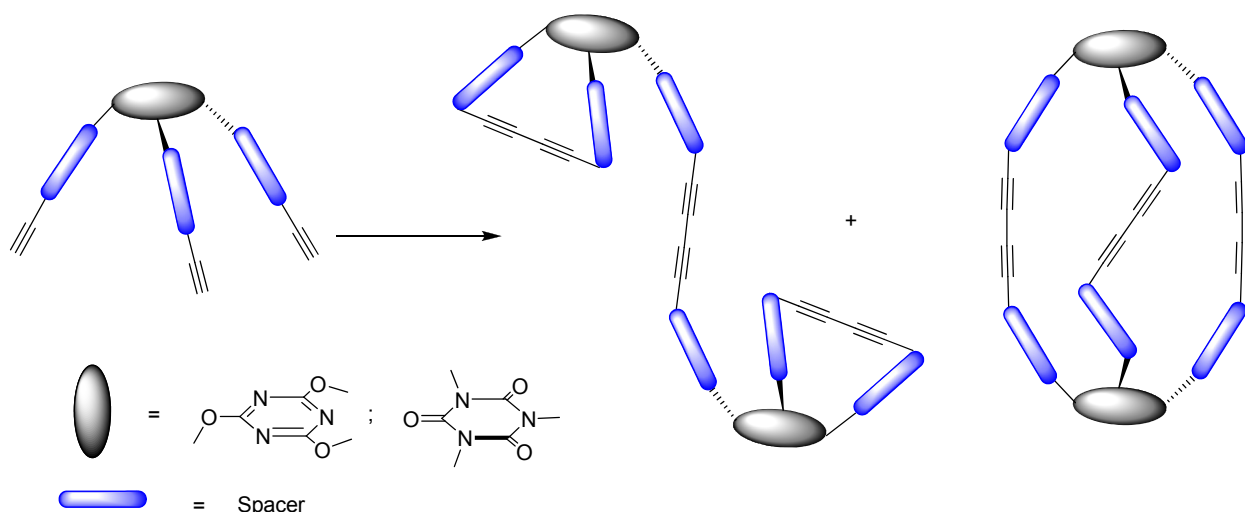


Scheme 21. Synthesis of isocyanurate bromo-derivatives

1.3. Macrocycles by Cu-catalyzed homoacetylenic coupling reactions

Encouraged by the results presented to date in the field of supramolecular chemistry using coupling procedures,⁵⁶ cyanuric and isocyanuric podands were used for the synthesis of new macrocyclic derivatives. Podands build up from 1,3,5-triazine ring as main core, with planar geometry, in direct junction with flexible ethyleneoxy side arms can embody three-dimensional cages with relatively rigid large cavity.

The purpose of this work consists in obtaining new functional molecular cages by three-fold oxidative coupling reactions. Oxidative acetylene coupling reactions in Hay's conditions⁵⁷ employed with these podands afforded two types of architectures depicted in Scheme 22.

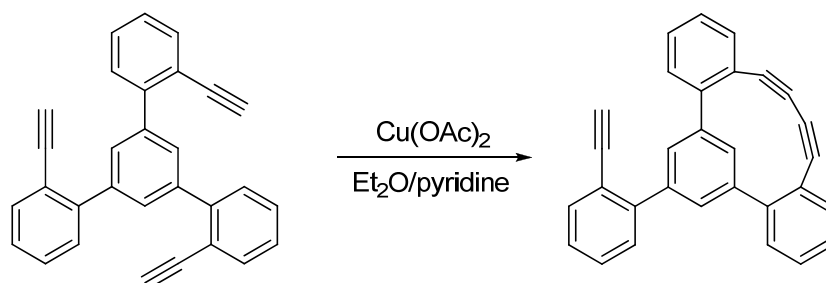


Scheme 22. Target molecules

⁵⁶ Piron, F.; Cismas, C.; Terec, A.; Roncali, J.; Grosu, I. *Mini-Reviews in Organic Chemistry* **2009**, *6*, 78-85

⁵⁷ Hamilton, D.G.; Prodi, L.; Feeder, N.; Sanders, J.K.M. *J. Chem. Soc., Perkin Trans 1*, **1999**, 1057-1065

Similar behavior of some triyne systems, which show substantial preference for intramolecular acetylenic coupling instead of intermolecular dimerization, was also noted by Fallis and coworkers.⁵⁸ They have obtained some excessively strained cyclophanes from joining either one or two of the terminal acetylenes by oxidative acetylenic coupling (Scheme 23).⁵⁹



Scheme 23. Intramolecular coupling

The flexibility of the side arms with terminal acetylene in case of our podands is determining the formation of two triply bridged members by joining all the acetylenes: a cryptand closed by three intermolecular couplings and a bis-macrocyclic formed by two intramolecular and one intermolecular oxidative couplings.

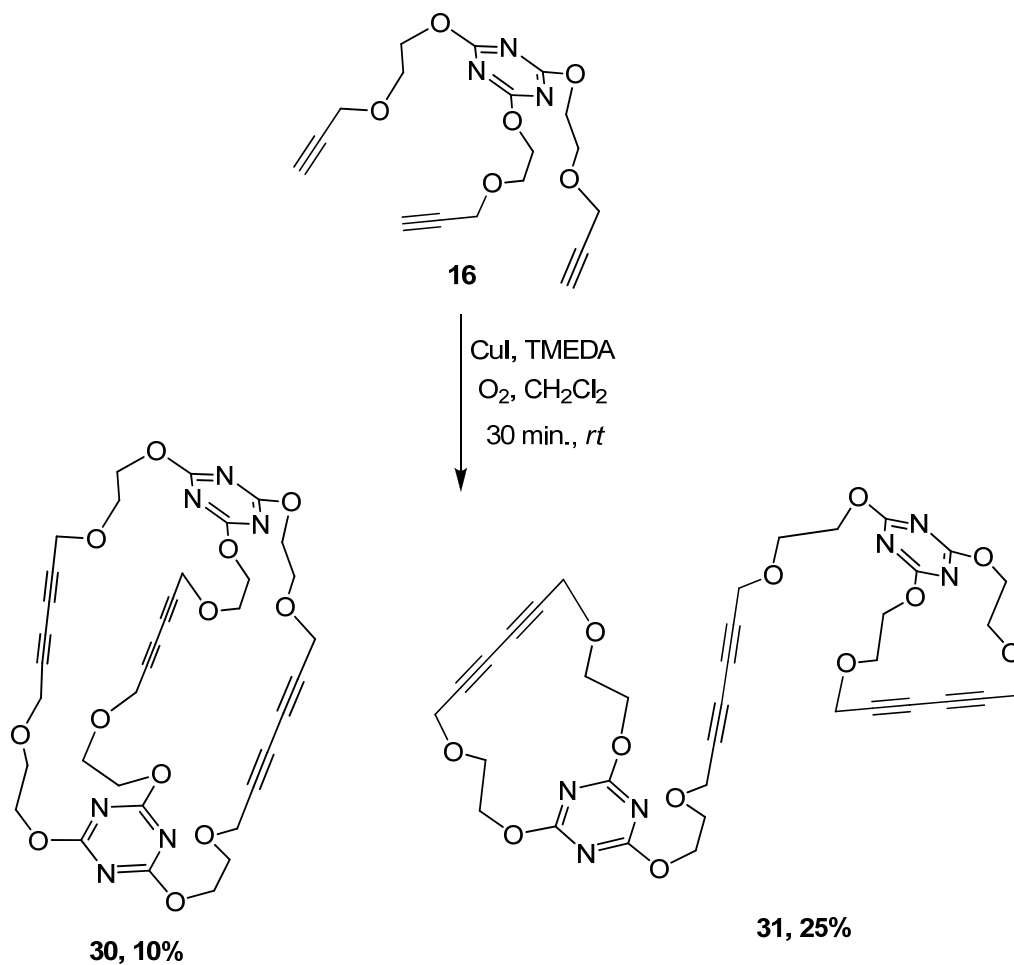
1.3.1. Synthesis and analysis of macrocycles with cyanurate units

Oxidative acetylenic coupling performed with podand **16** in dichloromethane, at room temperature using as catalyst Cu(I) salts and tetramethylethylenediamine (TMEDA) afforded a mixture of two homocoupled products (Scheme 24).

Both products cryptand **30** and bis-macrocyclic **31** were obtained in a 1 to 2.5 ratio with 10% and 25% yields, respectively and they could be separated by column chromatography using a mixture of toluene/acetone as eluent.

⁵⁸ Collins, S.K.; Yap, G.P.A.; Fallis, A.G. *Org. Lett.* **2002**, *4*, 11-14

⁵⁹ Fallis, A.G. *Synlett* **2004**, *13*, 2249-2267



Scheme 24. Synthesis of compounds **30** and **31**

In the mass spectrum of compound **31** we could identify signals corresponding to macrocycle molecular peak but also to the Na⁺ complex (Fig. 12). Mass analysis data revealed similar peaks for its isomer, cryptand **30**.

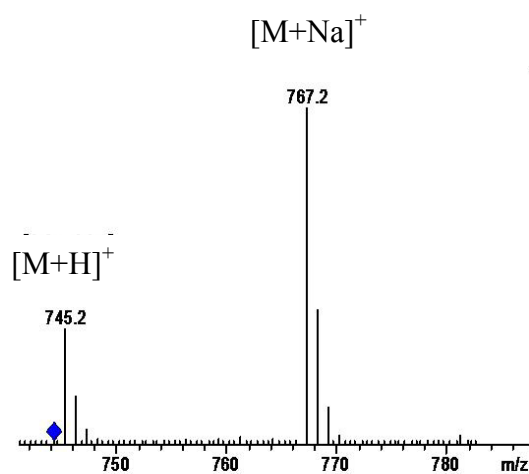


Figure 12. ESI-MS spectrum of compound **31** (n = 1)

^1H -NMR spectra of the two isolated compounds are different because of the magnetic nonequivalence of the protons belonging to the two types of branches. Thus the proton spectrum of cryptand **30** displays similar signals for the protons of the three connected branches, as expected for a symmetrical compound (Fig. 13).

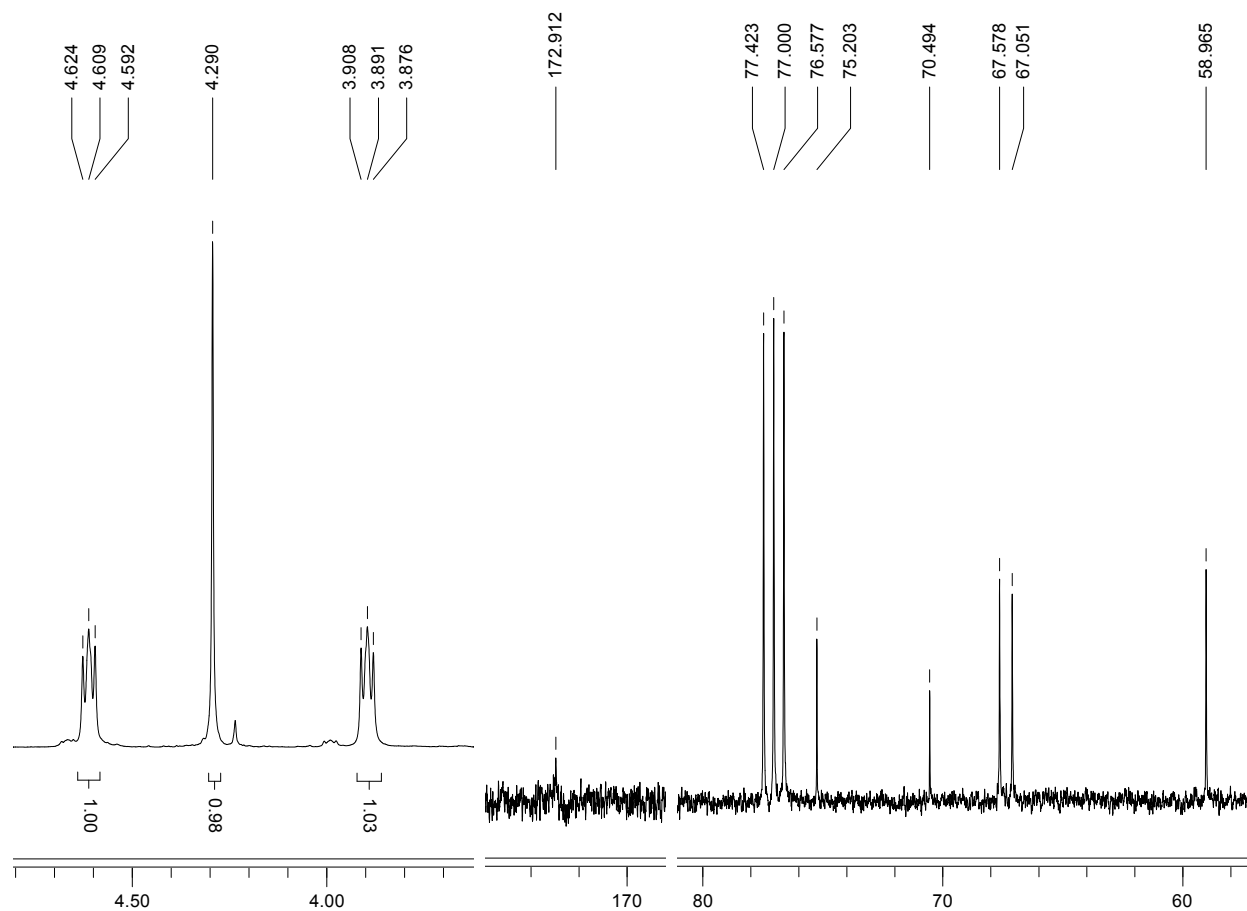


Fig. 13. ^1H -NMR and ^{13}C -NMR fragments spectra of compound **30** ($n = 1$) (CDCl_3 , 300 MHz and 75 MHz respectively)

^{13}C -NMR spectrum confirms the proposed structure displaying six types of signals corresponding to the six types of carbon atoms in the molecule, in agreement with a symmetrical structure (Fig. 14).

The proton spectrum of bis-macrocycle **31** ($n = 1$) displays two sets of signal for the protons corresponding to the two types of ethyleneoxy branches, with an integration rapport of 2/1. Due to the different connection of the side arms, twelve types of carbon atoms are presented in this molecule (Fig. 14) and the corresponding number of signals is recorded in the ^{13}C -NMR spectrum.

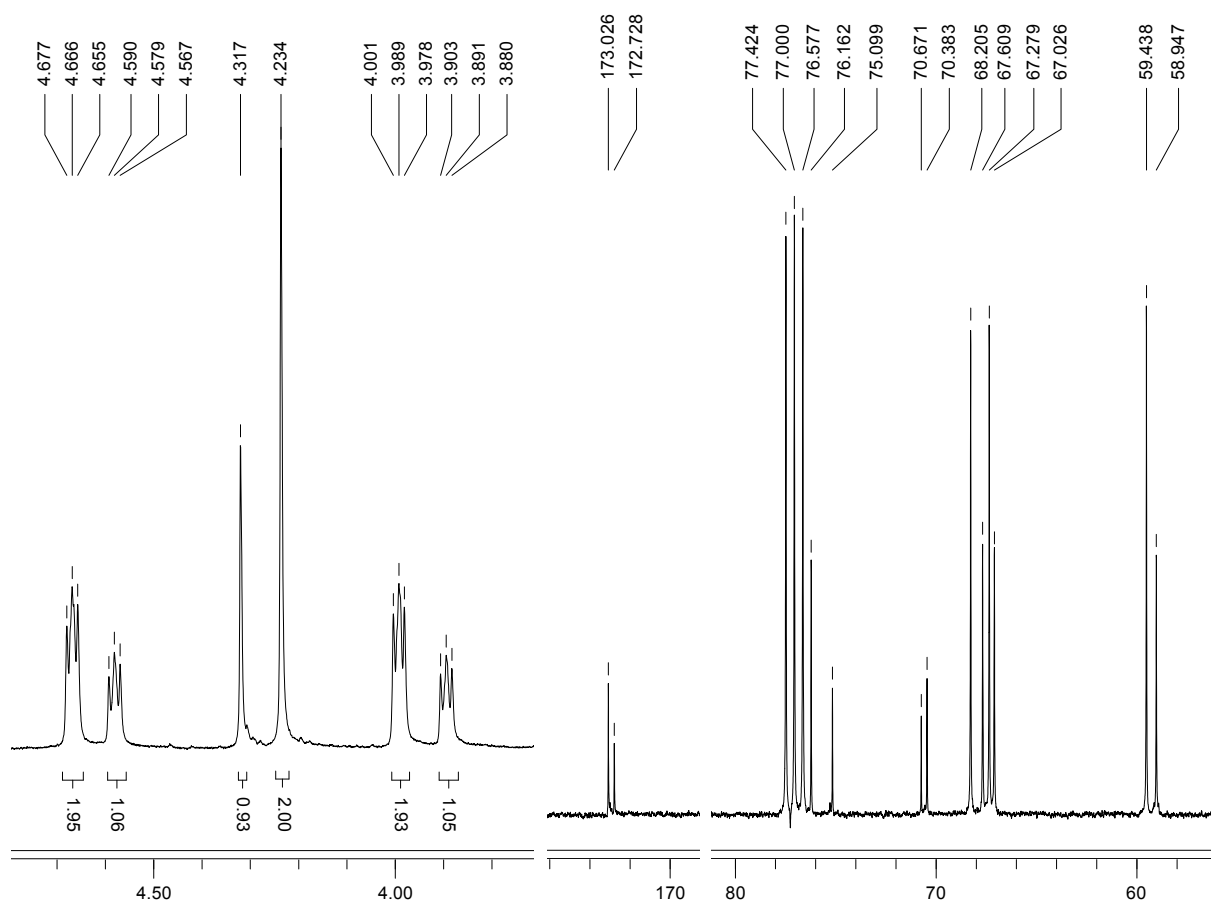
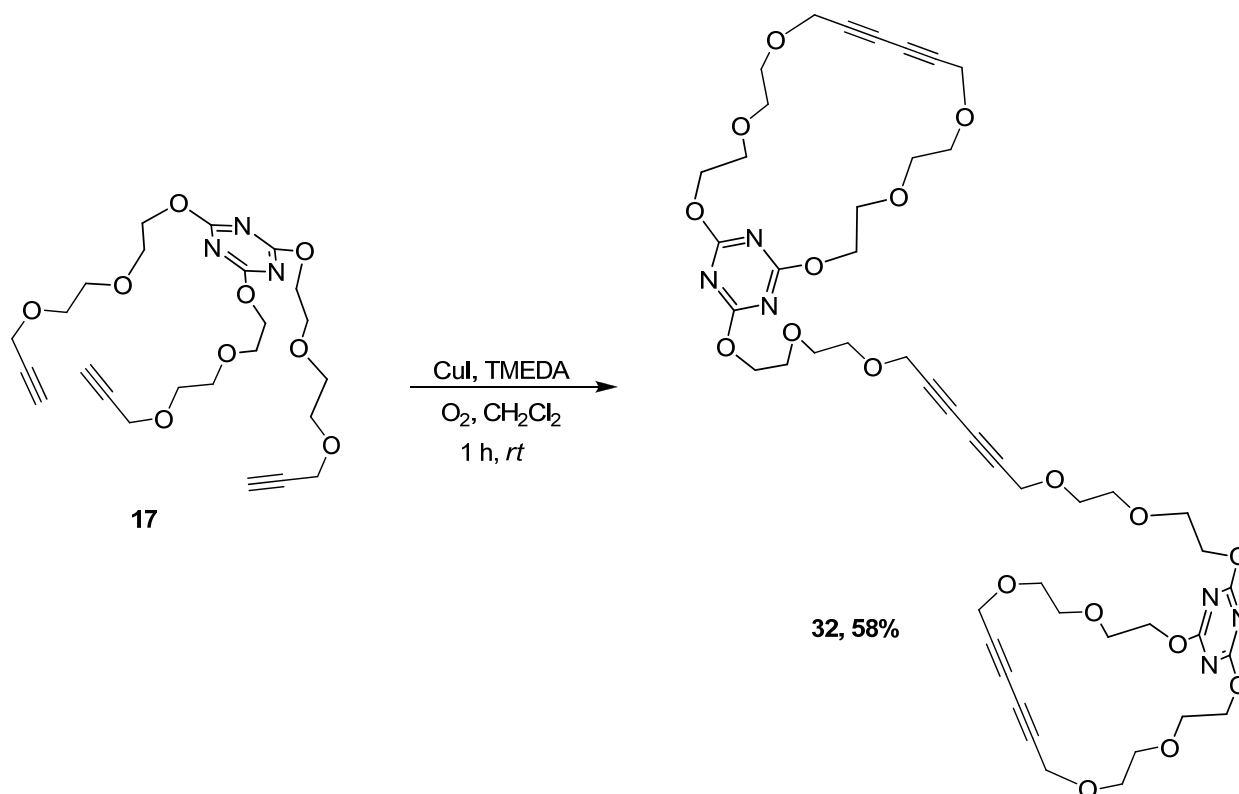


Figure 14. $^1\text{H-NMR}$ and $^{13}\text{C-NMR}$ fragments spectra of compound **31** ($n = 1$) (CDCl_3 , 300 MHz and 75 MHz respectively)

The same coupling conditions employed with podand **17** ($n = 2$) afforded as major product bis-macrocyclic **32** ($n = 2$) (Scheme 25). The lack of formation of the symmetrically closed cage derivative can be due to the increased flexibility of the side arms.



Scheme 25. Synthesis of bis-macrocycle **32** (n = 2)

Compound **32** (n = 2) was obtained after purification by column chromatography using a mixture of toluene/acetone as eluent, as a colorless oily liquid in 58% yield. ESI-MS spectrum of bis-macrocycle **32** (n = 2) exhibits $[M+H]^+$ and $[M+Na]^+$ peaks (Fig. 15).

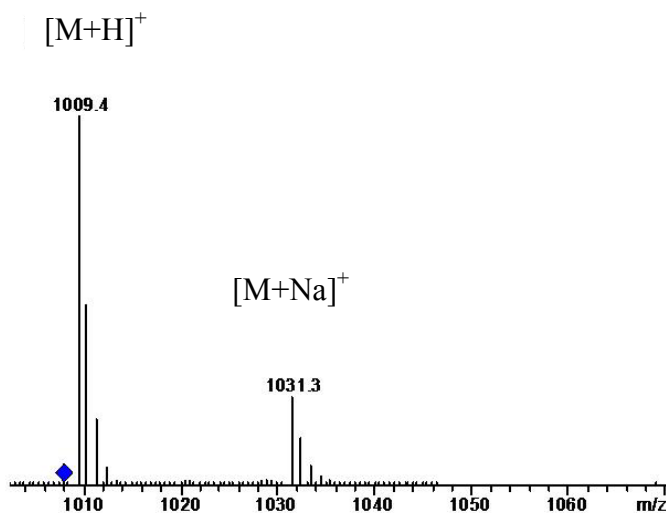


Fig. 15. ESI-MS spectrum of compounds **32** (n = 2)

The proton spectrum of bi-macrocycle **32** (n = 2) displays two sets of signal for the protons corresponding to the two types of branches with an integration ratio of 2/1 while the ¹³C-

NMR spectrum presents sixteen types of carbon atoms including the pairs corresponding to the two types of branches (Fig. 16).

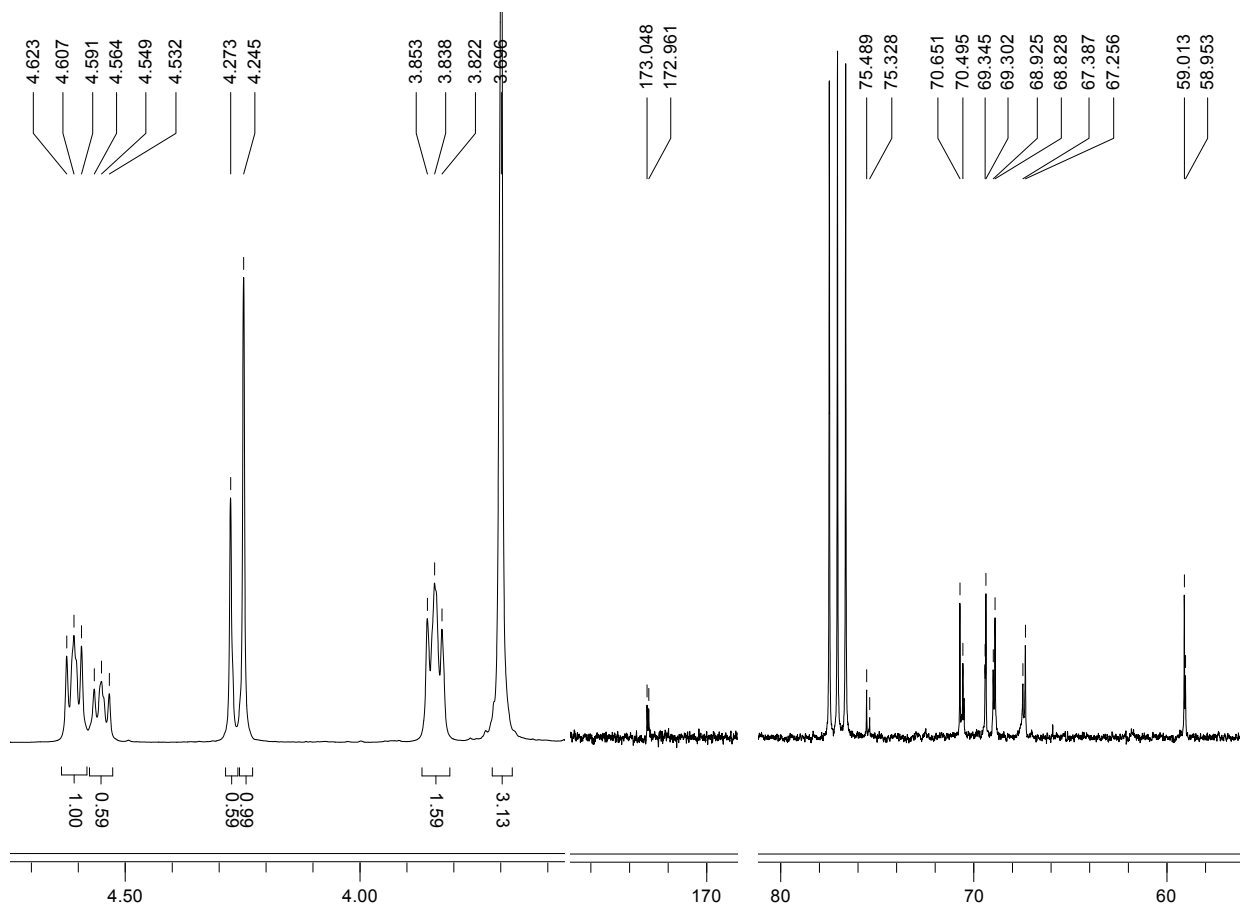
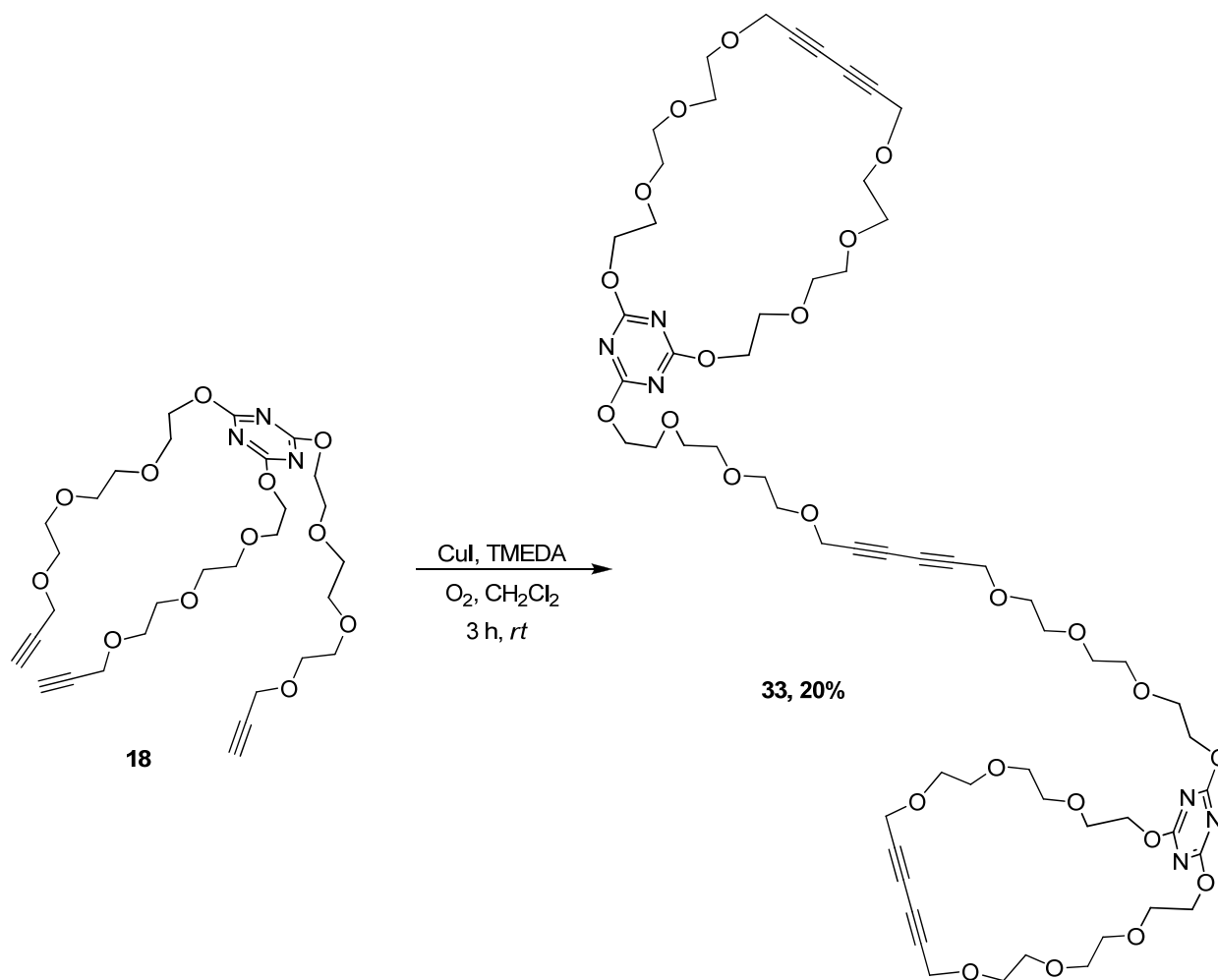


Fig. 16. ¹H-NMR and ¹³C-NMR fragments spectra of compound **32** (n = 2) (CDCl₃, 300 MHz and 75 MHz respectively)

Compound **18** (n = 3) reacts with the formation of bis-macrocyclic **33** (n = 3) as single product (Scheme 26). Proton and carbon spectra show similarities with compound **32** (n = 2) and display signals for each type of atom in the chains. ESI-MS spectrum shows signals for the molecular peak [M+H]⁺ at 1273.8 and for the complex with sodium cation [M+Na]⁺ at 1295.6.



Scheme 26. Synthesis of compound **33**

In order to test the reactivity of these podands in the coupling reaction we also employed Eglinton coupling conditions by performing the oxidative dimerization in dry-oxygen-free pyridine or in acetonitrile in the presence of copper (II) salts ($\text{Cu}(\text{OAc})_2$) (Table 3). For the synthesis of compound **32** ($n = 2$) we have tried similar procedures but we used the reflux of the solvent. The starting podand **18** was added dropwise during two hours, and then the mixture was heated to reflux for three hours. The yields were lower maybe due to polymerization of the starting compound at the higher temperatures. It is known for similar compounds that the presence of acetonitrile could improve the yields, due to a template effect. With $\text{Cu}(\text{II})$ in acetonitrile the yield of the reaction were significantly diminished in the case of compounds **30** and **31** ($n = 1$). Unfortunately when replacing acetonitrile with pyridine in the reaction catalyzed by copper(II) acetate, no traces of the desired compound **33** ($n = 3$) could be identified.

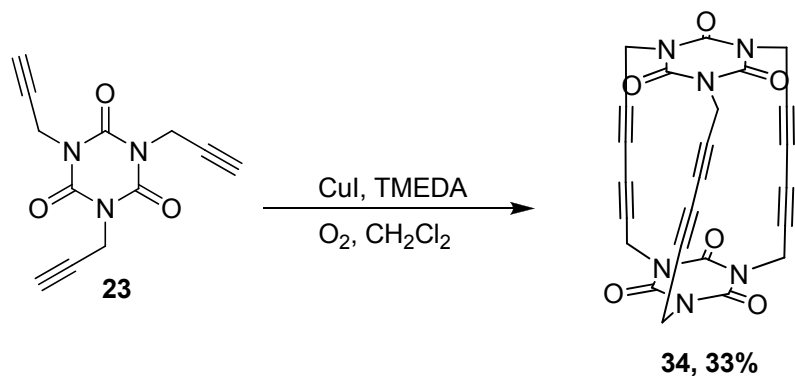
Table 3. Conditions for Cu-catalyzed coupling of cyanurate podands

Compd.	Reaction conditions	Yield (%)
30 , (n = 1)	CuCl, TMEDA in CH ₂ Cl ₂ , O ₂ , 30 min., <i>rt</i>	10%
	Cu(OAc) ₂ *H ₂ O in AcCN, 12h, air, 60 °C	3%
31 , (n = 1)	CuCl, TMEDA in CH ₂ Cl ₂ , O ₂ , 30 min., <i>rt</i>	25%
	Cu(OAc) ₂ *H ₂ O in AcCN, 12h, air, 60 °C	9%
32 , (n = 2)	CuI, TMEDA in CH ₂ Cl ₂ , O ₂ , 1h, <i>rt</i>	58%
	CuI, TMEDA in CHCl ₃ , O ₂ , 3h, reflux	25%
33 , (n = 3)	CuI, TMEDA in CH ₂ Cl ₂ , O ₂ , 3h, <i>rt</i>	20%
	Cu(OAc) ₂ *H ₂ O in pyridine, 12h, 60 °C	-

Reviewing all results obtained in the cyanurate derivatives series we can conclude that the synthesis of bis-macrocycle derivatives is determined by the length and flexibility of the branches, and thus the increased size of the podands creates favorable conditions for intramolecular coupling reactions instead of the intermolecular dimerization. Also it is hard to speak about the template effect of acetonitrile because the size of the formed cavities is expected to be higher than those already presented in the literature. It worth nothing that the oxidative acetylenic couplings performed with compound **15** (n = 0) were unsuccessful in both Hay (Cu(I) salts) and Eglinton (Cu(II) salts) conditions. The only available explanation found for its behavior could be the higher reactivity of the substrate compared with its superior analogues, affording insoluble polymers.

1.3.2. Synthesis and analysis of macrocycles with isocyanurate units

Similar coupling reactions were performed on the isocyanurate podands series, using Hay's or Eglinton coupling conditions. Acetylenic coupling carried out with compound **23** in Hay's conditions afforded as single product macrobicyclic cage molecule **34** (Scheme 27).



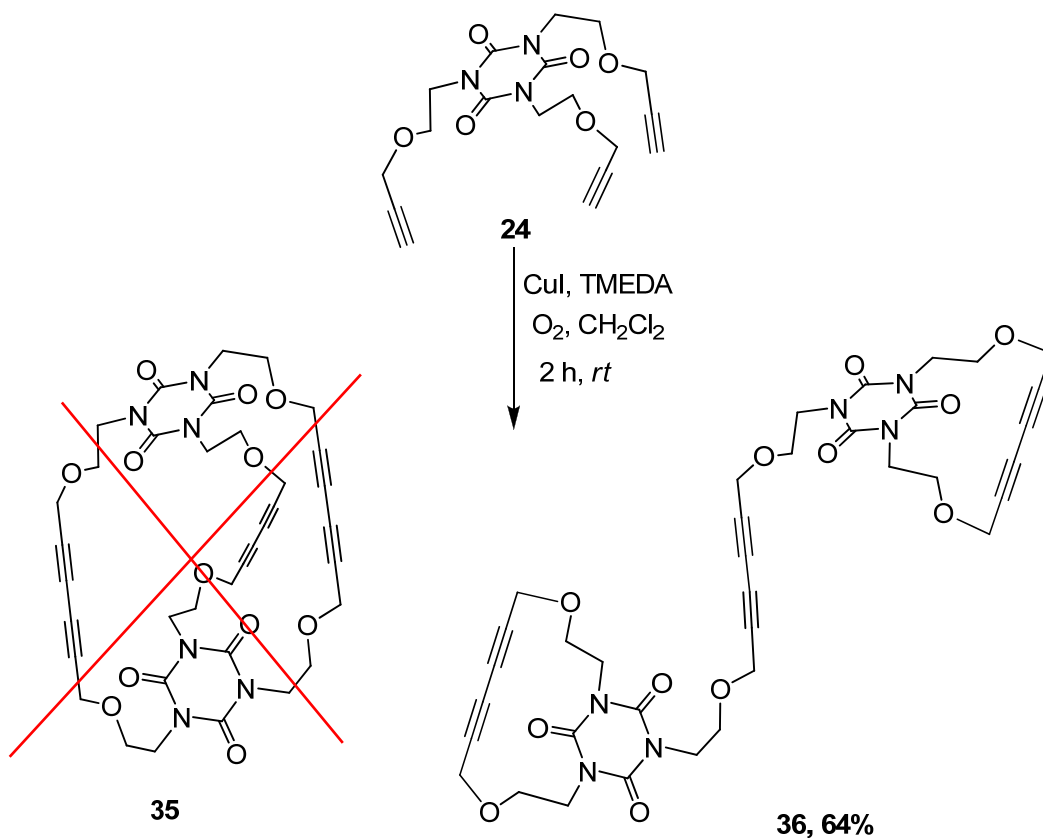
Scheme 27. Synthesis of cage molecule **34**

Proton and carbon NMR spectra of this compound show signals for each type of atom in the molecule: a singlet for the methylene protons and four signals for the carbon atoms. ESI-MS spectrum displays a peak at 481 corresponding to $[M+H]^+$. The yields of this reaction were significantly diminished when Cu(II) in pyridine was used (Table 4).

Table 4. Conditions for Cu-catalyzed coupling of isocyanurate podands

Compd.	Reaction conditions	Yield (%)
34 , (n = 0)	CuI, TMEDA in CH ₂ Cl ₂ , O ₂ , 2h, <i>rt</i>	33%
	Cu(OAc) ₂ *H ₂ O in pyridine, 12h, air, 60 °C	3%
36 , (n = 1)	CuI, TMEDA in CH ₂ Cl ₂ , O ₂ , 2h, <i>rt</i>	64%
	Cu(OAc) ₂ *H ₂ O in AcCN, 12h, air, 60 °C	27%

A similar behavior was observed in the case of compound **24** (n = 1) with lower yields when performing the reaction with Cu(II) in acetonitrile instead of Cu(I) and TMEDA (Table 5, Scheme 28). Surprisingly Hay's oxidative acetylenic conditions gave only bis-macrocyclic **36** (n = 1) in 64% yields with no evidence of its symmetric isomer, the cage dimer **35** (n = 1).



Scheme 28. Synthesis of compound **36** ($n = 1$)

¹H-NMR spectrum of compound **36** ($n = 1$) displays two sets of signals assigned for protons corresponding to the two types of branches (Fig. 17). Carbon and ESI-MS spectra are in accordance with the presumed structure. Mass spectrum shows a signal at 746.3 (in APCI) corresponding to the molecular peak and a signal at 768.4 (in ESI) for its complex with Na⁺.

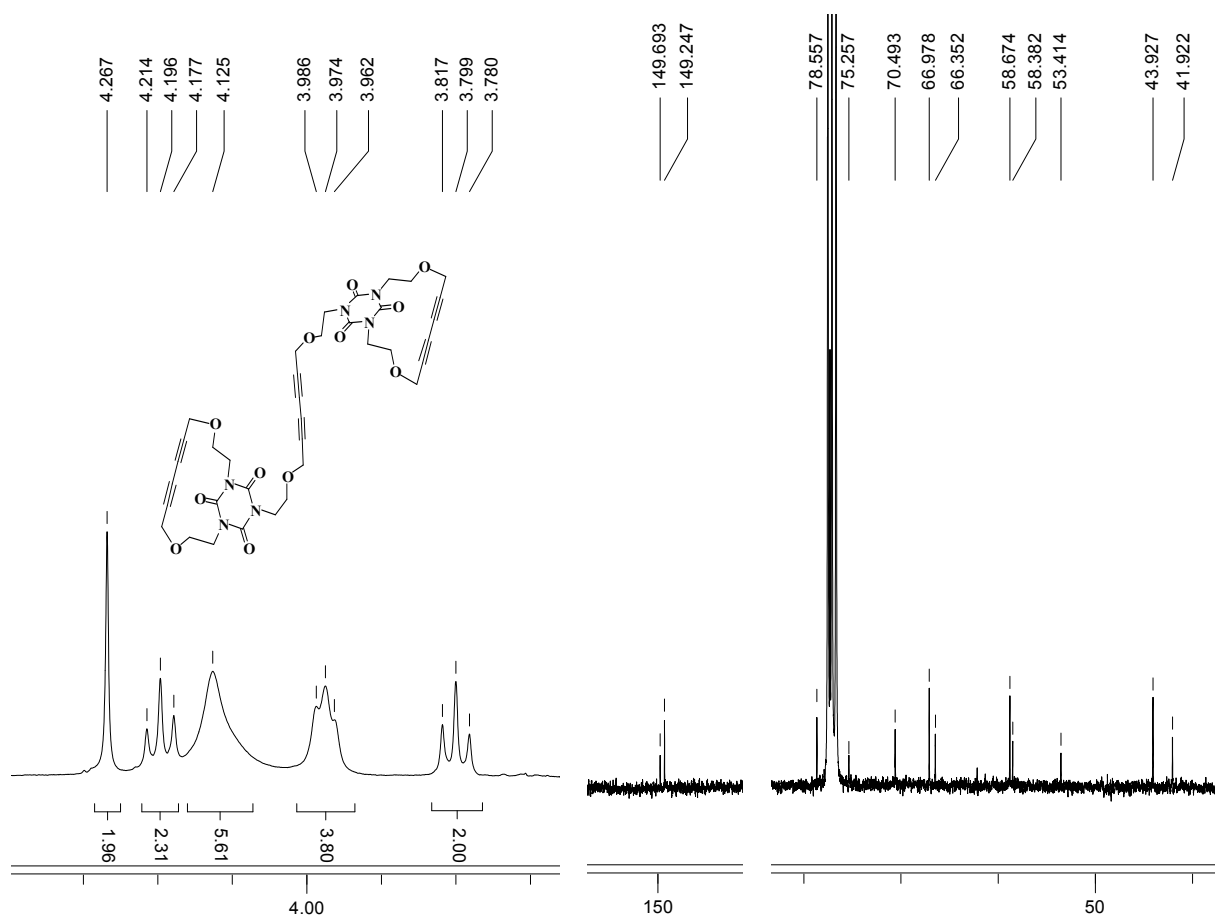


Fig. 17. ¹H-NMR and ¹³C-NMR fragments spectra of compound **36** (n = 1) (CDCl₃, 300 MHz and 75 MHz respectively)

Proton spectrum recorded in CDCl₃ at *rt* exhibits coalescence for the signals belonging to protons of the macrocycle branches. Variable temperature NMR spectra recorded in CDCl₃ show modification of the shape of the signals when the temperature is raised up to 323 K (Fig. 18).

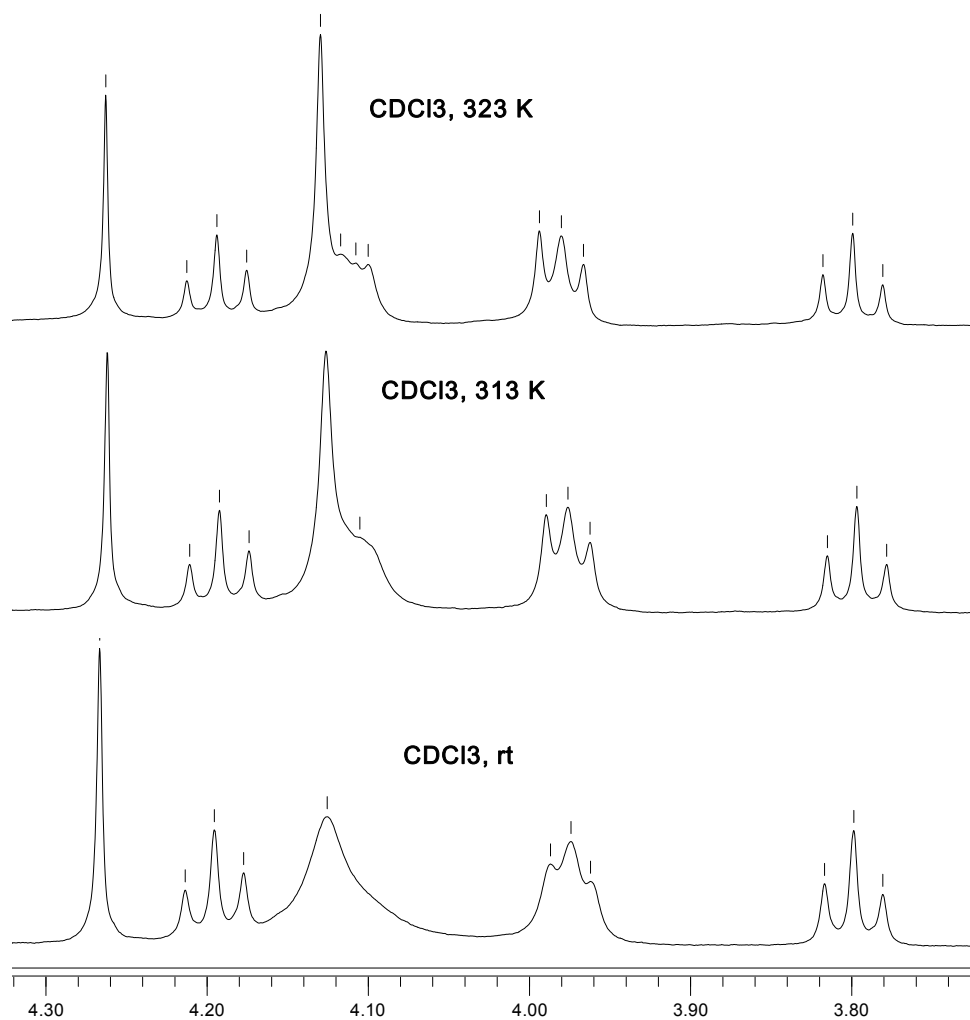


Fig. 18. Variable temperature ¹H-NMR spectra of compound **36** (n = 1) (CDCl₃, 300 MHz)

The spectrum of the same compound was also recorded in C₆D₆ at *rt* and high temperature. Although the use of deuterated benzene (ASIS solvent) sometimes improves and/or helps in the spectra interpretation, it did not work as expected with the spectra run at *rt* but it clearly shows two different signals for the two ethyleneoxy branches of compound **36** (n = 1) (Fig. 19).

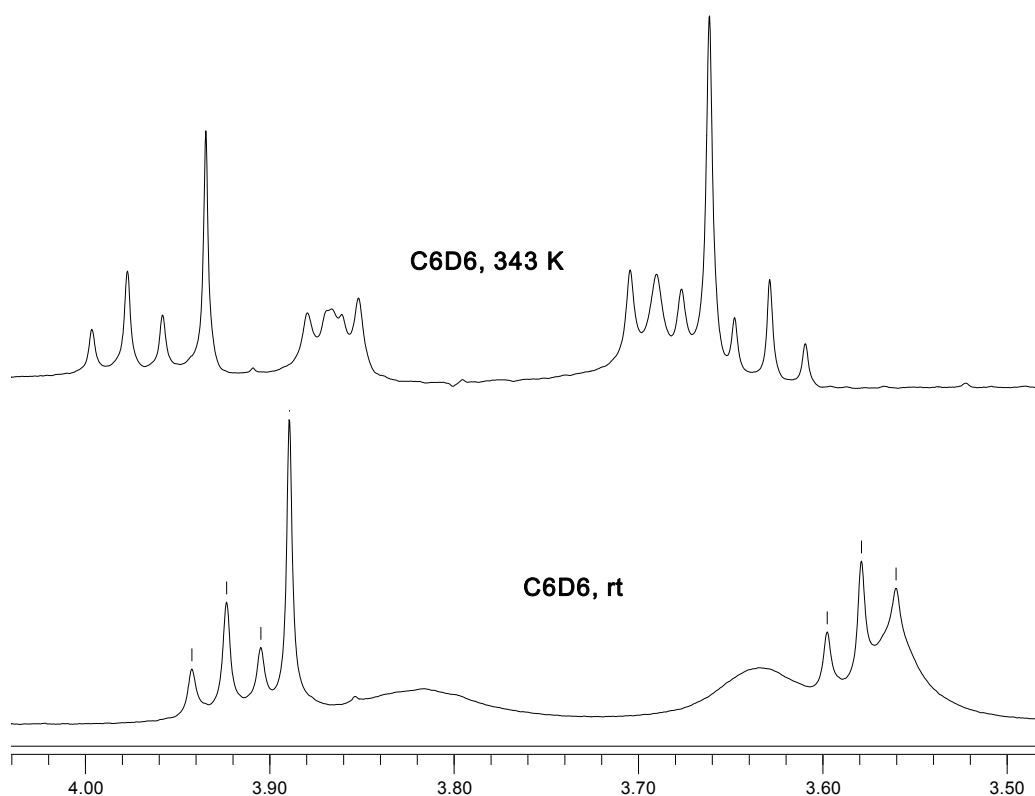


Fig. 19. Variable temperature ¹H-NMR spectra of compound **36** (n = 1) (C₆D₆, 300 MHz)

Taking into consideration the variable temperature NMR experiments for **36** (n = 1) we can assume that it exists as a mixture of two diastereoisomers. Thus we have proposed a diastereoisomeric equilibrium between *cis-cis* and *trans-trans* form (Fig. 20)

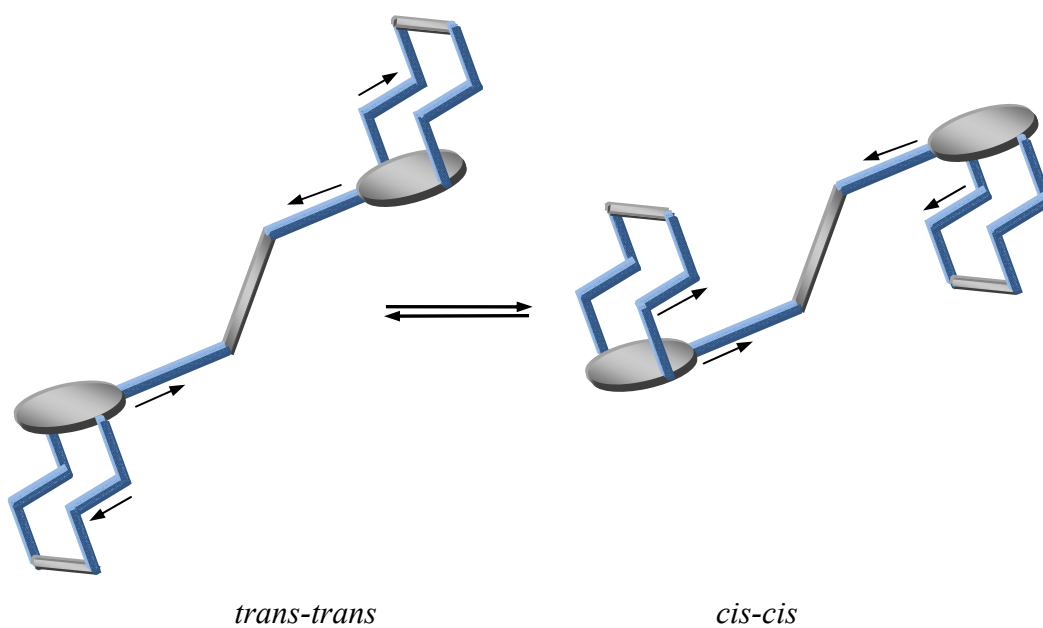


Fig. 20. The two conformations of compound **36** (n = 1)

1.3.3. Solid state structural investigations for bis-macrocycle **36** ($n = 1$)

The structural analysis performed by x-ray diffractometry on crystals obtained from double layered chloroform/hexane solutions showed the presence of centro-symmetrical conformation with *cis*- orientation of the two macrocycles. ORTEP diagram of the compound displays the parallel disposition of the two isocyanurate heterocycles (Fig. 21).

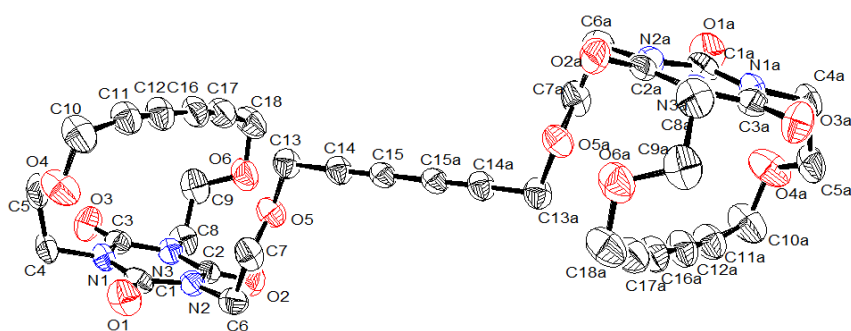


Fig. 21. ORTEP drawing of compound **36** ($n = 1$)

Investigations of the lattice reveals layered disposition of the molecules. The layers are formed by the capped macrocycles which are linked by diene connecting units (Fig. 22).

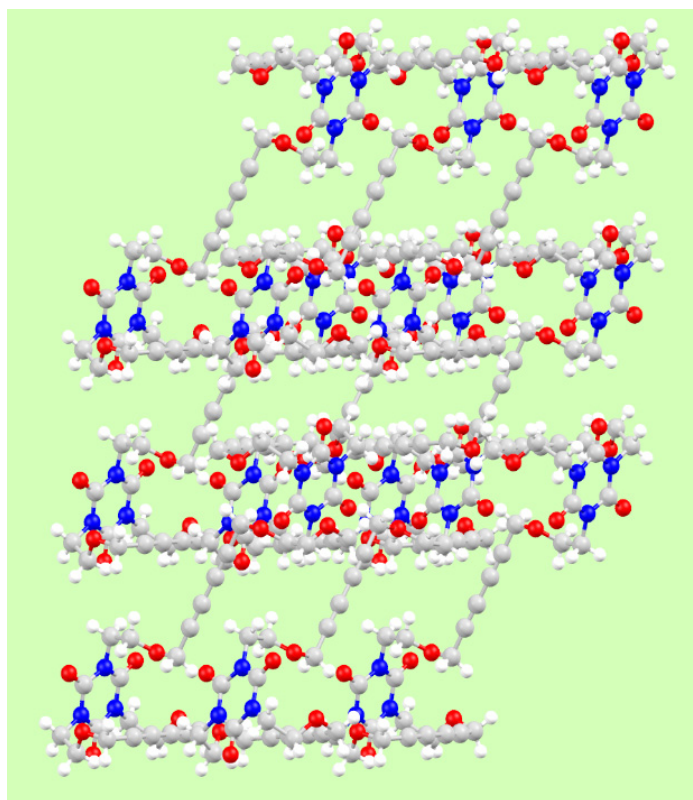


Fig. 22. Mercury drawings along the b axis showing the layered structure of the lattice of compound **36** ($n = 1$)

Three intermolecular carbonyl-proton short contacts could be observed in the lattice of **36**. Carbonyl units from the heterocycle have 2.728 Å, 2.613 Å, 2.664 Å contacts with protons belonging to the connecting branches, to the macrocycle branches, and to the -CH₂- groups of the macrocycle.

In the lattice we can observe two orientations of the molecules illustrated by the opposite disposition of the bridges which connect the macrocyclic units. The two types of molecules in the lattice are alternating and have short contacts of 2.718 Å (Fig. 23).

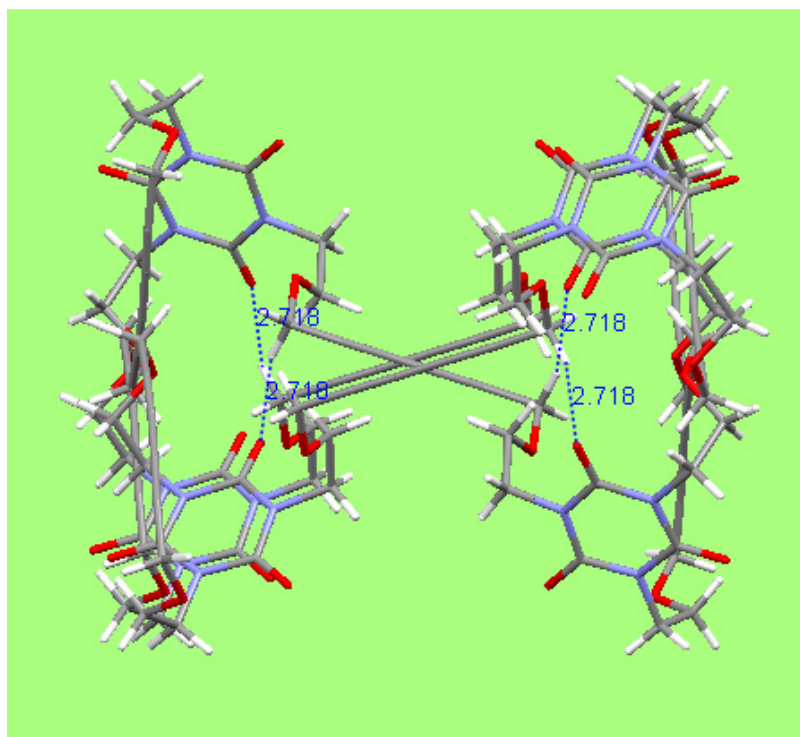


Fig. 23. Mercury drawing showing molecules disposition in the lattice of **36** (n = 1)

1.4. Conclusions

New tripodands corresponding to esters of both cyanuric and isocyanuric acids bearing terminal triple bonds were obtained and used as precursors for the synthesis of macrocyclic compounds.

Cyanurate podands were built up from 1,3,5-triazine, with planar geometry, in junction with flexible ethyleneoxy arms.

For the synthesis of the isocyanurate series several procedures were employed. Thus podands with 1,3,5-triazine-2,4,6-trione units have been obtained from cyanuric acid or 2,4,6-tris(2-hydroxyethyl)cyanuric acid in reaction with propargylbromide, and by isomerization of their cyanurate analogues.

Oxidative acetylenic homocoupling reactions were performed with this podands using Hay's or Eglinton coupling conditions.

Two new types of macrocyclic derivatives have been obtained: a) cryptands by three intermolecular oxidative couplings and b) bis-macrocycles by two intramolecular and one intermolecular coupling reaction.

Preliminary variable temperature NMR analyses of the bis-macrocycle **36** ($n = 1$) indicate a mixture of the *cis-cis* and *trans-trans* diastereoisomers.

1.5. Experimental part

1.5.1. General indications

^1H -NMR and ^{13}C -NMR spectra were recorded on a Bruker AVANCE 300 spectrometer operating at 300 MHz for proton and 75 MHz for carbon; δ are given in ppm (relative to TMS) and coupling constants (J) in Hz. Mass spectra were recorded under ESI Agilent 6320 Ion Trap mass spectrometer in positive mode and under EI mode (70eV) on a VG-Autospec mass spectrometer or under positive ionization ThermoFinnigan MSQ mass spectrometer.

The X-ray crystallographic data were collected at *rt*, using graphite-monochromated $\text{MoK}\alpha$ radiation. For structure solving and refinement the software package SHELX-97 was used.⁶⁰ The drawings were created with Mercury, Ortep⁶¹ and Diamond programs.⁶²

Solvents were dried and distilled under argon using standard procedures before use. Chemicals of commercial grade were used without further purification.

Melting points are uncorrected. Column chromatography purifications were carried out on Merck silica gel Si 60 (40-63 μm). Thin layer chromatography (TLC) was carried out on aluminium sheets coated with silica gel 60 F₂₅₄ using UV lamp (254 nm) and KMnO_4 visualization.

⁶⁰ a) Sheldrick, G. M. *SHELX-97*, Universität Göttingen, Germany, **1997**; b) Bruker (**1999**). SMART (Version 5.611), SAINT (Version 6.02a), SHELXTL (Version 5.10) and SADABS. Bruker AXS Inc., Madison, Wisconsin, USA; c) Claridge, J. B.; Layland, R. C.; Loye, H.-C. *Acta Cryst.* **1997**, C53, 1740

⁶¹ Farrugia, L. J. *J. Appl. Cryst.*, **1997**, 30, 565

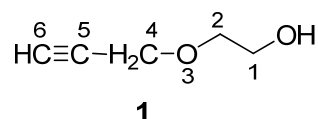
⁶² *DIAMOND* - Visual Crystal Structure Information System; CRYSTAL IMPACT: P.O.B. 1251, D-53002 Bonn, Germany

1.5.2. Synthesis and characterization of compounds

General methods for the synthesis of alkyne chains

Under argon atmosphere 0.044 mol (1.065 g) NaH 95% were added portionwise, under continuously stirring, to 0.25 mol of freshly distilled polyethyleneglycols cooled at 0°C. 0.044 mol (5.54 g, 1 equiv.) of 80% propargyl bromide is added dropwise at 0 °C after all the hydride was reacted. The mixture was stirred at room temperature overnight, extracted with dichloromethane and washed with water 2x50 ml. After drying over sodium sulfate organic phase was concentrated by evaporation. The crude obtained liquid was purified by chromatography over silica gel with ether/acetone 4/1 as eluent. As first fraction we have isolated the side products (di-substitution products) and as second fraction the desired alcohols.

3-oxaheptane-5-yn-1-ol (1, n = 1)

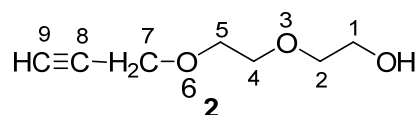


Colorless liquid, $R_f = 0.4$ (eluent: ether/acetone = 4/1). Yield: 23%.

$^1\text{H-NMR}$ (300 MHz, CDCl_3) δ ppm: 2.42 (t, 1H, $J = 2.4$, CCH), 2.8 (s, 1H, OH), 3.57 (t, 2H, CH_2O), 3.68 (t, 2H, CH_2OH), 4.13 (d, 2H, $J = 2.4$, OCH_2CC).

$^{13}\text{C-NMR}$ (75 MHz, CDCl_3) δ ppm: 58.16 (3-C), 61.3 (1-C), 71.08 (2-C), 74.6 (6-C), 79.33 (5-C).

3,6-dioxanonane-8-yn-1-ol (2, n = 2)

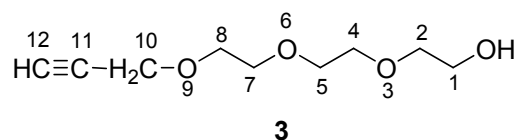


Colorless liquid, $R_f = 0.35$ (eluent: ether/acetone = 4/1). Yield: 25%.

$^1\text{H-NMR}$ (300 MHz, CDCl_3) δ ppm: 2.41 (t, 1H, $J = 2.4$, CCH), 2.96 (s, 1H, OH), 3.52-3.64 (m, 8H), 4.13 (d, 2H, $J = 2.4$, OCH_2CC).

$^{13}\text{C-NMR}$ (75 MHz, CDCl_3) δ ppm: 57.86 (7-C), 60.97 (1-C), 68.61 (2-C), 69.61(4-C), 72.17 (5-C), 74.54 (9-C), 79.08 (8-C).

3,6,9-trioxadodec-11-yn-1-ol (3, n = 3)

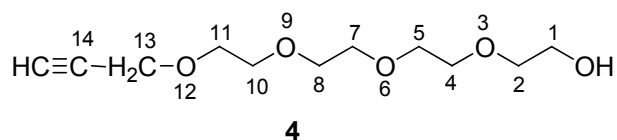


Colorless liquid, $R_f = 0.27$ (eluent: diisopropylether/acetone = 4/1). Yield: 21%.

$^1\text{H-NMR}$ (300 MHz, CDCl_3) δ ppm: 2.41 (t, 1H, $J = 2.4$, CCH), 2.88 (s, 1H, OH), 3.52-3.68 (m, 12H), 4.14 (d, 2H, $J = 2.4$, OCH_2CC).

$^{13}\text{C-NMR}$ (75 MHz, CDCl_3) δ ppm: 58.20 (10-C), 61.45 (1-C), 68.88, 70.08, 70.12, 70.41, 72.45 (2-C, 4-C, 5-C, 7-C, 8-C), 74.59 (12-C), 79.38 (11-C).

(3,6,9,12-tetraoxapentadec-14-yn-1-ol) (4, n = 4)

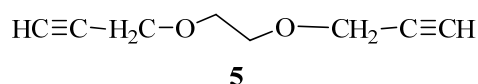


Colorless liquid, $R_f = 0.23$ (eluent: ether/acetone = 4/1). Yield: 27%.

$^1\text{H-NMR}$ (300 MHz, CDCl_3) δ ppm: 2.41 (t, 1H, $J = 2.4$, CCH), 2.86 (s, 1H, OH), 3.54-3.69 (m, 14H), 4.15 (d, 2H, $J = 2.4$, OCH_2CC).

$^{13}\text{C-NMR}$ (75 MHz, CDCl_3) δ ppm: 58.26 (13-C), 61.53 (1-C), 68.96, 70.09, 70.12, 70.35, 70.38, 70.46, 72.60 (2-C, 4-C, 5-C, 7-C, 8-C, 10-C, 11-C), 74.59 (15-C), 79.41 (14-C).

1,2-bis(prop-2-yn-1-yloxy)ethane (5, n = 1)



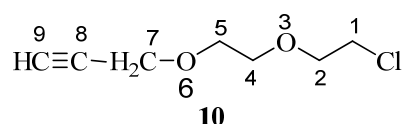
Colorless liquid, $R_f = 0.58$ (eluent: ether/acetone = 4/1). Yield: 10%.

$^1\text{H-NMR}$ (300 MHz, CDCl_3) δ ppm: 2.41 (t, 2H, $J = 2.4$, CCH), 3.68 (s, 4H, CH_2CH_2), 4.17 (d, 4H, $J = 2.4$, OCH_2CC).

General method for the synthesis of chloroalkynes

Chloro-poly(ethoxy)ethanol 20 mmol was added dropwise to a solution of 40 mmol (0.97 g) NaH 95% in 50 ml dry THF at -20 °C, under argon atmosphere. After 15 minutes at -78 °C propargyl bromide 80% solution 20 mmol (2.97 g) was added dropwise and the mixture was refluxed for 2 hours. The reaction mixture was concentrated by evaporation under pressure, washed with 50 ml of water and extracted with dichloromethane. After drying over dry sodium sulfate, the organic layer was concentrated and the resulting crude was purified by chromatography over silica, eluent pentane/ether 4/1.

1-chloro-3,6-dioxa-nona-8-yn (10, n = 2)

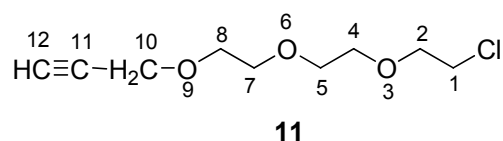


Colorless liquid, $R_f = 0.56$ (eluent: pentane/diethylether = 4/1). Yield: 70%.

$^1\text{H-NMR}$ (300 MHz, CDCl_3) δ ppm: 2.43 (t, 1H, $J = 2.1$, CCH), 3.61-3.77 (m, 8H), 4.20 (d, 2H, $J = 2.4$, OCH_2CC).

$^{13}\text{C-NMR}$ (75 MHz, CDCl_3) δ ppm: 42.29 (1-C), 57.08 (7-C), 68.53, 69.90, 70.81 (2-C, 4-C, 5-C), 74.35 (9-C), 78.11 (8-C).

1-chloro-3,6,9-trioxa-dodeca-11-yn (11, n = 3)



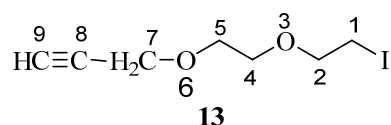
Colorless liquid, $R_f = 0.42$ (eluent: pentane/diethylether = 4/1). Yield: 84%.

$^1\text{H-NMR}$ (300 MHz, CDCl_3) δ ppm: 2.42 (t, 1H, $J = 2.4$, CCH), 3.60-3.77 (m, 12H), 4.19 (d, 2H, $J = 2.1$, OCH_2CC).

General method for the synthesis of iodo-alkynes

17 Mmol of chloro-alkynes **9-11** together with 68 mmol (10.2 g) of dry NaI powder in 170 ml dry acetone were refluxed 48-68 hours. Solvent was removed and the crude was washed with water and extracted with dichloromethane. The organic layer was dried over sodium sulfate and the solvent removed under reduced pressure. Products were purified by chromatography on silica gel.

1-iodo-3,6-dioxa-nona-8-yn (**13**, n = 2)

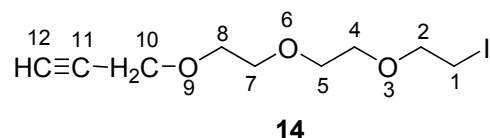


Brown liquid, $R_f = 0.5$ (eluent: pentane/diethylether = 4/1). Yield: 60%.

$^1\text{H-NMR}$ (300 MHz, CDCl_3) δ ppm: 2.42 (t, 1H, $J = 2.1$, CCH), 3.27 (t, 2H, $J = 6.9$, CH_2I), 3.65-3.76 (m, 6H), 4.19 (d, 2H, $J = 2.4$, OCH_2CC).

$^{13}\text{C-NMR}$ (75 MHz, CDCl_3) δ ppm: 2.72 (1-C), 58.28 (7-C), 68.83, 69.78, 71.75 (2-C, 4-C, 5-C), 74.56 (9-C), 79.34 (8-C).

1-iodo-3,6,9-trioxa-dodec-11-yn (**14**, n = 3)



Brown liquid, $R_f = 0.38$ (eluent: pentane/diethylether = 4/1). Yield: 79%.

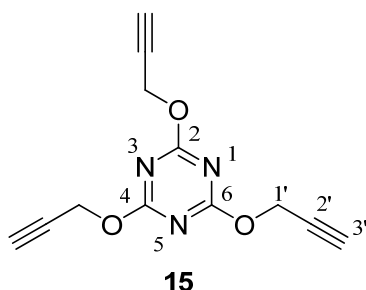
$^1\text{H-NMR}$ (300 MHz, CDCl_3) δ ppm: 2.42 (t, 1H, $J = 2.1$, CCH), 3.24 (t, 2H, $J = 6.6$, CH_2I), 3.64-3.76 (m, 10H), 4.19 (d, 2H, $J = 2.4$, OCH_2CC).

$^{13}\text{C-NMR}$ (75 MHz, CDCl_3) δ ppm: 2.88 (1-C), 58.18 (10-C), 68.85, 69.94, 70.24, 70.35, 71.69 (2-C, 4-C, 5-C, 7-C, 8-C), 74.46 (12-C), 79.40 (11-C).

General method for the synthesis of podands with 1,3,5-triazine units

Under argon atmosphere 5.32 mmol (3.34 ml 15% in hexane) n-BuLi were added over 5 minutes to a solution of 5.32 mmol alkyne chain and 40 ml of dry THF. Alchoxyde solution thus formed was stirred at this temperature for 15 minutes, then 1.77 mmol (327.2 mg) of cyanuril chloride dissolved in 10 ml of THF is added dropwise over 5 minutes. The mixture was stirred overnight at room temperature. After solvent removal the residuum is washed with 50 ml of water, extracted with dichloromethane, dried over sodium sulfate and concentrated. Product were purified by chromatography over silica gel.

2,4,6-tris(prop-2'-yn-1'-yloxy)-1,3,5-triazine (15, n = 0)

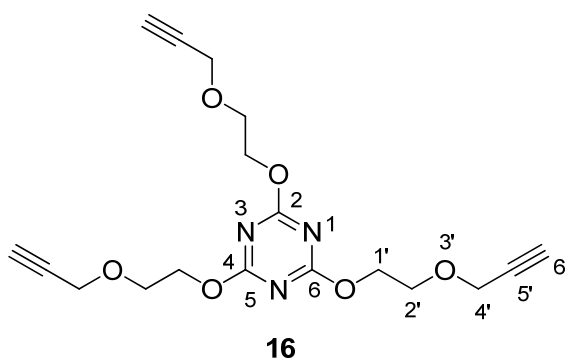


White solid, m.p. = 70 °C, R_f = 0.35 (eluent: pentane/ethylacetate = 9/1); Yield: 65%.

$^1\text{H-NMR}$ (300 MHz, CDCl_3) δ ppm: 2.53 (t, 3H, J = 2.4, 3'-H), 5.04 (d, 6H, J = 2.4, 1'-H).

$^{13}\text{C-NMR}$ (75 MHz, CDCl_3) δ ppm: 58.81 (1'-C), 75.81 (3'-C), 76.83 (2'-C), 172.30 (2-C).

2,4,6-tris(3'oxahexa-5'-yn-1'-yloxy)-1,3,5-triazine (16, n = 1)



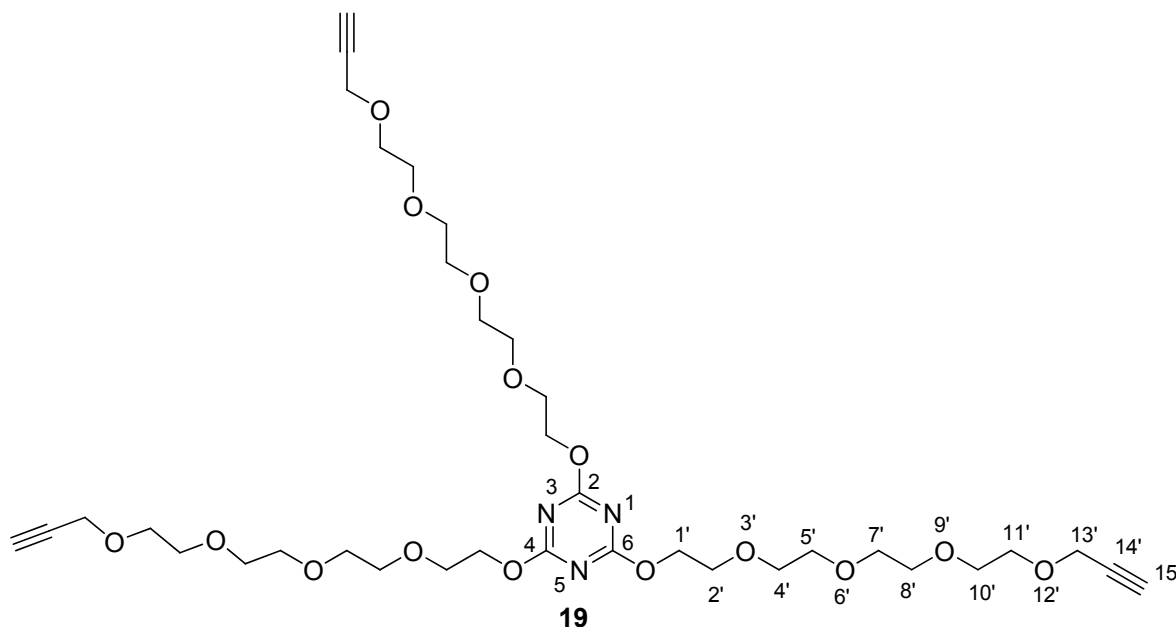
White solid, m.p. = 96 °C; R_f = 0.35 (eluent: ether/acetone/hexane = 4/1/1); Yield: 63%.

$^1\text{H-NMR}$ (300 MHz, CDCl_3) δ ppm: 2.43 (t, 3H, J = 2.4, 6'-H), 3.86 (t, 6H, J = 4.8, 2'-H), 4.21 (d, 6H, J = 2.4, 4'-H), 4.55 (t, 6H, J = 4.8, 1'-H).

$^{13}\text{C-NMR}$ (75 MHz, CDCl_3) δ ppm: 58.39 (4'-C), 67.17, 67.24 (1'-C, 2'-C), 74.87 (6'-C), 79.17 (5'-C), 172.88 (2-C).

ESI-MS $m/z = 640.3 ([M+H]^+)$, $662.3 ([M+Na]^+)$.

2,4,6-tris(3',6',9',12'-tetraoxapentadec-14'-yn-1'-yloxy)-1,3,5-triazine (19, n = 4)



Colorless liquid, $R_f = 0.35$ (eluent: ether/acetone/hexane = 4/1/1); Yield: 55%

$^1\text{H-NMR}$ (300 MHz, CDCl_3) δ ppm: 2.42 (t, 1H, $J = 2.4$, 15'-H), 3.64-3.67 (m, 12H, 2'-H, 4'-H, 5'-H, 7'-H, 8'-H, 10'-H), 3.81 (m, 2H, 11'-H), 4.18 (d, 2H, $J = 2.4$, 13'-H), 4.51 (m, 2H, 1'-H).

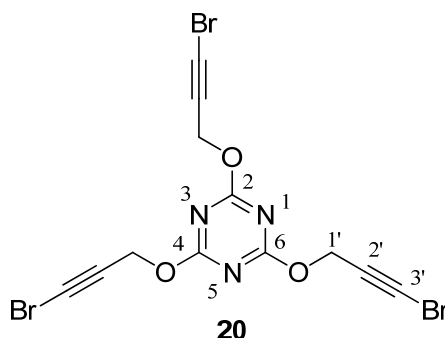
$^{13}\text{C-NMR}$ (75 MHz, CDCl_3) δ ppm: 58.34 (13'-C), 67.48, 68.79, 69.06, 70.35, 70.55 (2'-C, 4'-C, 5'-C, 7'-C, 8'-C, 10'-C, 11'-C), 70.68 (1'-C), 74.48 (15'-C), 79.63 (14'-C) 172.92 (2-C).

ESI-MS $m/z = 772.3 ([M+H]^+)$, $794.3 ([M+Na]^+)$.

General method for the bromination reaction

To a solution of 3.3 mmol of cyanurate or isocyanurate podand in 75 ml of degassed acetone 34.6 mmol of NBS and 4.9 mmol of AgNO₃ were added with stirring at room temperature under argon atmosphere. The mixture was stirred at room temperature over night, extracted with dichloromethane and washed with brine. The oily crude was purified on chromatography over silica gel using mixture of toluene/acetone as eluent.

2,4,6-tris(3'-bromoprop-2'-yn-1'-yloxy)-1,3,5-triazine (20)



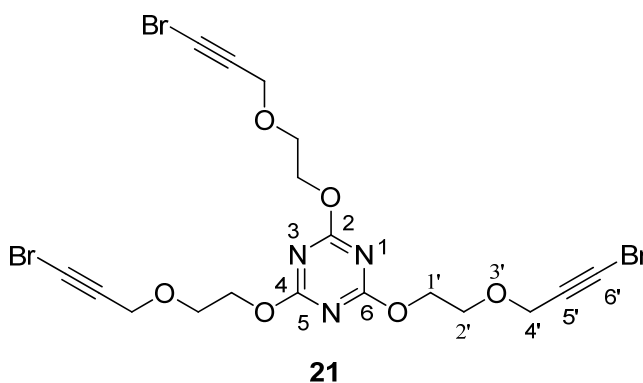
White solid, m.p. = 95 °C, R_f = 0.7 (eluent: toluene/acetone = 20/1); Yield: 36%.

¹H-NMR (300 MHz, CDCl₃) δ ppm: 5.05 (s, 6H, 1'-H).

¹³C-NMR (75 MHz, CDCl₃) δ ppm: 48.53 (3'-C), 56.76 (1'-C), 73.38 (2'-C), 172.34 (2-C).

ESI-MS m/z = 480.9 ([M+H]⁺).

2,4,6-tris(6'-bromo-3'-oxa-hexa-5'-yn-1'-yloxy)-1,3,5-triazine (21)



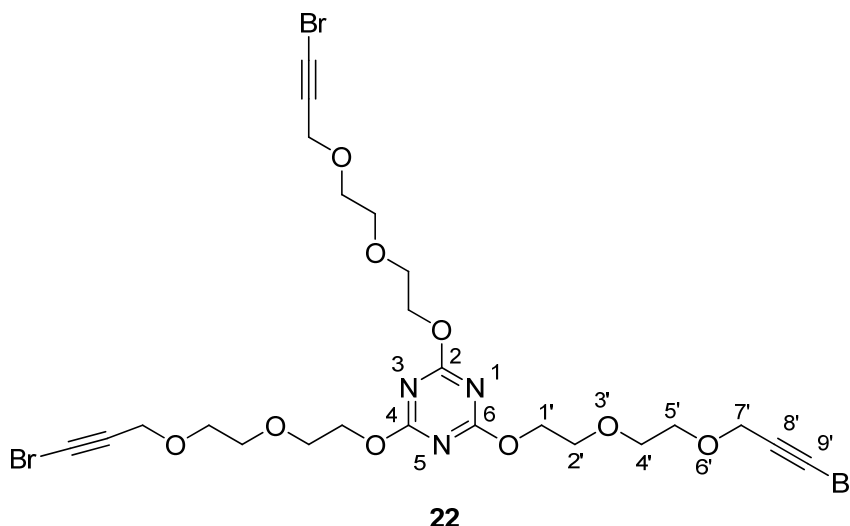
White solid, m.p. = 105 °C, R_f = 0.7 (eluent: toluene/acetone = 9/1); Yield: 36%.

¹H-NMR (300 MHz, CDCl₃) δ ppm: 3.86 (t, 6H, J = 3.6, 2'-H), 4.25 (s, 6H, 4'-H), 4.56 (t, 6H, J = 3.6, 1'-H).

¹³C-NMR (75 MHz, CDCl₃) δ ppm: 46.59 (6'-C), 59.42 (4'-C), 67.18, 67.45 (1'-C, 2'-C), 75.81 (5'-C), 172.94 (2-C).

ESI-MS $m/z = 613.9$ ($[M+H]^+$), 634.9 ($[M+Na]^+$).

2,4,6-tris(-9'-bromo-3', 6'-dioxanona-8'-yn-1'-yloxy)-1,3,5-triazine (22)



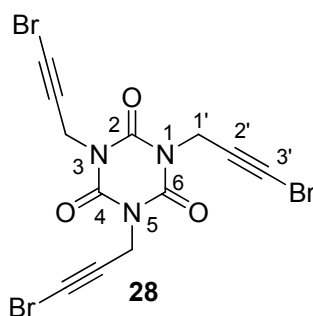
Brown liquid, $R_f = 0.31$ (eluent: toluene/acetone = 4/1); Yield: 20%.

$^1\text{H-NMR}$ (300 MHz, CDCl_3) δ ppm: 3.69 (m, 12H, 2'-H, 4'-H), 3.83 (m, 6H, 5'-H), 4.22 (s, 6H, 7'-C), 4.54 (m, 6H, 1'-H).

$^{13}\text{C-NMR}$ (75 MHz, CDCl_3) δ ppm: 46.16 (9'-C), 59.41 (7'-C), 67.47, 68.87, 69.20, 70.49 (1'-C, 2'-C, 4'-C, 5'-C), 76.09 (8'-C), 172.90 (2-C).

ESI-MS $m/z = 745.7$ ($[M+H]^+$) 767.1 ($[M+Na]^+$).

1,3,5-tris(3'-bromoprop-2'-yn-1'-yl)-1,3,5-triazinane-2,4,6-trione (28)



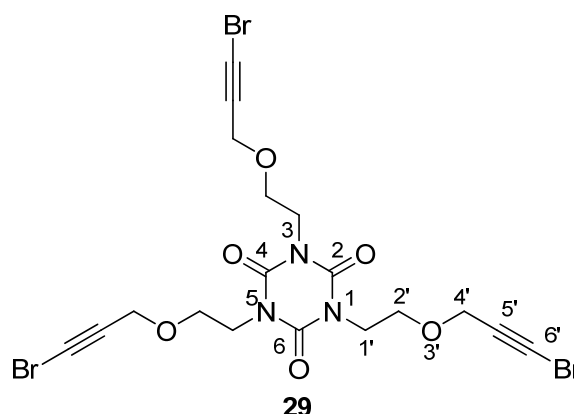
White solid, m.p. = 80 °C; Yield: 45%.

$^1\text{H-NMR}$ (300 MHz, CDCl_3) δ ppm: 4.70 (s, 6H, 1'-H).

$^{13}\text{C-NMR}$ (75 MHz, CDCl_3) δ ppm: 33.58 (1'-C), 44.81 (3'-C), 72.87 2'8-C), 147.14 (2-C).

EI-MS m/z (%) = 480 (M^+ , 10), 376 (12), 203 (100), 119 (73).

1,3,5-tris(6'-bromo-3'-oxahexa-5'-yn-1'-yl)-1,3,5-triazinane-2,4,6-trione (29)



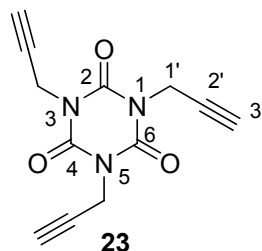
Brown liquid, $R_f = 0.56$ (eluent: toluene/acetone = 4/1); Yield: 73%.

$^1\text{H-NMR}$ (300 MHz, CDCl_3) δ ppm: 3.77 (t, 6H, $J = 4.2$, 2'-H), 4.13 (t, 6H, $J = 4.2$, 1'-H), 4.20 (s, 6H, 4'-H).

$^{13}\text{C-NMR}$ (75 MHz, CDCl_3) δ ppm: 41.80 (1'-C), 46.29 (6'-C), 58.89 (4'-C), 66.14 (2'-C), 75.91 (5'-C), 148.98 (2-C).

ESI-MS $m/z = 614.5$ ($[\text{M}+\text{H}]^+$), 634.5 ($[\text{M}+\text{Na}]^+$).

1,3,5-tris(prop-2'-yn-1'-yl)-1,3,5-triazinane-2,4,6-trione (23)



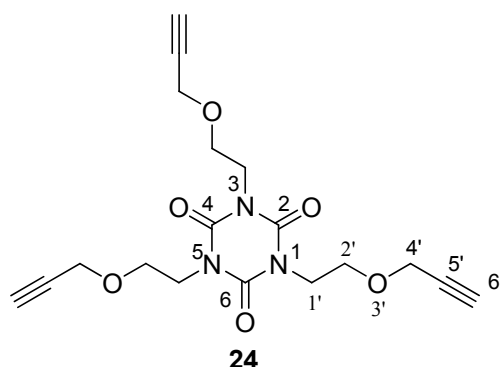
Cyanuric acid (1 g, 7.75 mmols, 1 equiv.) was solubilized in 12 ml of water containing 23.25 mmol (0.93 g, 3 equiv.) NaOH. After heating up to 50 °C, 23.25 mmol (3.48 g, 3 equiv.) of propargylbromide 80% solution in toluene were added to the mixture drop by drop. The mixture was refluxed for 5 hours, concentrated under reduced pressure and the crude was purified by recrystallization from methanol followed by ethanol.

Cream solid, m.p. = 158 °C; Yield: 45%.

$^1\text{H-NMR}$ (300 MHz, CDCl_3) δ ppm: 2.28 (t, 3H, $J = 2.4$, 3'-H), 4.70 (d, 6H, $J = 2.4$, 1'-H).

$^{13}\text{C-NMR}$ (75 MHz, CDCl_3) δ ppm: 32.55 (1'-C), 72.42 (3'-C), 76.2 (2'-C), 150 (2-C).

1,3,5-tris(3'-oxahexa-5'-yn-1'-yl)-1,3,5-triazinan-2,4,6-trione (24, n = 1)



8.4 mmol (100% excess) of NaH 95% were added to a solution of 22.8 mmol (6 g) 1,3,5-tris(2-hydroxyethyl)cyanuric acid in 50 ml of dry DMSO, under argon atmosphere and continuously cooling under cold water, without freezing the solvent. After stirring at room temperature for 1 hour 68.4 mmol (10.17 g) of propargylbromide 80% toluene solution were added dropwise at 20 °C and stirred for 2 hours at room temperature. The mixture was washed with water 3x50 ml and extracted with dichloromethane. The organic layer was concentrated and the crude purified by chromatography.

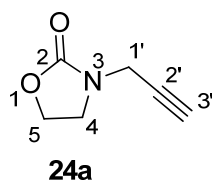
Colorless liquid, $R_f = 0.4$ (eluent: ethylacetate/pentane = 1/2); Yield: 20%.

$^1\text{H-NMR}$ (300 MHz, CDCl_3) δ ppm: 2.42 (t, 3H, $J = 2.4$, 6'-H), 3.78 (t, 6H, $J = 5.4$, 2'-H), 4.13 (t, 6H, $J = 5.4$, 1'-H), 4.16 (d, 6H, $J = 2.1$, 4'-H).

$^{13}\text{C-NMR}$ (75 MHz, CDCl_3) δ ppm: 41.73 (1'-C), 57.82 (4'-C), 65.91 (2'-C), 74.70 (6'-C), 79.27 (5'-C), 148.97 (2-C).

APCI-MS $m/z = 376.3$ ($[\text{M}+\text{H}]^+$).

3-(prop-2'-yn-1'-yl)oxazolidin-2-one (24a)



8.4 mmol (100% excess) of NaH 95% were added to a solution of 22.8 mmol (6 g) 1,3,5-tris(2-hydroxyethyl)cyanuric acid in 50 ml of dry DMSO, under argon atmosphere and continuously cooling under ice, without freezing the solvent. After stirring at room temperature for 1 hour 68.4 mmol (10.17 g) of propargylbromide 80% toluene solution were added dropwise at 35-40 °C and stirred for 2 hours. The mixture was washed with water 3x50 ml and extracted

with dichloromethane. The organic layer was concentrated and the crude purified by chromatography.

Colorless liquid; R_f = 0.30 (eluent: ethyl acetate/pentane 1/2); Yield: 31%.

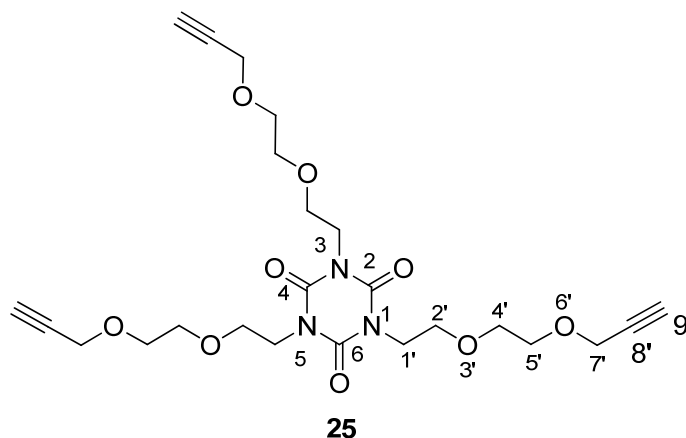
$^1\text{H-NMR}$ (300 MHz, CDCl_3) δ ppm: 2.30 (t, 1H, J = 2.4, 3'-H), 3.65 (m, 2H, 4-H), 4.07 (d, 2H, J = 2.4, 1'-H), 4.36 (m, 2H, 5-H).

$^{13}\text{C-NMR}$ (75 MHz, CDCl_3) δ ppm: 34.03 (1'-C), 43.79 (4-C), 61.92 (5-C), 73.29 (3'-C), 76.81 (2'-C), 157.83 (2-C).

General method for the synthesis of isocyanurate podands

0.66 mmol of podand with 1,3,5-triazine units and Bu_4NBr 0.2 mmol (53 mg) or Bu_4PBr 0.2 mmol (67.8 mg) were stirred at 125 °C for 48 hours. Extraction was made with dichloromethane and after washing with water, the organic layer was concentrated and the crude purified by chromatography on silica gel.

1,3,5-tris(3', 6'-dioxanona-8'-yn-1'-yl)-1,3,5-triazinan-2,4,6-trione (**25**, $n = 2$)



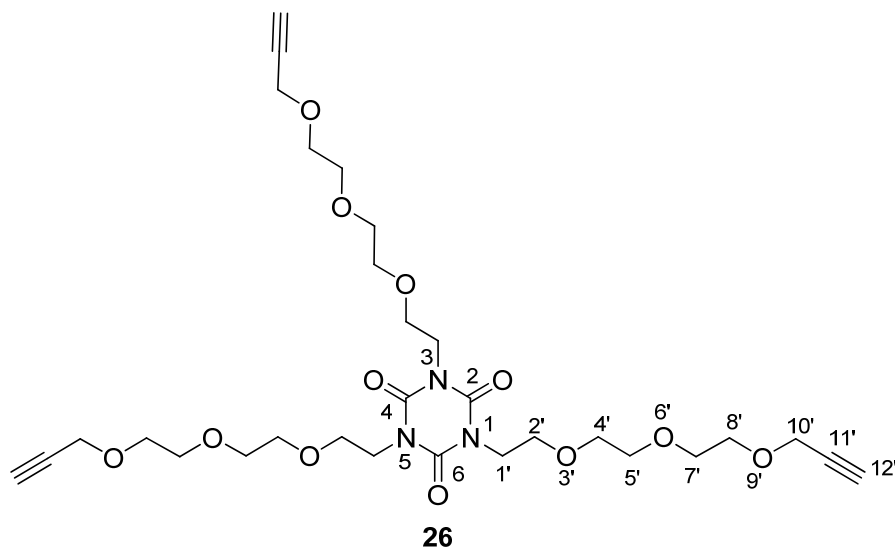
Yellow liquid; R_f = 0.64 (ethyl acetate/pentane 1/1); Yield: 33%.

$^1\text{H-NMR}$ (300 MHz, CDCl_3) δ ppm: 2.42 (t, 3H, J = 2.4, 9'-H), 3.66 (m, 12H, 4'-H, 5'-H), (t, 6H, J = 4.5, 2'-H), 4.10 (t, 6H, J = 4.5, 1'-H), 4.17 (d, 6H, J = 2.1, 7'-H).

$^{13}\text{C-NMR}$ (75 MHz, CDCl_3) δ ppm: 41.67 (1'-C), 58.38 (7'-C), 67.48 (2'-C), 69.04, 69.81 (4'-C, 5'-C), 74.54 (9'-C), 79.60 (8'-C), 149.02 (2-C).

ESI-MS m/z = 508.4 ($[\text{M}+\text{H}]^+$), 530.4 ($[\text{M}+\text{Na}]^+$), 546.3 ($[\text{M}+\text{K}]^+$).

1,3,5-tris(3', 6', 9'-trioxadodeca-11'-yn-1'-yl)-1,3,5-triazinan-2,4,6-trione (26, n = 3)



Yellow liquid; $R_f = 0.5$ (ethyl acetate/pentane 1/1); Yield: 20%.

$^1\text{H-NMR}$ (300 MHz, CDCl_3) δ ppm: 2.43 (t, 3H, $J = 2.4$, 12'-H), 3.61-6.71 (m, 30H, 2'-H, 4'-H, 5'-H, 7'-H, 8'-H), 4.09 (t, 6H, $J = 4.5$, 1'-H), 4.19 (d, 6H, $J = 2.4$, 10'-H)

$^{13}\text{C-NMR}$ (75 MHz, CDCl_3) δ ppm: 41.68 (1'-C), 58.40 (10'-C), 67.45, 69.10, 69.99, 70.42, 70.63 (2'-C, 4'-C, 5'-C, 7'-C, 8'-C), 74.54 (12'-C), 149.00 (2-C).

ESI-MS $m/z = 640.4$ ($[\text{M}+\text{H}]^+$).

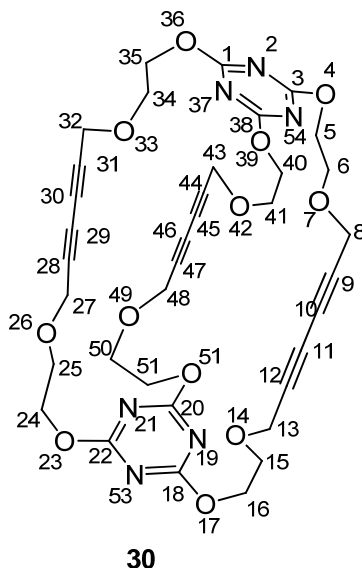
General method for the Eglinton acetylenic coupling

To a solution of 19 mmol $\text{Cu}(\text{OAc})_2$ in 150 ml acetonitrile heated at 60 °C a 2 mmol podand solution in 15 ml acetonitrile was added at once and the mixture was stirred over night at this temperature. 300 ml of water were added and the precipitate was filtered and washed with 200 ml water. The solid thus obtained was purified by chromatography on silica gel, eluent toluene/acetone 4/1.

General method for the Hay's acetylenic coupling

To a solution of 1 mmol (1 equiv.) podand in 200 ml (5mM) dry CH_2Cl_2 containing 40 mmol (120 equiv.) dry TMEDA 20 mmol (60 equiv.) of dry CuI (or dry CuCl) were added and the mixture was stirred for 2 hours at room temperature under oxygen atmosphere. After solvent evaporation, extraction with dichloromethane and washing several times with water (for complete removing of the copper salts), the organic layer was purified by chromatography on silica gel, eluent toluene/acetone 4/1.

4, 7, 14, 17, 23, 26, 33, 36, 39, 42, 49, 51-dodecaoxa-2, 19, 21, 37, 53, 54-hexaazapentacyclo[18. 18. 14. 1^{1,3}. 1^{18,20}]-tetrapentaconta-1, 3(54), 18, 20, 22(54), 25-hexaene-9, 11, 28, 31, 44, 46-hexayne (30)



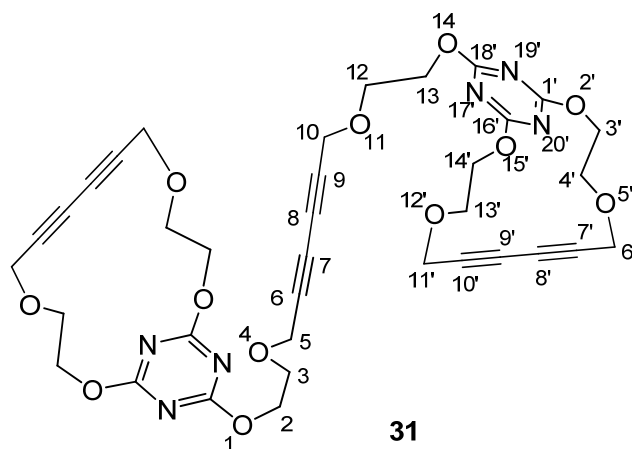
Colorless liquid, $R_f = 0.44$ (eluent: toluene/acetone= 4/1). Yield: 10%.

$^1\text{H-NMR}$ (300 MHz, CDCl_3) δ ppm: 3.89 (m, 12H, 12H, 6-H, 15-H, 25-H, 34-H, 41-H, 50-H), 4.29 (s, 12H, 8-H, 13-H, 27-H, 32-H, 43-H, 48-H), 4.60 (m, 12H, 5-H, 16-H, 24-H, 35-H, 40-H, 51-H).

$^{13}\text{C-NMR}$ (75 MHz, CDCl_3) δ ppm: 59.01 (8-C, 13-C, 27-C, 32-C, 43-C, 48-C), 67.10 (5-C, 16-C, 24-C, 35-C, 40-C, 51-C), 67.63 (6-C, 15-C, 25-C, 34-C, 41-C, 50-C), 70.54, 75.25 (9,10-C, 11,12-C, 28,29-C, 30,31-C, 44,45-C, 46,47-C) 172.96 (2,19,21,37,53,54-C-triazine).

ESI-MS $m/z = 745.2$ ($[\text{M}+\text{H}^+]$), 767.2 ($[\text{M}+\text{Na}^+]$).

1,14-bis(2', 5', 12', 15'-tetraoxa-17', 19', 20'-triazia-bicyclo[14. 3. 1]icosa-16', 18', 20'(1')-triene-7', 9'-diyne-18'-yl)-1, 4, 11, 14-tetraoxatetradeca-6, 8-diyne (31)



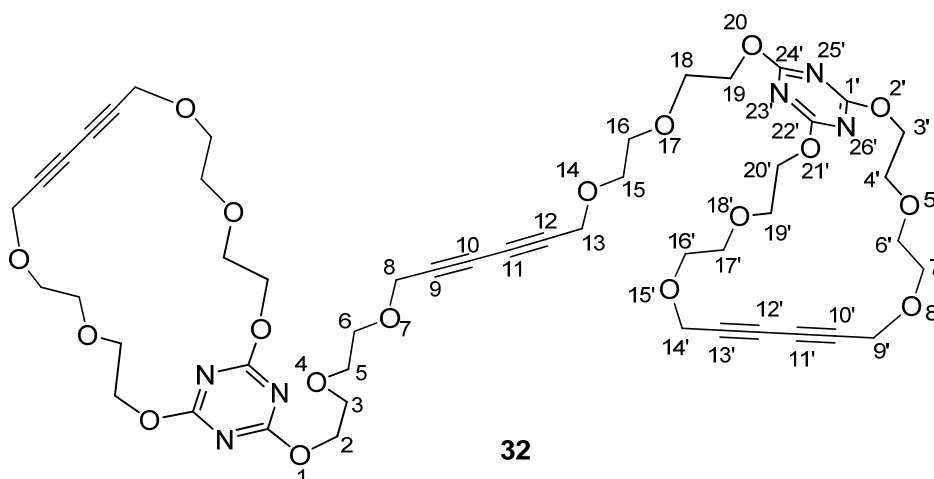
White solid; m.p. = 175°C (decomp.), R_f = 0.39 (eluent: toluene/acetone= 4/1). Yield: 25%.

$^1\text{H-NMR}$ (300 MHz, CDCl_3) δ ppm: 3.89 (m, 4H, 3-H, 12-H), 3.98 (m, 8H, 2X4'-H, 2X13'-H), 4.23 (s, 8H, 2X6'-H, 2X11'-H), 4.31 (s, 4H, 5-H, 10-H), 4.57 (m, 4H, 2-H, 13-H), 4.66 (m, 8H, 2X3'-H, 2X14'-H).

$^{13}\text{C-NMR}$ (75 MHz, CDCl_3) δ ppm: 58.94 (5-C, 10-C); 59.43 (2X6'-C, 2X11'-C), 67.02 (2-C, 13-C); 67.27 (2X3'-C, 2X14'-C), 67.60 (3-C, 12-C); 68.20 (2X4'-C, 2X13'-C), 70.38, 76.16 (6,7-C, 8,9-C); 70.87, 75.09 (2X7',8'-C, 2X9',10'-C) 172.72 (2X18'-C-triazine) 173.02 (2X17',19'-C-triazine).

ESI-MS m/z = 745.2 ($[\text{M}+\text{H}^+]$), 767.2 ($[\text{M}+\text{Na}^+]$).

1,20-bis(2', 5', 8', 15', 18', 21'-hexaoxa-23', 25', 26'-triazabicyclo[20.3.1]hexacos-22', 24', 26' (1')-triene-10', 12'-diyne-24'-yl)-1, 4, 7, 14, 17, 20-hexaoxaicosa-9, 11-diyne (32)



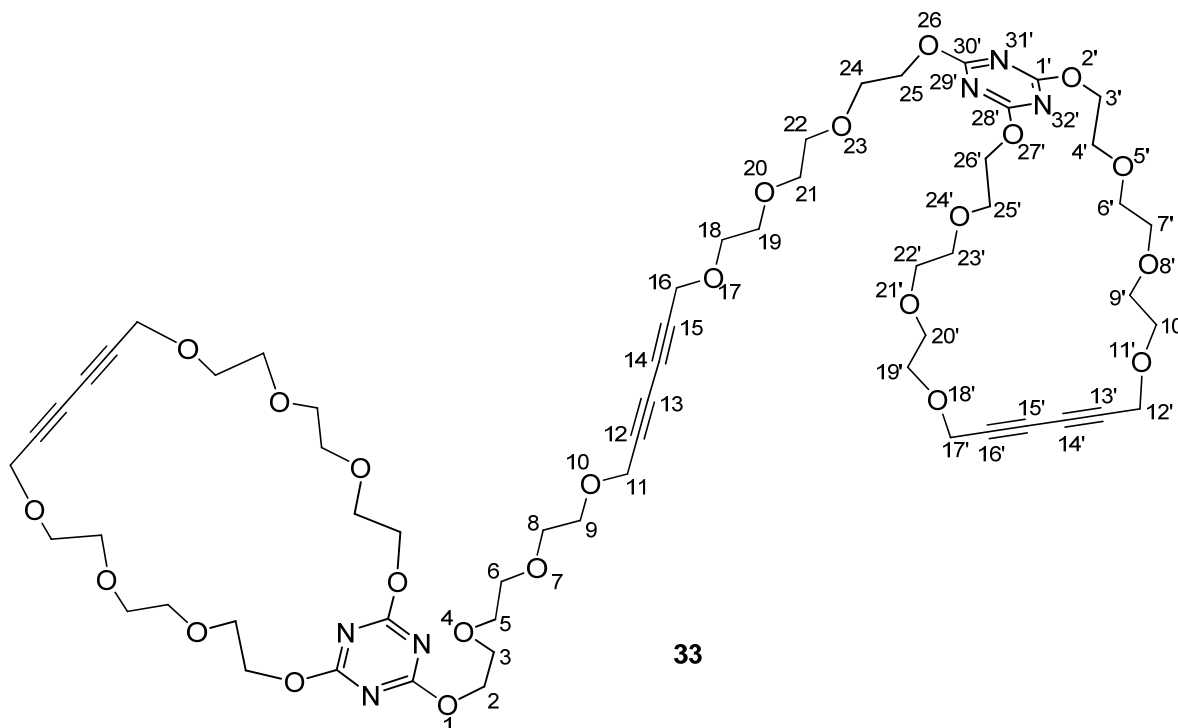
Yellow liquid; $R_f = 0.34$ (eluent: toluene/acetone= 4/1). Yield: 58%.

$^1\text{H-NMR}$ (300 MHz, CDCl_3) δ ppm: 3.69 (s, 24H, 5-H, 6-H, 15-H, 16-H, 2X6'-H, 2X7'-H, 2X16'-H, 2X17'-H), 3.83 (m, 12H, 3-H, 18-H, 2X4'-H, 2X19'-H), 4.24 (s, 8H, 2X9'-H, 2X14'-H), 4.27 (s, 4H, 8-H, 13-H), 4.54 (m, 4H, 2-H, 19-H), 4.60 (m, 8H, 2X3'-H, 2X20'-H).

$^{13}\text{C-NMR}$ (75 MHz, CDCl_3) δ ppm: 58.95 (8-C, 13-C); 59.01 (2X9'-C, 2X14'-C), 67.25 (2X3'-C, 2X20'-C); 67.38 (2-C, 19-C), 68.82 (2X4'-C, 2X19'-C); 68.92 (3-C, 18-C), 69.30, 69.34, 70.43, 70.56 (5-C, 6-C, 15-C, 16-C, 2X6'-C, 2X7'-C, 2X16'-C, 2X17'-C), 70.49, 70.65, 75.32, 75.48 (9,10-C, 11,12-C, 2X10',11'-C, 2X12',13'-C) 172.96, 173.04 (2X24'-C, 2X23',26'-C-triazine).

ESI-MS $m/z = 1009.4$ ($[\text{M}+\text{H}^+]$), 1031.3 ($[\text{M}+\text{Na}^+]$).

1,26-bis(2', 5', 8', 11', 18', 21', 24', 27'-octaoxa-29', 31', 32'-triazabicyclo[26.3.1]dotriaconta-28', 30', 32' (1')-triene-13', 15'-diyne-30'-yl)-1, 4, 7, 10, 17, 20, 23, 26-octaoxahexacos-12, 14-diyne (33)



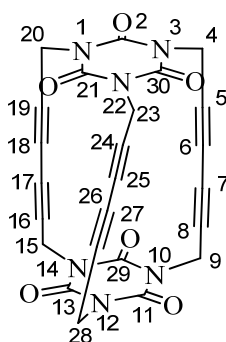
Yellow liquid; $R_f = 0.39$ (eluent: toluene/acetone= 1/1). Yield: 20%.

$^1\text{H-NMR}$ (300 MHz, CDCl_3) δ ppm: 3.66 (m, 48H, 5-H, 6-H, 8-H, 9-H, 18-H, 19-H, 21-H, 22-H, 2X6'-H, 2X7'-H, 2X9'-H, 2X10'-H, 2X19'-H, 2X20'-H, 2X22'-H, 2X23'-H), 3.82 (m, 12H, 3-H, 24-H, 2X4'-H, 2X25'-H), 4.25 (s, 4H, 11-H, 16-H), 4.26 (s, 8H, 2X12'-H, 2X17'-H), 4.52 (m, 12H, 2-H, 25-H, 2X3'-H, 2X26'-H).

$^{13}\text{C-NMR}$ (75 MHz, CDCl_3) δ ppm: 58.86 (11-C, 16-C, 2X12'-C, 2X17'-C), 67.42, 67.60, 68.79, 69.13, 69.28, 70.34, 70.40, 70.46, 70.55, 70.64, 70.92, 75.38, 75.40, 75.41, 172.90 (C-triazine).

ESI-MS $m/z = 1273.6$ ($[\text{M}+\text{H}^+]$), 1295.6 ($[\text{M}+\text{Na}^+]$).

2, 11, 13, 21, 29, 30-hexaoxo-1, 3, 10, 12, 14, 22-hexaazapentacyclo[11. 11. 6. 1^{1,3}.1^{10,12}]-triaeconta-5, 7, 16, 18, 24, 26-hexayne (34)



34

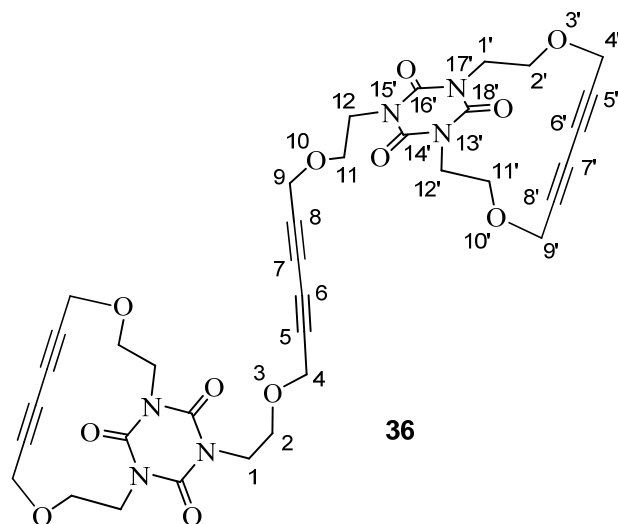
Brown solid; mp = 20 °C (decomp.); R_f = 0.62 (eluent: dichloromethane/ether= 3/7). Yield: 33%.

$^1\text{H-NMR}$ (300 MHz, CDCl_3) δ ppm: 34.65 (s, 12H, 4-H, 9-H, 15-H, 20-H, 23-H, 28-H).

$^{13}\text{C-NMR}$ (75 MHz, CDCl_3) δ ppm: 53.40 (4-C, 9-C, 15-C, 20-C, 23-C, 28-C), 89.64 (5-C, 8-C, 16-C, 19-C, 24-C, 27-C), 131.04 (6-C, 7-C, 17-C, 18-C, 25-C, 26-C), 161.17 (2-C, 11-C, 13-C, 21-C, 29-C, 30-C-izocyanurate).

ESI-MS m/z = 481.1($[\text{M}+\text{H}]^+$).

1,12-bis(3', 10'-dioxo-13',15',17'-triazza-bicyclo[12. 3. 1]octadeca-14',16',18'-trioxo-5', 7'-diyne-15'-yl)-3,10-dioxadodeca-5, 7-diyne (36)



White solid; m.p. = >300°C (>150 °C brown), $R_f = 0.5$ (eluent: toluene/acetone= 4/1). Yield: 64%.

$^1\text{H-NMR}$ (300 MHz, CDCl_3) δ ppm: 3.89 (m, 4H, 3-H, 12-H), 3.98 (m, 8H, 2X4'-H, 2X13'-H), 4.23 (s, 8H, 2X6'-H, 2X11'-H), 4.31 (s, 4H, 5-H, 10-H), 4.57 (m, 4H, 2-H, 13-H), 4.66 (m, 8H, 2X3'-H, 2X14'-H).

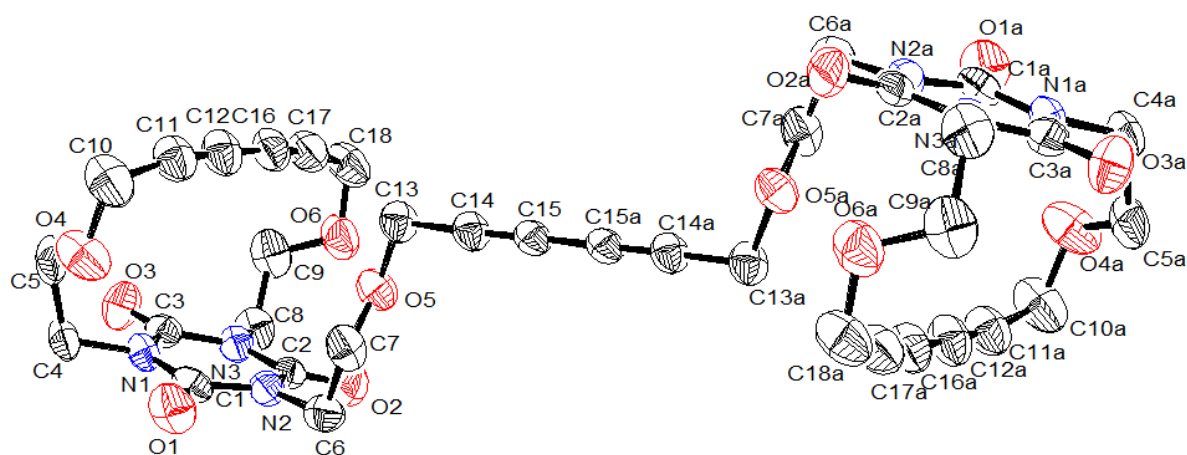
$^{13}\text{C-NMR}$ (75 MHz, CDCl_3) δ ppm: 41.92 (1-C, 12-C), 43.92 (2X1'-C, 2X12'-C), 53.41 (6-C, 7-C), 58.38 (4-C, 9-C), 58.67 (2X4'-C, 2X9'-C), 66.35 (2-C, 11-C), 66.97 (2X2'-C, 2X11'-C), 70.49 (2X6'-C, 2X7'-C), 75.25 (5-C, 7-C), 78.55 (2X5'-C, 2X7'-C), 149.24 (2X16'-C, 2X14'-C), 149.69 (18'-C).

APCI-MS $m/z = 745.3$ ($[\text{M}+\text{H}]^+$), 767.3 ($[\text{M}+\text{Na}]^+$).

Annex 1

Crystal data and structure refinement for compound **36**

Empirical formula	C ₃₆ H ₃₆ N ₆ O ₁₂	
Formula weight	744.71	
Temperature (K)	297(2)	
Wavelength, Å	0.71073	
Crystal system	Monoclinic	
Space group	C2 / C	
Unit cell dimensions, Å	a = 16.651(3)	α = 90°
	b = 17.434(3)	β = 93.549(4)°
	c = 12.609(3)	γ = 90°
Volume, Å ³	3653.4(12)	
Z	4	
Density (calculated) mg/m ³	1.354	
Absorption coefficient, mm ⁻¹	0.103	
F(000)	1560	
Crystal size/mm	0.33 x 0.30 x 0.28	
Theta range for data collection/ (°)	2.29 to 25.00	
Index ranges	-19 ≤ h ≤ 19, -20 ≤ k ≤ 20, -14 ≤ l ≤ 14	
Reflections collected	17404	
Independent reflections	3224 [R(int) = 0.0703]	
Refinement method	Full-matrix least-squares on F ²	
Data/restraints/parameters	3224 / 0 / 244	
Goodness-of-method on F ²	1.258	
Final R indices [I > 2σ(I)]	R1 = 0.1097, wR2 = 0.2063	
R indices (all data)	R1 = 0.1473, wR2 = 0.2224	
Largest diff. peak and hole, eÅ ⁻³	0.629 and -0.20	



Chapter 2

**Synthesis, structural analysis and chiral investigations of new atropisomers
with *EE*-tetrahalogeno-1,3-butadiene core**

Table of contents

2.1.	Introduction	67
2.2.	Synthesis and analysis of chiral 1,3-dienes	71
2.2.1.	Synthesis of 1,3-oxazolidin-2-one-3-yl-1,3-dienes	72
2.2.2.	NMR and MS analysis of 1,3-oxazolidin-2-one-3-yl-1,3-dienes	74
2.2.3.	Solid state structural investigations of 1,3-oxazolidin-2-one-3-yl-1,3-dienes	76
2.2.4.	Synthesis of bis(polyethyleneoxy)-tetrahalo-1,3-dienes	82
2.2.5.	NMR and MS analysis of bis(polyethyleneoxy)-tetrahalo-1,3-diene	83
2.3.	Chiral structural investigations for 1,3-oxazolidin-2-one-3-yl-tetrahalo-1,3-dienes	85
2.3.1.	Chromatography on chiral support	86
2.3.1.1.	Chiral HPLC separation of 1,3-oxazolidin-2-one-3-yltetraiodo-1,3-diene (2)	88
2.3.1.2.	Chiral HPLC separation of 1,3-oxazolidin-2-one-3-yl-tetrabromo-1,3-diene (3)	89
2.3.1.3.	Resolution of 1,3-oxazolidin-2-one-3-yl-tetrachloro-1,3-diene (4)	91
2.3.2.	Determination of the rotation barriers by DHPLC	92
2.3.2.1.	Rate of racemization for the isolated enantiomers of 1,3-oxazolidin-2-one-3-yl-tetraiodo-1,3-diene (2)	92
2.3.2.2.	Rate of racemization for the isolated enantiomers of 1,3-oxazolidin-2-one-3-yl-tetrabromo-1,3-diene (3)	93
2.3.2.3.	Estimation of the enantiomerization barrier for 1,3-oxazolidin-2-one-3-yl-tetrabromo-1,3-diene (3) using Schurig equation	95
2.3.3.	Determination of the enantiomerization barriers by dynamic NMR experiments	97
2.3.4.	Correlations between halogens and rotation barriers in 2 – 4	99
2.4.	Assignment of the absolute configuration	102
2.5.	Conclusions	107
2.6.	Experimental part	108
2.6.1.	General remarks	108
2.6.2.	Synthesis and characterization of compounds	110
	Annexes	120

2.1. Introduction

Axially chiral compounds represent important target in organic chemistry¹ due to their interesting stereochemistry and their potential use as ligands for catalyze in asymmetric synthesis.²

The first resolution as atropisomers of 6,6'-dinitro-2,2'-diphenic acid³ enantiomers opened a new path for investigation of various compounds exhibiting atropisomerism. Their high enantiomeric stability and racemization barriers are of a great importance in the field of organic chemistry.⁴

Atropisomerism and axial chirality in the case of highly substituted 1,3-dienes is due to the non planarity caused by bulky substituents which hinder the formation of *s-cis* (*cisoid*) and *s-trans* (*transoid*) coplanar conformations.⁵ Atropisomers are stereoisomers resulted from hindered rotation about single bonds where the barrier to rotation is high enough to allow the isolation of the conformers.

Chirality of non planar butadienes was introduced by Kobrich et al.⁶, demonstrated by ¹H-NMR spectroscopy based on the anisochronism of the prochiral substituents revealed by signal splitting in the presence of an optically active chemical shift reagent⁷, but also differentiated by chromatography on optically active stationary phases, such as triacetylcellulose.⁸

Non substituted acyclic diene molecules may exist in *s-cis* or *s-trans* conformation (Fig. 1). It is generally accepted that the planar *s-trans* conformation is the global minimum, separated from the *s-cis* rotamer by a barrier of some 6-7 kcal/mol.⁹

¹ Eliel, E. L.; Wilen, S. H. *Stereochemistry of Organic Compounds*, Wiley, New-York, **1994**, p. 1142

² Clayden, J. *Angew. Chem. Int. Ed.* **1997**, *36*, 949-951

³ Christie, G.H.; Kenner, J. H. *J. Chem. Soc.* **1922**, *121*, 614

⁴ a) Roussel, C.; Vanthuynne, N.; Bouchekara, M.; Djafri, A.; Elguero, J.; Alkorta, I. *J. Org. Chem.* **2008**, *73*, 403-411; b) Vanthuynne, N.; Andreoli, F.; Fernandez, S.; Roman, M.; Roussel, C. *Lett. Org. Chem.* **2005**, *2*, 433-443; c) Roussel, C.; Popescu, C. *Chirality* **1994**, *6*, 251-260.; d) Roussel, C.; Stein, J.L.; Beauvais, F. *New J. Chem.* **1990**, *14*, 169-173

⁵ Rosner, M. and Kobrich, G. *Angew. Chem.* **1974**, *86*, 775-776; *Angew. Chem. Int. Ed.* **1974**, *13*, 741-742

⁶ Kobrich, G.; Mannschreck, A.; Misra, R.A.; Rissmann, G.; Rosner, M.; Zundorf, W. *Chem. Ber.* **1972**, *105*, 3794-3806

⁷ Mannschreck, A.; Jonas, V.; Bodecker, H.O.; Elbe, H.L.; Kobrich, G. *Tetrahedron Lett.* **1974**, 2153

⁸ Becher, G. and Mannschreck, A. *Chem. Ber.* **1981**, *114*, 2365-2368

⁹ Squillacote, M.E.; Liang, F. *J. Org. Chem.* **2005**, *70*, 6564-6573

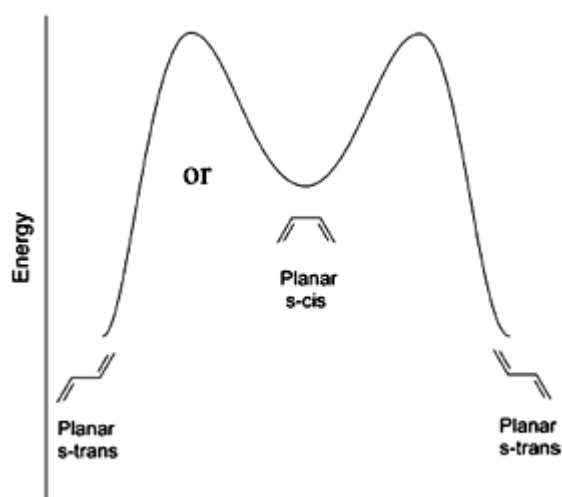


Fig. 1. Planar conformations of non substituted acyclic dienes

Nonplanar substituted 1,3-dienes belong to point group C_2 or C_1 and are always chiral. Dynamic experiments and molecular modeling indicate a considerably higher barrier of the inversion through the *s-cis* form.¹⁰ The bulky substituents slow down the rotation about the chiral axis and thus interconversion of the enantiomers takes place via *s-trans* transition (achiral coplanar conformation) (Fig. 2) corresponding to a partial rotation around the central bond.^{11,12}

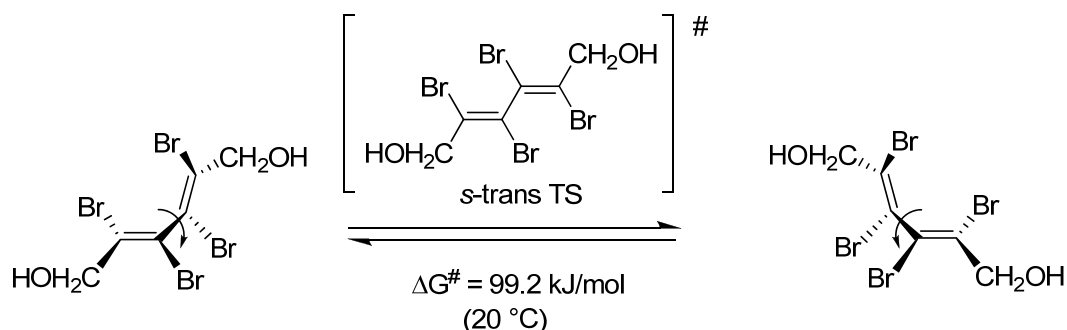


Fig. 2. Enantiomer interconversion of substituted butadienes

The considerable dependence of the rotation barriers around the central C-C single bond, upon the size of terminal substituent and the nature of internal substituents, is discussed in terms of buttressing effect. Barriers to rotation $\Delta G_{\text{rot}}^\ddagger$, determined by NMR spectroscopy at 140°C for some dihalo-1,3-dienes, increase in the series from chloro- to iodo-derivative (Table 1): 87.92 KJ/mol (chloro-), >92.10 KJ/mol (bromo-), >100.48 KJ/mol (iodo).⁵ In the case of tetrahalo-1.3-

¹⁰ a) Devaquet, A. J. P.; Townshend, R. E.; Hehre, W. J. *J. Am. Chem. Soc.* **1976**, *98*, 4068-4076, b) Bachrach, S. M.; Liu, M. *J. Am. Chem. Soc.* **1991**, *113*, 7929-7937; c) Hansen, A. E.; Bak, K. L. *J. Phys. Chem. A* **2000**, *104*, 11362-11370

¹¹ Kobrich, G.; Kolb, B.; Mannschreck, A.; Misra, R.A. *Chem. Ber.* **1973**, *106*, 1601-1611

¹² Mannschreck, A.; Mintas, M.; Becher, G.; Stühler, G. *Angew. Chem.* **1980**, *92*, 490-491

dienes (Table 2) the barrier to rotation is due to the bulky outlying substituents and an increase of this barrier was observed and interpreted as a buttressing effect of these groups.^{13,14,15}

Table 1. Rotation barrier for dihalo-dienes

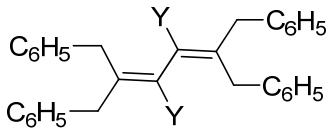
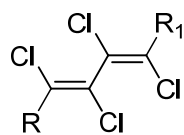
Y	ΔG^\ddagger Kobrlich ⁵ at 140°C
	
I	>100.48 kJ/mol
Br	>92.10 kJ/mol
Cl	87.92 kJ/mol

Table 2. Rotation barriers for several buttressed tetrachloro-dienes

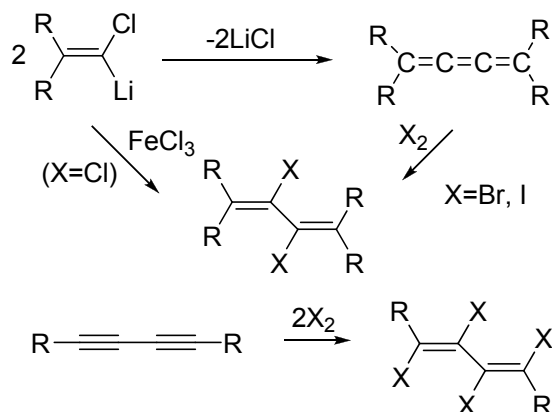
R	R ₁	ΔG^\ddagger (dienes)
		
CH ₂ C ₆ H ₅	H	55.23 kJ/mol at -7°C
Si(CH ₃) ₂ C ₆ H ₅	Si(CH ₃) ₂ C ₆ H ₅	65.68 kJ/mol at 12°C
CH ₂ C ₆ H ₅	Si(CH ₃) ₂ C ₆ H ₅	69.87 kJ/mol at 72°C
OCH ₃	OCH ₃	70.29 kJ/mol at 54°C
CH ₂ C ₆ H ₅	CH ₂ C ₆ H ₅	73.64 kJ/mol at 79°C

¹³ Bodecker, H.O.; Jonas, V.; Kolb, B.; Mannschreck, A.; Kobrlich, G. *Chem. Ber.* **1975**, *108*, 3497-3508

¹⁴ Becher, G.; Mannschreck, A. *Chem. Ber.* **1983**, *116*, 264-272

¹⁵ Elbe, H.-L.; Köbrlich, G. *Chem. Ber.* **1974**, *107*, 1654-1666

Chiral halo-1,3-dienes bearing chlorine and bromine can be obtained by oxidative coupling reactions of vinyl derivatives or by halogen addition reactions to diynes or cumulenes (Scheme 1).^{8,12,16}



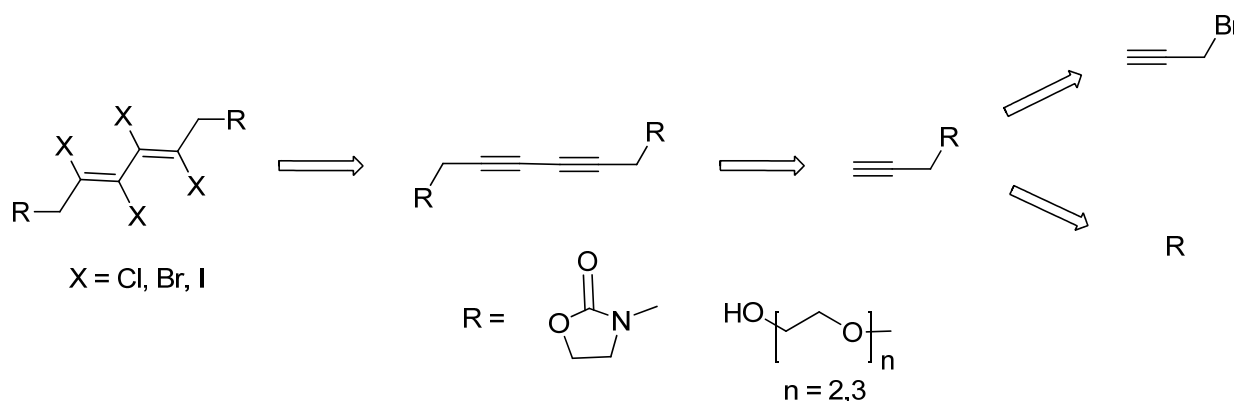
Scheme 1. Synthesis of halo-1,3-dienes

Atropisomerism is significant because induces a chirality element in the absence of stereogenic atoms. Atropisomers are of great interest in asymmetric synthesis, asymmetric catalysis as well as in natural product chemistry. We have considered of interest the development of investigations in the field of chiral 1,3-dienes by obtaining new chiral tetrahalo-1,3-dienes, to determine their structure, to separate the enantiomers, to measure the barriers of racemization and to determine the absolute configuration of the enantiomers.

¹⁶ Rosner, M. and Kobrich, G. *Angew. Chem.* **1975**, *19*, 715-717

2.2. Synthesis and analysis of chiral 1,3-dienes

We have proposed the synthesis, analysis and structure investigation of some new chiral 1,3-dienes bearing different substituents. The followed route consists in three steps: synthesis of the starting materials with terminal alkyne units, oxidative coupling dimerization with the obtainment of the corresponding 1,3-diynes and final halogen addition to the two triple bonds (Scheme 2).



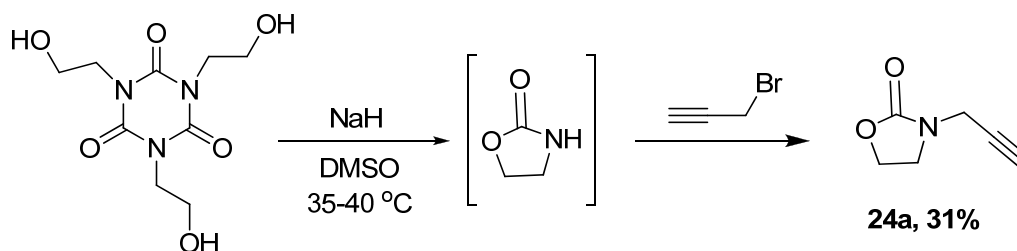
Scheme 2. Route for the synthesis of 1,3-dienes

New chiral 1,3-dienes with different internal substituents have been obtained in low to moderate yields. Their synthesis, analysis by NMR spectroscopy and mass spectrometry are presented.

2.2.1. Synthesis of 1,3-oxazolidin-2-one-3-yl-1,3-dienes

3-(prop-2'-ynyl)-Oxazolidin-2-one **24a** (Chapter 1, Scheme 18) has been previously obtained from 2-oxazolidinone with sodium hydride in tetrahydrofuran (THF) or dimethylformamide (DMF).¹⁷ We have managed to obtain this compound from the reaction of 1,3,5-tris(2-hydroxyethyl)cyanuric acid and propargylbromide in presence of sodium hydride (Chapter 1, Scheme 18).

Formation of compound **24a** requests as first step the transposition reaction of 1,3,5-tris(2-hydroxyethyl)cyanuric acid to 2-oxazolidone followed by *in situ* reaction with propargylbromide (Scheme 3). This type of reaction was already reported^{18,19} using sodium hydride as base in DMF but at higher temperatures.



Scheme 3. Synthesis of 3-(prop-2'-ynyl)-oxazolidin-2-one **24a**

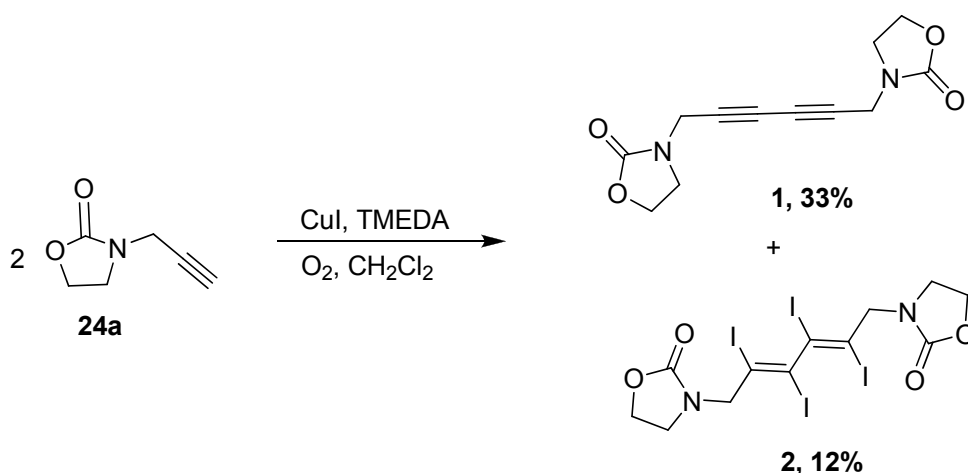
Compound **24a** was obtained in various yields depending on the conditions employed for the reaction (Chapter 1). Therefore we could achieve its synthesis as major product up to 31% yields, by modifying the temperature of the reaction. Separation of the desired compound was achieved by column chromatography using ethyl acetate/pentane 1/2 as eluent.

1,6-Bis(1',3'-oxazolidin-2'-one-3'-yl)-2,4-hexadiyne **1** is accessible by acetylene coupling of **24a** under Hay's reaction conditions, in dichloromethane at room temperature and with a large excess of copper(I) iodide. Diyne **1** was obtained in a mixture with tetraiodo-1,3-diene **2** as byproduct (Scheme 4). The two products of the reaction **1** and **2** were subjected to column chromatography to afford pure compounds in 33% (**1**) and 12% (**2**) yield, respectively.

¹⁷ Wei, L.L.; Xiong, H.; Douglas, C.J. and Hsung, R.P. *Tetrahedron Letters*, **1999**, 40, 6903-6907

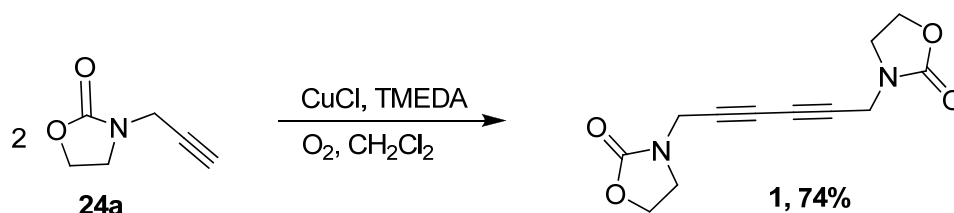
¹⁸ Cummins, R.W. *J. Org. Chem.* **1963**, 28, 85-89

¹⁹ Frazier, T.C.; Little, E.D. and Lloyd, B.E. *J. Org. Chem.* **1960**, 15, 1944-1946



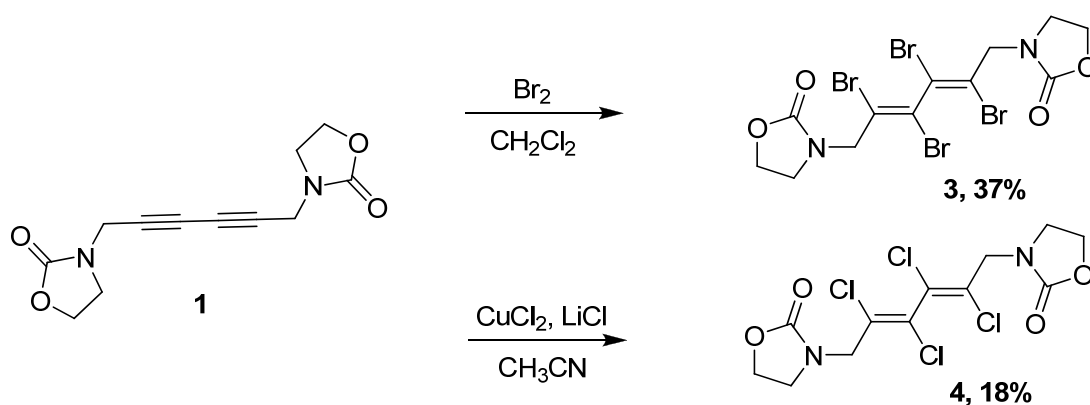
Scheme 4. Synthesis of compounds **1** and **2**

1,6-Bis(1',3'-oxazolidine-2'-one-3'-yl)-2,4-hexadiyne **1** could be obtained as single reaction product in higher yields, up to 74%, using similar reaction by replacing CuI(I) with CuCl(I) thus avoiding the formation of unwanted byproducts (Scheme 5).



Scheme 5. Synthesis of compound **1**

Tetrabromo- and tetrachloro- 1,3-dienes (**3** and **4**) were synthesized as single *EE*-isomers by direct halogen addition to the corresponding 1,6-Bis(1',3'-oxazolidine-2'-one-3'-yl)-2,4-hexadiyne **1** (Scheme 6). The use of copper(II) chloride and lithium chloride for chlorine addition decreases significantly the yield for this type of reaction.



Scheme 6. Synthesis of 2,3,4,5-tetrabromo- et tetrachloro-1,6-bis(1',3'-oxazolidin-2'-one-3'-yl)-2,4-hexadiene **3** and **4**

2.2.2. NMR and MS analysis of 1,3-oxazolidin-2-one-3-yl-1,3-dienes

$^1\text{H-NMR}$ and $^{13}\text{C-NMR}$ spectroscopy together with mass spectrometry confirm the anticipated structure for these 1,3-oxazolidin-2-one-derivatives. Proton spectroscopic data of compound **1** show well-defined signals for each type of proton in accordance with the symmetrical structure of the molecule. $^1\text{H-NMR}$ spectra clearly reveals the chirality of these compounds by non-equivalence of the protons at position 4' (4'') of the heterocyclic ring which are diastereotopic (Fig. 3).

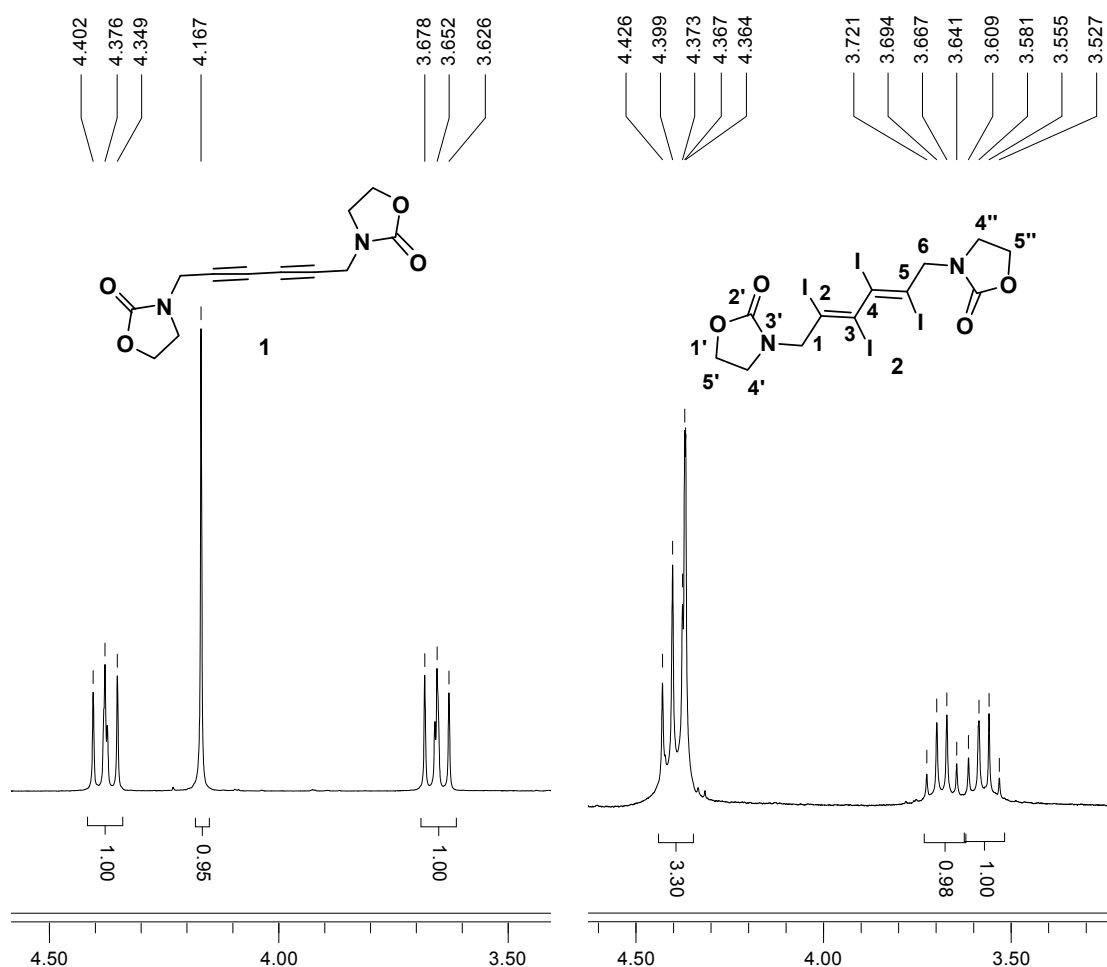


Fig. 3. Fragment of $^1\text{H-NMR}$ spectra of diyne **1** (left) and tetraiodo-1,3-diene **2** (right) (CDCl_3 , 300 MHz)

Comparison between proton spectra of tetrabromo-1,3-diene **3** and tetraiodo-1,3-diene **2** shows a unique pattern for signal splitting corresponding to diastereotopic protons at position 4' (4'') (Fig. 4). Switching from iodine to bromine proton spectrum shows a superposition of the diastereotopic protons signals (at position 4' (4'')), due to smaller internal substituents ($\text{I} > \text{Br} >$

Cl) and thus less sterical hindrances, effect further observed in the case of tetrachloro-derivative (4).

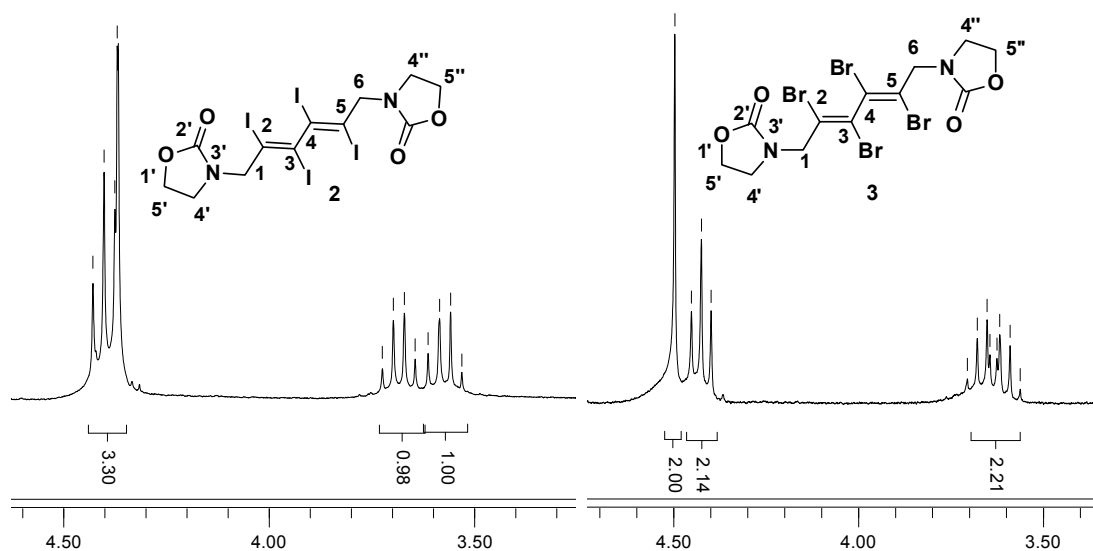


Fig. 4. Fragment of ^1H -NMR spectra of **2** (left) and **3** (right) (CDCl_3 , 300 MHz)

^1H -NMR spectra of these compounds recorded in deuterated chloroform (CDCl_3) do not differentiate the diastereotopic protons at position 1(6) and 5'(5''), displaying unique signals. Changing CDCl_3 with deuterated benzene (C_6D_6), a shift in signals positions was observed in the proton spectra, showing at room temperature different signals for diastereotopic protons (non-equivalent protons 1(6) and 4'(4'')) in the molecule (Fig. 5). These experiments reveal important ASIS (Aromatic Solvent Induced Shifts)²⁰ effects for the NMR spectra of **2** - **4**. As an example the ^1H NMR spectrum of **4** (Figure 5) exhibits an AB system ($\delta_{1,6} = 3.92$, $\delta'_{1,6} = 3.81$ ppm; $J = 15.4$ Hz) for the protons of the CH_2 groups connected to the diene units and two overlapped doublets of doublets of doublets ($\delta_{5',5''} = 3.275$, $\delta'_{5',5''} = 3.272$ ppm; $J = J' = 8.1$; $J'' \approx 0$ Hz) and two doublets of doublets ($\delta_{4',4''} = 2.51$, $\delta'_{4',4''} = 2.35$ ppm; $J = 15.7$, $J' = 8.1$; $J'' \approx 0$ Hz) for the protons at positions 5'(5'') and 4'(4''), respectively. In the case of proton at position 5'(5'') similar situations were observed for some N-substituted-1,3-oxazolidone derivatives bearing – $\text{CH}_2\text{-R}^*$ groups ($\text{R}^* = \text{chiral substituent}$).²¹

²⁰ a) Stewart, W. E.; Siddall, T. H. *Chem. Rev.* **1970**, *70*, 517-551; b) Roussel, C.; Liden, A.; Chanon, M.; Metzger, J.; Sandstrom, J. *J. Am. Chem. Soc.* **1976**, *98*, 2847-2852; c) Liden, A.; Roussel, C.; Liljefors, T.; Chanon, M.; Carter, R. E.; Metzger, J.; Sandstrom, J. *J. Am. Chem. Soc.* **1976**, *98*, 2853-2860; d) Grosu, I.; Plé, G.; Mager, S.; Martinez, R.; Mesaros, C.; Camacho, B. C. *Tetrahedron* **1997**, *53*, 6215-6232.; e) Mesaros, E.; Grosu, I.; Mager, S.; Plé, G.; Farcas, S. I. *Monatsh. Chem.* **1998**, *129*, 723-733

²¹ Ng, S.S.; Ho, C.Y.; Jamison, T.F. *J. Am. Chem. Soc.* **2006**, *128*, 11513-11528

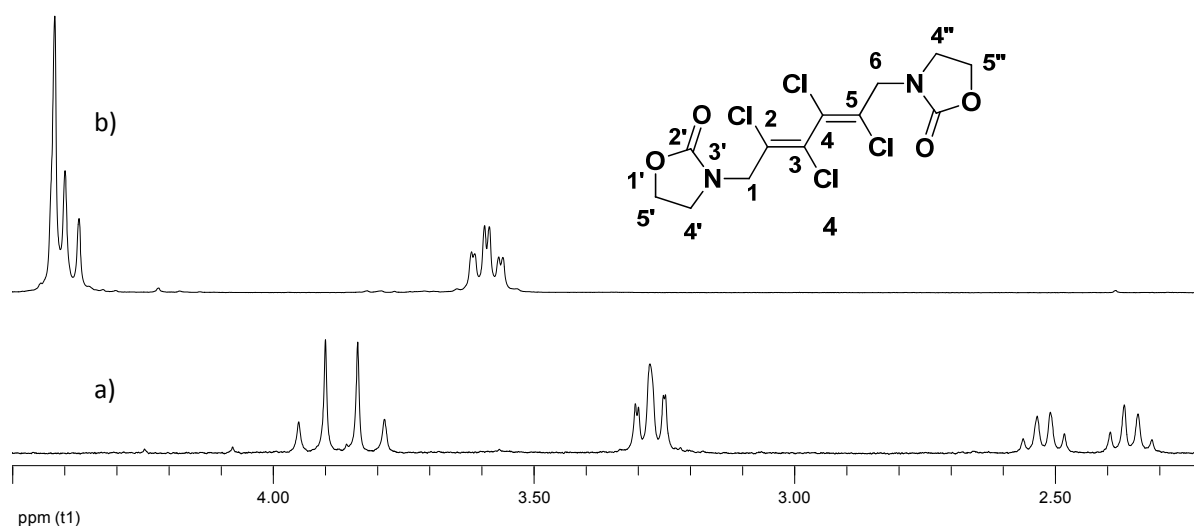


Fig. 5. $^1\text{H-NMR}$ of compound **4** at room temperature in C_6D_6 (a) and CDCl_3 (b) (300 MHz)

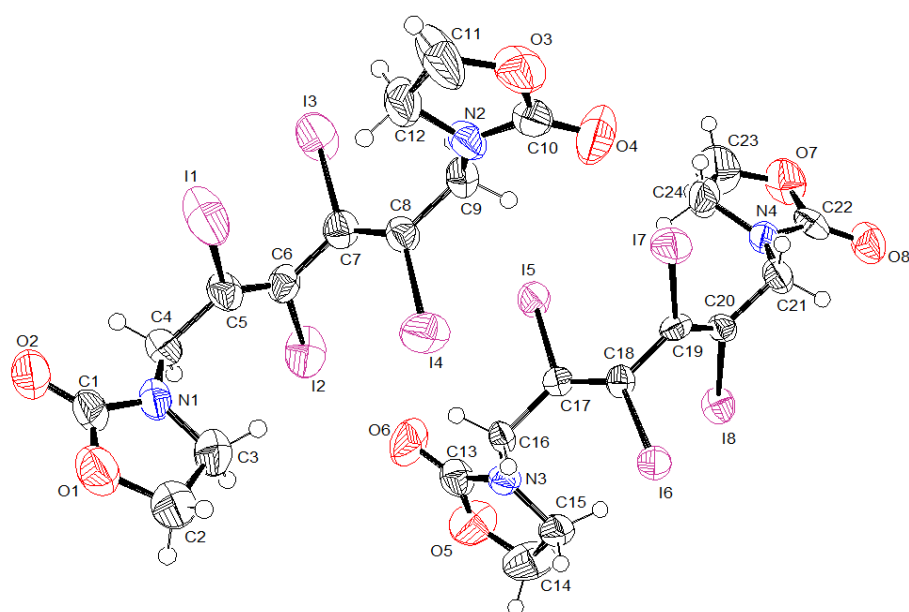
ESI-MS and EI-MS spectra of these compounds show signals for the molecular peak but also for the Na^+ complexes (Table 3).

Table 3. Relevant ESI-MS and EI-MS data

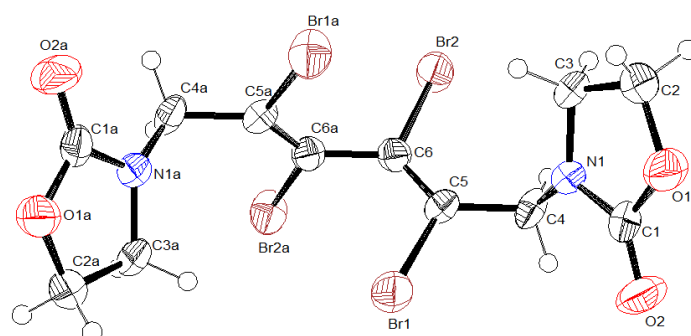
Compd.	Exact mass	m/z LR ESI-MS		m/z (%) EI-MS
		$[\text{M}+\text{H}]^+$	$[\text{M}+\text{Na}]^+$	
2 (I)	755.70	564.7	587.7	
3 (Br)	563.75	756.7	778.6	
4 (Cl)	390.05			354.5 (M^+-Cl)

2.2.3. Solid state structural investigations of 1,3-oxazolidin-2-one-3-yl-1,3-dienes

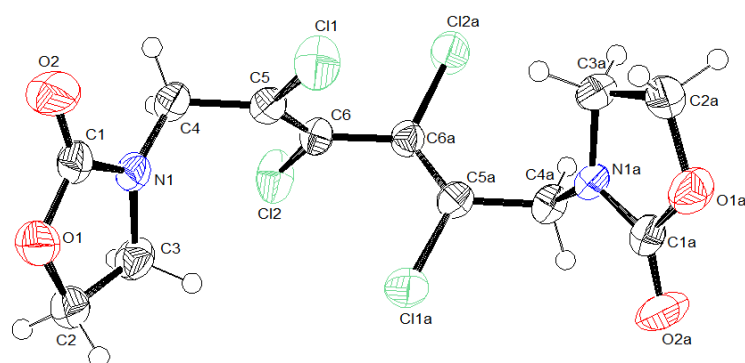
Single crystal molecular structures for **2-4** (Fig. 6) were obtained by X-ray diffraction using suitable crystals obtained from double layered $\text{CHCl}_3/\text{hexane}$ solutions. The presence of the two enantiomers could be observed in the lattice of the crystal. The molecular structures reveal perpendicular orientation for the planes of the double bonds (torsion angles in the range $88.33\text{-}91.13^\circ$). Tetraiodo-1,3-diene presents two different types of molecules in the crystal due to the packing effects seen by the interatomic distances, bond and angles in the lattice.



Compound 2



Compound 3



Compound 4

Fig. 6. ORTEP diagrams for compounds 2, 3 and 4

The perpendicular orientation of the double bonds in the molecule and the ground strains induced by the methylene-1,3-oxazolidine-2-one groups determine a diminishing of the bond

angles $X^1-C^5-C^6$ ($X^{1a}-C^{5a}-C^{6a}$) and $C^{6a}-C^6-X^2$ ($C^6-C^{6a}-X^{2a}$) correlated with the van der Waals radii (vdW) of the halogens. Compound **2** bond angles $X^1-C^5-C^6$ ($X^{1a}-C^{5a}-C^{6a}$) are higher than expected probably due to spatial intramolecular halogen-hydrogen interactions [$X^2-H(C^3)$; $X^{2a}-H(C^{3a})$] which can be appreciated by the amplitude of the difference between the sum of the vdW of the atoms and the corresponding measured distances in the X-ray structure (Table 4).

Table 4. Values (°) of some selected bonds angles (the numbering corresponds to ORTEP diagrams).*

Compd.	Bond angles (°)		d [Distances (Å)]	
	$X^1-C^5-C^6$ $X^{1a}-C^{5a}-C^{6a}$	$C^{6a}-C^6-X^2$ $C^6-C^{6a}-X^2$	$X^2-H(C^3)$ $X^{2a}-H(C^{3a})$	$\Delta d = d-(r_x-r_H)$ (r_x and r_H are the vdW radii of X and H) **
2 (A)	118.01; 118.30	110.89; 112.72	2.903; 2.836	-0.288; -0.240
2 (A)	118.04; 119.18	110.49; 111.56	2.782; 2.830	-0.167; -0.234
3	116.27	112.00	2.784	-0.156
4	117.86	113.39	2.691	-0.149

*For **4** the crystal exhibits two type of molecules denoted with A and B (see Fig. 6)

** $r_H = 1.09$ Å; $r_{Cl} = 1.75$ Å; $r_{Br} = 1.85$ Å; $r_I = 1.98$ Å

Other supramolecular interactions were observed in the lattice of compound **2** which can also influence the values of the bond angles (Fig. 7). Thus halogen-halogen, proton-halogen, proton-carbonyl oxygen and halogen bonding (halogen-carbonyl oxygen interactions) which are smaller than the corresponding vdW radii sum are revealed in Table 5.

Table 5. Intramolecular interactions for compound **2**

Atoms		d [Distances (Å)]
I	I	3.784
I	O=C	2.982, 3.069, 3.143, 3.154, 3.360
I	H	3.101, 3.148
C=O	H	2.594, 2.614, 2.704
C	H	2.858

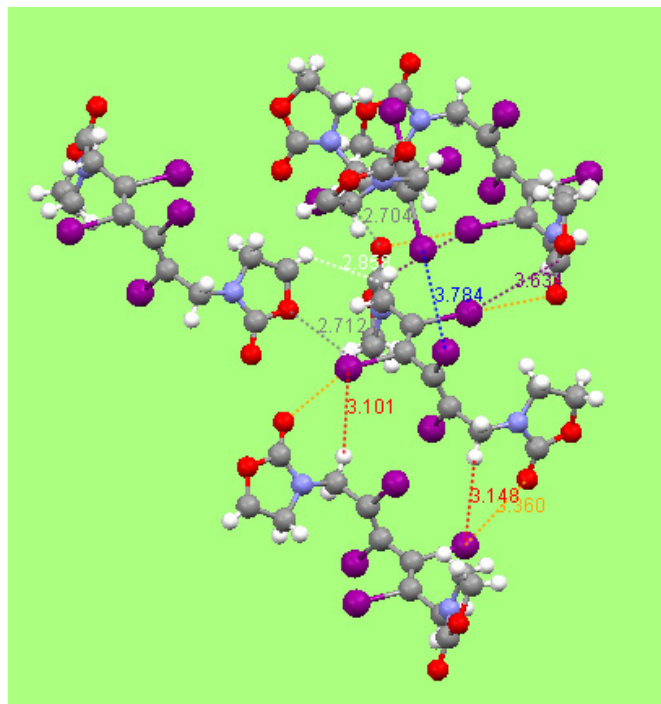


Fig. 7. Mercury view for intermolecular interaction of compound 2 lattice

Checking the associations of molecules in the lattices revealed for **3** and **4** layered structures (Fig. 8, Fig. 9) in which the $C^{4(4a)}$ -X bonds of different molecules exhibit antiparallel orientations generating favorable dipole-dipole interactions ($d_{C^{4(4a)}-X}$ of neighboring molecules are 3.943 Å for X=Br and 3.743 Å for X=Cl, respectively). In addition halogen-halogen interactions ($d_{Cl-Cl} = 3.454$ Å; $d_{Br-Br} = 3.550$ Å; type I interactions),²² $C^{4(4a)}$ -H---X ($d_{H-Br} = 2.985$, 3.020 Å and $d_{H-Cl} = 2.946$ Å) and $C^{2(2a),3(3a)}$ -H---O=C² interactions ($d_{H-O} = 2.652$; 2.639 Å for **4**) and halogen supramolecular bonding interactions (X---O=C²; $d_{Cl-O} = 3.225$ Å and $d_{Br-O} = 3.125$ Å) were observed (Table 6).^{23,24}

²² Bui, T.T.T.; Dahaoui, S.; Lecomte, C.; Desiraju, G.R.; Espinosa, E. *Angew. Chem. Int. Ed.* **2009**, *48*, 3838–3841

²³ a) Metrangolo, P.; Resnati, G.; Arman, H. D. *Halogen Bonding: Fundamentals and Applications*, Springer-Verlag, Berlin, **2008**; b) Metrangolo, P.; Meyer, F.; Pilati, T.; Resnati, G.; Terraneo G. *Angew. Chem. Int. Ed.* **2008**, *47*, 6114-6127; c) Zou, W.S.; Han, J.; Jin W.J. *J. Phys. Chem. A* **2009**, *113*, 10125-10132

²⁴ Csoregh, I.; Brehmer, T.; Bombicz, P.; Weber, E. *Cryst. Eng.* **2001**, *4*, 343–357

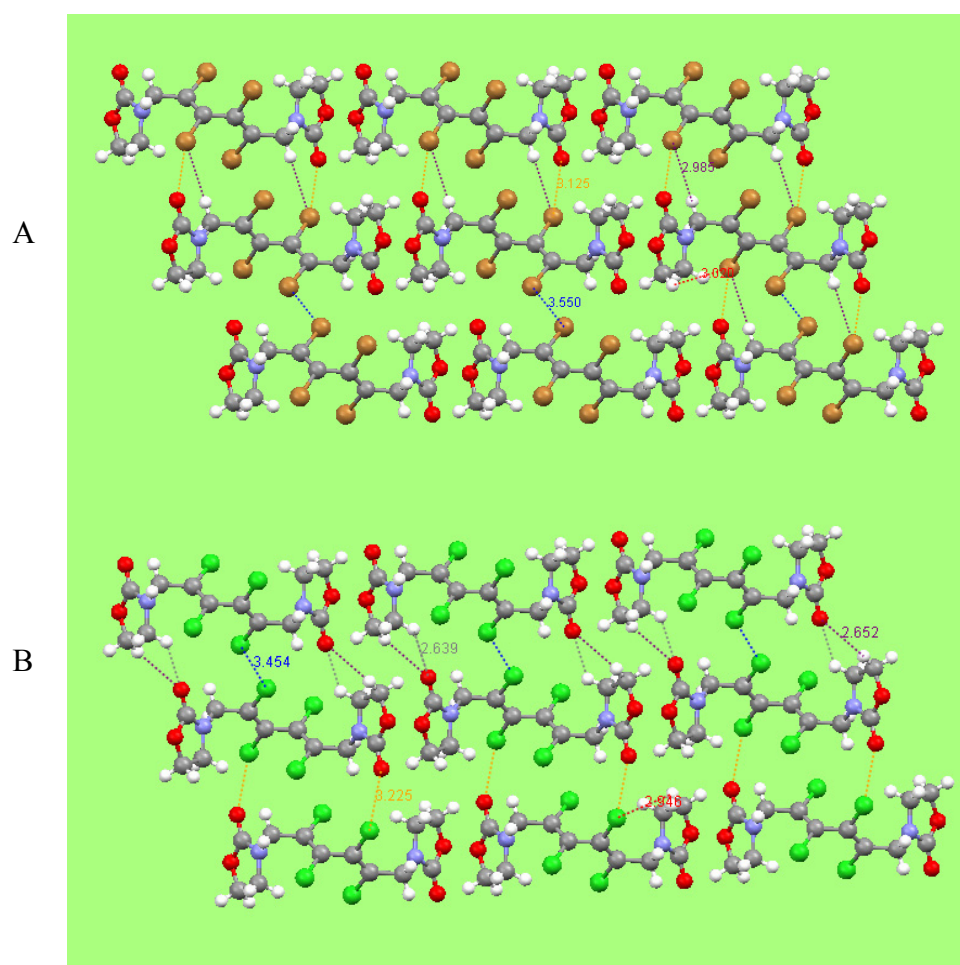


Fig. 8. Mercury view (along the axis b) of the lattice of A) **3** and B) **4**

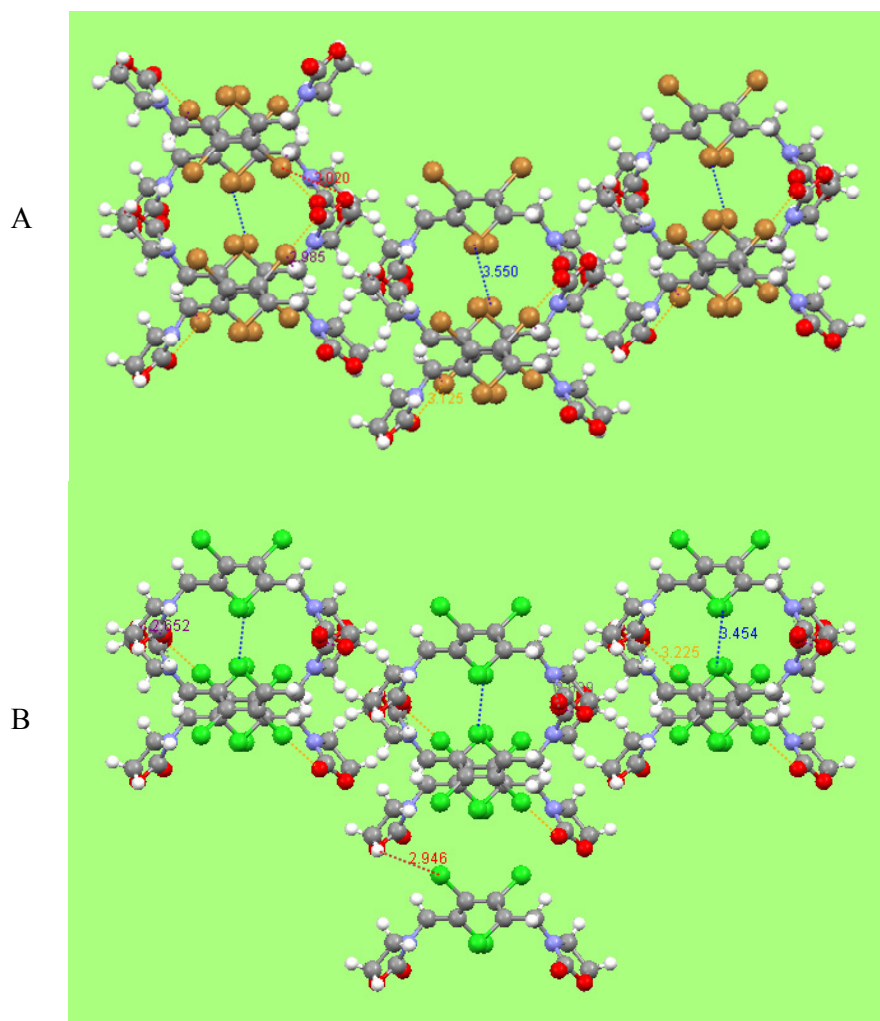


Fig. 9. Mercury view (along the axis *c*) of the lattice of A) **3** and B) **4**

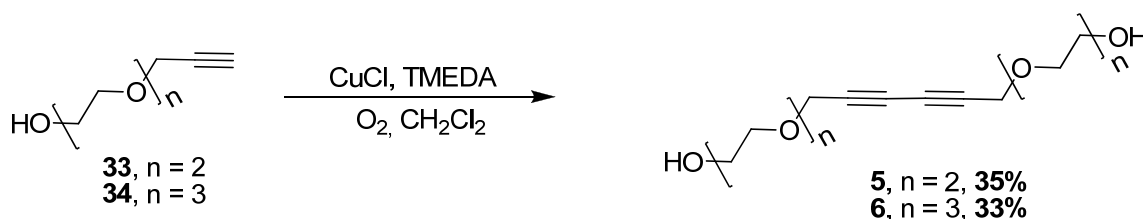
Table 6. Intramolecular interactions for compounds **3** and **4**

Compd.	Atoms		d [Distances (Å)]
3	Br	Br	3.550
	Br	H	2.985
	Br	H	3.020
	Br	O=C	3.125
	Br	C	3.943
	Cl	Cl	3.454
4	Cl	H	2.946
	Cl	O=C	3.225
	C=O	H	2.652, 2.639
	Cl	C	3.743

2.2.4. Synthesis of bis(polyethyleneoxy)-tetrahalo-1,3-dienes

Other substituted halo-1,3-dienes were synthesized in order to separate their enantiomers and to try to determine their absolute configuration by IR and VCD analysis, in comparison with the previous ones. Thus previously obtained precursor, alcohols with terminal alkyne units **2** and **3**, (Chapter 1, Scheme 12) were used for the synthesis of other halo-1,3-dienes. Following the same three steps synthetic route two other series of chiral halo-1,3-dienes have been synthesized and characterized.

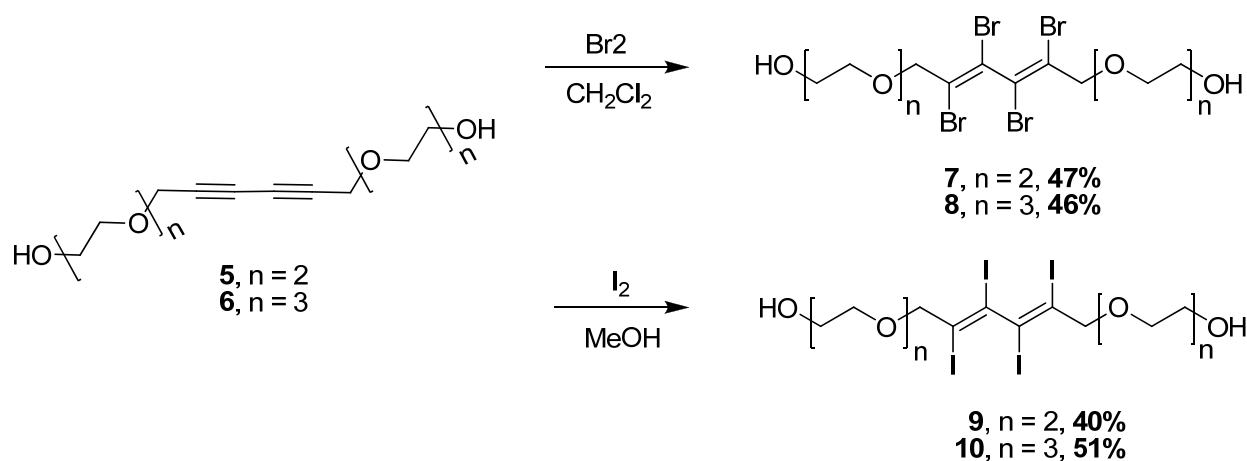
Earlier published diyne **5**²⁵ was obtained in moderate yields as well as diyne **6** by oxidative coupling reaction starting from mono-alkyne **33** and **34**, respectively (Scheme 7).



Scheme 7. Synthesis of diynes **5** and **6**

New tetrahalo-dienes (**7** - **10**) were synthesized by halogen addition to the corresponding diynes (Scheme 8). The reactions underwent stereoselectively with the formation of the *E,E* isomers.

²⁵ Wegner, G. *Makromolekulare Chemie* **1970**, 134, 219



Scheme 8. Synthesis of bis(polyethyleneoxy)-tetrahalo- and tetraiodo-1,3-dienes

2.2.5. NMR and MS analysis of bis(polyethyleneoxy)-tetrahalo-1,3-dienes

Structural investigations of compounds **7** - **10** were performed using NMR spectroscopy and ESI MS spectrometry. ^1H -NMR spectra clearly evidence the chirality of these compounds by presence of non-equivalent signals of the protons belonging to the CH_2 groups connected directly to the diene system (allylic positions). In this situation the spectrum should exhibit two doublets (AB system) for the protons of the allyl CH_2 groups (Fig. 10, Table 7) prove the hindrance for the rotation around the central bond in the diene unit.

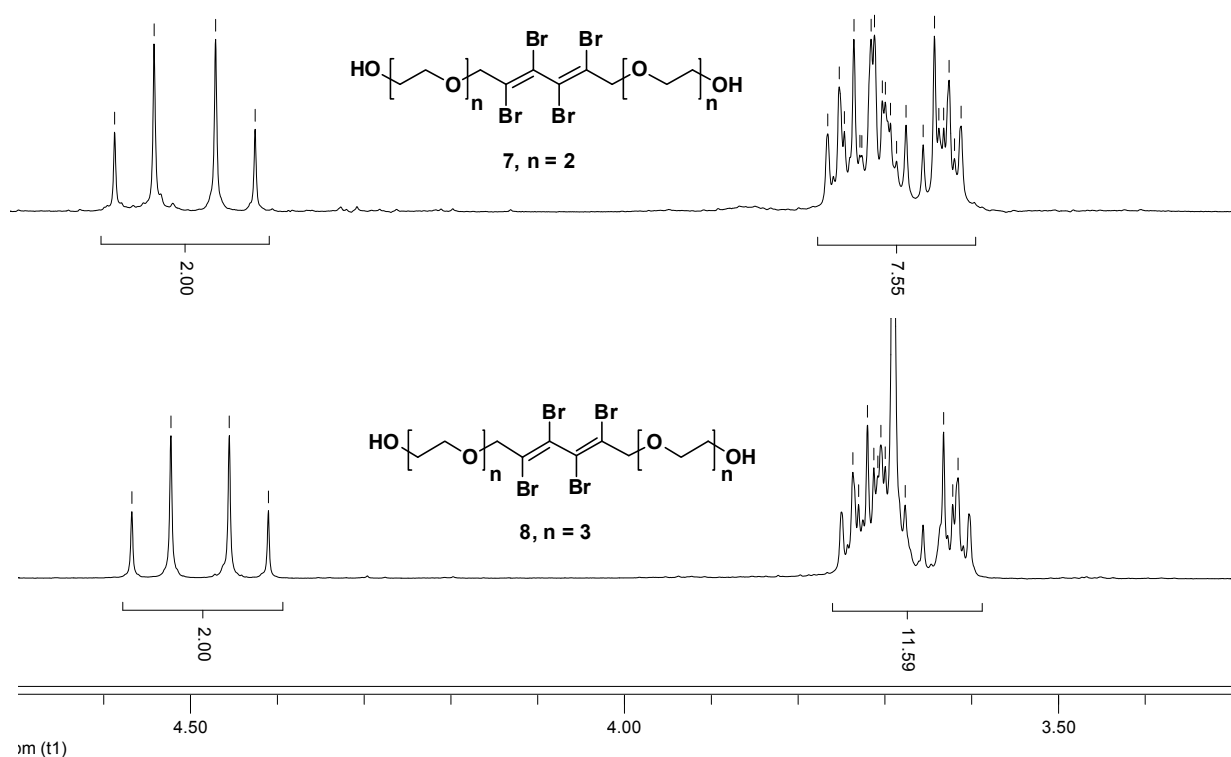


Fig. 10. ^1H -NMR fragment spectra of compounds **7** and **8** (CDCl_3 , 300 MHz)

Table 7. Relevant NMR data for **7 - 10**

Compd.	δ (ppm)		$\Delta\delta$ (ppm)	J (Hz)
	-CX=CX- CH(H)-	-CX=CX- CH(H)-		
7 (Br)	4.44	4.55	0.10	13.5
8 (Br)	4.43	4.54	0.09	13.5
9 (I)	4.30	4.40	0.10	13.5
10 (I)	4.28	4.38	0.10	13.5

The $^1\text{H-NMR}$ spectrum of **8** run at *rt* (Fig. 10) shows the two reference doublets at $\delta = 4.43; 4.53$ ppm ($J = 13.5$ Hz), while the signals for the other protons of the CH_2 groups could not be assigned and they are all overlapped in the range 3.6-3.75 ppm. Proton spectrum of this compound does not show any modifications of signals when heated up to 60 °C. This result is in agreement with the reported barriers of racemization for other chiral tetrabromo dienes⁷ and reveals the high stability of the atropenantiomers of these compounds.

ESI-MS spectra of these compounds show signal for the molecular peak and for the complexes formed with Na^+ (Table 8).

Table 8. LR ESI-MS data for compounds **5 - 10**

Compd.	Exact mass	m/z LR ESI-MS	
		$[\text{M}+\text{H}]^+$	$[\text{M}+\text{Na}]^+$
5	286.1	287.1	309.1
6	374.1	375.2	397.2
7 (Br)	605.9	606.7	628.8
8 (Br)	694.04	694.9	716.9
9 (I)	793.9	794.7	816.7
10 (I)	881.8	882.7	903.7

Enantiomers of these compounds will be separated by chiral chromatography and the pure enantiomers will be analyzed by IR and VCD spectra in order to determine their absolute configuration by means of signature bands corresponding to the butadiene core.

2.3. Chiral structural investigations for 1,3-oxazolidin-2-one-3-yl-tetrahalo-1,3-dienes

Chiral 1,3-dienes exist as a mixture of two enantiomers (Fig. 11) with non-planar conformation and which can interconvert through the *trans*-planar conformation. Highly substituted 1,3-dienes prefer a conformation with perpendicular arrangement of the double bonds thus ensuring the longest distance between the substituent and decreasing the steric hindrances between molecule fragments. The barrier to rotation is influenced by the geometry of the system, its mode of relaxation, the size and the steric constrains of the substituents.

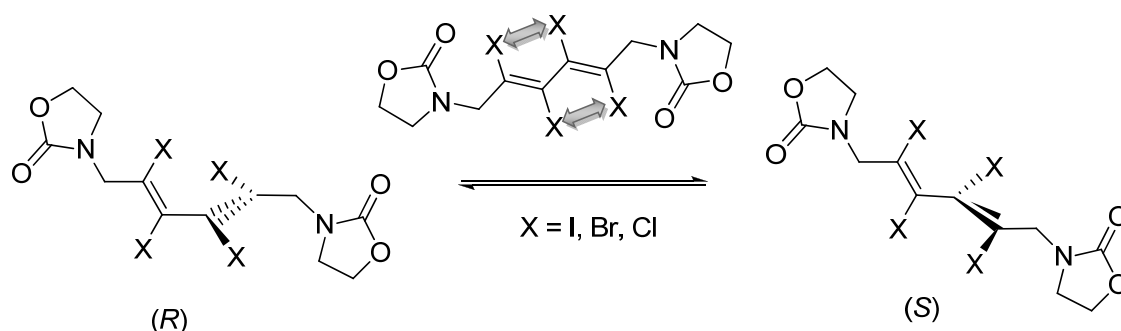


Fig. 11. *R, S* conformations of the tetrahalo-butadienes

Compounds **2**, **3** and **4** exist as a mixture of atropisomers with racemization energies depending on the substituents nature. The rate of partial rotation about the central C-C single bond can be estimated by dynamic NMR experiments, in the case of smaller internal substituents (Cl) and by polarimetry or chiral chromatography in the case of larger internal substituents (Br, I).

Proton spectra of these compounds, recorded in different deuterated solvents, displays two diastereotopic groups the -CH₂- from position 4' (4'') of the 1,3-oxazolidinone ring and the -CH₂- groups in position 1(6) (Fig. 12).

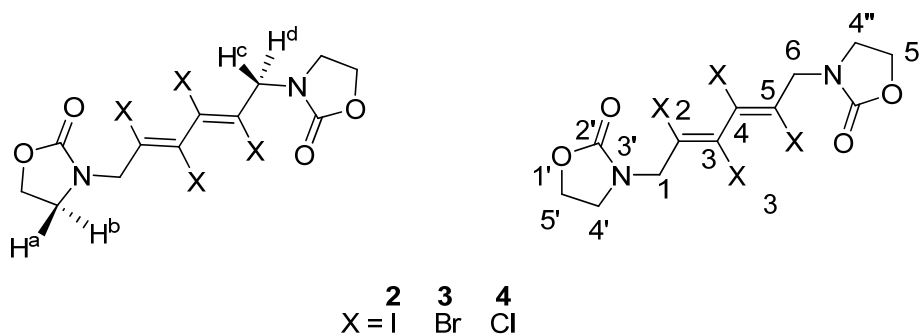


Fig. 12. Diastereotopic protons observed in NMR spectra of 1,3-oxazolidin-2-one-3-yl-tetrahalo-1,3-dienes

Resolution of these compounds via chiral HPLC and the determination of their activation barriers to enantiomerization are presented. The enantiomers of compounds **2** and **3** were resolved on several chiral stationary phases at variable temperature. As known from DNMR experiments, compound **4** presents a too low barrier for a separation at room temperature and accordingly a single peak was observed. Cryogenic chromatography²⁶ might be helpful in that case but no attempts were performed in that direction since the barrier was already available from NMR experiments.

2.3.1. Chromatography on chiral support

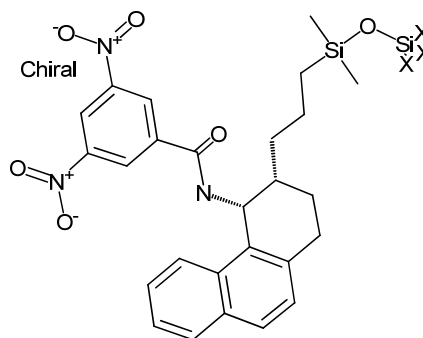
If the barrier to rotation is high enough ($\Delta G_{\text{rot}}^{\ddagger} > 100$ kJ/mol), the enantiomers of these compounds can be baseline separated by chiral HPLC at 25°C. They were isolated by semi-preparative chiral HPLC and the barriers to rotation were determined by a kinetic of enantiomerization of an optically pure enantiomer.

Resolution of 1,3-diene **2** and **3** enantiomers was achieved by chiral HPLC. Analytical separations of enantiomers were performed with 1 mL/min as flow-rate, detection using classic UV at 254 nm and on-line chiral detection by a polarimeter. Retention times R_t in minutes, retention factors $k_i = (R_{t_i} - R_{t_0})/R_{t_0}$ are given. R_{t_0} was determined by injection of tri-tert-butyl benzene. For the separation of the enantiomers we used different chiral stationary phases (Fig. 13). Chiralpak IC column from Daicel composed of cellulose *tris*(3,5-dichlorophenylcarbamate) immobilized on silica afforded baseline separation of the enantiomers of **2** and **3** at 25°C. In both cases the enantiomer with a (-) sign was eluted first on Chiralpak IC using various mixtures of Hexane-CHCl₃-EtOH.

²⁶ a) Gasparrini, F.; Grilli, S.; Leardini, R.; Lunazzi, L.; Mazzanti, A.; Nanni, D.; Pierini, M.; Pinamonti, M. *J. Org. Chem.* **2002**, *67*, 3089-3095; b) Wolf, C.; Tumambac, G.E. *J. Phys. Chem. A* **2003**, *107*, 815-817

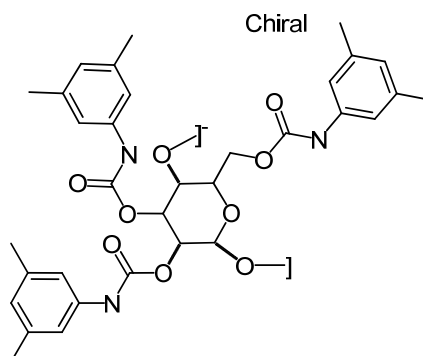
Whelk O1-(R,R)

(3*S*,4*R*)-4-(3,5-Dinitrobenzamido)-3-[3-(dimethylsilyloxy)propyl]-1,2,3,4-tetrahydrophenanthrene



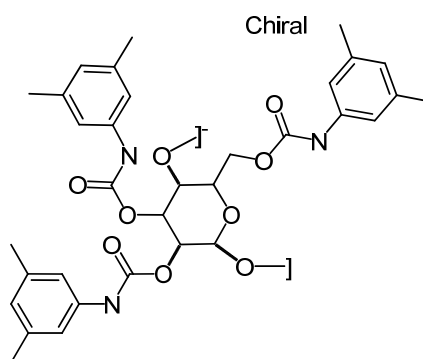
Chiralpak IA

Amylose tris(3,5-dimethylphenylcarbamate) immobilized on silica



Chiralcel IB

Cellulose tris(3,5-dimethylphenylcarbamate) immobilized on silica



Chiralpak IC

Cellulose tris(3,5-dichlorophenylcarbamate) immobilized on silica

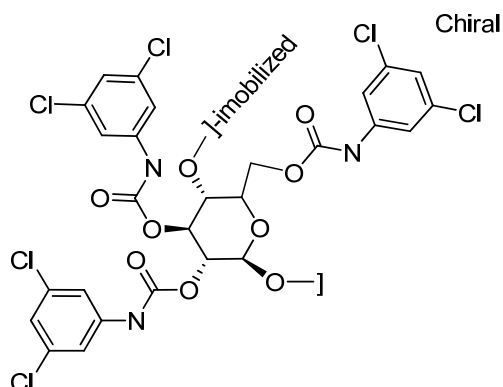


Fig. 13. Different chiral stationary phases

2.3.1.1. Chiral HPLC separation of 1,3-oxazolidin-2-one-3-yl-tetraiodo-1,3-diene (**2**)

Compound **2** was injected on the four columns with different eluting conditions, at 25°C, with 1 mL/min as flow-rate and detected by UV at 254 nm and by a polarimeter. Several stationary phases were tried in order to separate the enantiomers of tetraiodo-1,3-diene **2** (Table 9).

Table 9. Separation condition used of the compound **2**

Column type	Mobile phase	Rt ₁ (min)	Rt ₂ (min)	k ₁	k ₂	α	R _s
Chiralpak IC	Hexane/ethanol/CHCl ₃ 3/3/1	28.89 (-)	34.71 (+)	8.32	10.20	1.23	3.04
	Ethanol/CHCl ₃ 1/1	5.80 (-)	6.47 (+)	0.87	1.09	1.25	1.89
	Ethanol/CHCl ₃ /hexane 3/3/1	8.20 (-)	9.63 (+)	1.65	2.11	1.28	2.68
Chiralpak IB	Hexane/CHCl ₃ 1/1	23.97	23.97	6.73	6.73	1	0
Chiralpak IA	Hexane/CHCl ₃ 1/1	26.31	26.31	7.49	7.49	1	0
Whelk-O1 (R,R)	Hexane/ethanol/CHCl ₃ 3/3/1	13.95	13.95	3.50	3.50	1	0
	Hexane/ethanol/CHCl ₃ 1/1/1	9.18	9.18	1.96	1.96	1	0

The tetraiodo derivative (**2**) was separated on Chiralpak IC with a mixture ethanol/CHCl₃/hexane 3/3/1 as mobile phase; the enantiomers are baseline separated with short retention times (Fig. 14).

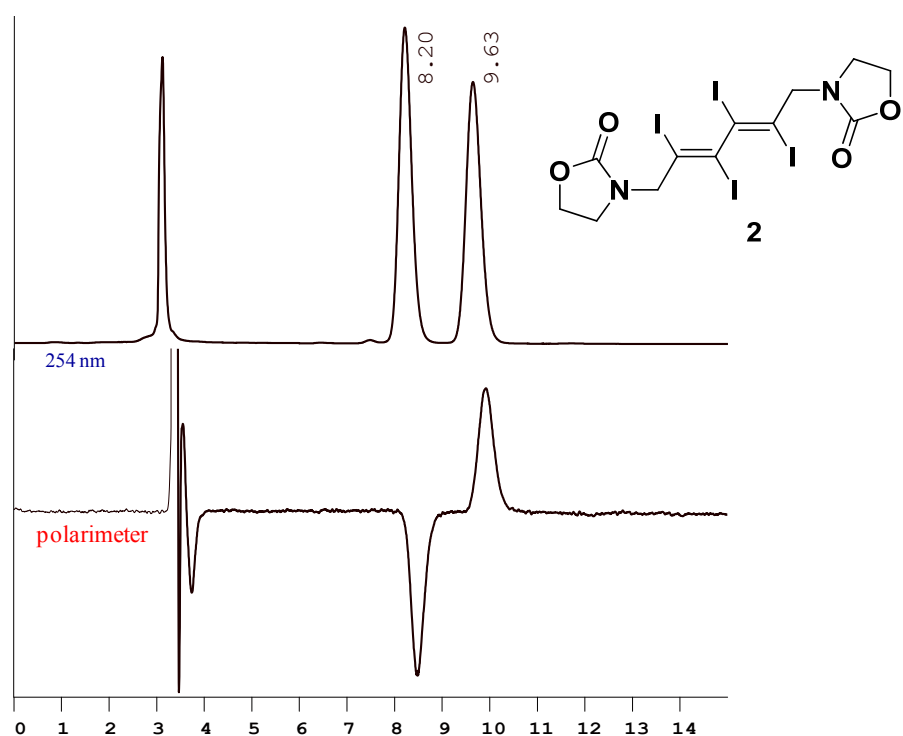


Fig. 14. Enantiomers separation of tetraiodo-1,3-diene (2), UV and polarimeter detection

2.3.1.2. Chiral HPLC separation of 1,3-oxazolidin-2-one-3-yl-tetrabromo-1,3-diene (3)

Compound 3 was injected on the four columns with different eluting conditions, at 25°C, with 1 mL/min as flow-rate and detected by UV at 254 nm and by a polarimeter. Tetrabromo (3) is separated on Chiralpak IC, Chiralpak IA and Whelk-O1 (R,R). On Chiralpak IC and Chiralpak IA, the (-)-enantiomer is the first eluted. When we used Whelk-O1 (R,R) as stationary phase, the elution order is reversed (Table 10, Fig. 15).

Table 10. Separation condition used of the compound **3**

Column type	Mobile phase	Rt ₁ (min)	Rt ₂ (min)	k ₁	k ₂	α	Rs
Chiralpak IC	Hexane/ethanol/CHCl ₃ 3/3/1	28.67 (-)	34.97 (+)	8.25	10.28	1.23	3.49
	Ethanol/CHCl ₃ 1/1	5.75 (-)	6.41 (+)	0.85	1.07	1.25	1.28
	Ethanol/CHCl ₃ /hexane 3/3/1	7.92 (-)	9.32 (+)	1.56	2.01	1.29	2.88
Chiralpak IB	Hexane/CHCl ₃ 1/1	16.57	16.57	4.35	4.35	1	0
Chiralpak IA	Hexane/CHCl ₃ 1/1	18.39 (-)	20.29 (+)	4.93	5.55	1.12	1.79
Whelk-O1 (R,R)	Hexane/ethanol/CHCl ₃ 3/3/1	12.06 (+)	12.89 (-)	2.89	3.16	1.09	0.86
	Hexane/ethanol/CHCl ₃ 1/1/1	7.82 (+)	8.29 (-)	1.52	1.67	1.10	0.93

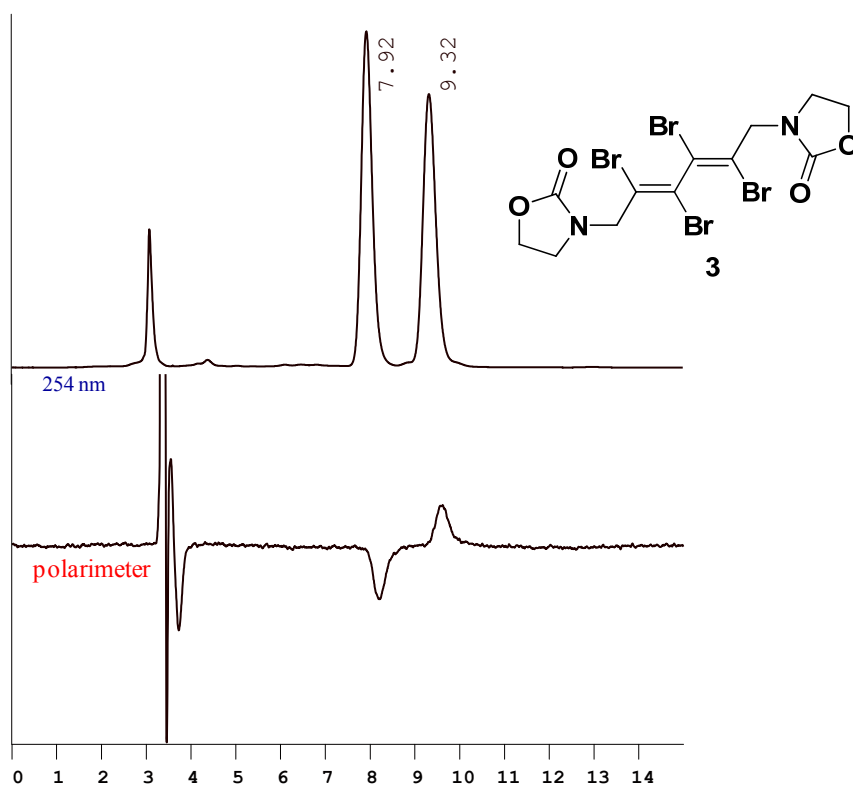


Fig. 15. Enantiomers separation of tetrabromo-1,3-diene (**3**), UV and polarimeter detection

2.3.1.3. Resolution of 1,3-oxazolidin-2-one-3-yl-tetrachloro-1,3-diene (4)

As in the case of tetraiodo- and tetrabromo-1,3-dienes, different stationary phases were tried in order to separate the enantiomers of the tetrachloro-1,3-diene (4) at room temperature (Table 11, Fig. 16).

Table 11. Separation condition used of the compound 4

Column type	Mobile phase	Rt ₁ (min)	Rt ₂ (min)	k ₁	k ₂	α	Rs
Chiralpak IC	Hexane/ethanol/CHCl ₃ 3/3/1	24.69	24.69	6.96	6.96	1	0
	Ethanol/CHCl ₃ 1/1	5.54	5.54	0.79	0.79	1	0
	Ethanol/CHCl ₃ /hexane 3/3/1	7.50	7.50	1.42	1.42	1	0
Chiralpak IB	Hexane/CHCl ₃ 1/1	14.65	14.65	3.73	3.73	1	0
Chiralpak IA	Hexane/CHCl ₃ 1/1	16.00	16.00	4.16	4.16	1	0
Whelk-O1 (R,R)	Hexane/ethanol/CHCl ₃ 3/3/1	10.97	10.97	2.54	2.54	1	0
	Hexane/ethanol/CHCl ₃ 1/1/1	7.38	7.38	1.38	1.38	1	0

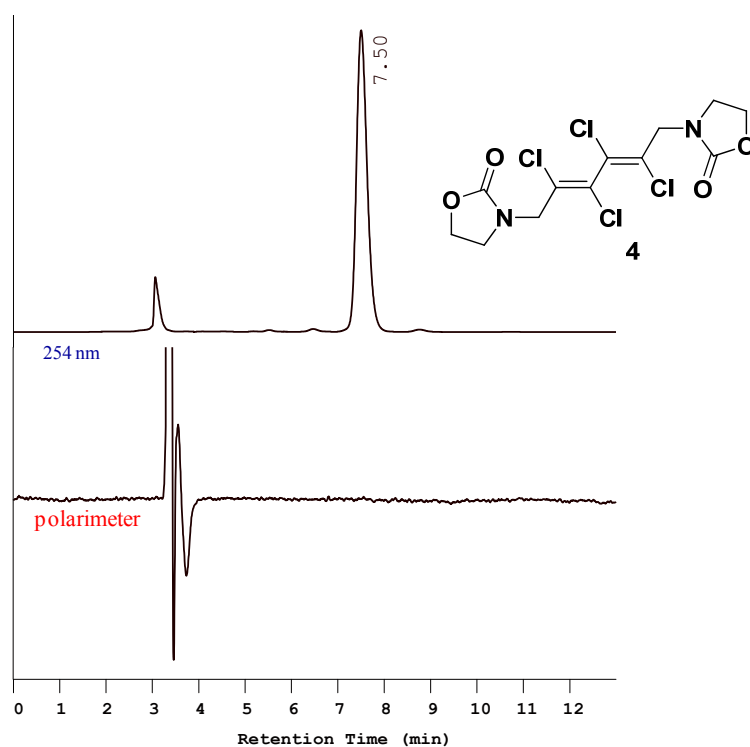


Fig. 16. UV and polarimeter detection in the case of tetrachloro-1,3-diene (4)

Tetrachloro derivative **4** could not be separated on chiral HPLC at 25°C. Compound **4** presents a too low barrier for a separation at room temperature and accordingly a single peak was observed.

2.3.2. Determination of the rotation barriers by DHPLC

Enantiomers of tetraiodo- and tetrabromo-1,3-dienes (**2** and **3**) were stable enough at room temperature to be isolated. About 2 mg of each enantiomer were collected by semi-preparative HPLC on Chiralpak IC, and thermal racemizations were performed on the single enantiomers in order to determine their energy barrier.

2.3.2.1. Rate of racemization for the isolated enantiomers of 1,3-oxazolidin-2-one-3-yl-tetraiodo-1,3-diene (2)

About 1.5 mg of (+)-enantiomer of the tetraiodo-1,3-diene **2** were diluted in 2 mL of chlorobenzene and heated to reflux. The enantiomeric excess was followed by chiral HPLC (Chiralpak IC, Ethanol/CHCl₃/hexane 3/3/1, 1 mL/min, UV detection at 254 nm) (Table 12).

Table 12. Rate of enantimerization in time for compound **2**

Time (min)	% enantiomer (+)	$\ln ((\%t-\%e)/(\%0-\%e))$
0	87.123	0.0000
150	85.461	-0.0458
345	83.377	-0.1064

The slope of the kinetic line gives the kinetic rate for enantiomerization where from we could deduce the barrier to rotation for tetraiodo-diene (**2**): $\Delta G_{\text{rot}}^{\ddagger} = 143 \pm 1$ kJ/mol at 131°C in chlorobenzene (Fig. 17).

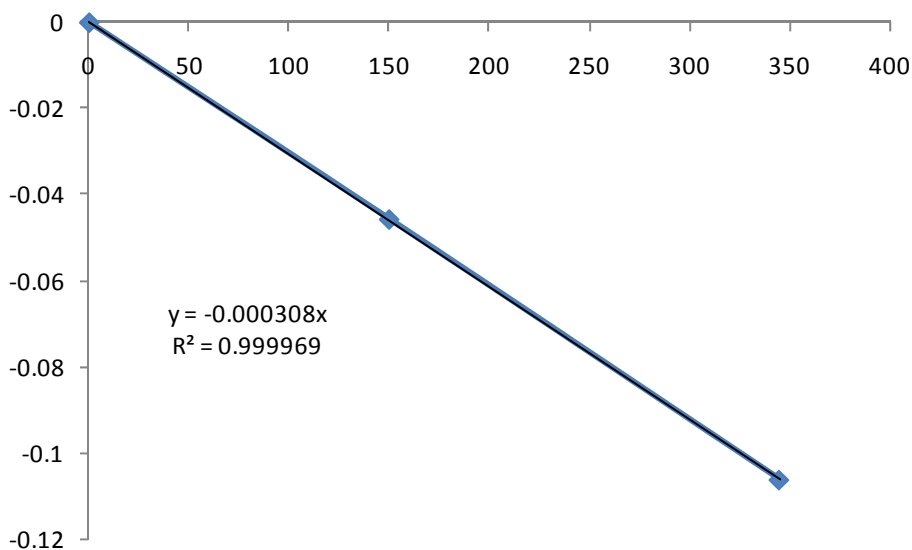


Fig. 17. Kinetic line for enantiomerization of 2,3,4,5-tetraiodo-1,6-bis(1,3-oxazolidinone)-2,4-hexadiene (**2**) at 131°C

2.3.2.2. Rate of racemization for the isolated enantiomers of 1,3-oxazolidin-2-one-3-yl-tetrabromo-1,3-diene (**3**)

About 2 mg of (+)-enantiomer of the tetrabromo-1,3-diene **3** were diluted in 5 mL of chloroform and heated at 40°C. The enantiomeric excess was followed by chiral HPLC (Chiralpak IC, Ethanol/CHCl₃/hexane 3/3/1, 1 mL/min, UV detection at 254 nm) every 15 minutes (Table 13).

Table 13. Rate of enantimerization in time for compound **3**

Time (min)	% enantiomer (+)	ln ((%t-%e)/(%0-%e))
0	90.878	0.0000
15	86.426	-0.1153
30	81.99	-0.2452
45	79.828	-0.3151
60	77.874	-0.3829
75	75.385	-0.4764
90	72.789	-0.5843
105	70.794	-0.6759
120	67.909	-0.8253
135	65.891	-0.9448
150	64.425	-1.0416
165	62.830	-1.1588
180	61.79	-1.2433
195	60.682	-1.3420
210	59.856	-1.4225

The slope of the kinetic line gives the kinetic rate for enantimerization, so we deduce the barrier to rotation for tetra-bromo-diene: $\Delta G^{\ddagger}_{\text{rot}} = 102.3 \pm 0.5$ kJ/mol at 40°C in chloroform (Fig. 18).

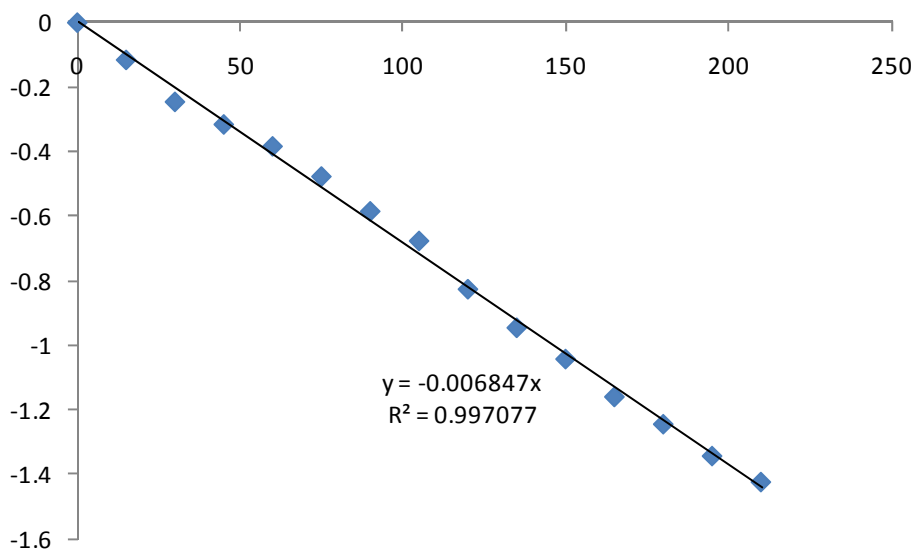


Fig. 18. Kinetic line for 2,3,4,5-tetrabromo-1,6-bis(1,3-oxazolidinone)-2,4-hexadiene (**3**) at 40°C

2.3.2.3. Estimation of the enantiomerization barrier for 1,3-oxazolidin-2-one-3-yl-tetrabromo-1,3-diene (**3**) using Schurig equation

For compound **3** the rotation barrier is in the range of a possible observation of a plateau during chiral chromatography.²⁷ Thus the racemate of tetrabromo-1,3,-diene **3** was injected on Chiralpak IC at 50°C, using Ethanol/CHCl₃/hexane 3/3/1 as eluent, in order to see a plateau between the two enantiomers (Fig. 19).

The tetraiodo-derivative **2** did not show a plateau, the off-line measured barrier of enantiomerization at 131°C in chlorobenzene was 143 ± 1 kJ/mol corresponding to a 1.56 day half-life at 131°C.

²⁷ a) Schurig, V. *J. Chromatogr. A* **2009**, 1216, 1723–1736; b) Wolf, C. *Chem. Soc. Rev.* **2005**, 34, 595-608; c) Trapp, O. *Anal. Chem.* **2006**, 78, 189-198; d) Trapp, O. *Chirality* **2006**, 18, 489-497

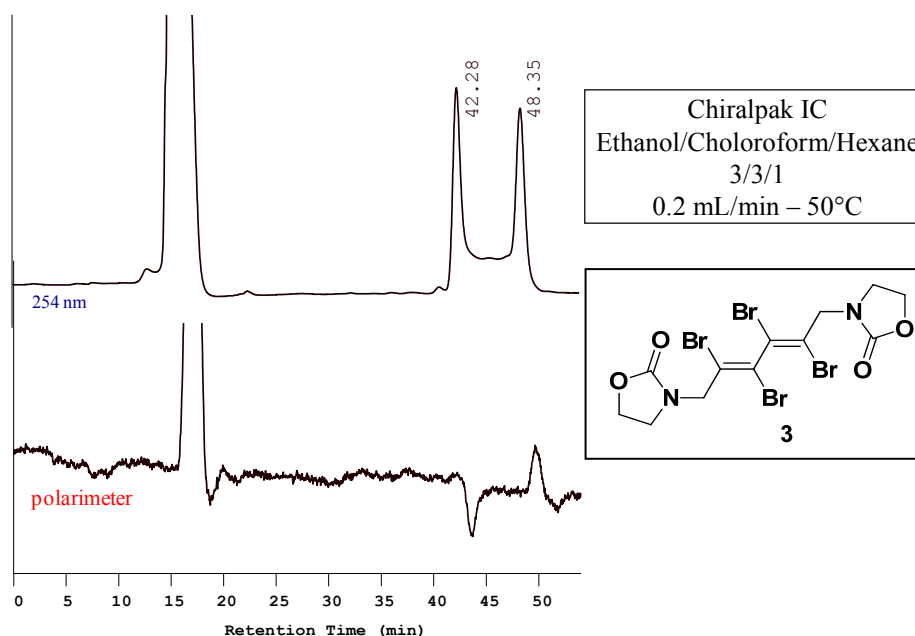


Fig. 19. Racemate of tetrabromo-1,3-diene (**3**), UV and polarimeter detection

When running chiral chromatography at 50°C with the same mobile phase a very nice plateau was observed allowing an estimation of the barrier using Trapp and Schurig equation²⁸ from the chromatogram shape and the height of the plateau (Fig. 20).

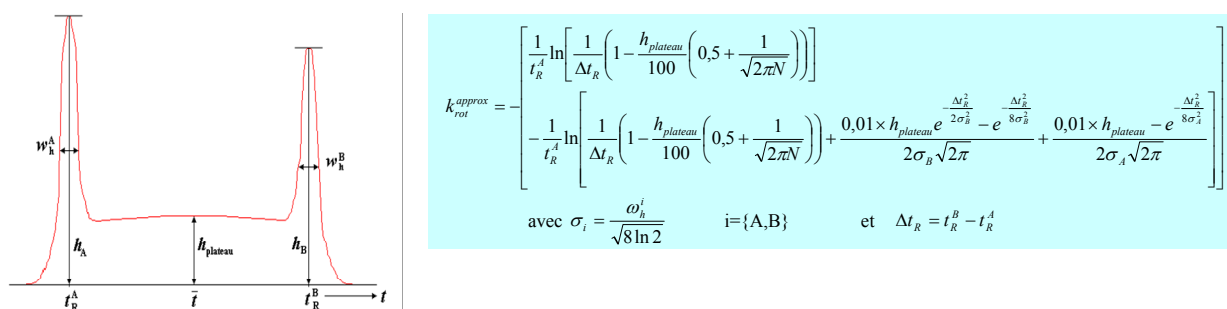


Fig. 20. Plateau formed by the enantiomers of the tetrabromo-1,3-diene (**3**)

Using this method and Schurig equation we have calculated the barrier to rotation for compound **3**: $\Delta G^{\ddagger}_{rot} = 103.6$ kJ/mol at 50°C in ethanol/chloroform/hexane 3/3/1 mixture.

The barriers of enantiomerization of two butadienes having in common with compound **3** the core of four bromides and differing by the so-called external group CH_2R' [$R' = OH, OMe$ or oxazolidinone unit ($C_3H_4NO_2$) for **3**] have been reported in the literature.⁷ The barriers in acetone were 102.2 kJ/mol (recalculated at 53.5°C) for $R' = OH$ and 104.5 kJ/mol (recalculated at

²⁸ Trapp, O.; Schurig, V. *Chirality* **2002**, *14*, 465-470

53.5°C) for R' = OMe. Difference in barriers determined by DHPLC and off-line racemisation have been already observed and discussed in terms of different rates of racemisation on the chiral support and in the mobile phase in the DHPLC experiments. A serious issue is a possible temperature gradient in the column which is difficult to evaluate.²⁹

2.3.3. Determination of the enantiomerization barriers by dynamic NMR experiments

In order to determine the barriers induced by hindered rotation of the molecules around C³-C⁴ bonds we carried out variable temperature NMR experiments by increasing the temperature.

Attempts to determine the barrier to rotation for chiral tetrabromo-dienes by dynamic NMR have been made in 1975 by Rosner and Kobrich³⁰, when they heated the solution up to 140°C in order to see the coalescence. They could determine the barrier only by other kinetic studies. The same authors^{8, 12, 16} managed to determine, by dynamic NMR, the barrier to rotation of a tetrachloro-diene as being 67.82±0.2 kJ/mol at 54°C. All these values depend not only of the nature of halogen but also of the type of other substituents. Substituents bulkiness would also influence the barrier to rotation around the central C-C bond.

Proton spectra of compound **2** and **3** recorded in CDCl₃ at 300 MHz at *rt* partially differentiate the diastereotopic proton in position 4'(4'') while spectrum of compound **4** could not differentiate any diastereotopic groups in the molecule. Proton spectrum of the same compound **4** recorded at 500 MHz at *rt* partially differentiate the diastereotopic protons in position 4'(4''). The same spectra recorded in CDCl₃ at 300 MHz at *rt* with chemical shift agent (Eu(FOD)₃-*d*₂₇) shifted the signals displaying all diastereotopic protons in the molecule.

Similar NMR experiments using C₆D₆ as solvent gave interesting results with different signals for the diastereotopic protons in positions 4'(4'') and 1(6) (Table 14). For compounds **2** and **3** the spectra recorded in DMSO-*d*₆ at higher temperatures (up to 400 K) did not show significant modifications in comparison with the spectra recorded at *rt*, indicating that the barrier is too high to be determined by this method, results found in accordance with literature data.¹⁴

²⁹ a) D'Acquarica, I.; Gasparrini, F.; Pierini, M.; Villani, C.; Zappia, G. *J. Sep. Sci.* **2006**, *29*, 1508 – 1516; b) Villani, C.; Gasparrini, F.; Pierini, M.; Mortera, S. L.; D'Acquarica, I.; Ciogli, A.; Zappia, G. *Chirality* **2009**, *21*, 97–103.

³⁰ Rosner, M. and Kobrich, G. *Angew.Chem.* **1975**, *19*, 715-717

Table 14. Relevant data for proton signals of compounds **2** – **4** in CDCl₃ and C₆D₆ (300 MHz)

Compd.	¹ H-NMR (CDCl ₃ , 300MHz)			¹ H-NMR (C ₆ D ₆ , 300MHz)		
	4'(4'')	5'(5'')	1(6)	4'(4'')	5'(5'')	1(6)
	δ ppm	δ ppm	δ ppm	δ (ppm) J (Hz)	δ (ppm) J (Hz)	δ (ppm) J (Hz)
2 (I)	3.61	4.40	4.36	2.47 (15.6, 8.1)	3.36	3.83 (15.4)
				2.69 (15.6, 8.1)		3.93 (15.4)
3 (Br)	3.60	4.39	4.47	2.41 (15.4, 8.1)	3.31	3.88 (15.4)
				2.60 (15.4, 8.1)		3.99 (15.4)
4 (Cl)	3.59	4.39	4.41	2.35 (15.7, 8.1)	3.27	3.81 (15.4)
				2.51 (15.7, 8.1)		3.92 (15.4)

Variable temperature ¹H-NMR experiment of compound **4** (in C₆D₆) was performed by recording the spectra in the range of temperatures from 293 K to 343 K. Spectra were recorded after repeatedly increasing the temperature with 10 Celsius degrees (Fig. 21).

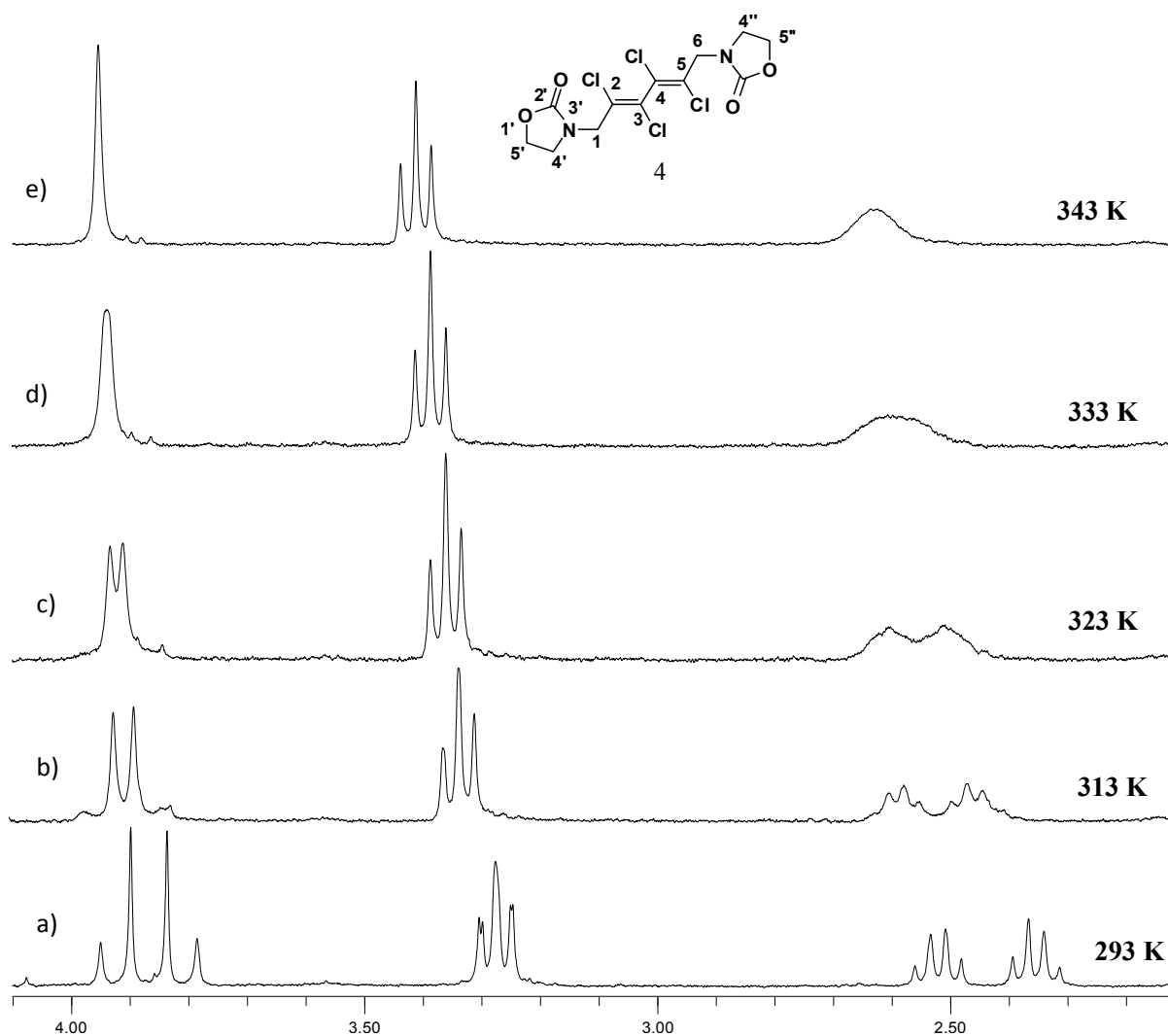


Fig. 21. ¹H-NMR (300 MHz) of compound **4** in C₆D₆ at 293 K (a), 313 K (b), 323 K (c), 333 K (d), 343 K (e)

Spectrum at 293 K is complex and reveals the anancomeric structure of compound **4**. Coalescence signals was observed at 333 K (T_c) while the spectrum recorded at 343 K corresponds to the flexible structure of compound **4**. Using the values of the chemical shifts obtained at 293 K ($\delta_{1,6} = 3.92$, $\delta'_{1,6} = 3.81$ ppm; $^2J = 15.4$ Hz; $\delta_{4,4''} = 2.51$, $\delta'_{4,4} = 2.35$ ppm; $J = 15.7$, $J' = 8.1$; $J'' \approx 0$ Hz) and the equations of Eyring (1 and 2) the barrier for the rotation of the molecule around the C³-C⁴ bond was estimated to be $\Delta G^\ddagger = 69.57 \pm 0.627$ kJ/mol (16.62 ± 0.627 kcal/mol), in agreement with the data reported for other similar compounds.¹⁴

Standard deviation was established using the ΔG^\ddagger values calculated at $\Delta G^\ddagger_{T_c} = 16.62$ kcal/mol, $\Delta G^\ddagger_{T_{c-10}} = 16.18$ kcal/mol and $\Delta G^\ddagger_{T_{c+10}} = 17.14$ kcal/mol at the temperatures (T_c), T_{c-10} and T_{c+10} .

$$k_{coal.} = \frac{\pi}{2} \sqrt{2} \sqrt{(\delta_1 - \delta_2)^2 + 6J^2} \quad (1)$$

$$k_{coal.} = k(k_B T_c / h) e^{-\Delta G^\ddagger / RT_c} \quad (2)$$

where: $k_{coal.}$ – rate of site exchange between two equally populated sites; $\Delta\delta = \delta_1 - \delta_2$ – is the chemical shift difference (in hertz) between the two exchanging nuclei at a temperature well below coalescence; J – coupling constant of the two nuclei in question; k – the transmission coefficient (usually taken as unity); k_B – Boltzmann's constant; h – Plank's constant; T_c – the coalescence temperature; ΔG^\ddagger – free energy of activation.

2.3.4. Correlations between halogens and rotation barriers in **2** - **4**

Inspection of the relevant literature data revealed a single example of a complete set of dihalogen (chlorine, bromine and iodine) substituted butadiene, reported by Mannschreck et al.⁵ They have estimated the barriers for dichloro-derivative and gave the lower limits for dibromo- and diiodo-derivatives. Thus correlations of the halogen steric size with the energy barriers will be made comparing the barriers of our set of halogen derivatives with the barriers disclosed in literature for some other halogen frameworks. The barriers of some biphenyls carrying halogen groups were determined by DMNR by Sternhell et al.³¹ He studied the interactions between the non buttressed substituents X (chlorine, bromine and iodine) and C_{ar}-H and the influences of these interactions (lone pair of electrons with C-H group) onto the rotation barriers. Plotting the barriers reported in Sternhell series against those determined for **2**, **3**, and **4** reveals a significant

³¹ Bott, G.; Field, L.D.; Sternhell, S. *J. Am. Chem. Soc.* **1980**, *102*, 5618-5626.

Table 15. Listed barrier to rotation values for some halo-derivatives (1,3-dienes- this work, Sternhell³³ and Dogan³⁴)

X	ΔG^\ddagger (kJ/mol) Sternhell	ΔG^\ddagger (kJ/mol) 1,3-dienes (this work)	ΔG^\ddagger (kJ/mol) Dogan Z = O, R = CH ₃	ΔG^\ddagger (kJ/mol) Dogan Z = S, R = CH ₃	ΔG^\ddagger (kJ/mol) Dogan Z = S, R = H
I	86.3 ± 1.8	143 ± 1	124.0±0.7	128.2±0.7	129.0±0.7
Br	82.9 ± 1.4	102.3 ± 0.5	117.2±0.7	121.6±0.7	123.6±0.7
Cl	78.5 ± 1.1	69.57±0.627	112.6±0.7	116.3±0.7	119.5±0.7

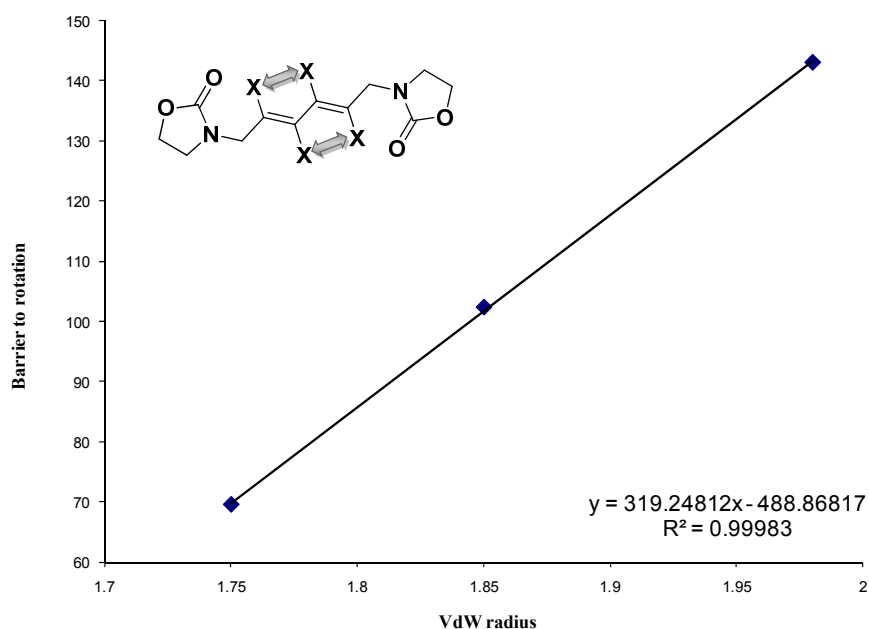


Figure 24. Correlation between barriers to rotation found in compounds **2-4** with van der Waals radii of the halogen atoms

Comparing the two types of halogen series we can conclude that no buttressing effect induced by the external substituents in **2**, **3**, and **4** can be detected and that any existent steric effect is linearly correlated with the size of the interacting groups.

2.4. Assignment of the absolute configuration

The absolute configuration of (+)-**2** (second eluted on Chiralpak IC column) and (-)-**2** (first eluted on Chiralpak IC column) was determined by means of vibrational circular dichroism (VCD) by comparing experimental spectra of both enantiomers with the calculated VCD spectra of the (*aR*) enantiomer.³³ The geometry optimizations, vibrational frequencies, IR absorption and VCD intensities were calculated using Density Functional Theory (DFT) with B3LYP functional and a 6-31+G(d,p) basis set, using the Gaussian 03 program.³⁴

Conformational study of **2** has shown that, among the twenty conformations found (Table 16), only four, (*aR*)-**2a-d**, have a Boltzmann population higher than 5% (Fig. 25). Normal mode analysis confirmed that **2a-d** correspond to minima on the potential energy surface since no imaginary frequency was found. Similar results were obtained for **3** (Table 16).

³³ a) Nafie, L. A.; Keiderling, T. A.; Stephens, P. J. *J. Am. Chem. Soc.* **1976**, *98*, 2715-2723; b) Nafie, L. A. *Annu. Rev. Phys. Chem.* **1997**, *48*, 357-386; c) Stephens, P. J.; Devlin, F. J. *Chirality* **2000**, *117*, 172-179; d) Freedman, T. B.; Cao, X.; Dukor, R. K.; Nafie, L. A. *Chirality* **2003**, *15*, 743-758; e) Polavarapu, P. L.; He, J. *Anal. Chem.* **2004**, *76*, 61-67; f) Bürgi, T.; Urakawa, U.; Behzadi, B.; Ernst, K.-H.; Baiker, A. *New J. Chem.* **2004**, *28*, 332-334; g) Naubron, J.-V.; Giodano, L.; Fotiadu, F.; Bürgi, T.; Vanthuyne, N.; Roussel, C.; Buono, G. *J. Org. Chem.* **2006**, *71*, 5586-5593; h) Polavarapu, P. L. *The Chemical Record* **2007**, *7*, 125-136. i) Polavarapu, P. L.; Petrovic, A. G.; Vick, S. E.; Wulff, W. D.; Ren, H.; Ding, Z.; Staples, R. J. *J. Org. Chem.* **2009**, *74*, 5451-5457.

³⁴ Gaussian 03, Revision E.01, Frisch, M. J.; Trucks, G. W.; Schlegel, H. B.; Scuseria, G. E.; Robb, M. A.; Cheeseman, J. R.; Montgomery, Jr., J. A.; Vreven, T.; Kudin, K. N.; Burant, J. C.; Millam, J. M.; Iyengar, S. S.; Tomasi, J.; Barone, V.; Mennucci, B.; Cossi, M.; Scalmani, G.; Rega, N.; Petersson, G. A.; Nakatsuji, H.; Hada, M.; Ehara, M.; Toyota, K.; Fukuda, R.; Hasegawa, J.; Ishida, M.; Nakajima, T.; Honda, Y.; Kitao, O.; Nakai, H.; Klene, M.; Li, X.; Knox, J. E.; Hratchian, H. P.; Cross, J. B.; Bakken, V.; Adamo, C.; Jaramillo, J.; Gomperts, R.; Stratmann, R. E.; Yazyev, O.; Austin, A. J.; Cammi, R.; Pomelli, C.; Ochterski, J. W.; Ayala, P. Y.; Morokuma, K.; Voth, G. A.; Salvador, P.; Dannenberg, J. J.; Zakrzewski, V. G.; Dapprich, S.; Daniels, A. D.; Strain, M. C.; Farkas, O.; Malick, D. K.; Rabuck, A. D.; Raghavachari, K.; Foresman, J. B.; Ortiz, J. V.; Cui, Q.; Baboul, A. G.; Clifford, S.; Cioslowski, J.; Stefanov, B. B.; Liu, G.; Liashenko, A.; Piskorz, P.; Komaromi, I.; Martin, R. L.; Fox, D. J.; Keith, T.; Al-Laham, M. A.; Peng, C. Y.; Nanayakkara, A.; Challacombe, M.; Gill, P. M. W.; Johnson, B.; Chen, W.; Wong, M. W.; Gonzalez, C.; and Pople, J. A.; Gaussian, Inc., Wallingford CT, **2004**.

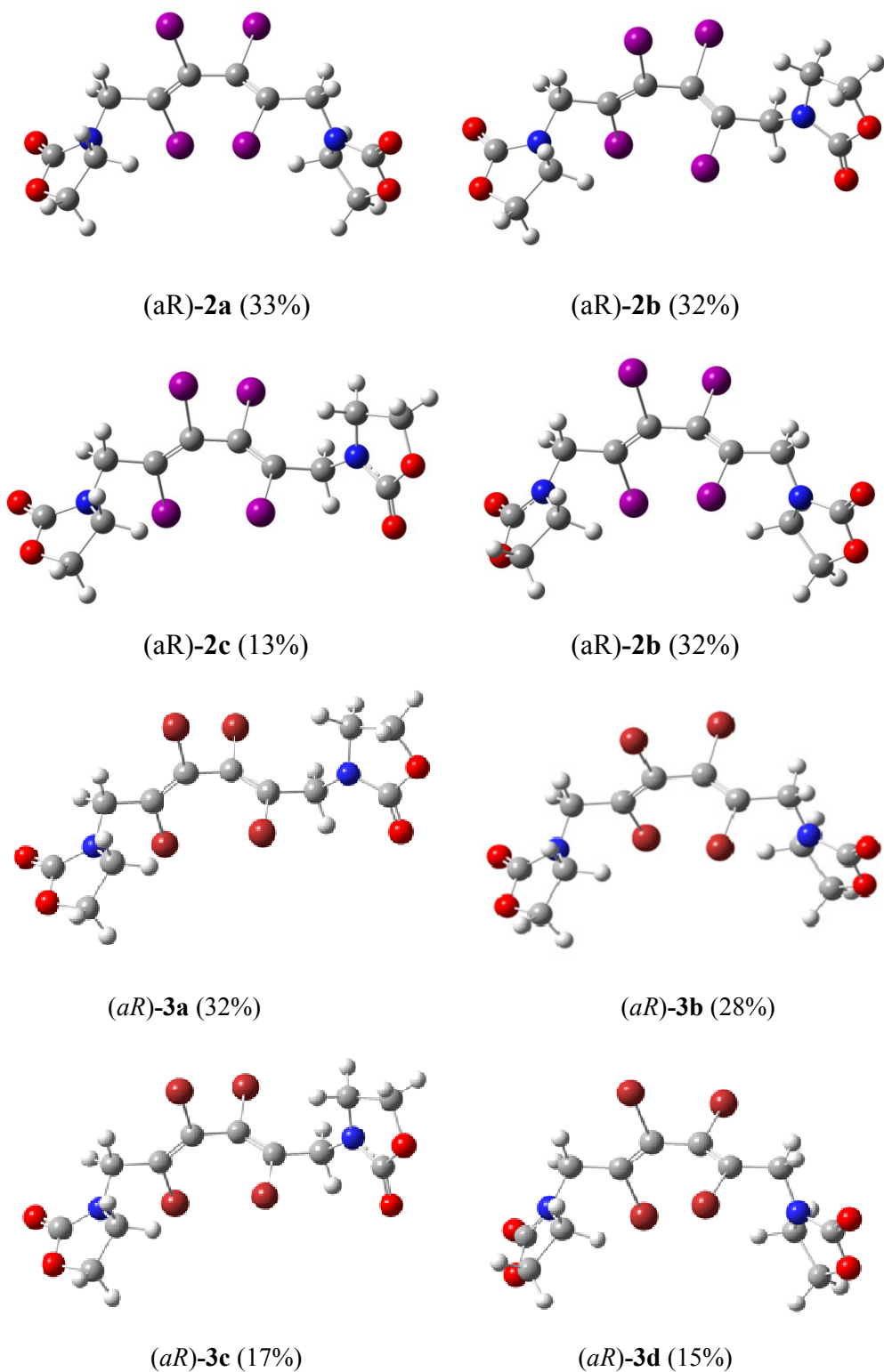


Fig. 25. Optimized B3LYP/6-31+G(d,p) structures of conformers (*aR*)-**2a-d** and (*aR*)-**3a-d**

Table 16. B3LYP/6-31+G(d,p) Energies of (*aR*)-**2a-d** and (*aR*)-**3a-d**

Conformers	Energies + ZPE (a.u)	ΔE^{ZPE} (kJ.mol ⁻¹)	Boltzmann population (%)
2a	-920.3194935	0.00	33
2b	-920.3194672	0.07	32
2c	-920.3186295	2.27	13
2d	-920.3184769	2.67	11
3a	-928,165204	0.00	32
3b	-928,1650985	0.28	28
3c	-928,1645934	1.60	17
3d	-928,1645149	1.81	15

As shown in Fig. 26 - 29, the experimental IR absorption and VCD spectra of (+)-**3** and (+)-**2** (second eluted enantiomer on Chiralpak IC column) in CD₂Cl₂ solution are in good agreement with the predicted spectra of (*aR*)-**3** and (*aR*)-**2** which were obtained by weighting the spectrum of each conformer by its Boltzmann population. The shape and the relative intensities of the IR and VCD bands were well reproduced by the calculations. It should be noted that VCD spectra of enantiomers have opposite signs. The calculated bands at 1647 cm⁻¹ in **3** (experimental 1647 cm⁻¹) and 1624 cm⁻¹ in **2** (experimental 1625 cm⁻¹) are particularly interesting.

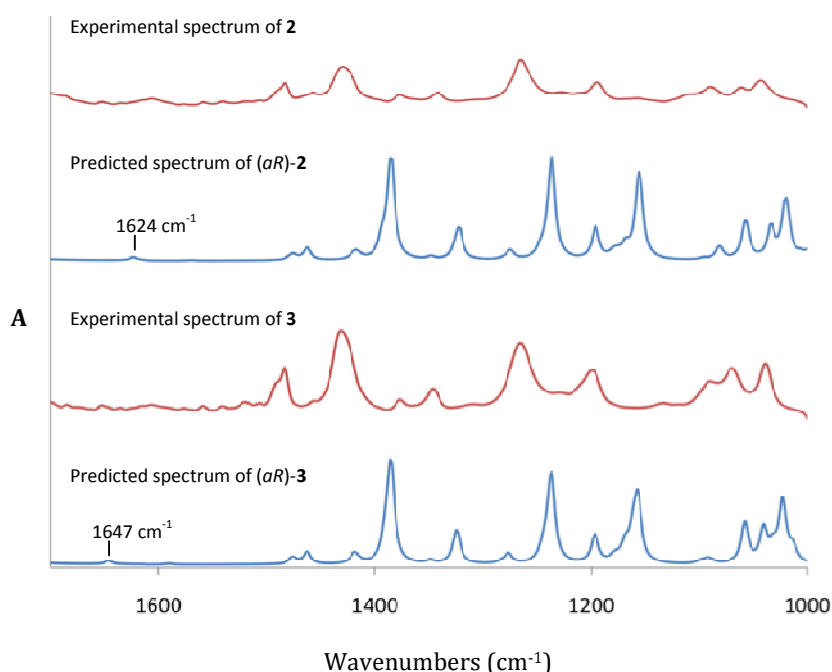


Fig. 26. Comparison of experimental IR spectra of **2** and **3** in CD₂Cl₂ solution (top two traces) with predicted IR spectrum (bottom trace) of the (*aR,M*) configuration of **2** and **3** obtained with B3LYP/6-31+G(d,p) level. For predicted spectra, wave numbers are scaled by the factor 0.96. The trace labeled «predicted» is the population-weighted spectrum with populations given in Fig. 25.

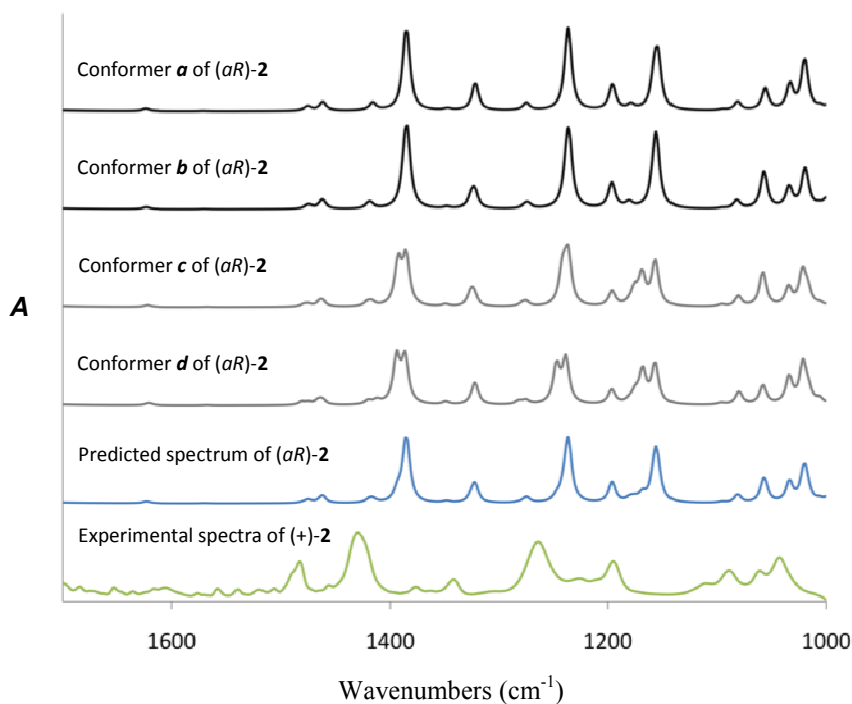


Fig. 27. Experimental IR absorption spectrum in CD₂Cl₂ of (+)-**2** together with calculated spectra of populated conformations of (*aR*)-**2** (structure and conformation labels in Figure 25) obtained with B3LYP/6-31+G(d,p):MWB46 level. For predicted spectra, wavenumbers are scaled by the factor 0.96. The trace labeled «predicted» (second from bottom) is the population-weighted spectrum with populations given in Table 16.

The bottle neck of the VCD method for the determination of absolute configuration being the calculations of the predicted spectra, we looked for VCD bands which can be used as a signature of the absolute configuration of the butadiene framework independently of the various conformations of the attached groups. The calculated band at 1624 cm⁻¹ in **2** (experimental 1625 cm⁻¹) is a good candidate; it comes from the symmetric stretching mode of the butadiene moiety (Fig. 29) and it is weakly affected by the attached groups. As expected, the IR intensity of this band is very weak but from the sign of that band it can be concluded that the absolute configuration of (+)-**2** (second eluted on Chiralpak IC column) is (+)-(*aR*)-**2** (Fig. 27). The experimental VCD spectra of the isolated enantiomers of **3** showed the presence of that signature band which is slightly shifted (1647 cm⁻¹) due to the drastic change of four iodine into four bromine atoms on the butadiene framework (Fig 28). From the examination of the sign of that band it can be concluded that here again the absolute configuration of (+)-**3** (second eluted on Chiralpak IC column) is (+)-(*aR*)-**3**. Moreover, we have made theoretical and experimental studies confirming that the symmetric stretching mode of the butadiene moiety can be safely used as a signature for the determination of the absolute configuration.

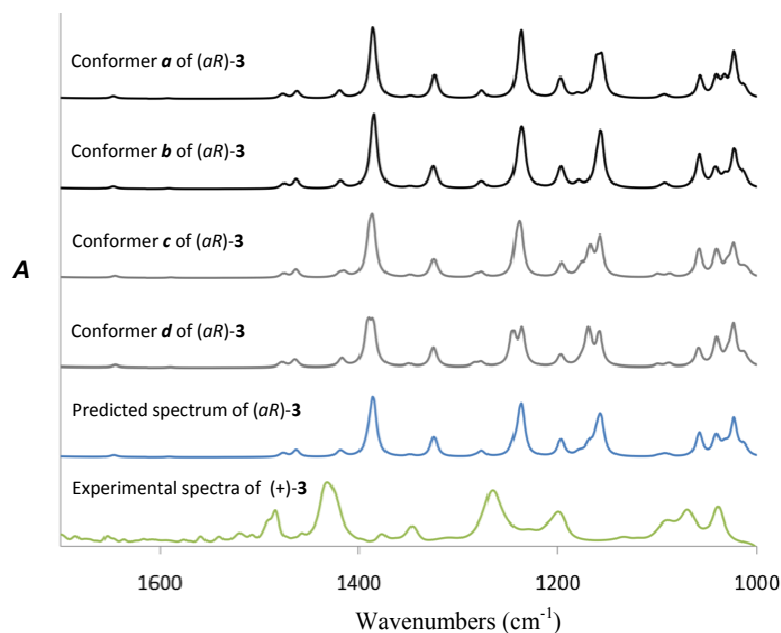


Fig. 28. Experimental IR absorption spectrum in CD₂Cl₂ of (+)-**3** together with calculated spectra of populated conformations of (aR)-**3** (structure and conformation labels in Figure 25) obtained with B3LYP/6-31+G(d,p):MWB28 level. For predicted spectra, wavenumbers are scaled by the factor 0.96. The trace labeled «predicted» (second from bottom) is the population-weighted spectrum with populations given in Table 16.

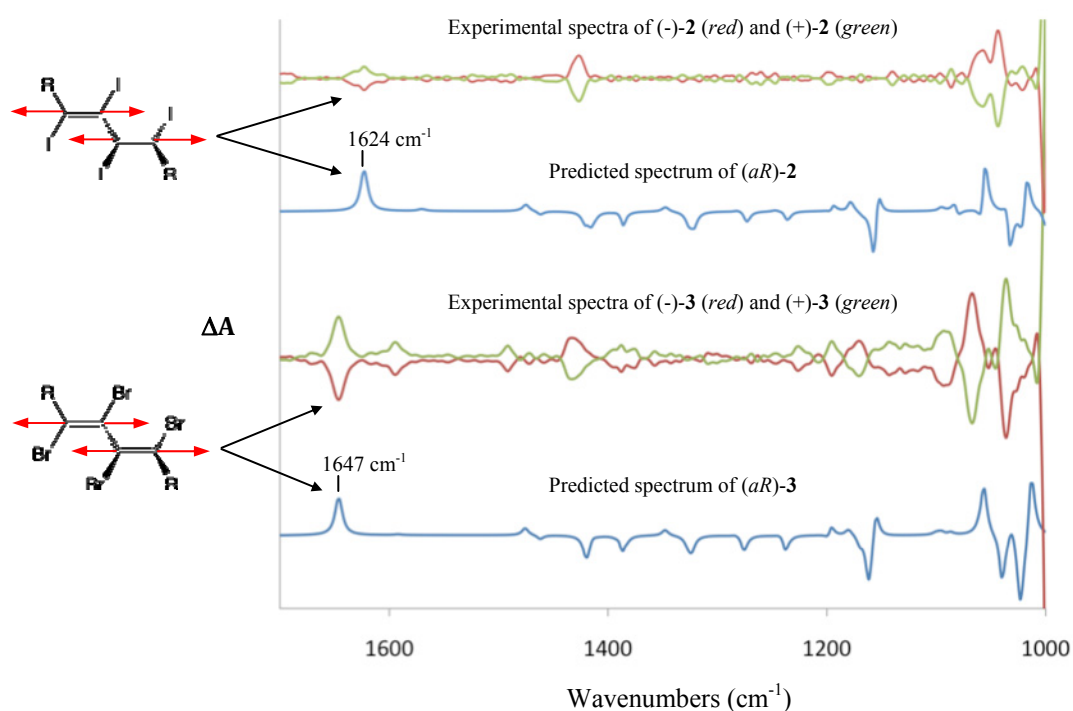


Fig. 29. Comparison of the experimental VCD spectra of (-)-**3** (in red), (+)-**3** (in green), (-)-**2** (in red) and (+)-**2** (in green) in CD₂Cl₂ solution with predicted VCD spectrum of the aR configuration of **3** and **2** (in blue) obtained with B3LYP/6-31+G(d,p) level. For predicted spectra, wave numbers are scaled by the factor 0.96. The traces labeled «predicted» are the population-weighted spectra with populations given in Figure 25.

2.5. Conclusions

New axially chiral butadienes have been synthesized and completely analyzed by NMR spectroscopy, mass spectrometry, IR, VCD and X-ray diffractometry.

Chirality of the compounds has been proven by the presence of the diastereotopic protons in the ^1H -NMR spectra.

A study of the atropisomers belonging to a complete set of tetra-halo-1,3-dienes substituted by two 1,3-oxazolidin-2-one units was presented.

Stable atropisomers of the tetraiodo- and tetrabromo 1,3-dienes were for the first time separated by chiral stationary phase chromatography, yielding pure enantiomers.

Barriers to rotation about the single C-C bonds were determined by DHPLC for tetraiodo- and tetrabromo- derivatives and by DNMR spectroscopy for the tetrachloro-derivative.

A linear correlation of the barriers energy with the van der Waals radii of the halogen was observed in this halogen series as observed in other axially chiral halogen series. Thus any existent steric effect is correlated with the size of the interacting groups.

Assignment of the absolute configuration for tetraiodo- and tetrabromo-1,3-dienes was made by theoretical calculations and VCD spectra.

A VCD spectra was performed for the first time for the isolated stable atropisomers of substituted-1,3-butadienes. A signature band arising from the chirality of the sole 1,3-butadiene framework was identified. The sign of that band allow a safe assignment of the absolute configuration of other stable 1,3-butadiene atropisomers.

2.6. Experimental part

2.6.1. General remarks

¹H-NMR and ¹³C-NMR spectra were recorded on a Bruker AVANCE 300 spectrometer operating at 300 and 75 MHz; δ are given in ppm (relative to TMS) and coupling constants (J) in Hz. Mass spectra were recorded under ESI ion trap mass spectrometer in positive mode.

The X-ray crystallographic data were collected at *rt*, using graphite-monochromated MoK α radiation. For structure solving and refinement the software package SHELX-97 was used.³⁵ The drawings were created with Ortep³⁶, Mercury and Diamond programs.³⁷

Solvents were dried and distilled under argon using standard procedures before use. Chemicals of commercial grade were used without further purification.

Melting points are uncorrected. Column chromatography purifications were carried out on Merck silica gel Si 60 (40-63 μ m). Thin layer chromatography (TLC) was carried out on aluminium sheets coated with silica gel 60 F₂₅₄ using UV lamp (254 nm) and KMnO₄ visualization.

The analytical chiral HPLC experiments were performed on a unit composed of a Merck D-7000 system manager, Merck L-6000 pump, Merck-Lachrom L-7360 oven, Merck L-4200 UV-detector, and on-line Jasco OR-1590 polarimeter. Hexane, chloroform, and ethanol, HPLC grade, were degassed and filtered on a 0.45 μ m membrane before use. Retention times R_t in minutes, retention factors $k_i = (R_{t_i} - R_{t_0}) / R_{t_0}$ are given. R_{t_0} was determined by injection of tri-tertio-butyl benzene. The sign given by the on-line polarimeter is the sign of the product in the solvent used for the chromatographic separation. The columns (250 x 4.6 mm) used are Whelk-O1 (R,R) and Chiralpak IA, Chiralpak IB and Chiralpak IC from Daicel. The analyses were performed with 1 mL/min as flow-rate, detection by UV at 254 nm and by a polarimeter.

Infrared (IR) and vibrational circular dichroism (VCD) spectra were recorded on a Bruker PMA 50 accessory coupled to a Vertex 70 Fourier transform infrared spectrometer. All solutions were prepared from 2.1 mg sample in 80 μ L CD₂Cl₂. The VCD spectra of each pure enantiomer were measured and subtracted to each other in order to eliminate artefacts. For the

³⁵ a) Sheldrick, G. M. *SHELX-97*, Universität Göttingen, Germany, **1997**; b) Bruker (**1999**). SMART (Version 5.611), SAINT (Version 6.02a), SHELXTL (Version 5.10) and SADABS. Bruker AXS Inc., Madison, Wisconsin, USA; c) Claridge, J. B.; Layland, R. C.; Loye, H.-C. *Acta Cryst.* **1997**, C53, 1740

³⁶ Farrugia, L. J. *J. Appl. Cryst.* **1997**, 30, 565

³⁷ *DIAMOND* - Visual Crystal Structure Information System; CRYSTAL IMPACT: P.O.B. 1251, D-53002 Bonn, Germany

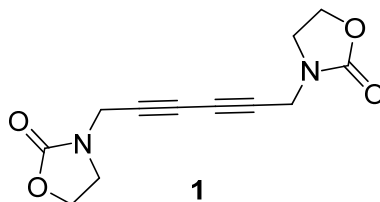
individual spectra of the enantiomers, about 12'000 scans were averaged at 4 cm⁻¹ resolution (corresponding to three hours measurement time). For the infrared spectrum the cell filled with CD₂Cl₂ served as reference. The spectra are presented without smoothing and further data processing.

The geometry optimizations, vibrational frequencies, IR absorption and VCD intensities were calculated using Density Functional Theory (DFT) with B3LYP functional and a 6-31+G(d,p) basis set, using the Gaussian 03 program. Frequencies were scaled by a factor of 0.96. IR absorption and VCD spectra were constructed from calculated dipole and rotational strengths assuming Lorentzian band shape with a half-width at half maximum of 8 cm⁻¹.

For the conformational study, it was used annealing at RM1 semi-empirical level, with B3LYP/6-31+G(d,p) optimized geometry as starting structure. During the annealing, only the dihedral angles were allowed to relax, the bond lengths and valence angles were kept fixed. Many annealing, starting from different geometries, were done in order to explore the whole potential energy surface. All semi-empirical calculations were done using AMPAC 9 program.

2.6.2. Synthesis and characterization of compounds

1,6-Bis(1',3'-oxazolidin-2'-one-3-yl)-2,4-hexadiyne (1)



A solution of N-propargyl-1,3-oxazolidine-2-one (0.2g, 1.59 mmol) in dry dichloromethane (100 mL) containing dry TMEDA (7.37 g, 190.8 mmol) was treated with CuI (6.07g, 95.4 mmol) and stirred for 1 hour in an atmosphere of dry air. The mixture was then diluted with dichloromethane (50 ml) transferred to a separating funnel and washed with 2M HCl (2 x 50 ml) and then several times with water. The organic layer was then separated, dried over Na₂SO₄ and evaporated. The residue was purified by chromatography (silica gel, toluene/acetone 4/1) affording a white solid, 66 mg (0.27 mmol), m.p. = 201°C (decom), **R_f** = 0.37. Yield: 33%.

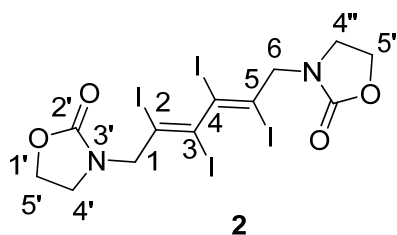
Calculated for C₁₂H₁₂N₂O₄ (%): C, 58.06; H, 4.87; N, 11.29. Found: C, 57.83; H, 4.66; N, 11.52.

¹H-NMR (300 MHz, CDCl₃) δ ppm: 3.65 (m, 2H, 4'-H), 4.16 (s, 2H, 1-H, 6-H), 4.37 (m, 2H, 5'-H).

¹³C-NMR (75 MHz, CDCl₃) δ ppm: 34.74 (1-C, 6-C), 43.97 (4'-C), 61.98 (5'-C), 68.93 (3-C, 4-C), 72.30 (2-C, 5-C), 157.75 (2'-C).

MS - EI m/z (%): 100 (62), 117 (100), 148 (2), 248 (M, 14).

1,6-bis(1',3'-oxazolidin-2'-one-3'-yl)-2,3,4,5-tetraiodo-hexane-2*E*,4*E*-diene (2)



CuI (6.07g, 95.4 mmol) was added to a solution of N-propargyl-1,3-oxazolidine-2-one (0.2 g, 1.59 mmol) in dry dichloromethane (100 mL) containing dry TMEDA (7.37 g, 190.8 mmol). The reaction mixture was stirred for 1 hour in dry air. The mixture was then diluted with dichloromethane (50 ml) transferred into a separating funnel and washed with 2M HCl (2 x 50 ml) and then several times with water till the aqueous layer remains colourless. The organic layer was then separated, dried over Na₂SO₄ and evaporated. The final product was then purified by column chromatography (silica gel, toluene/acetone 4/1) affording 72 mg of yellow solid, m.p. = 190°C (dec), *R_f* = 0.21. Yield: 12%.

Calculated for C₁₂H₁₂I₄N₂O₄ (%): C, 19.07; H, 1.60; I, 67.16; N, 3.71. Found: C, 18.89; H, 1.51; I, 66.97; N, 3.88.

¹H-NMR (300 MHz, CDCl₃) δ ppm: 3.61 (overlapped peaks, 4H, 4'-H, 4''-H), 4.36 (s, 4H, 1-H, 6-H), 4.40 (overlapped peaks, 4H, 5'-H, 5''-H);

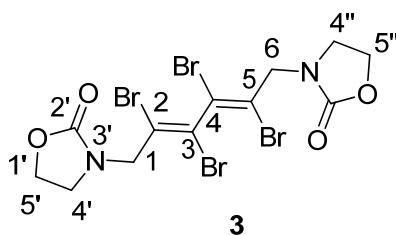
¹H-NMR (300 MHz, C₆D₆) δ ppm: 2.47 (dd, 2H, *J* = 15.6, 8.1 Hz, 4'-H, 4''-H), 2.69 (dd, 2H, *J* = 15.6, 8.1 Hz, 4'-H', 4''-H'), 3.36 (overlapped peaks, 4H, 5'-H, 5''-H), 3.83 (d, 2H, *J* = 15.4 Hz, 1-H, 6-H), 3.93 (d, 2H, *J* = 15.4 Hz, 1-H', 6-H').

¹³C-NMR (75 MHz, CDCl₃) δ ppm: 44.18 (4'-C, 4''-C), 59.19 (1-C, 6-C), 62.06 (5'-C, 5''-C), 102.64 (2-C, 5-C), 105.58 (3-C, 4-C), 158.01 (2'-C, 2''-C).

ESI-MS; *m/z* = 756.7 [M+H]⁺, 778.6 [M+Na]⁺, calculated for C₁₂H₁₂I₄N₂O₄ 755.7.

Chiral HPLC: Chiralpak IC, 25°C, Ethanol/CHCl₃/Hexane 3/3/1, 1 mL/min, *R_{t1}* = 8.20 min (-), *R_{t2}* = 9.63 min (+), *k*₁ = 1.65, *k*₂ = 2.11, α = 1.28 and *R_s* = 2.68.

1,6-bis(1',3'-oxazolidin-2'-one-3'-yl)-2,3,4,5-tetrabromo-hexane-2E,4E-diene (3)



To a solution of diacetylene **1** (125 mg, 0.5 mmol) in dichloromethane (50 ml), bromine (1 mmol, 160 mg solved in 1 ml dichloromethane) was added dropwise. The mixture was stirred at room temperature overnight, and at the end the organic phase was washed with a solution of sodium sulfite and then with water. After drying over sodium sulfate, the solvent was removed and the crude product was purified by chromatography (silica gel, toluene/acetone 4/1) affording 106 mg of yellow solid, m.p. = 215°C (dec), $R_f = 0.35$. Yield: 37%.

Calculated for $C_{12}H_{12}Br_4N_2O_4$ (%): C, 25.38; H, 2.13; Br, 56.29; N, 4.93. Found: C, 25.49; H, 2.28; Br, 56.11; N, 4.77.

1H -NMR (300 MHz, $CDCl_3$) δ ppm: 3.60 (overlapped peaks, 4H, 4'-H, 4''-H), 4.39 (overlapped peaks, 4H, 5'-H, 5''-H), 4.47 (s, 4H, 1-H, 6-H);

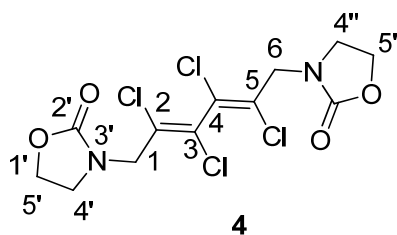
1H -NMR (300 MHz, C_6D_6) δ ppm: 2.41 (2H, dd, $J = 15.4, 8.1$ Hz, 4'-H, 4''-H), 2.60 (2H, dd, $J = 15.4, 8.1$ Hz, 4'-H', 4''-H'), 3.31 (overlapped peaks, 4H, 5'-H, 5''-H), 3.88 (d, 2H, $J = 15.4$ Hz, 1-H, 6-H), 3.99 (d, 2H, $J = 15.4$ Hz, 1-H', 6-H').

^{13}C -NMR (75 MHz, $CDCl_3$) δ ppm: 43.82 (4'-C, 4''-C), 50.43 (1-C, 6-C), 61.97 (5'-C, 5''-C), 118.07 (2-C, 5-C), 122.53 (3-C, 4-C), 158.05 (2'-C, 2''-C).

ESI-MS; $m/z = 564.7 [M+H]^+$, $586.7 [M+Na]^+$, calculated for $C_{12}H_{12}Br_4N_2O_4$ 563.75.

Chiral HPLC: Chiralpak IC, 25°C, Ethanol/ $CHCl_3$ /Hexane 3/3/1, 1 mL/min, $R_{t1} = 7.92$ min (-), $R_{t2} = 9.32$ min (+), $k_1 = 1.56$, $k_2 = 2.01$, $\alpha = 1.29$ and $R_s = 2.88$.

1,6-bis(1',3'-oxazolidin-2'-one-3'-yl)-2,3,4,5-tetrachloro-hexane-2*E*,4*E*-diene (4)



A solution of diacetylene **1** (80 mg, 0.32 mmol), CuCl₂ (174 mg, 1.29 mmol), LiCl (22 mg, 0.512 mmol) in dry acetonitrile (7 ml) was refluxed over night. Compound **4** was precipitated with acetone affording 22 mg of white crystals, m.p. = 201°C. Yield: 18%.

Calculated for C₁₂H₁₂Cl₄N₂O₄ (%): C, 36.95; H, 3.10; Cl, 36.36; N, 7.18. Found: C, 37.11; H, 3.02; Cl, 36.16; N, 7.31.

¹H-NMR (300 MHz, CDCl₃) δ ppm: 3.59 (overlapped peaks, 2H, 4'-H, 4''-H), 4.39 (overlapped peaks, 2H, 5'-H, 5''-H), 4.41 (s, 2H, 1-H, 6-H);

¹H-NMR (300 MHz, C₆D₆) δ ppm: 2.35 (2H, dd, *J* = 15.7, 8.1 Hz, 4'-H, 4''-H), 2.51 (2H, dd, *J* = 15.7, 8.1 Hz, 4'-H', 4''-H'), 3.27 (overlapped peaks, 4H, 5'-H, 5''-H), 3.81 (2H, d, *J* = 15.4 Hz, 1-H, 6-H), 3.92 (2H, d, *J* = 15.4 Hz, 1-H', 6-H');

¹³C-NMR (75 MHz, CDCl₃) δ ppm: 43.88 (4'-C, 4''-C), 46.59 (1-C, 6-C), 61.92 (5'-C, 5''-C), 125.41 (2-C, 5-C), 131.49 (3-C, 4-C), 158.14 (2'-C, 2''-C).

EI-MS *m/z* (%): 354 (7.5, [M⁺-Cl]), 308 (23), 264 (42), 216 (65), (literature data for similar cases 0.1% M⁺, and 100% [M⁺-Cl]).³⁸

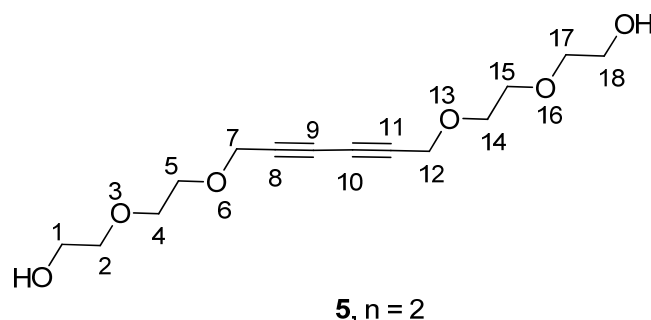
Chiral HPLC: Chiralpak IC, 25°C, Ethanol/CHCl₃/Hexane 3/3/1, 1 mL/min, one peak at 7.50 min, *k* = 1.42.

³⁸ Walsh, J.G.; Furlong, P.J.; Byrne, L.A.; Gilheany, D.G. *Tetrahedron* **1999**, *55*, 11519-11536

General procedure for the acetylenic coupling

CuI (60 mmol) was added to a solution of alkynes **7** or **8** (3 mmol) in dry dichloromethane (200 mL) containing dry TMEDA (120 mmol). The reaction mixture was stirred for 1 hour under a stream of dry air. The mixture was then diluted with dichloromethane (100 ml) transferred into a separating funnel and washed with a solution of HCl 2M (2 x 30 ml) and then several times with water till the aqueous layer remains colourless. The organic layer was then separated, dried over Na₂SO₄ and evaporated. The final product was then purified by column chromatography (silica gel, diisopropylether/acetone 1/1).

3,6,13,16-tetraoxaoctadeca-8,10-diyne-1,18-diol (**5**)



Transparent liquid, 300 mg. Yield: 35%.

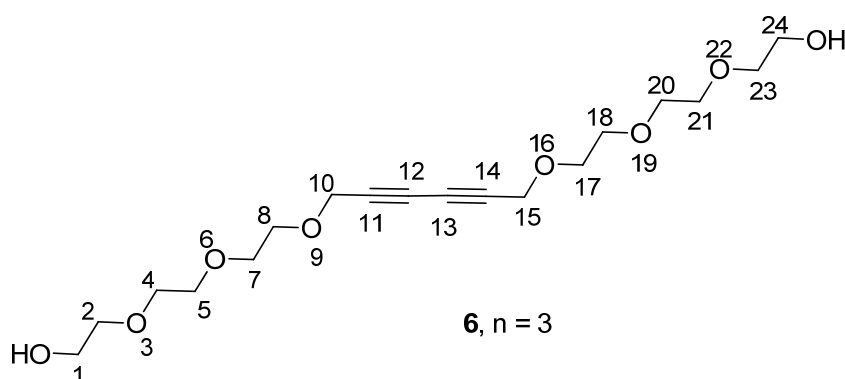
Calculated for C₁₄H₂₂O₆ (%): C, 58.73; H, 7.74. Found: C, 58.89; H, 7.51.

¹H-NMR (300 MHz, CDCl₃) δ ppm: 2.03 (2H, OH), 3.55-3.75 (m, 16H, 1-H, 2-H, 4-H, 5-H, 14-H, 15-H, 17-H, 18-H), 4.27 (s, 4H, 7-H, 12-H).

¹³C-NMR (75 MHz, CDCl₃) δ ppm: 58.91 (7-C, 12-C), 61.70 (1-C, 18-C), 69.37, 70.13 (2-C, 4-C, 15-C, 17-C), 70.53 (9-C, 10-C), 72.47 (5-C, 14-C), 75.22 (8-C, 11-C).

ESI-MS m/z = 287.1 [M+H]⁺, 309.1 [M+Na]⁺, calculated for C₁₄H₂₂O₈ 286.14.

3,6,9,16,19,22-hexaoxatetracos-11,13-diyne-1,24-diol (6)



Transparent liquid, 400 mg. Yield: 33%.

Calculated for $C_{18}H_{30}O_8$ (%): C, 57.74; H, 8.08. Found: C, 57.63; H, 8.28.

$^1\text{H-NMR}$ (300 MHz, CDCl_3) δ ppm: 2.13 (2H, OH), 3.59-3.74 (m, 24H, 1-H, 2-H, 4-H, 5-H, 7-H, 8-H, 17-H, 18-H, 20-H, 21-H, 23-H, 24-H), 4.27 (s, 4H, 10-H, 15-H).

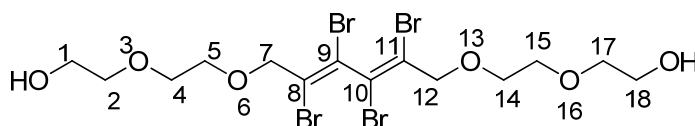
$^{13}\text{C-NMR}$ (75 MHz, CDCl_3) δ ppm: 58.89 (10-C, 15-C), 61.69 (1-C, 24-C), 69.28, 70.24, 70.27, 70.60 (2-C, 4-C, 5-C, 7-C, 18-C, 20-C, 21-C, 23-C), 70.50 (12-C, 13-C), 72.51 (8-C, 17-C), 75.25 (11-C, 14-C).

ESI-MS $m/z = 375.2$ $[\text{M}+\text{H}]^+$, 397.2 $[\text{M}+\text{Na}]^+$, calculated for $C_{18}H_{30}O_8$ 374.43.

General bromination procedure

To a solution of compounds **5** or **6** (0.26 mmol) in dichloromethane (20 ml), bromine (0.82 mmol, 130 mg solved in 1 ml dichloromethane) was added dropwise. The mixture was stirred at room temperature overnight, and at the end the organic phase was washed with a solution of sodium sulfite and then with water. After drying over sodium sulfate, the solvent was removed and the crude product was purified by chromatography (silica gel, diisopropylether/acetone 1/1).

(8E,10E)-8,9,10,11-tetrabromo-3,6,13,16-tetraoxaoctadeca-8,10-diene-1,18-diol (**7**)



Yellow liquid, 74 mg. Yield: 47%.

Calculated for C₁₄H₂₂Br₄O₆ (%): C, 27.75; H, 3.66; Br, 52.75. Found: C, 27.49; H, 3.78; Br, 52.91.

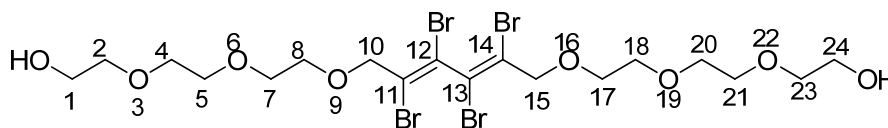
¹H-NMR (300 MHz, CDCl₃) δ ppm: 1.88 (2H, OH), 3.61-3.76 (m, 16H, 1-H, 2-H, 4-H, 5-H, 14-H, 15-H, 17-H, 18-H), 4.44 (d, 2H, *J* = 13.5, 7-H, 12-H), 4.55 (2d 2H, *J* = 13.5, 7'-H, 12'-H).

¹³C-NMR (75 MHz, CDCl₃) δ ppm: 61.79 (1-C, 18-C), 69.35, 70.18 (2-C, 4-C, 15-C, 17-C), 72.42 (5-C, 14-C), 73.06 (7-C, 12-C), 117.53 (8-C, 11-C), 124.79 (9-C, 10-C).

ESI-MS *m/z* = 606.7 [M+H]⁺, 628.8 [M+Na]⁺, calculated for C₁₄H₂₂Br₄O₈ 601.81 (exact mass), 605.94 (molecular weight).

(11E,13E)-11,12,13,14-tetrabromo-3,6,9,16,19,22-hexaoxatetracos-11,13-diene-1,24-diol

(8)



8, n = 3

Yellow liquid, 85 mg. Yield: 46%.

Calculated for $C_{18}H_{30}Br_4O_8$ (%): C, 31.15; H, 4.36; Br, 46.05. Found: C, 31.44; H, 4.09; Br, 46.33.

1H -NMR (300 MHz, $CDCl_3$) δ ppm: 2.07 (2H, OH), 3.61-3.73 (m, 24H, 1-H, 2-H, 4-H, 5-H, 7-H, 8-H, 17-H, 18-H, 20-H, 21-H, 23-H, 24-H), 4.43, (d, 2H, $J = 13.5$, 10-H, 15-H), 4.54 (d, 2H, $J = 13.5$, 10'-H, 15'-H).

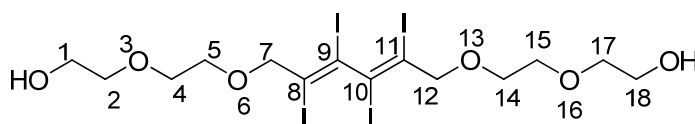
^{13}C -NMR (75 MHz, $CDCl_3$) δ ppm: 61.75 (1-C, 24-C), 69.35, 70.29, 70.33, 70.67 (2-C, 4-C, 5-C, 7-C, 18-C, 20-C, 21-C, 23-C), 72.50 (8-C, 17-C), 73.09 (10-C, 15-C), 117.44 (11-C, 14-C), 124.85 (12-C, 13-C).

ESI-MS $m/z = 694.9 [M+H]^+$, $716.9 [M+Na]^+$, calculated for $C_{18}H_{30}Br_4O_8$ 689.87 (exact mass), 694.04 (molecular weight).

General iodination procedure

To a solution of compounds **1** or **2** (0.26 mmol) in methanol (10 ml), iodine (0.82 mmol) was added. The mixture was stirred at room temperature overnight, and at the end solvent was removed by low pressure evaporation. Extraction was made with dichloromethane and was washed with water. After drying over sodium sulfate, the solvent was removed and the crude product was purified by chromatography (silica gel, diisopropylether/acetone 1/1).

(8E,10E)-8,9,10,11-tetraiodo-3,6,13,16-tetraoxaoctadeca-8,10-diene-1,18-diol (**9**)



Red-brown liquid, 83 mg. Yield: 40%.

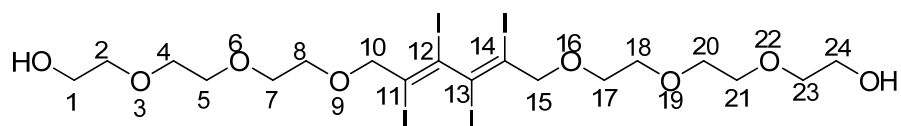
Calculated for C₁₄H₂₂I₄O₆ (%): C, 21.18; H, 2.79; I, 63.94. Found: C, 20.95; H, 2.93; I, 64.07.

¹H-NMR (300 MHz, CDCl₃) δ ppm: 2.09 (2H, OH), 3.63-3.78 (m, 16H, 1-H, 2-H, 4-H, 5-H, 14-H, 15-H, 17-H, 18-H), 4.30 (d, 2H, *J* = 13.5, 7-H, 12-H), 4.40 (d, 2H, *J* = 13.5, 7'-H, 12'-H).

¹³C-NMR (75 MHz, CDCl₃) δ ppm: 61.81 (1-C, 18-C), 69.27, 70.25 (2-C, 4-C, 15-C, 17-C), 72.40 (5-C, 14-C), 80.84 (7-C, 12-C), 97.08 (8-C, 11-C), 105.90 (9-C, 10-C).

ESI-MS *m/z* = 794.7 [M+H]⁺, 816.7 [M+Na]⁺, calculated for C₁₄H₂₂I₄O₈ 793.76.

(11*E*,13*E*)-11,12,13,14-tetraiodo-3,6,9,16,19,22-hexaoxatetracos-11,13-diene-1,24-diol (10)



10, n = 3

Red-brown liquid, 120 mg. Yield: 51%.

Calculated for $C_{18}H_{30}I_4O_8$ (%): C, 24.51; H, 3.43; I, 57.55. Found: C, 24.44; H, 3.56; I, 57.74.

1H -NMR (300 MHz, $CDCl_3$) δ ppm: 1.86 (2H, OH), 3.61-3.74 (m, 24H, 1-H, 2-H, 4-H, 5-H, 7-H, 8-H, 17-H, 18-H, 20-H, 21-H, 23-H, 24-H), 4.28, (d, 2H, $J = 13.5$, 10-H, 15-H), 4.38 (d, 2H, $J = 13.5$, 10'-H, 15'-H).

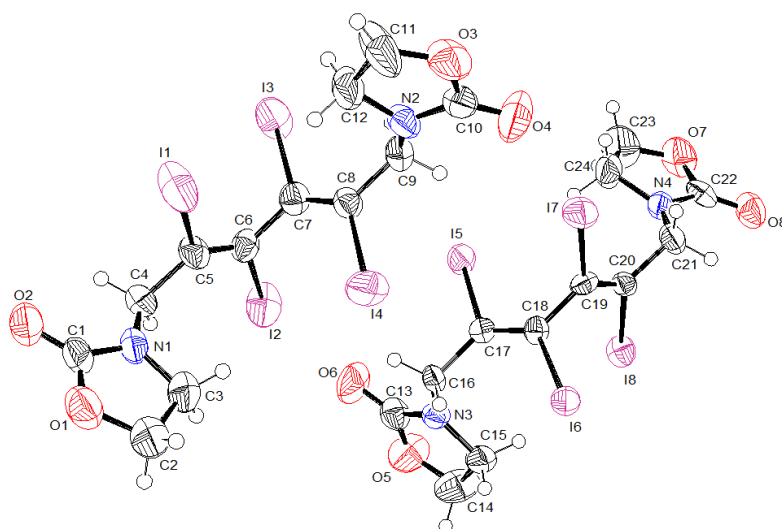
^{13}C -NMR (75 MHz, $CDCl_3$) δ ppm: 61.79 (1-C, 24-C), 69.30, 70.38, 70.73 (2-C, 4-C, 5-C, 7-C, 18-C, 20-C, 21-C, 23-C), 72.50 (8-C, 17-C), 80.87 (10-C, 15-C), 104.27 (11-C, 14-C), 106.02 (12-C, 13-C).

ESI-MS $m/z = 882.7 [M+H]^+$, $903.7 [M+Na]^+$, calculated for $C_{18}H_{30}I_4O_8$ 881.81.

Annex 1

Crystal data and structure refinement for compound 2

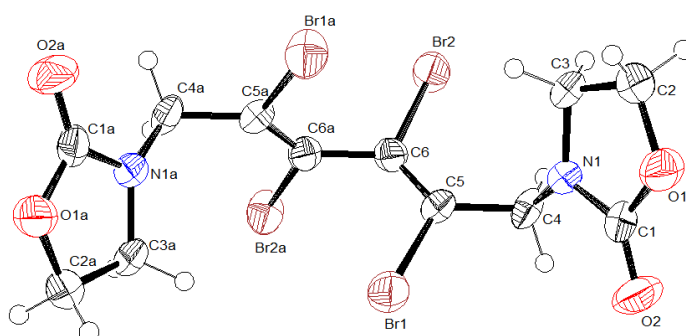
Empirical formula	C ₂₄ H ₂₄ I ₈ N ₄ O ₈	
Formula weight	1510.66	
Temperature (K)	297(2)	
Wavelength, Å	0.71073	
Crystal system	Monoclinic	
Space group	P2(1)/n	
Unit cell dimensions, Å	a = 17.1722(10) b = 11.5894(7) c = 19.7178(12)	α = 90° β = 103.0730(10) ° γ = 90°
Volume, Å ³	3822.4(4)	
Z	4	
Density (calculated) mg/m ³	2.625	
Absorption coefficient, mm ⁻¹	6.537	
F(000)	2732	
Crystal size/mm	0.27 x 0.22 x 0.20	
Theta range for data collection/ (°)	1.79 to 25.00	
Index ranges	-20 ≤ h ≤ 20, -13 ≤ k ≤ 13, -23 ≤ l ≤ 23	
Reflections collected	27157	
Independent reflections	6738 [R(int) = 0.0458]	
Refinement method	Full matrix least-squares on F ²	
Data/restraints/parameters	6738 / 0 / 398	
Goodness-of-method on F ²	1.103	
Final R indices [I > 2σ(I)]	R1 = 0.0554, wR2 = 0.1142	
R indices (all data)	R1 = 0.0639, wR2 = 0.1181	
Largest diff. peak and hole, eÅ ⁻³	2.548 and -1.913	



Annex 2

Crystal data and structure refinement for compound 3

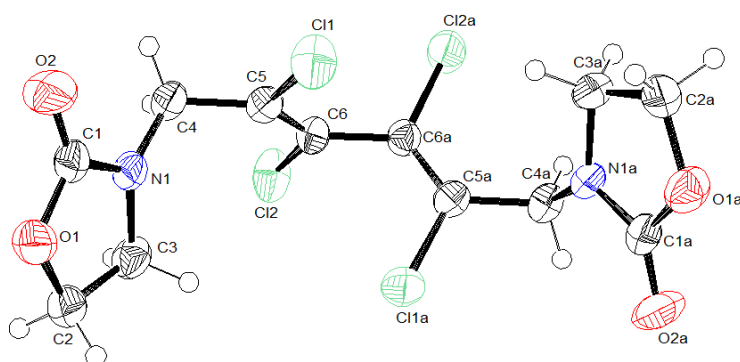
Empirical formula	C ₁₂ H ₁₂ Br ₄ N ₂ O ₄	
Formula weight	567.84	
Temperature (K)	297(2)	
Wavelength, Å	0.71073	
Crystal system	Monoclinic	
Space group	C 2/c	
Unit cell dimensions, Å	a = 22.162(4)	α = 90°
	b = 6.3307(10)	β = 113.885(2) °
	c = 12.776(2)	γ = 90°
Volume, Å ³	1639.0(4)	
Z	4	
Density (calculated) mg/m ³	2.301	
Absorption coefficient, mm ⁻¹	9.839	
F(000)	1080	
Crystal size/mm	0.28 x 0.22 x 0.15	
Theta range for data collection/ (°)	2.01 to 25.00	
Index ranges	-25 ≤ h ≤ 26, -7 ≤ k ≤ 7, -15 ≤ l ≤ 15	
Reflections collected	5636	
Independent reflections	1448 [R(int) = 0.0976]	
Refinement method	Full matrix least-squares on F ²	
Data/restraints/parameters	1448 / 0 / 100	
Goodness-of-method on F ²	1.041	
Final R indices [I > 2σ(I)]	R1 = 0.0585, wR2 = 0.1403	
R indices (all data)	R1 = 0.0722, wR2 = 0.1486	
Largest diff. peak and hole, eÅ ⁻³	1.139 and -0.633	



Annex 3

Crystal data and structure refinement for compound 4

Empirical formula	C ₁₂ H ₁₂ Cl ₄ N ₂ O ₄	
Formula weight	390.04	
Temperature (K)	297(2)	
Wavelength, Å	0.71073	
Crystal system	Monoclinic	
Space group	C 2/c	
Unit cell dimensions, Å	a = 22.379(4)	α = 90°
	b = 5.8742(10)	β = 111.065(3)°
	c = 12.425(2)	γ = 90°
Volume, Å ³	1524.2(5)	
Z	4	
Density (calculated) mg/m ³	1.700	
Absorption coefficient, mm ⁻¹	0.794	
F(000)	792	
Crystal size/mm	0.35 x 0.23 x 0.22	
Theta range for data collection/ (°)	1.95 to 25.05	
Index ranges	-26 ≤ h ≤ 26, -6 ≤ k ≤ 6, -14 ≤ l ≤ 14	
Reflections collected	5236 /	
Independent reflections	1343 [R(int) = 0.0316]	
Refinement method	Full-matrix least-squares on F ²	
Data/restraints/parameters	1343 / 0 / 100	
Goodness-of-method on F ²	1.137	
Final R indices [I > 2σ(I)]	R1 = 0.0554, wR2 = 0.1088	
R indices (all data)	R1 = 0.0657, wR2 = 0.1133	
Largest diff. peak and hole, eÅ ⁻³	0.466 and -0.342	



Chapter 3

**New building blocks for the synthesis of low band gap conjugated polymers
as active materials for organic solar cells**

Table of contents

3.1.Introduction	125
3.2.Monomer synthesis	130
3.2.1. Synthesis and reactivity of benzo[2,1-b:3,4-b']-dithiophene-4,5-dione	130
3.2.2. Synthesis and reactivity of 4,4'-bis(2-ethyl-hexyl)-4H-cyclopenta[2,1-b:3,4-b']dithiophene	137
3.3.Polymer synthesis	138
3.4.Conclusions	140
3.5.Experimental part	141
3.5.1. General remarks	141
3.5.2. Synthesis and characterization of compounds	142
Annexes	147

3.1. Introduction

At the end of 1970s began the search in the field of conducting polymers, when an increase in conductivity upon charge transfer doping was observed in the case of polyacetylene.¹ An ongoing research goal for conducting polymers has been the reduction of the energy bandgap (E_g) so that the absorbance of the undoped polymer shifts from the visible towards the near infrared region of the electromagnetic spectrum.

A number of low band gap polymers have been developed in recent years in the attempt to increase the device efficiency and to use them as active donors in polymer-based bulk heterojunction BHJ photovoltaic devices.

An organic photovoltaic device is fabricated by sandwiching a thin layer (or layers) of organic optoelectric materials between two conducting electrodes, one of which is transparent to allow incident light to reach the interior. In the active layer the organic materials absorb light, create separated charge carriers, and transport holes and electrons to the electrodes to furnish electric power.²

The design of new organic semiconductive conjugated materials is based on the band gap control of the material and thus on the control the energy level of the highest occupied molecular orbital (HOMO) -lowest unoccupied molecular orbital (LUMO) energy gap of the central unit of this materials.

Several structural factors influence the band gap of a polyaromatic conjugated system: the alternation of single and double bonds, the planarity of the conjugated system, the resonance energy of the aromatic cycle, the electronic effects of the substituents and intermolecular interactions³ (Fig. 1).

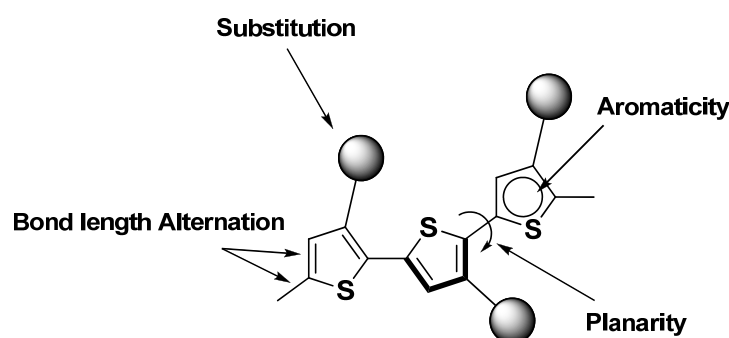


Fig. 1. Structural factors determining the band gap of linear conjugated systems

¹ Hardy Sze On Chan, Siu Choon Ng *Prog. Polym. Sci.* **1998**, *23*, 1167–1231

² Zhu, Z.; Waller, D.; Gaudiana, R.; Morana, M.; Muhlbacher, D.; Scharber, M. and Brabec, C. *Macromolecules* **2007**, *40*, 1981–1986

³Roncali, J. *Macromol. Rapid Commun.* **2007**, *28*, 1761–1775

Bond length alternation (BLA) which can be defined⁴ as the average of the difference in length between adjacent carbon-carbon bonds in a polyene chain, represent the major contribution to the magnitude of the energy gap and it is expected that structural modification that reduces bond length alternation to decrease the HOMO - LUMO gap. The two limiting mesomeric forms obtained by the flip of the double bond are not equivalent, thus the energy needed to switch from the aromatic to the quinoid form depends on the aromatic stabilization resonance energy of the aromatic unit. The dihedral angle between two consecutive contributes, tends to limit the delocalization of π -electrons and to increase the energy gap. Another way to modulate the HOMO - LUMO difference is to introduce electron-withdrawing or electron-releasing substituents.

Based on the structural factors presented, several solutions for the synthesis of low bang gap systems are proposed:

A. Resonance energy

The skeleton of a polyaromatic conjugated system,⁵ such as polyphenylene (**P1**) or polythiophene (**P2**) present two possible resonance structures: the aromatic form, in which each group maintains its aromaticity, and a quinoid form where π -electrons are delocalized by converting double bonds into single bonds and single bonds into double bonds.

BLA starts to decrease as the contribution of the quinoid form, in the ground state, increases, and thus HOMO - LUMO gap decreases. Polyphenylene has a higher band gap (3.2 eV) than poly(phenylenevinylene) (2.4 eV) due to benzenes high degree of aromaticity compared with phenylenevinylene, where the insertion of a double bond between the rings reduces the aromaticity. An even lower band gap was observed for polythiophene which is more likely to adopt a quinoid form determined by thiophenes lower aromaticity (Fig. 2).

⁴ Cheng, Y.J.; Yang, S.H.; Hsu, C.S. *Chem. Rev.* **2009**, doi: 10.1021/cr900182s

⁵ Roncali J. *Chem. Rev.* **1997**, *97*, 173-205

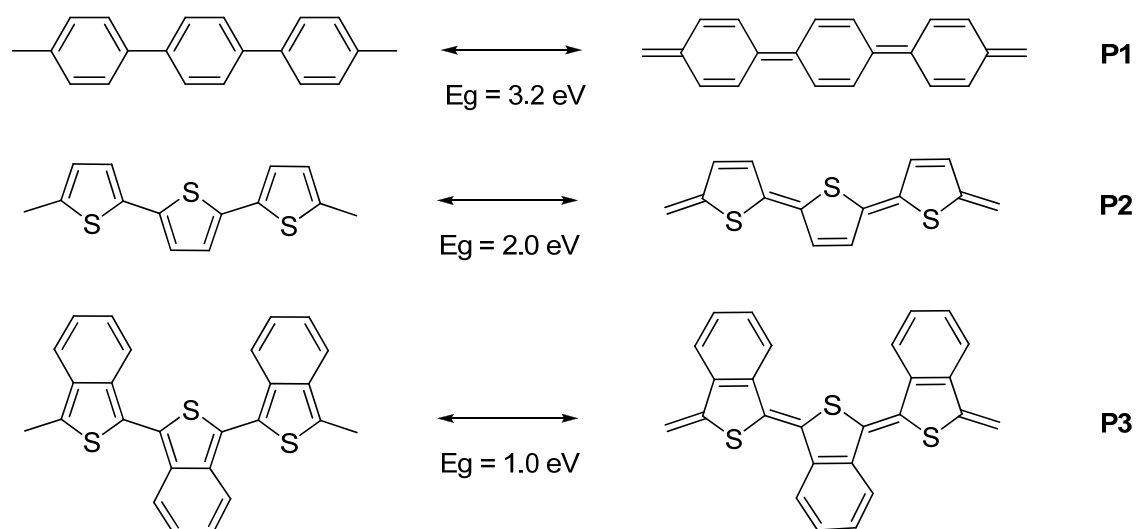


Fig. 2. Aromatic and quinoid forms of some polyaromatic systems

The first reported conjugated low band gap polymer, polyisothionaphthene⁶ (PITN – **P3**) represents the best example with effectively increased quinoid form and it was intensively used as model by changing benzene with other aromatic units such as pyrazine.⁷

B. Planarization of the conjugated system

Covalent rigidification between adjacent aromatic units leads to decreases BLA and determines band gap reduction by extending the conjugation and facilitating electron delocalization. For example, rigidified bithiophene by bridging with a sp^3 carbon (**P4**),⁸ exhibits fully planar conjugated structure and thus lower band gap. Extending the bridged systems (**P5**)⁹ a further decrease of the band gap is observed compared with parent compound polydithienylethylene (Fig. 3).

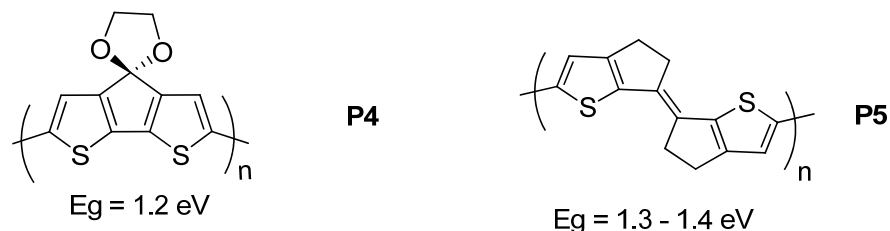


Fig. 3. Chemical structure of **P4** and **P5**

⁶ Wudl, f.; Kobayashi, M.; Heeger, A.J. *J. Org. Chem.* **1984**, *49*, 3382-3384

⁷ a) Pomerantz, M.; Chaloner-Gill, B.; Harding, L.O.; Tseng, J.J.; Pomerantz, W.J. *J. Chem. Soc. Chem. Commun.* **1992**, 1585-1586; b) Pomerantz, M.; Chaloner-Gill, B.; Harding, L.O.; Tseng, J.J.; Pomerantz, W.J. *Synth. Met.* **1993**, *55*, 960-965

⁸ Brisset, H.; Thobie-Gautier, C.; Jubault, M.; Gorgue, A.; Roncali, J. *J. Chem. Soc. Chem. Commun.* **1994**, 1305-1306

⁹ Roncali, J.; Thobie-Gautier, C.; Elandaloussi, E.H.; Frere, P. *J. Chem. Soc. Chem. Commun.* **1994**, 2249-2250

C. Electron withdrawing and electron-donating units

Electron donating groups raise the HOMO energy level while electron withdrawing groups lower the LUMO level decreasing the band gap. Poly(cyclopentabithiophene)s bearing electron withdrawing keto (**P6**)¹⁰ or dicyano (**P7**)¹¹ units (Fig. 4) have a band gap of 1.2 eV and 0.8 eV respectively. The low band gap in these structures was also attributed to the increased quinoid character of the ground state. The presence of electron donating alkoxy groups, in the case of poly(ethylenedioxy)thiophene (**P8**),¹² decrease with 0.5 eV the band gap compared with polythiophene (Fig. 4).

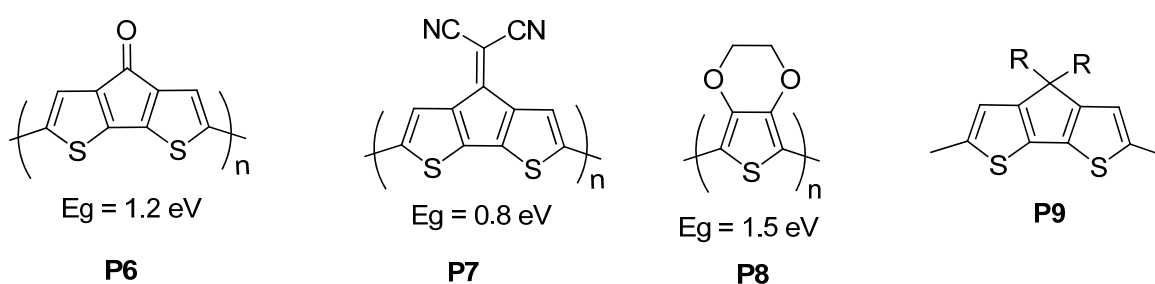


Fig. 4. Chemical structure of **P6 – P9**

An interesting example is cyclopenta[*c*]dithiophene (**P9**), which combines rigidly plan structure with inductive effect of the covalent bridge thus becoming an interesting building block for the synthesis of low band gap polymers.¹³

D. Alternate electron-rich (D) and electron-deficient (A) units

Reduced optical band gap in D-A polymers can be achieved by regular alternation of donor and acceptor units in the conjugated system. The interactions of the D-A units facilitate electron delocalization ensuring a higher HOMO and a lower LUMO. The degree of the band gap reduction is dependent of the strength of donor and acceptor. Thus **P11** (1.1 eV),¹⁴ having

¹⁰ Lambert, T.L.; Ferraris, J.P. *J. Chem. Soc., Chem. Commun.* **1991**, 752-753

¹¹ Lambert, T.L.; Ferraris, J.P. *J. Chem. Soc., Chem. Commun.* **1991**, 1268-1269

¹² Pei, Q.; Zuccarello, G.; Ahlskog, M.; Inganas, O. *Polymer* **1994**, *35*, 1347-1351

¹³ Coppo, P.; Turner, M.I. *J. Mater. Chem.* **2005**, *15*, 1123-1133

¹⁴ Van Mullekom, H.A.M.; Vekemans, J.A.J.M.; Meijer, E.W. *Chem Commun.* **1996**, 2163-2164

stronger pyrrole (D) and stronger benzothiadiazole (A) has a very low band gap when compared with similar D-A copolymers **P10** (1.7 eV)¹⁵ (Fig. 5).

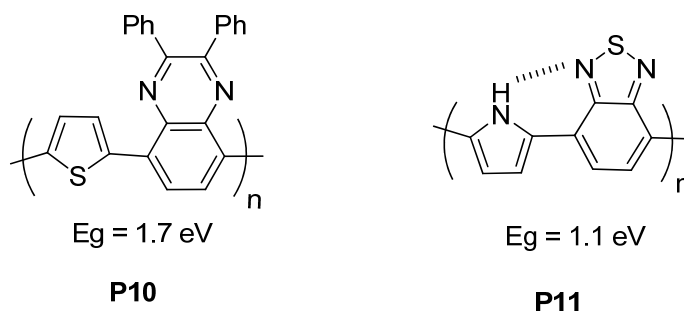
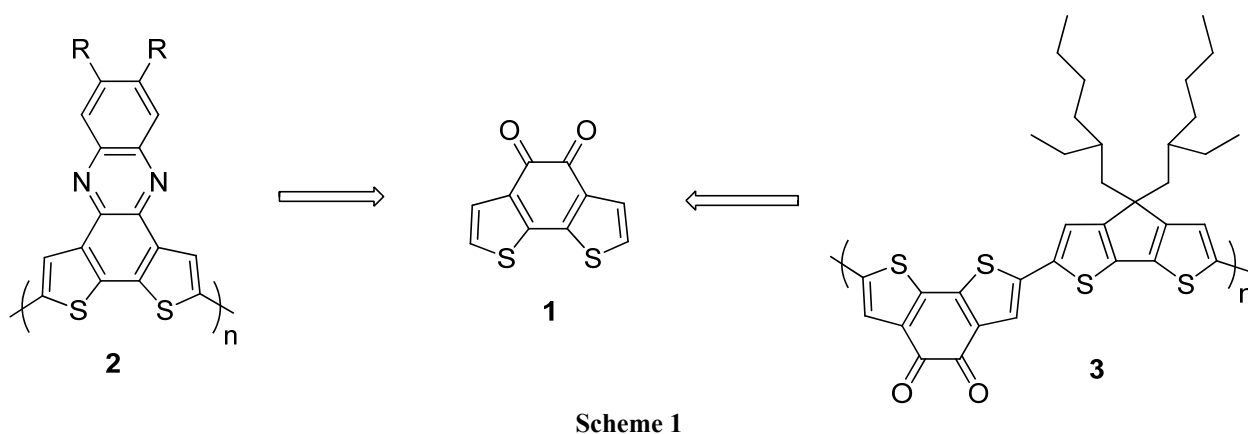


Fig. 5. Chemical structures of **P11** and **P12**

Intermolecular interactions can contribute to reduce the band gap of conjugated systems but can also influence their stability. Polymer insolubility is due to their very compact structure of unsubstituted conjugated systems. The presence of alkyl chains improve solubility but can also decrease their stability.

Our purpose is to synthesize some building blocks and the corresponding conjugated polymers, employing some of the above discussed approaches for band gap engineering. To this end we have envisioned the use of benzo[2,1-b:3,4-b']-dithiophene-4,5-dione (**1**) (Scheme 1) as key unit to develop acceptor building blocks that can be combined with donor units to produce low band gap systems.

The rigidity and planarity of these systems could lead to more effective π -electron delocalization when incorporated into a conjugated polymer backbone. This would lead to a smaller optical band gap while providing π - π interactions between polymer chains in thin solid film and improving charge carrier mobility in devices.⁵



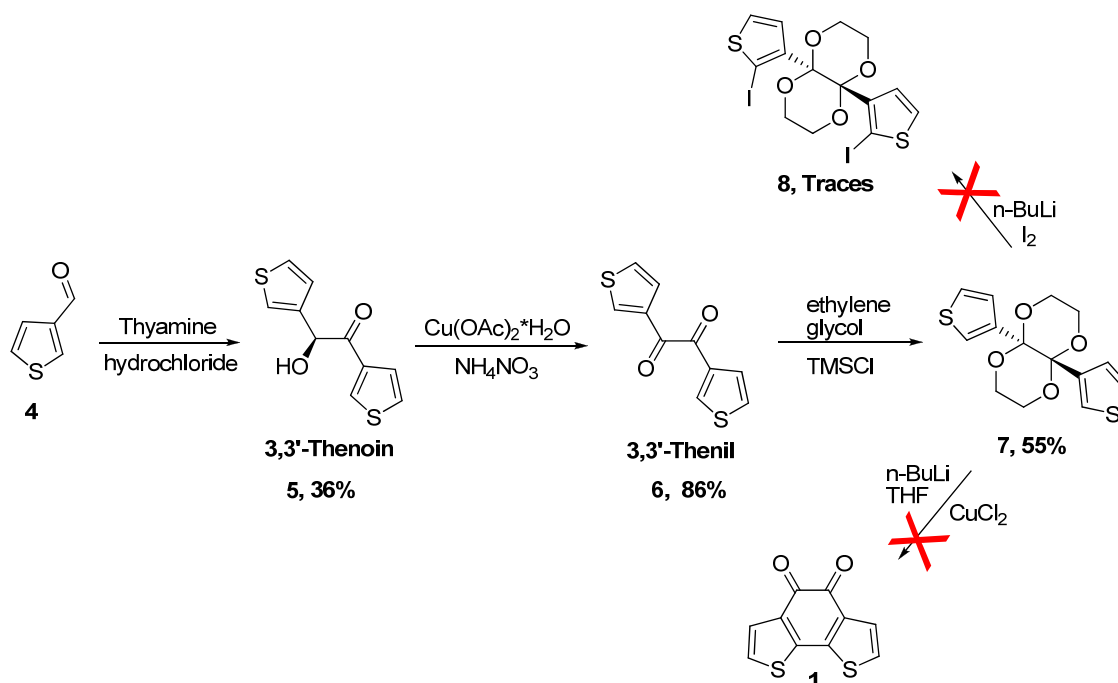
¹⁵ Yamamoto, T.; Zhou, Z.-H.; Kanbara, T.; Shimura, M.; Kizu, K.; Maruyama, T.; Nakamura, Y.; Fukuda, T.; Lee, B.-L.; Ooba, N.; Tomaru, S.; Kurihara, T.; Kaino, T.; Kubota, K.; Sasaki, S. *J. Am. Chem. Soc.* **1996**, *118*, 10389-10399

Starting from benzo[2,1-b:3,4-b']-dithiophene-4,5-dione (**1**) two types of π -conjugated polymers can be synthesized. Dithieno[3,2-a:2',3'-c]phenazine can be polymerized and the resulting polymers (**2**) can be used as donor material in bulk heterojunction solar cells. On the other hand, block-copolymers (**3**) can be synthesized by combining the alkylated cyclopentadithiophene as donor block with benzo[2,1-b:3,4-b']-dithiophene-4,5-dione (**1**) as acceptor block.

3.2. Monomer synthesis

3.2.1. Synthesis of and reactivity of benzo[2,1-b:3,4-b']-dithiophene-4,5-dione

The first route used for the synthesis of compound **1** was based on the synthesis of **7** starting from 3-thiophene carboxaldehyde (**4**) to obtain 3,3'-thenoin (**5**) which was subsequently used for the synthesis of 3,3'-thenil.^{16,17} Compound **6** was then reacted with ethyleneglycol to afford compound **1** in good yield. This later compound was then di-iodinated to give derivative **8** (Scheme 2). Unfortunately this compound was being obtained only in traces.



Scheme 2

¹⁶ Hyatt, J.L.; Stacy, V.; Wadkins, R.M.; Yoon, K.J.P.; Wierdl, M.; Edwards, C.C.; Zeller, M.; Hunter, A.D.; Danks, M.K.; Crundwell, G. and Potter, P.M. *J. Med. Chem.* **2005**, *48*, 5543-5550

¹⁷ Hoyos, P.; Fernandez, M.; Sinisterra, J.V. and Alcantara, A.R. *J. Org. Chem.* **2006**, *71*, 7632-7637

Attempts to synthesize dione (**1**) from compound **7** by a coupling reaction with copper II failed (Scheme 2). The X-ray analysis of a single crystal of **7** confirms the proposed structure (Fig. 6) but does not explain the lack of reactivity in the coupling reaction.

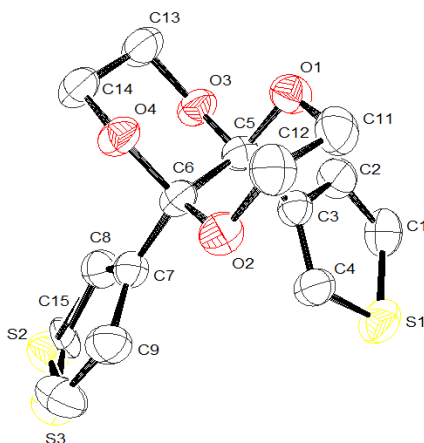
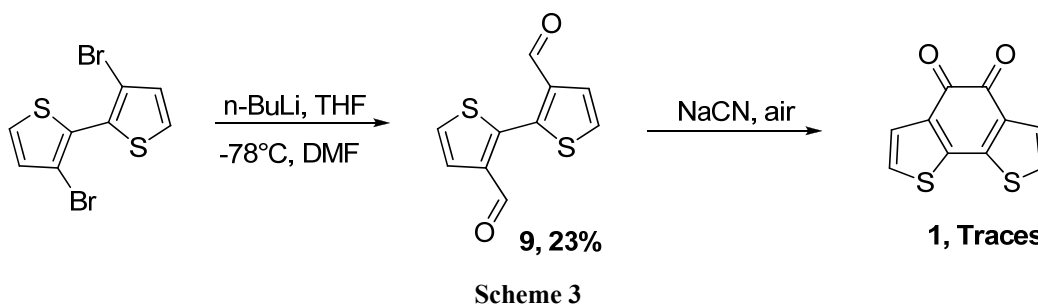


Fig. 6. ORTEP diagram of compound **7**

3,3'-Thiophene dicarboxaldehyde (**9**) was synthesized starting from 3,3'-dibromobithiophene, obtained in two steps from bithiophene¹⁸ or from 2,3-dibromothiophene in a coupling reaction in the presence of copper (II) chloride¹⁹, and was further used for the synthesis of the corresponding ketone (**1**). Following a synthetic route reported by Okada and coworkers²⁰ the dialdehyde was reacted with NaCN in presence of air affording the desired product **1** in traces (Scheme 3).

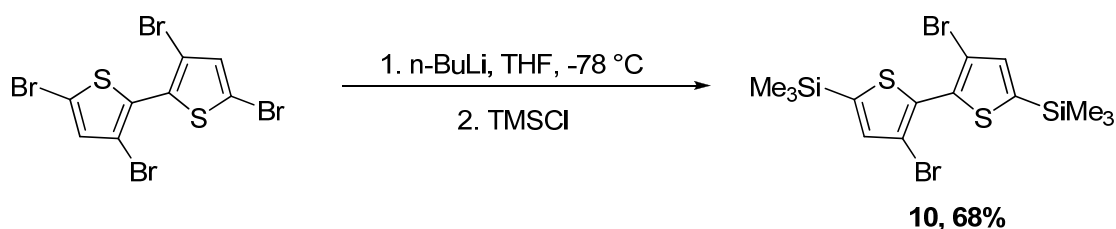


In order to limit possible secondary reactions we have protected the 5,5'-positions of the thiophene units. In this context 2,2',5,5'-tetrabromo-bithiophene was reacted with trimethylsilyl chloride to synthesize 5,5'-trisilyl derivative **10** in good yields (Scheme 4).

¹⁸ Khor, E.; Choon Ng, S.; Chze Li, H.; Chai, S. *Heterocycles* **1991**, 32, 9, 1805-1812

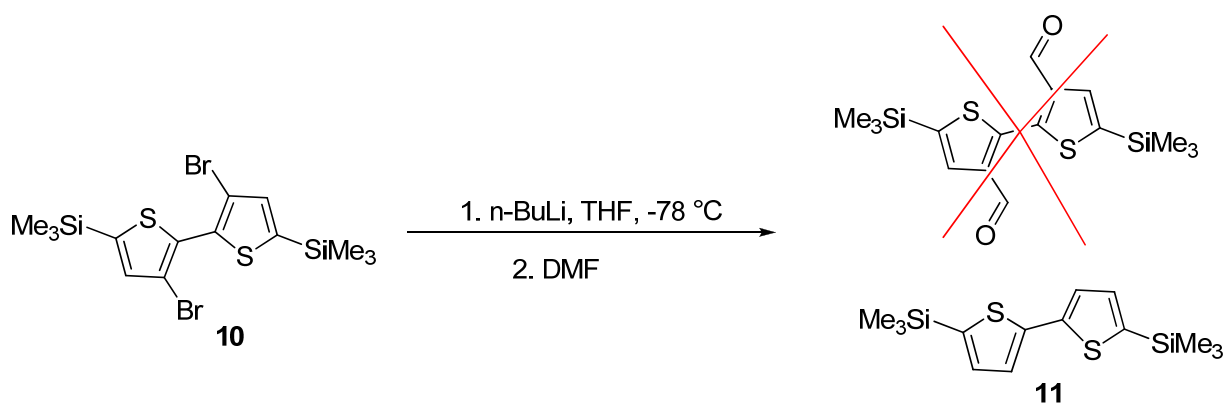
¹⁹ Allared, F.; Hellberg, J. and Remonen, T. *Tetrahedron Letters* **2002**, 43, 1553-1554

²⁰ Ohnishi, H.; Kozaki, M.; Okada, K. *Synthetic Metals* **2003**, 135-136, 85-86



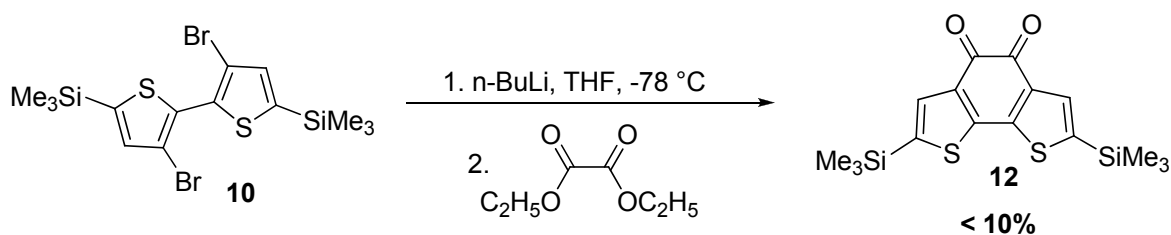
Scheme 4

The dibromo-silylated derivative, thus obtained, was reacted with dimethylformamide in order to obtain the corresponding dialdehyde, which could be further used for the synthesis of the dione **1**. No desired compound was isolated, the main product from the synthesis being 5,5'-trimethylsilyl-bithiophene (**11**) (Scheme 5).



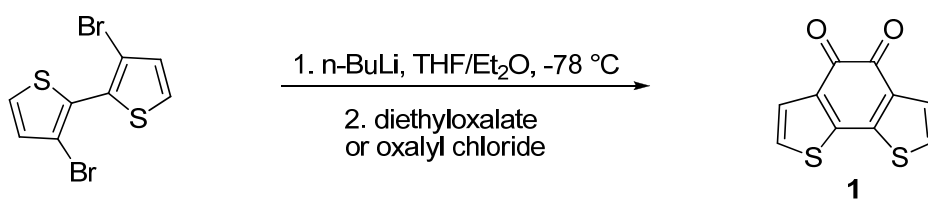
Scheme 5

The desired compound (**12**) was isolated in very low yields from the reaction of the silylated derivative (**10**) with diethyloxalate in the presence of n-BuLi at low temperature (Scheme 6).



Scheme 6

The third synthetic route tried for the synthesis of benzo[2,1-b:3,4-b']-dithiophene-4,5-dione (**1**) involved the reaction of the 3,3'-dibromo-bithiophene with diethyloxalate or oxalyl chloride and n-BuLi in a mixture of THF and diethylether (Scheme 7).



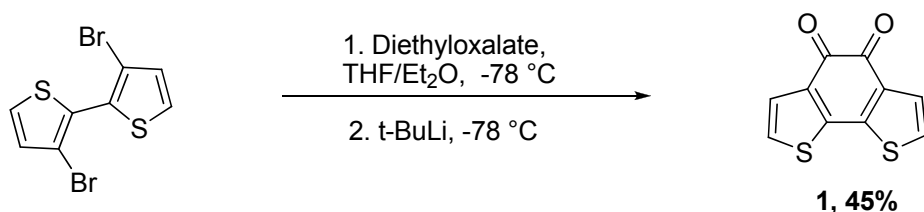
Scheme 7

Although very low, the yields of this reaction were the best we could get from the various synthetic routes investigated. In order to improve these low yields we have tried different working conditions starting with increasing or decreasing the reaction time of the substrate with *n*-BuLi, in order to generate the lithiated derivative, and by using diethyl oxalate or the more reactive oxalyl chloride as electrophile. In each case the yields for the diketone were very low and no starting material was recovered (Table 1).

Table 1. Used conditions for the synthesis of compound **1**

Work conditions	Yield (%)
1 - 30 min; 2 – diethyl oxalate in ether	< 10
1 - 1h; 2 - diethyl oxalate in ether	< 10
1 – 5 min; 2 – diethyl oxalate in ether	< 10
1 – 10 min; 2 – oxalyl chloride	< 10

Finally benzo[2,1-b:3,4-b']-dithiophene-4,5-dione (**1**) was obtained in 45% yields starting from 3,3'-dibromobithiophene and diethyloxalate in reaction with *t*-BuLi at low temperature (Scheme 8). The best working conditions consist in base and electrophile addition in the same time at low temperature in a mixture of dry diethylether and tetrahydrofuran as solvent.



Scheme 8

The UV-Vis spectrum of benzo[2,1-b:3,4-b']-dithiophene-4,5-dione (**1**), shows two absorption maximum at 320 nm and at 500 nm (Fig. 7).

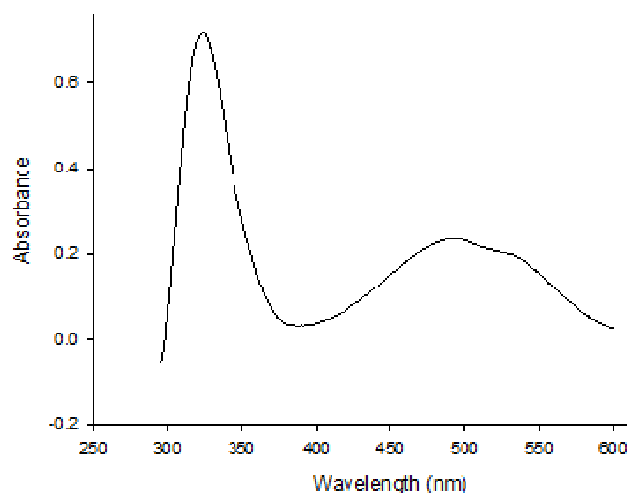
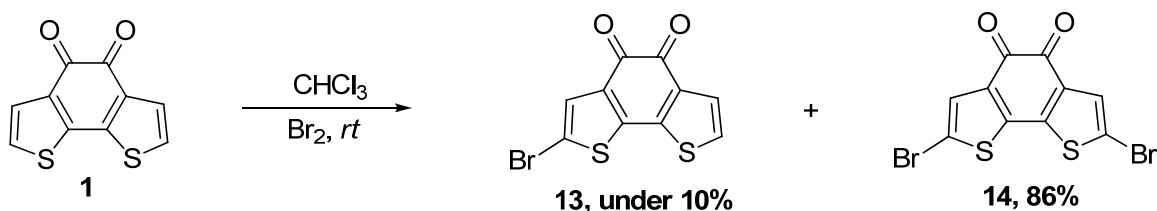


Fig. 7. UV-Vis absorption spectrum of **1** in methylene chloride

Compound **1** thus obtained was brominated to give the corresponding mono- and di-bromo derivatives (**13** and **14**) which were separated on chromatography silica gel using dichloromethane as eluent (Scheme 9). With a long time reaction and repetitive addition of an excess of bromine, compound **14** could be synthesized as single product with 86% yield.



Scheme 9

Single crystals of compound **14** were obtained from dichloromethane. The X-Ray analysis confirms the planar structure of the molecule, which is an important factor for the synthesis of low band gap polymer (Fig. 8).

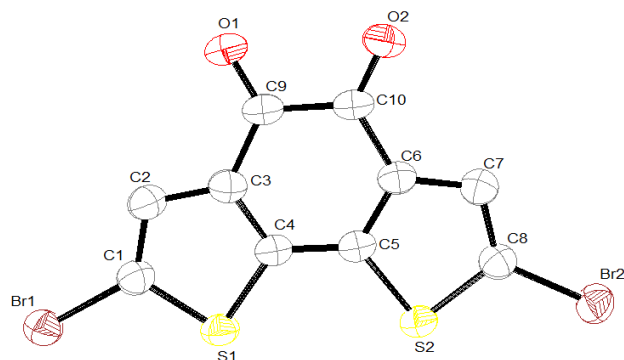


Fig. 8. ORTEP diagram of compound **14**

The UV-Vis spectrum of compound **14** shows a maximum of absorption at 530 nm, with a bathochromic shift of 30 nm compared with the ketone (Fig. 9).

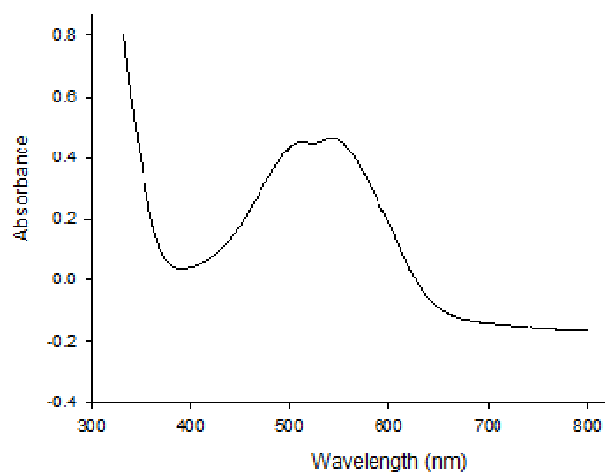
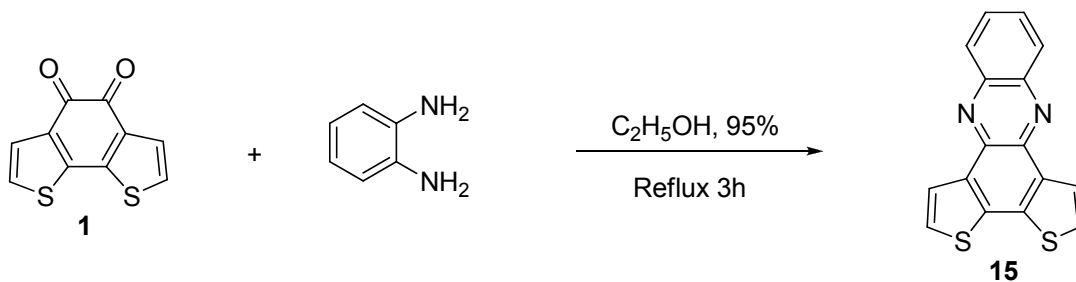


Fig. 9. UV-Vis absorption spectrum of **14** in methylene chloride

Reaction of compound **1** with *o*-phenylenediamine gave the condensation product, dithieno[3,2-*a*:2',3'-*c*]phenazine (**15**) in a quantitative yield (Scheme 10). The UV-Vis spectrum of the compound shows two maxima of absorption at 290 nm and 390 nm respectively (Fig. 10).



Scheme 10

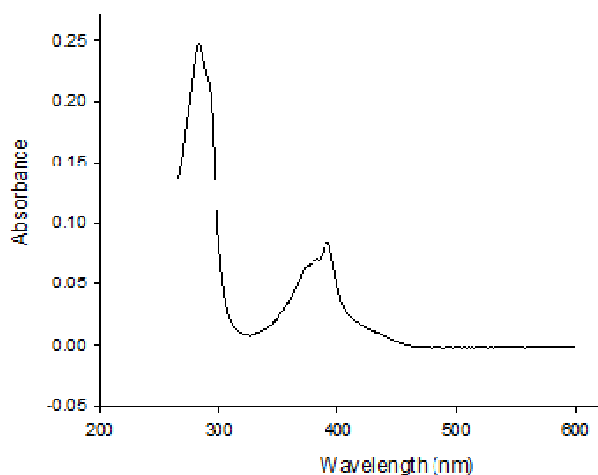
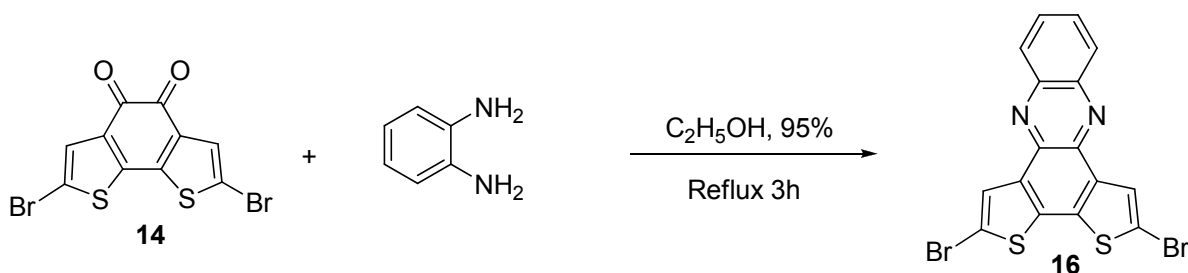


Fig. 10. UV-Vis absorption spectrum of **15** in methylene chloride

The condensation reaction between di-bromoderivative **14** and o-phenylenediamine gave a fully insoluble yellow product, phenazine **16** (Scheme 11).

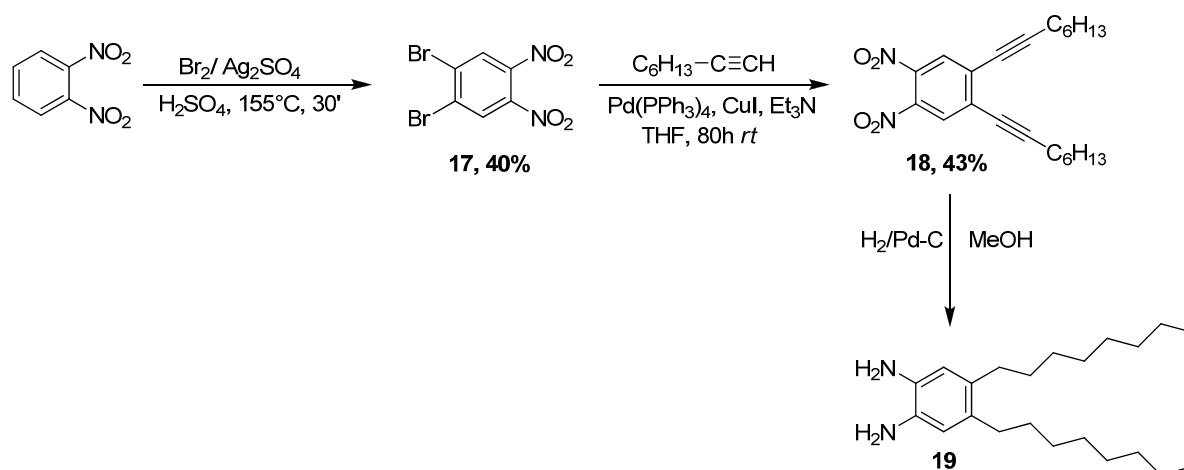


Scheme 11

In order to increase the solubility of this type of compounds, as well as the solubility of the future polymers, alkyl chains were attached to the phenyl ring. Thus 1,2-diamino-4,5-dioctylbenzene (**19**) was synthesized following the strategy used by Lin Pu and coworkers^{21,22} (Scheme 12)

²¹ Zhang, H.C.; Huang, W.S. and Pu, L. *J. Org. Chem.* **2001**, *66*, 2, 481-487

²² Ma, L.; Hu, Q.S.; Vitharana, D.; Wu, C.; Kwan, C. S. and Pu, L. *Macromolecules* **1997**, *30*, 204-218

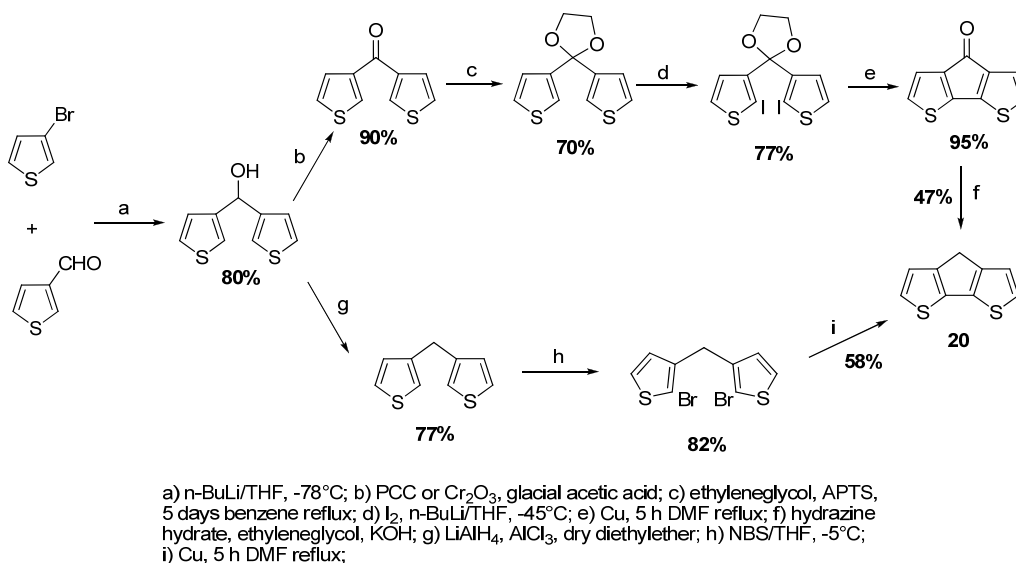


Scheme 12

Compound **19**, thus obtained will be used in reaction with benzo[2,1-b:3,4-b']-dithiophene-4,5-dione (**1**) to afford the corresponding condensation product. This monomer will be used as precursors for polymerization.

3.2.2. Synthesis and reactivity of 4,4'-bis(2-ethyl-hexyl)-4H-cyclopenta[2,1-b:3,4-b']dithiophene

Two synthetic routes were followed for the synthesis of 4H-cyclopenta[2,1-b:3,4-b']dithiophene (**20**), starting from 3-bromothiophene and 3-thiophene-carboxaldehyde^{1,23,24} (Scheme 13).

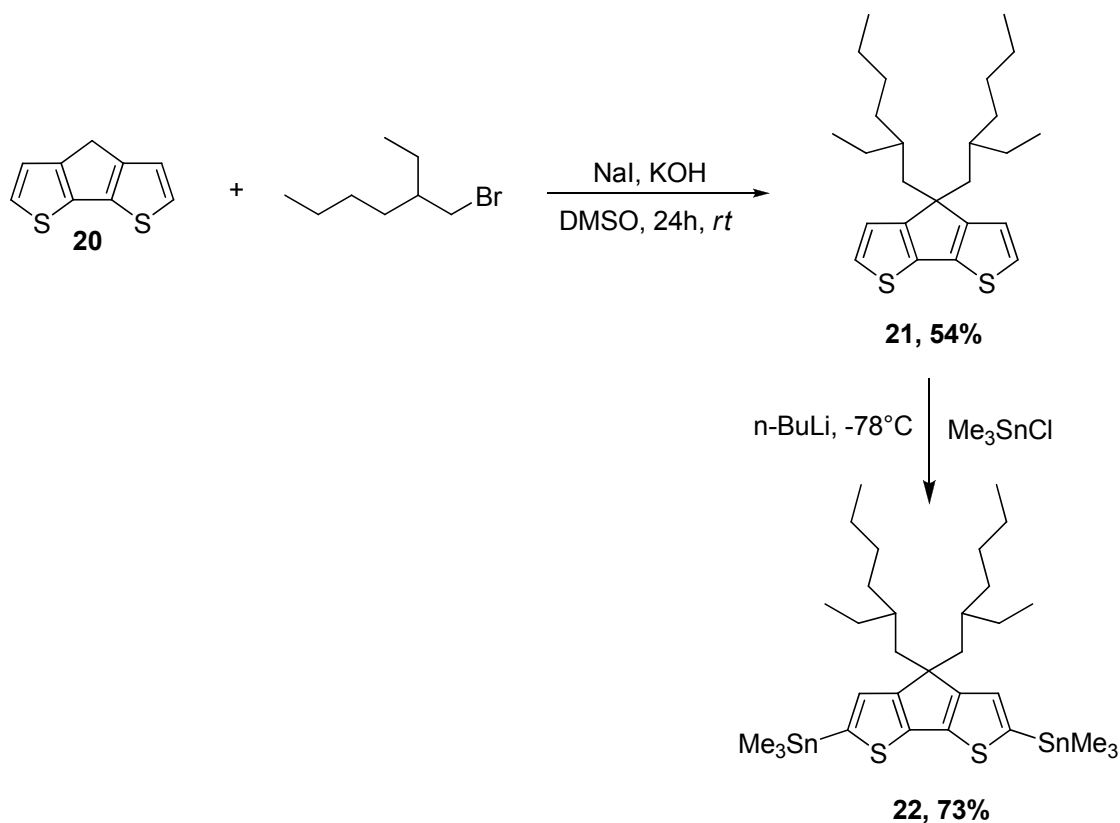


Scheme 13

²³ Brzezinski, J.Z.; Reynolds, J.R. *Synthesis* **2002**, 8, 1052-1056

²⁴ Amer, A.; Burkhardt, A.; Nkansah, A.; Shabana, R.; Galal, A.; Mark, A.B. and Zimmer, H. *Phosphorus, Sulfur, and Silicon* **1989**, 42, 63-71

Side alkyl chains were incorporated to improve solubility of the resulting polymers, thus cyclopentadithiophene (**20**) was alkylated to form 4,4'-bis(2-ethyl-hexyl)-4*H*-cyclopenta[2,1-*b*:3,4-*b'*]dithiophene (**21**) and was used for the synthesis of the bis(trimethylstannyl) derivative (**22**) (Scheme 14).



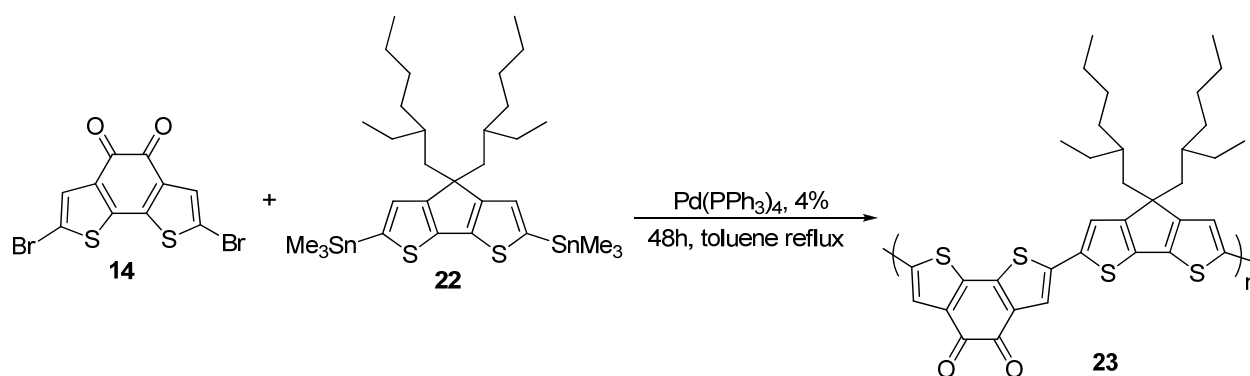
Scheme 14

Compounds **21** and **22**, thus obtained will then serve as building blocks for the synthesis of conjugated polymers with reduced bandgap.

3.3. Polymers synthesis

The preferred route for the synthesis of polymers for BHJ solar cells is based on the association of donor and acceptor units, to create intramolecular charge transfer and very low band gap polymers.

The first copolymer synthesis was performed by polycondensation of di-bromo-benzo[2,1-*b*:3,4-*b'*]dithiophene-4,5-dione (**14**) with 4,4'-bis(2-ethylhexyl)-2,6-bis(trimethylstannanyl)-4*H*-cyclopenta-[2,1-*b*:3,4-*b'*]dithiophene (**22**), through a Stille coupling reaction (Scheme 15).



Scheme 15

The crude polymer was washed with methanol in order to remove by products and short chain oligomers. The crude solid was extracted successively with hexane, chloroform, tetrahydrofuran and chlorobenzene using a Soxhlet apparatus.

The UV-Vis spectra of the fractions obtained after extraction show an insignificant bathochromic shift of the maximum of the absorption (Fig. 11).

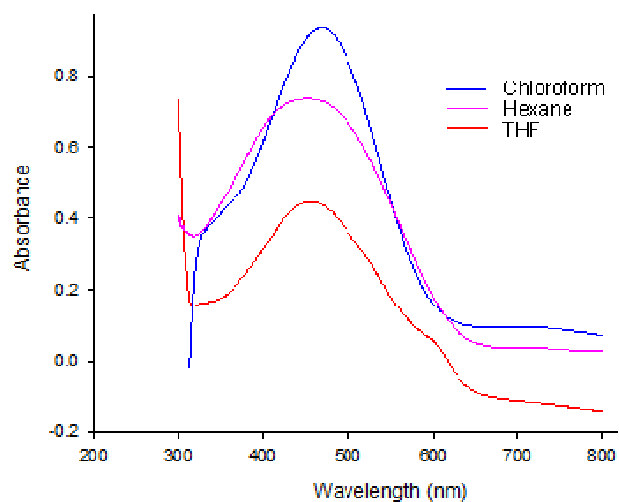


Fig. 11. UV-Vis absorption spectrum of the polymerization fraction in methylene chloride

The obtained fractions will be further analyzed by MALDI-TOF mass spectrometry in order to establish the polymerization degree.

As a perspective we will try to improve the polymerization conditions along with a proper analyze and characterization of the products.

Studies in the case of low band gap polymers will be continued using these intermediates either as single monomers or as copolymers by alternating donor and acceptor groups.

3.4. Conclusions

Benzo[2,1-b:3,4-b']-dithiophene-4,5-dione was used as key unit to develop acceptor building blocks to be combined with donor units to produce low band gap systems.

Several synthetic routes were envisaged and followed for the synthesis of benzo[2,1-b:3,4-b']-dithiophene-4,5-dione (**1**). The best obtained yield is 45% by a concomitant addition of the base and electrophile at low temperature in a mixture of dry diethylether and tetrahydrofurane as solvent.

Two dithieno[3,2-a:2',3'-c]phenazine derivatives were obtained in quantitative yields using dione **1** but could not be further used due to their low solubility. The synthesis of alkylated derivatives was presented as alternative to increase the solubility.

4,4'-Bis(2-ethyl-hexyl)-4*H*-cyclopenta[2,1-b:3,4-b']dithiophene (**21**) was obtained and used as donor block for the synthesis of conjugated polymers.

As a perspective, the obtained blocks will be further used for the development of low band gap systems, either as single monomer or as donor/acceptor alternating copolymers.

3.5. Experimental Part

3.5.1. General remarks

^1H NMR and ^{13}C NMR spectra were recorded on a Bruker AVANCE DRX 500 spectrometer operating at 500.13 and 125.7 MHz; δ are given in ppm (relative to TMS) and coupling constants (J) in Hz.

Mass spectra were recorded under EI mode on a VG-Autospec mass spectrometer or under MALDI-TOF mode on a MALDI-TOF-MS BIFLEX III Bruker Daltonics spectrometer.

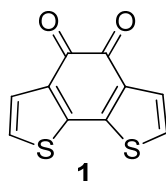
UV-Vis optical data were recorded with a Perkin-Elmer lambda 19 and lambda 950 spectrophotometers.

Melting points were obtained from a Reichert-Jung Thermovar hot-stage microscope apparatus and are uncorrected.

Column chromatography purifications were carried out on Merck silica gel Si 60 (40-63 μm).

2.4.2. Synthesis and characterization of compounds

benzo[2,1-b:3,4-b']-dithiophene-4,5-dione (1)



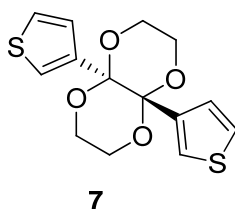
Under a nitrogen atmosphere, 1.5 M *t*-butyllithium in hexane (1.94 mL, 2.92 mmol) and diethyl oxalate (1.75 mmol) were added dropwise, in the same time, to a stirred solution of 3,3'-dibromobithiophene (0.5 g, 1.46 mmol) in dry tetrahydrofurane/diethylether (10/80 mL) at -78°C. After the complete addition the mixture was allowed to warm to room temperature and stirred for another 30 minutes at this temperature. Water was added and the extraction was made with diethylether and dichloromethane. The combined organic phase was dried over MgSO₄ and the solvent was evaporated affording the crude product as a black solid. Purification by column chromatography on silicagel with dichloromethane as eluent afforded the title compound as a black powder 142 mg in 44% yield.

¹H NMR (500 MHz, CDCl₃) δ ppm: 7.51 (d, 2H, *J* = 5Hz), 7.21 (d, 2H, *J* = 5Hz).

¹³C NMR (125 MHz, CDCl₃) δ ppm: 174.54, 143.87, 135.04, 127.80, 125.

MS-EI *m/z* 219.7, calculated for C₁₀H₄O₂S₂ 219.97.

(4*as*,8*as*)-4*a*,8*a*-di(thiophen-3-yl)hexahydro-[1,4]dioxino[2,3-*b*][1,4]dioxine (7)



In a 50 ml round-bottomed flask, 0.9 g (4.05 mmol) of 3,3'-thenil and 25 ml of dry ethyleneglycol, were added under nitrogen atmosphere. Chlorotrimethylsilane (2.25 ml, 17.82 mmol) was added in three portions, and the mixture was stirred at room temperature for 16h. Extraction was made with diethylether and the organic layer was washed with 5% NaHCO₃, brine and dried over magnesium sulfate. The solvent was evaporated and the resulting white

solid was purified by column chromatography on silica gel (petroleum spirits) to give compound **5** as white crystals 0.7 g in 55% yield, m.p. 185 °C.

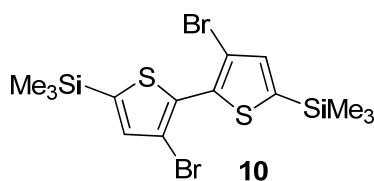
¹H NMR (500 MHz, CDCl₃) δ ppm: 3.72-3.76 (m, 4H), 4.17-4.18 (m, 4H), 7.15 (d, 2H, *J* = 5Hz), 7.24 (dd, 2H, *J* = 5Hz), 7.28 (dd, 2H).

¹³C NMR (125 MHz, CDCl₃) δ ppm: 139.09, 127.24, 125.44, 124.09, 93.89, 66.06, 61.15.

EI-MS found 310.8, calculated for C₁₄H₁₄O₄S₂ 310.03.

MS (MALDI-TOF) 311.17.

3,3'-dibromo-5,5'-bis(trimethylsilane)-2,2'-bithiophene (**10**)

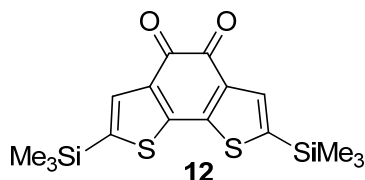


Under a nitrogen atmosphere, 2.5 M n-butyllithium in hexane (3.32 mL, 8.3 mmol) was added dropwise to a stirred solution of 3,3',5,5'-tetrabromobithiophene (2 g, 4.25 mmol) in dry tetrahydrofuran (45 mL) at -78°C. After 15 minutes at this temperature chlorotrimethylsilane (1.26 mL, 10 mmol) was added dropwise. The mixture was allowed to warm to room temperature and the solvent was evaporated to reduce pressure. The crude was taken up in diethylether and washed with saturated NH₄Cl solution. The organic layer was dried over MgSO₄, concentrated and the crude purified by chromatography on silicagel with hexane as eluent affording 1.3g of product, yield 68%.

¹H NMR (500 MHz, CDCl₃) δ ppm: 7.25 (s, 2H), 0.33 (s, 18H).

MS-EI m/z 467.8, calculated for C₁₄H₂₀Br₂S₂Si₂ 465.89.

2,7-trimethylsilyl-benzo[2,1-b:3,4-b']-dithiophene-4,5-dione (**12**)



Under a nitrogen atmosphere, 2.5 M n-butyllithium in hexane (2.22 mL, 5.55 mmols) was added dropwise to a stirred solution of 3,3'-dibromo-5,5'-bis(trimethylsilyl)bithiophene (1.3 g, 2.77 mmols) in dry tetrahydrofuran/diethylether (60/160 mL) at -78°C. After 1 hour at this

temperature diethyl oxalate (0.45mL, 3.32 mmols) was added dropwise. Saturated NH₄Cl solution was added and extraction was made with diethylether. The organic layer was dried over MgSO₄, concentrated and the crude was purified by chromatography on silicagel with pentane/diethylether 4/1 as eluent affording the desired product in traces.

¹H NMR (500 MHz, CDCl₃) δ ppm: 7.59 (s, 2H), 0.35 (s, 18H)

¹³C NMR (125 MHz, CDCl₃): δ ppm: 175.19, 148.33, 142.45, 135.80, 134.35, 29.68.

2-bromo-benzo[2,1-b:3,4-b']-dithiophene-4,5-dione (13) and 2,7-dibromo-benzo[2,1-b:3,4-b']-dithiophene-4,5-dione (14)



To a solution of benzo[2,1-b:3,4-b']-dithiophene-4,5-dione (0.3 g, 1.362 mmols) in 30 mL CHCl₃ was added portionwise a solution of 0.16 mL Br₂ in 10 mL of CHCl₃ during 2 days. The mixture was stirred at room temperature for another 1 day, the solvent was concentrated and the black crude was purified on chromatography on silica gel with dichloromethane as eluent. Dibromo-derivative (14) was obtained from the first fraction 354 mg in 86% yield.

¹H NMR (500 MHz, CDCl₃) δ ppm: 7.46 (s, 2H).

¹³C NMR (125 MHz, CDCl₃) δ ppm: 172.52, 143.57, 135.34, 129.99, 114.59.

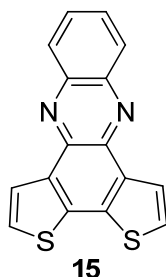
MS-EI m/z = 377.7, calculated for C₁₀H₂Br₂O₂S₂ 375.79.

From the second fraction we obtained the monobromo-derivative (13) in small amount.

¹H NMR (500 MHz, CDCl₃) δ ppm: 7.50 (d, 2H, *J* = 5Hz), 7.45 (s, 2H); 7.24 (d, 2H, *J* = 5Hz).

¹³C NMR (125 MHz, CDCl₃) δ ppm: 173.68, 173.33, 144.89, 142.44, 134.99, 129.81, 127.99, 126.12, 114.04.

bis-thieno[3,2-a:2',3'-c]-phenazine (15)

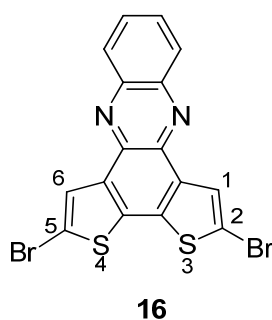


A mixture of benzo[2,1-b:3,4-b']-dithiophene-4,5-dione (40 mg, 0.18 mmols) and o-phenylenediamine (19.63 mg, 0.18 mmols) in 4 mL of ethanol 95% were refluxed for 3 hours. After 1 hour a yellow precipitate appeared in the solution. The solution was cooled to room temperature and the solvent was removed under reduced pressure. The yellow crude was solubilized in dichloromethane and filtered over a pad of silica, affording the product as a yellow solid in quantitative yield (50 mg).

¹H NMR (500 MHz, CDCl₃) δ ppm: 8.47 (d, 2H, *J* = 5Hz), 8.34 (dd, 2H, *J* = 3.5Hz), 7.87 (dd, 2H, *J* = 3.5Hz), 7.58 (d, 2H, *J* = 5Hz).

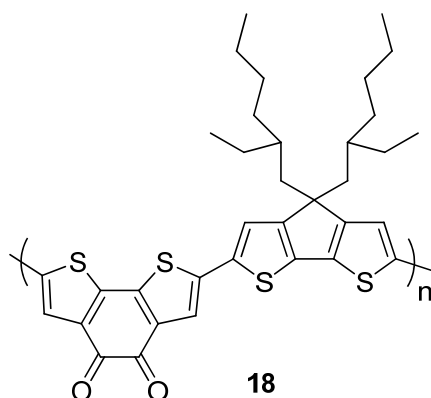
¹³C NMR (125 MHz, CDCl₃) δ ppm: 141.68, 139.97, 136.01, 134.89, 129.66, 129.38, 125.07, 124.54.

2,5-dibromo-bis-thieno[3,2-a:2',3'-c]-phenazine (15)



A mixture of the bromoderivative **14** (187.5 mg, 0.5 mmol) and o-phenylenediamine (54 mg, 0.5 mmol) in 10 mL of ethanol 95% were refluxed during 3 hours. After 1 hour a yellow precipitate appeared in the solution. The solution was cooled to room temperature and the solvent was removed under reduced pressure. The yellow crude was solubilized in dichloromethane (1L) and filtered over a pad of celite, affording the product as a yellow solid in quantitative yield (200 mg). The analysis of the compound could not be made because of its reduced solubility.

MS-EI *m/z* = 449.9, calculated for C₁₆H₆Br₂N₂S₂ 447.83.

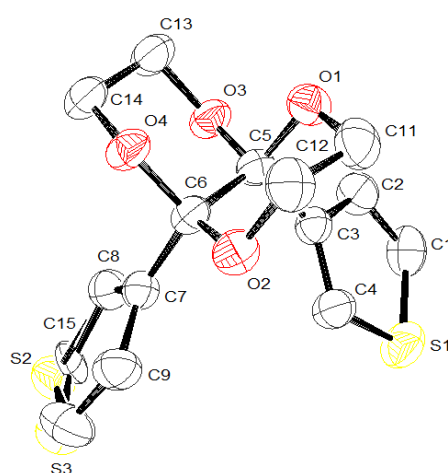


Bis(trimethylstannyl)-4,4-di(2-ethylhexyl)-cyclopenta[2,1-*b*:3,4-*b*]dithiophene (0.874 g, 1.2 mmol) and 2,2'-dibromo- benzo[2,1-*b*:3,4-*b'*]dithiophene-4,5-dione (0.453 g, 1.2 mmol) were dissolved in toluene (100 mL). The reaction was purged with nitrogen, and Pd(PPh₃)₄ catalyst (27.73 mg, 0.0234 mmol) was added. The reaction was further purged with nitrogen for 10 min and heated to 120 °C under nitrogen for 48 h. The reaction was poured into methanol (400 mL), and the black precipitate was collected by filtration, washed with methanol, and dried.

Annex 1

Crystal data and structure refinement for compound 7

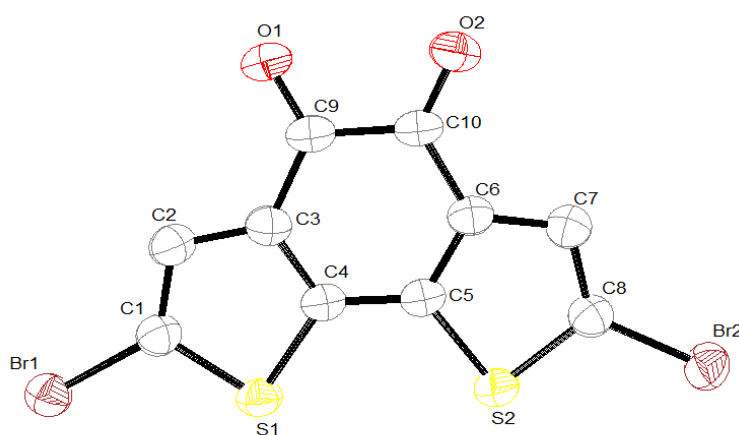
Empirical formula	C ₁₄ H ₁₄ O ₄ S ₂	
Formula weight	310.37	
Temperature (K)	293(2)	
Wavelength, Å	0.71073	
Crystal system	Orthorhombic	
Space group	P 21 21 21	
Unit cell dimensions, Å	a = 9.4943(9) b = 11.681(1) c = 12.244(1)	$\alpha = 90^\circ$ $\beta = 90^\circ$ $\gamma = 90^\circ$
Volume, Å ³	1357.9(2)	
Z	4	
Density (calculated) mg/m ³	1.518	
Absorption coefficient, mm ⁻¹	0.402	
F(000)	648	
Crystal size/mm	0.54 x 0.15 x 0.12	
Theta range for data collection/ (°)	2.41 to 26.13	
Index ranges	-11 ≤ h ≤ 11, -13 ≤ k ≤ 14, -14 ≤ l ≤ 15	
Reflections collected	10566 / 2661	
Independent reflections	[R(int) = 0.0517]	
Refinement method	Full-matrix least-squares on F ²	
Data/restraints/parameters	2661 / 0 / 193	
Goodness-of-method on F ²	1.056	
Final R indices [I > 2σ(I)]	R1 = 0.0370, wR2 = 0.0762	
R indices (all data)	R1 = 0.0606, wR2 = 0.0905	
Largest diff. peak and hole, eÅ ⁻³	0.212 and -0.251	



Annex 2

Crystal data and structure refinement for compound **14**

Empirical formula	C ₁₀ H ₂ Br ₂ O ₂ S ₂	
Formula weight	378.06	
Temperature (K)	293(2)	
Wavelength, Å	0.71073	
Crystal system	Monoclinic	
Space group	C 2 / C	
Unit cell dimensions, Å	a = 21.981(2)	$\alpha = 90^\circ$
	b = 5.7278(4)	$\beta = 104.78(1)^\circ$
	c = 17.877(2)	$\gamma = 90^\circ$
Volume, Å ³	2176.3(3)	
Z	8	
Density (calculated) mg/m ³	2.308	
Absorption coefficient, mm ⁻¹	7.810	
F(000)	1440	
Crystal size/mm	0.73 x 0.15 x 0.04	
Theta range for data collection/ (°)	1.92 to 26.02	
Index ranges	-26<=h<=26, -6<=k<=6, -22<=l<=21	
Reflections collected	10190 / 2092	
Independent reflections	[R(int) = 0.0465]	
Refinement method	Full-matrix least-squares on F ²	
Data/restraints/parameters	2092 / 0 / 153	
Goodness-of-method on F ²	0.979	
Final R indices [I>2σ(I)]	R1 = 0.0348, wR2 = 0.0884	
R indices (all data)	R1 = 0.0408, wR2 = 0.0917	
Largest diff. peak and hole, eÅ ⁻³	0.596 and -0.487	



Chapter 4

Three-dimensional π -conjugated architectures based on a twisted bithiophene core

Table of contents

4.1. Introduction	149
4.2. Synthesis	153
4.2.1. Synthesis and reactivity of 3,3',5,5'-(3,4-ethylenedioxythiophene)-2,2'-bithiophene (E₄T₂) and tetra(3,4-ethylenedioxythiophene)-3,3'-dithienyl-2,2'-bithiophene (E₄T₄)	154
4.2.2. Derivatization of twisted 2,2'-bithiophene by thiophene and alkylthiophenes: synthesis and reactivity	157
4.2.3. 3D conjugated systems containing 3,4-ethylenedioxythiophene (EDOT) block	163
4.3. Electronic properties of 3D π -conjugated systems based on twisted 2,2'-bithiophene	167
4.3.1. Optical properties of the 3D precursors	167
4.3.2. Electrochemical properties of the monomers	170
4.3.3. Electropolymerization of the 3D precursors	173
4.3.4. Electrochemical and optical properties of the polymers	181
4.3.5. Chemical polymerization of 3D systems	183
4.4. 3D conjugated systems containing 2-ethylhexyl-carbazole units	185
4.5. Conclusions	189
4.6. Experimental part	190
4.6.1. General remarks	190
4.6.2. Synthesis and characterization of compounds	191
Annexes	206

4.1. Introduction

Since the scientists from Bayer company¹ described a novel conducting polymer poly(3,4-ethylenedioxythiophene) (PEDOT) with moderate band gap, low oxidation potential and good optical transparency in the conducting state, widespread applications have been developed on the basis of its conducting properties. Although initially envisioned for antistatic coatings,² PEDOT has been then considered for other applications like active materials in capacitors or hole injection layer in OLEDs³ and solar cells.^{4,5,6}

From a different point of view, 3,4-ethylenedioxythiophene (EDOT) has attracted increasing interest as a building block for the design of various classes of molecular functional π -conjugated systems⁷ because of its specific electronic properties in terms of reactivity and donor effect combined with the structuring effect of the EDOT unit.⁸ The presence of ether groups in the structure of EDOT confer a high reactivity to the free α , α' positions and also prevent the formation of parasitic α - β' linkages during the polymerization process. The self-rigidification effect resulted from non-covalent intramolecular S-O interactions^{7,9} represents another advantage associated with the use of EDOT for the design of functional π -conjugated systems.¹⁰

The electronic properties of the EDOT derivatives can be tuned by structural modification using different functional substituents¹¹ or by association of the EDOT units with electron withdrawing groups¹² in copolymers.¹³ A related approach has been initially developed in Reynolds group who inserted different aromatic units between two EDOT groups in view of the synthesis of various precursors.¹⁴ Electropolymerization of this type of precursors, using the

¹ Jonas, F.; Schrader, L. *Synth. Met.* **1991**, *41*, 831-836

² Jonas, F.; Morrison, J.T. *Synth. Met.* **1997**, *85*, 1397-1398

³ Granstrom, M.; Inganas, O. *Adv. Mater.* **1995**, *7*, 1012-1015

⁴ Brabec, C.J.; Sariciftei, N.S.; Hummelen, J.C. *Adv. Funct. Mater.* **2001**, *11*, 15-26

⁵ Kirchmeyer, S.; Reuter, K. *J. Mater. Chem.* **2005**, *15*, 2077-2088

⁶ Groenendaal, L.G.; Jonas, F.; Freitag, D.; Pielartzik, H.; Reynolds, J.R. *Adv. Mater.* **2000**, *7*, 481-494

⁷ Roncali, J.; Blanchard, P.; Frere, P. *J. Mater. Chem.* **2005**, *15*, 1589-1610

⁸ Spencer, H.J.; Skabara, P.J.; Giles, M.; McCulloch, I.; Coles, S.J.; Hursthouse, M.B. *J. Mater. Chem.* **2005**, *15*, 4783-4792

⁹ a) Raimundo, J.M.; Blanchard, P.; Frere, P.; Mercier, N.; Ledoux-Rak, I.; Hierle, R.; Roncali, J. *Tetrahedron Letters* **2001**, *42*, 1507-1510; b) Leriche, P.; Turbiez, M.; Monroche, V.; Blanchard, P.; Skabara, P.J.; Roncali, J. *Tetrahedron Letters* **2003**, *44*, 649-652

¹⁰ Turbiez, M.; Frere, P.; Roncali, J. *Tetrahedron* **2005**, *61*, 3045-3053

¹¹ a) Mohanakrishnan, A.K.; Hucke, A.; Lyon, M.A.; Lakshmikantham, M.V.; Cava, M.P. *Tetrahedron*, **1999**, *55*, 11745-11754

¹² Groenendaal, L.G.; Zotti, G.; Aubert, P.H.; Waybright, S.M.; Reynolds, J.R. *Adv. Mater.* **2003**, *15*, 855-879

¹³ a) Akoudad, S.; Roncali, J. *Chem. Commun.* **1998**, 2081-2082; b) Roncali, J. *J. Mater. Chem.* **1999**, *9*, 1875-1893; c) Raimundo, J-M.; Blanchard, P.; Brisset, H.; Akoudad, S.; Roncali, J. *Chem. Commun.* **2000**, 939-940; d) Turbiez, M.; Frere, P.; Blanchard, P.; Roncali, J. *Tetrahedron Letters* **2000**, *41*, 5521-5525

¹⁴ Sotzing, G.A.; Reynolds, J.R.; Steel, P.J. *Chem. Mater.* **1996**, *8*, 882-889

high reactivity of the lateral EDOT units can generate electroactive materials, with different conjugation lengths along the polymer depending on the nature of the central building block.

The synthesis of hybrid oligomers based on different combinations of EDOT and thiophene units was also developed in our group. Thus some alternating EDOT-Thiophene oligomers¹⁵ were synthesized in which self-rigidification was demonstrated.¹⁶ Some of these conjugated systems can function as organic semiconductors.

Microporous materials have received a great scientific interest because of the large specific surface area associated with their porous structure which allows to envision numerous potential applications.¹⁷ Aluminosilicate zeolites and the following aluminum phosphates, discovered by Flanigen and coworkers at the beginning of the 1980s,¹⁸ represent the predominant class of microporous materials with three-dimensional framework. Zeolites were the first class of nanoporous materials discovered and due to their stability a large number of applications find utility in the area of ion-exchange, separations and catalysis.¹⁹ Metal-organic frameworks (MOFs) have received great interest, in the last years, among nanoporous materials due to the possibility to reach large overall pore volume and adjustable pore sizes combining organic ligands with metals. Intensively studied by Ferey and coworkers, MOFs find applications as gas sorbent (H₂, N₂, CO₂, CH₄),²⁰ drug delivery²¹ or catalyst.²²

In the past two years a new class of microporous materials based on conjugated systems has emerged in the literature. Thus, Copper and workers have described the first conjugated microporous polymers (CMPs) based on poly(aryleneethylene)s structure.²³ Although this novel class of purely organic microporous materials tend to complement the classical ones (zeolites, activated carbons and metal organic frameworks) in a variety of applications, the presence of π -conjugated systems in their structure allows to envision quite new applications in particular in

¹⁵ Turbiez, M.; Frere, P.; Allain, M.; Videlot, C.; Ackermann, J.; Roncali, J. *Chem. Eur. J.* **2005**, *11*, 3742-3735

¹⁶ Turbiez, M.; Frere, P.; Roncali, J. *J. Org. Chem.* **2003**, *68*, 5357-5360

¹⁷ Thomas, A.; Kuhn, P.; Weber, J.; Titirici, M.M., Antonietti, M. *Macromol. Rapid Commun.* **2009**, *30*, 221-236

¹⁸ Wilson, S.T.; Lok, B.M.; Messina, C.A.; Cannan, T.R.; Flanigen, E.M. *J. Am. Chem. Soc.* **1982**, *104*, 1146-1147

¹⁹ Cheetham, A.K.; Ferey, G.; Loiseau, T. *Angew. Chem. Int. Ed.* **1999**, *38*, 3268-3292

²⁰ a) Ferey, G.; Latroche, M.; Serre, C.; Millange, F.; Loiseau, T.; Percheron-guegan, A. *Chem. Commun.*, **2003**, 2976-2977; b) Cote, A.P.; Benin, A.I.; Ockwig, N.W.; O'Keeffe, M.; Matzger, A.J.; Yaghi, O.M. *Science*, **2005**, *310*, 1166-1170; c) Ramsahye, N.A.; Maurin, G.; Bourrelly, S.; Llewellyn, P.; Loiseau, T.; Fery, G. *Phys. Chem. Chem. Phys.*, **2007**, *9*, 1059-1063; d) Surble, S.; Millange, F.; Serre, C.; Duren, T.; Latroche, M.; Bourrelly, S.; Llewellyn, P.L.; Ferey, G. *J. Am. Chem. Soc.*, **2006**, *128*, 14889-14896; d) Collins, D.J.; Zhou, H.C. *J. Mater. Chem.* **2007**, *17*, 3154-3160; d) Bourrelly, S.; Llewellyn, P.L.; Serre, C.; Millange, F.; Loiseau, T.; Ferey, G. *J. Am. Chem. Soc.*, **2005**, *127*, 1359-13521

²¹ Horcajada, P.; Serre, C.; Vallet-Regi, M.; Sebban, M.; Taulelle, F.; Ferey, G. *Angew. Chem. Int. Ed.* **2006**, *45*, 5974-5978

²² Horcajada, P.; Surble, S.; Serre, S.; Hong, D.Y.; Seo, Y.Y.; Chang, J.S.; Greneche, J.M.; Margiolaki, I.; Ferey, G. *Chem. Commun.* **2007**, 2820-2822

²³ Jiang, J.X.; Su, F.; Trewin, A.; Wood, C.D.; Campbell, N.L.; Niu, H.; Dickinson, C.; Ganin, A.Y.; Rosseinsky, M.J.; Khimiyak, Y.Z.; Cooper, A.I. *Angew. Chem. Int. Ed.* **2007**, *46*, 8574-8578

the field of electrode materials for sensors or electrochemical energy storage fields where a high surface-to-volume ratio is crucial.

CMPs already described in the literature are chemically generated and the only characterizations performed on these materials are elemental analysis and gas sorption. They can be obtained via different synthetic routes, using C-C coupling reactions already described for the synthesis of linear conjugated polymers. Thus, Sonogashira-Hagihara coupling has been used to synthesize microporous poly(aryleneethylene) and poly(phenylene butadiynylene) based on 1,3,5-substituted-benzenes^{24,25} or tetraphenylmethane and -silane compounds,²⁶ Suzuki coupling was used for the synthesis of microporous poly(phenyleneethylene) and poly(*p*-phenylene) based on a spirobifluorene²⁷ and Yamamoto coupling for poly(spirobifluorene) and poly(arylene spirobifluorene).²⁸ Oxidative polymerization was also employed for the synthesis of poly(arylene thienylene)s microporous conjugated polymers based on thiophene linkage.²⁹

It has been showed that the micropore size and specific surface area can be easily tuned by changing the length of the central connecting precursor.³⁰ Thus pore size control in microporous conjugated polymers can be achieved by using highly rigid, bulk nonplanar architectures.³¹

Three dimensional conjugated architectures have been recently synthesized and used as new classes of organic-semiconductors with isotropic charge transport and optical properties.³² Thus, tetrahedral molecules consisting of four conjugated oligothiophenes chains attached onto a central node such as silicon or twisted bithiophene, have been synthesized in our group, and used as donor materials in bulk hetero-junction solar cells.³³

In this work, various new types of 3D conjugated architectures have been synthesized in view of the electrochemical generation of electroactive microporous conjugated networks. To this end, we have taken advantage of the high reactivity of the EDOT moiety to generate conjugate networks by polymerization. As a first step in this direction we have used as starting

²⁴ Jiang, J.X.; Su, F.; Niu, H.; Wood, C.D.; Campbell, N.L.; Khimyak, Y.Z.; Cooper, A.I. *Chem. Commun.* **2008**, 486-488

²⁵ Kobayashi, N.; Kijima, M. *J. Mater. Chem.* **2007**, 4289-4296

²⁶ Stockel, E.; Wu, X.; Trewin, A.; Wood, C.D.; Clowes, R.; Campbell, N.L.; Jones, J.T.A.; Khimyak, Y.Z.; Adams, D.J.; Cooper, A.I. *Chem. Commun.* **2009**, 212-214

²⁷ Weber, J.; Thomas, A. *J. Am. Chem. Soc.* **2008**, *130*, 6334-6335

²⁸ Schmidt, J.; Werner, M.; Thomas, A. *Macromolecules* **2009**, *42*, 4426-4429

²⁹ Schmidt, J.; Weber, J.; Epping, J.D.; Antonietti, M.; Thomas, A. *Adv. Mater.* **2009**, *21*, 702-705

³⁰ Jiang, J.X.; Su, F.; Trewin, A.; Wood, C.D.; Niu, H.; Jones, J.T.A.; Khimyak, Y.Z.; Cooper, A.I. *J. Am. Chem. Soc.* **2008**, *130*, 7710-7720

³¹ Weber, C. *Angew. Chem. Int. Ed.* **2008**, *47*, 448-450

³² Roncali, J.; Leriche, P.; Cravino, A. *Adv. Mater.*, **2007**, *19*, 2045-2060

³³ (a) Roncali, J.; Thobie-Gautier, C.; Brisset, H.; Favard, J.F.; Guy, A. *J. Electroanal. Chem.* **1995**, *381*, 257; (b) Roncali, J. *J. Mater. Chem.* **1999**, *9*, 1875-1893; (c) Roquet, S.; de Bettignies, R.; Leriche, P.; Cravino, A.; Roncali, J. *J. Mater. Chem.* **2006**, *16*, 3040-3045

node a bithiophene unit twisted by steric effects already reported in the laboratory of Angers by Karpe et al.³⁴ In that previous work a series of 3D conjugation architectures built by fixation of short-chains oligothiophenes onto a twisted bithiophene has been synthesized in order to analyze the influence of the conjugation and electron delocalization along the main axis by changing the dihedral angle between the two thiophene of the bithiophene core by different twisting groups.

X-ray crystallographic structures of this type of compounds have demonstrated that twisted bithiophene represent an interesting node for building 3D conjugated architectures. The steric hindrance between the bulky groups attached at the 3,3'-positions of the bithiophene core produces a dihedral angle up to 90° between the two thiophene units thus leading to a tetrahedral starting unit which can be used for the construction of 3D conjugated systems.³⁵

In this context, it could be expected that combining the 3D structure of the twisted bithiophene core with the high polymerizability of the terminal EDOTs could represent an interesting approach for the formation of electroactive 3D networks. The size and surface area, but also the electronic properties of these materials could be tuned by using different blocks for the construction of the lateral chains (Fig. 1). We present here the synthesis of the 3D precursors and the characterization of the electronic properties of the materials obtained by electrochemical and chemical polymerization of these precursors.

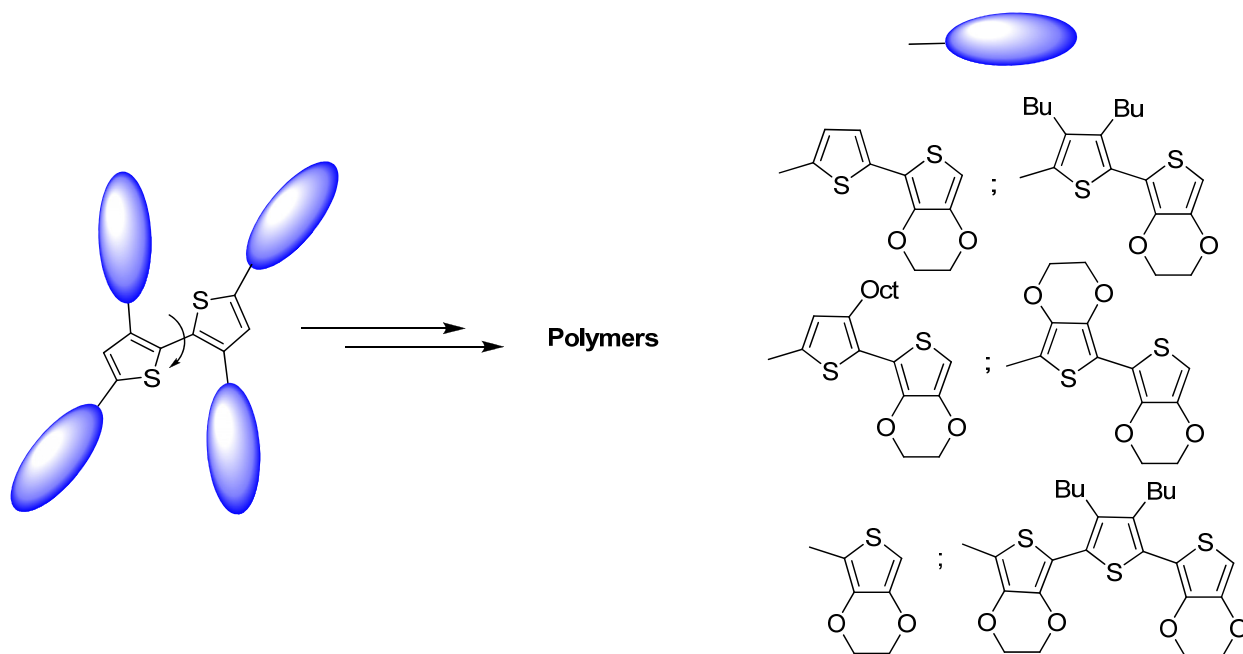


Fig. 1. Target molecules

³⁴ Karpe, S.; Cravino, A.; Frere, P.; Allain, M.; Mabon, G.; Roncali, J. *Adv. Funct. Mater.*, **2007**, *17*, 1163-1171

³⁵ Roncali, J. *Acc. Chem. Res.*, doi:10.1021/ar900041b

Figure 1 shows the structure of the various target molecules. An easily available precursor is the tetra-EDOT-bithiophene obtained by the direct connection of four EDOT units onto the bithiophene core. The solubility of these types of precursors could be increased using octyl- and dibutyl-thiophene. Extension of the conjugated branches can also be achieved by replacing the thiophene with EDOT units and alternated thiophene-EDOT unit.

Electropolymerization of this type of precursor could produce electroactive nanoporous material with potential applications in areas such as gas and energy storage, sensors or heterogenous catalysis.^{36,37}

In the following we present our results on different size monomer synthesis, their electropolymerization behavior and electronic properties by UV-Vis spectroscopy and cyclic voltammetry.

4.2. Synthesis

Different routes have been envisaged for the synthesis of the target 3D systems using two types of materials: 3,3',5,5'-tetrabromo-2,2'-bithiophene (**1**) and tetrabromo-3,3'-dithienyl-2,2'-bithiophene (**2**).

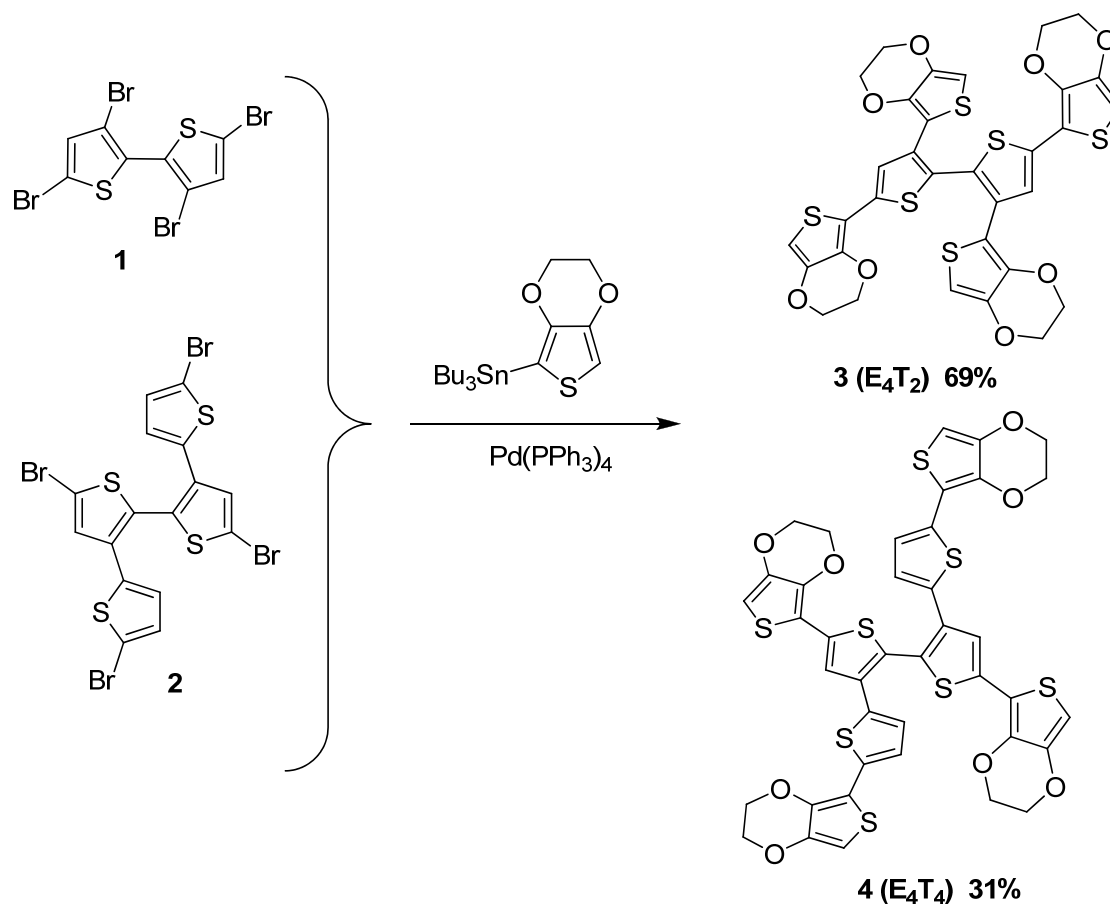
- A first route involves the direct coupling reaction between the thiophenic core and EDOT.
- The second route aims at an extension of the conjugation length of the precursors in three steps namely i) a coupling reaction of the bithiophenic units with different thiophene and alkylthiophene, ii) a bromination reaction at the α -position of the terminal thiophene units and iii) a further coupling reaction to attach the terminal EDOT units.
- A third route is based on the synthesis of some EDOT and thiophene-EDOT oligomers followed by fixation onto the main bithiophenic core.

³⁶ Cheetham, A.; Ferey, G.; Loiseau, T. *Angew. Chem. Int. Ed.* **1999**, *38*, 3268-3292

³⁷ Kitagawa, S; Kitaura, R; Noro, S. *Angew. Chem. Int. Ed.* **2004**, *43*, 2334-2375

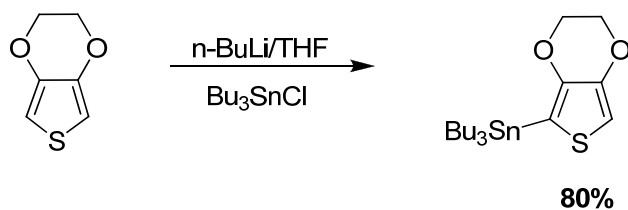
4.2.1. Synthesis and reactivity of 3,3',5,5'-(3,4-ethylenedioxythiophene)-2,2'-bithiophene (E_4T_2) and tetra(3,4-ethylenedioxythiophene)-3,3'-dithienyl-2,2'-bithiophene (E_4T_4)

Compounds **3** (E_4T_2)³⁸ and **4** (E_4T_4) have been synthesized by a Stille coupling reaction between the 2,2'-bithiophene cores (**1**, **2**) and the stannic derivative of EDOT as depicted in Scheme 1.



Scheme 1

Tributylstannyl-EDOT was obtained in good yields from EDOT following a known procedure³⁹ (Scheme 2).

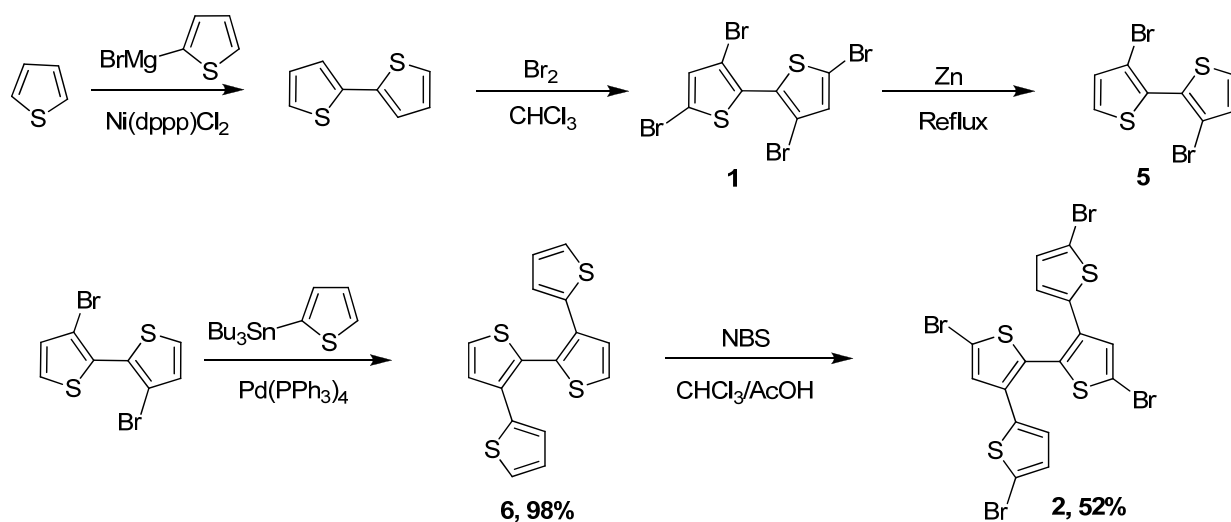


Scheme 2

³⁸ Piron, F.; Mabon, G.; Leriche, P.; Grosu, I.; Roncali, J. *Electrochem. Commun.* **2008**, *10*, 1427-1430

³⁹ Zhu, S.S.; Swager, T.M. *J. Am. Chem. Soc.* **1997**, *119*, 12568-12577

The two starting tetrabromo-derivatives were obtained in good yields by using the reported bromination procedure of 2,2'-bithiophene⁴⁰ and 3,3'-di(2-thienyl)-2,2'-bithiophene⁴¹ respectively (Scheme 3). A Stille coupling between compound **5** and tributylstannylthiophene gave compound **6** in 90% yields. Bromination of compound **6** at the four α -positions using bromine in chloroform/acetic acid at room temperature gave the 3,3'-di(2-thienyl)-2,2'-bithiophene **2** in 52% yield.



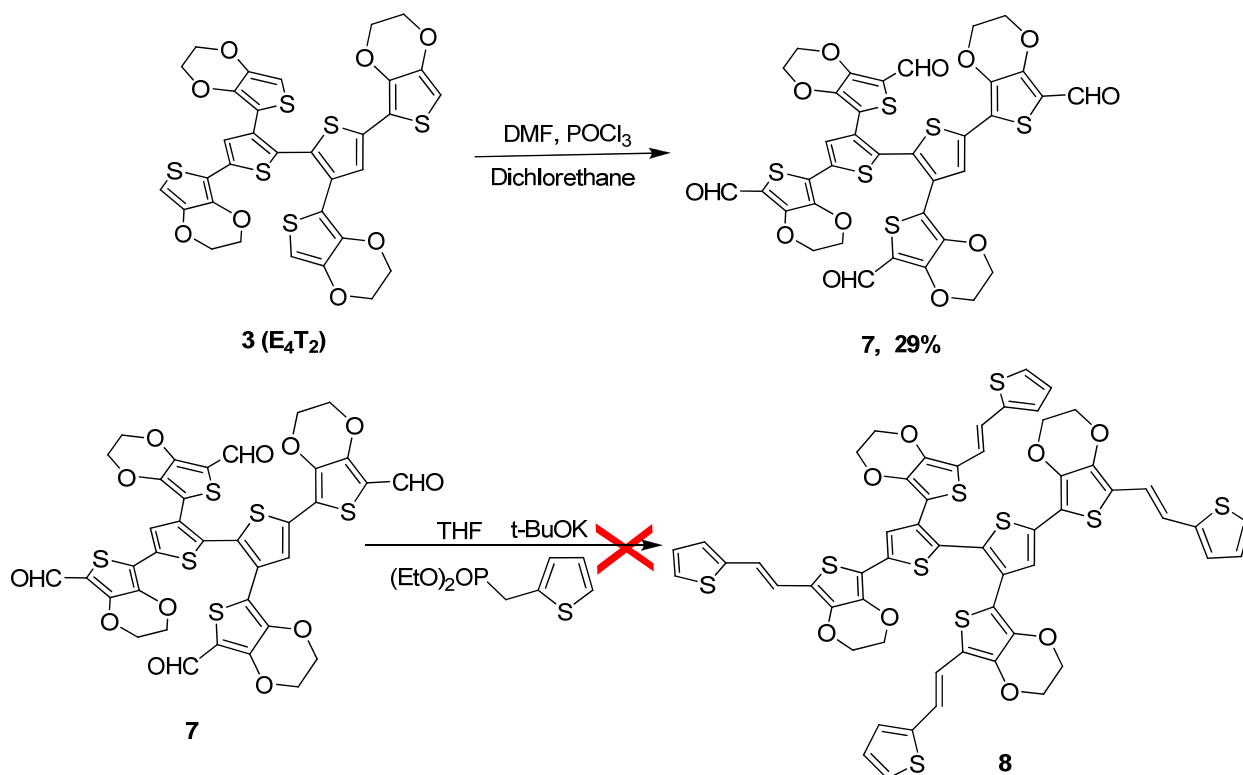
Scheme 3

Finally derivatives **3** (E_4T_2) and **4** (E_4T_4) were obtained by Stille coupling reaction between the stannic of EDOT and compound **1** and **2** respectively in 69% and 31% yield respectively.

Starting from these two compounds with terminal EDOT unit, we have tried different synthetic approaches in order to extend the conjugated branches by introducing thienylenevinylene side chains. Thus we have synthesized the tetra-aldehyde **7** in moderate yields, by a Vilsmeier-Haack reaction (Scheme 4). Fourfold Wittig-Horner olefination between tetra-aldehyde **7** and thiophene-phosphonate in the presence of potassium *tert*-butoxide (*t*-BuOK) at room temperature failed due to the low solubility of the starting material which was entirely recovered.

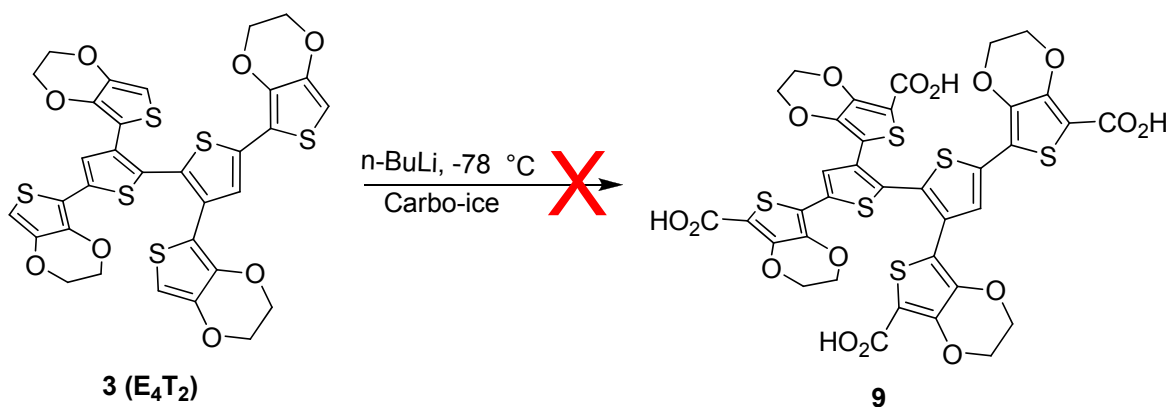
⁴⁰ Khor, E.; Choon Ng, S.; Chze Li, H.; Chai, S. *Heterocycles* **1991**, *32* (9), 1805-1812

⁴¹ Chan, H.S.O.; Ng, S.N.; Seow, S.H.; Moderschein, M.J.G. *J. Mater. Chem.* **1992**, *56*, 5059



Scheme 4

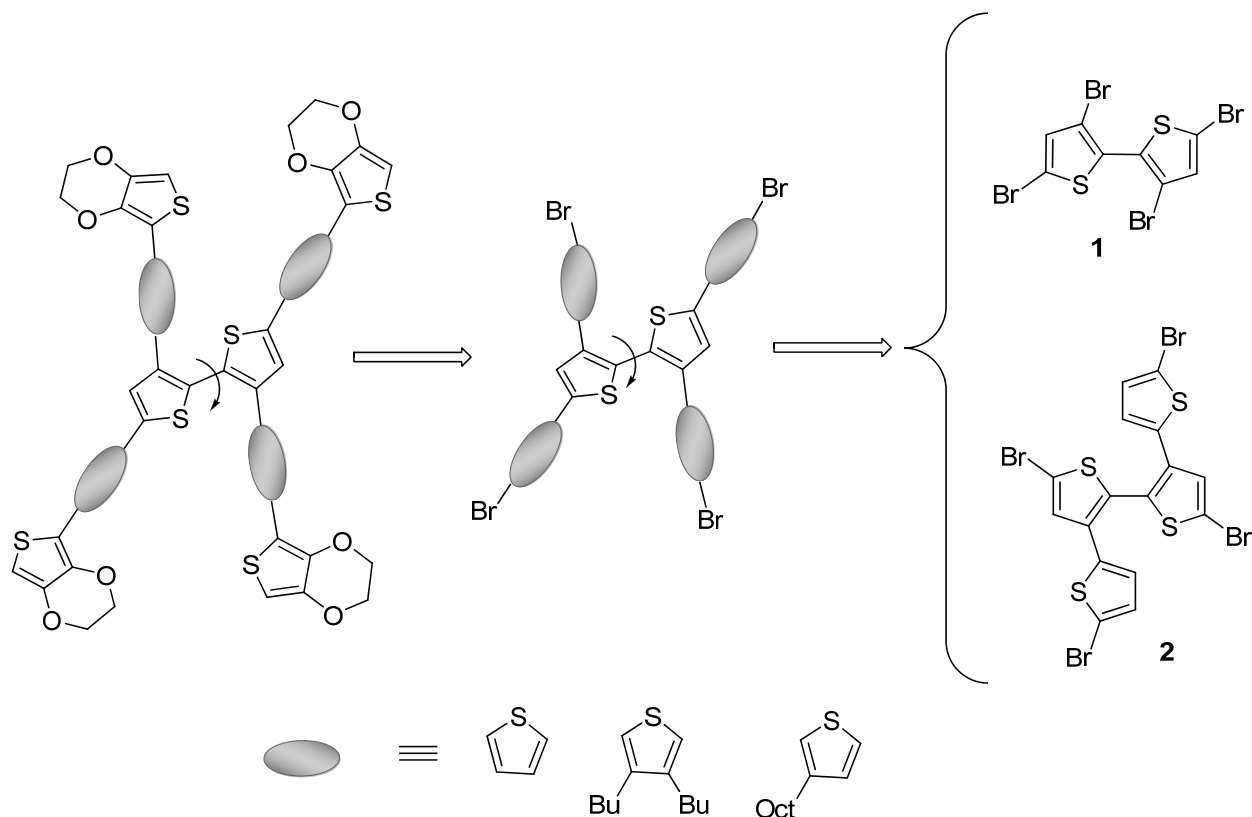
Aiming the access analogue compounds with longer branches and thus different electronic properties, we have also attempted to directly attach other functional groups to our scaffold. Thus, we have tried to synthesize the tetracarboxylic derivative 9 using *n*-butyl-lithium (*n*-BuLi) and carbonic ice at low temperature (Scheme 5). Reaction occurred but the product could not be characterized and analyzed because of its instability in ambient conditions.



Scheme 5

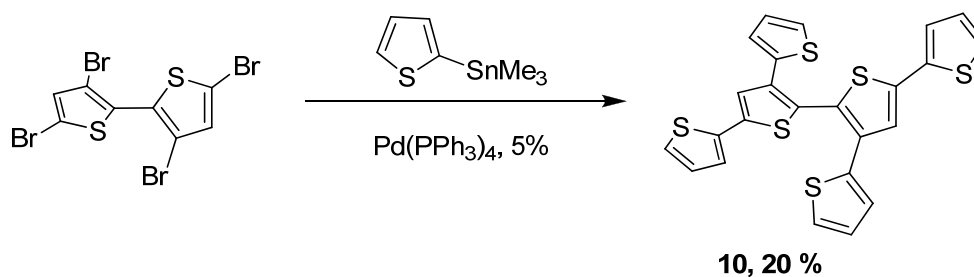
4.2.2. Derivatization of twisted 2,2'-bithiophene by thiophene and alkylthiophenes: synthesis and reactivity

In order to increase the conjugated framework we have envisaged the introduction of an additional thiophene ring between the twisted bithiophene node and the terminal EDOT moiety (Scheme 6). Thus, we have performed the synthesis of the Stille reagents of thiophene and alkylthiophene and their coupling products on the appropriate bromo-derivatives.



Scheme 6

The Stille coupling between 3,3',5,5'-tetrabromo-2,2'-bithiophene (**1**) and 2-tributylstannyl-thiophene gave compound **10** in 20% yield (Scheme 7).



Scheme 7

A crystal suitable for X-ray diffraction analysis was obtained from a 2/1 petroleum ether/diethylether solution of compound **10** (Fig. 2). The results from the crystallographic structure determination, reveals a 80° dihedral angle between the two thiophene rings that form the 2,2'-bithiophene core, thus confirming that this type of compound represents an interesting structure for building 3D-conjugated systems.

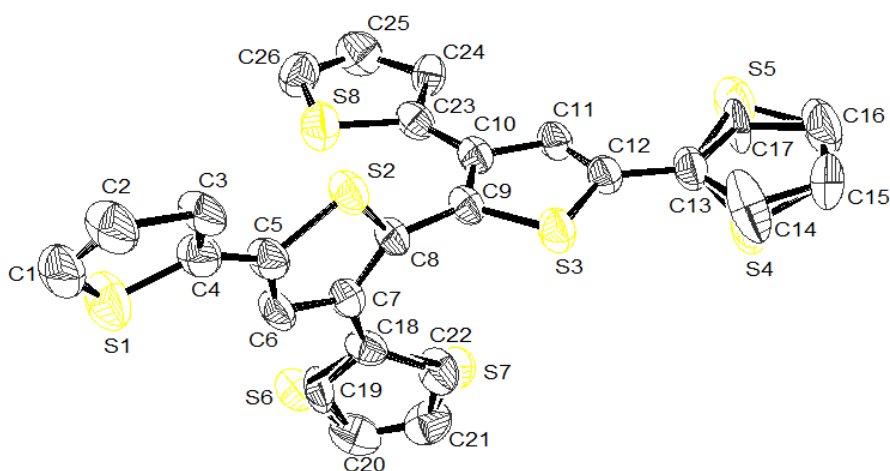
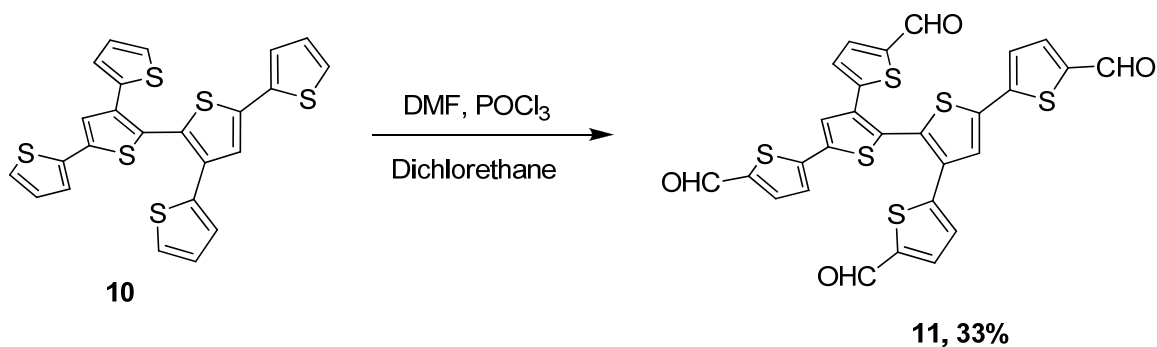


Fig. 2. ORTEP diagram of compound **10**

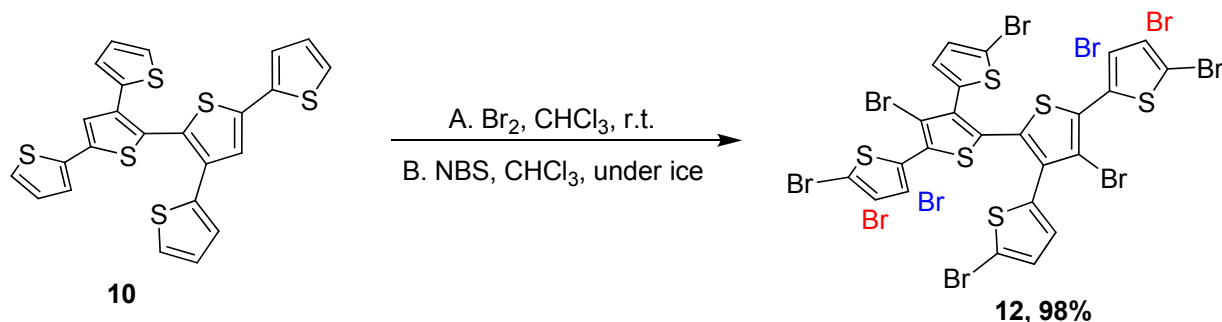
Tetraaldehyde **12** was synthesized by Vilsmeier-Haack formylation on compound **10** (Scheme 8). In spite of the low yield, (33%) the tetra electrophilic substitution works well on this type of thiophene or EDOT tetra-substituted 2,2'-bithiophenes.



Scheme 8

Attempts to achieve bromination of compound **10** at the four α -positions using bromine in chloroform at room temperature or *N*-bromo-succinimide in chloroform remained unsuccessful. At low temperature we have obtained an unseparable mixture of several bromo-derivatives while at room temperature compound **12** was obtained as major product (Scheme 9). Surprisingly, we observed that bromination takes place not only at the terminal thiophene units but also at the 4,4'-positions of the central bithiophenic core. In the case of α, α' -linked

thiophene the two bromine atoms are localized at α position and at one of the β positions (in blue or in red, in Scheme 9). Spectrometric analysis did not allow to discriminate between these two possibilities.

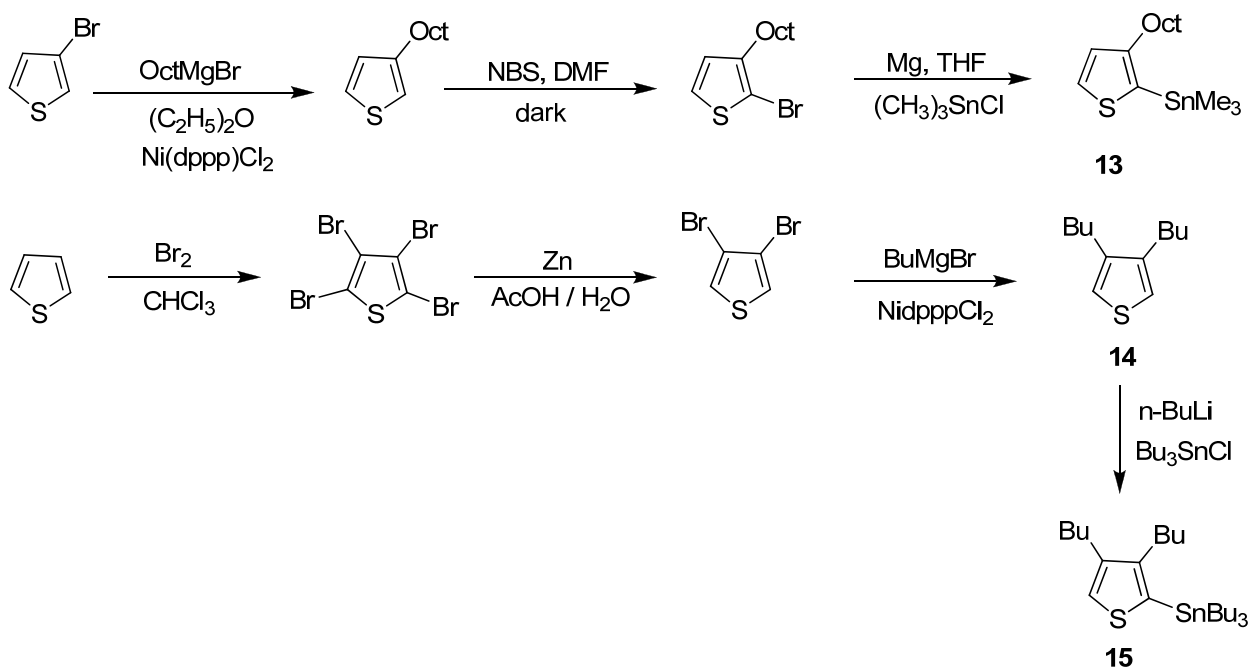


Scheme 9

In order to avoid this problem of regioselectivity, we have envisaged to graft on the bithiophenic core, 2 or 4 thiophene rings already substituted at their 3 and/or 4 position(s). For this purpose we have synthesized 3-octyl-thiophene and 3,4-dibutyl-thiophene. The presence of the alkyl chain will prevent the attack of bromine at these positions and thus avoid polybromination. Moreover, these alkyl chains will contribute to increase the solubility of the products.

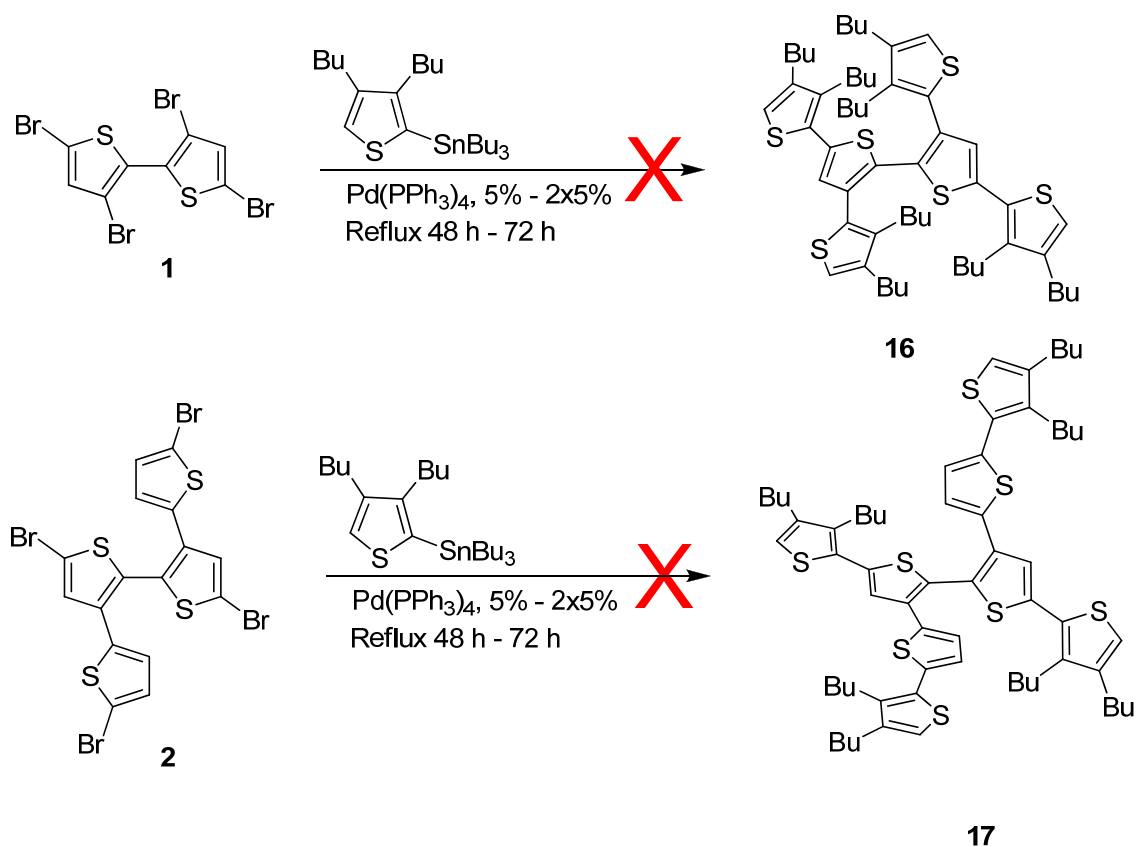
Easily accessible 2-trimethylstannyl-3-octyl-thiophene (**13**) was obtained in three steps from 3-bromo-thiophene (Scheme 10). 3,4-Dibromo-thiophene was synthesized following a known method⁴² and 3,4-dibutyl-thiophene (**14**) was obtained in good yields by Kumada coupling. Compound **14** was then stannylated in good yields to lead to 3,4-dibutyl-2-stannylthiophene **15** (Scheme 10).

⁴² Araki, K.; Endo, H.; Masuda, G.; Ogawa, T. *Chem. Eur. J.* **2004**, *10*, 3331 - 3340



Scheme 10

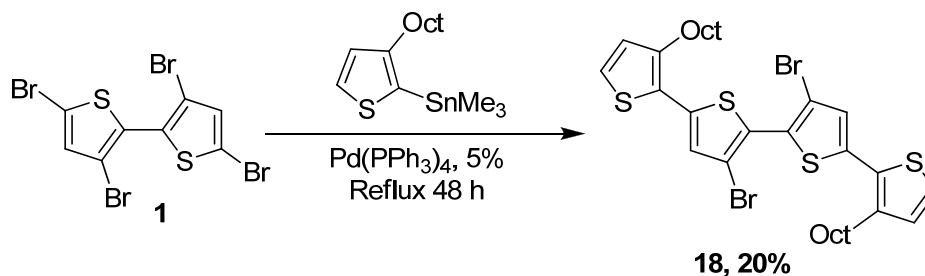
Compound **15** was used in a Stille reaction with 3,3',5,5'-tetrabromo-2,2'-bithiophene (**1**) together with tetrabromo-3,3'-di(2-thienyl)-2,2'-bithiophene (**2**) (Scheme 11).



Scheme 11

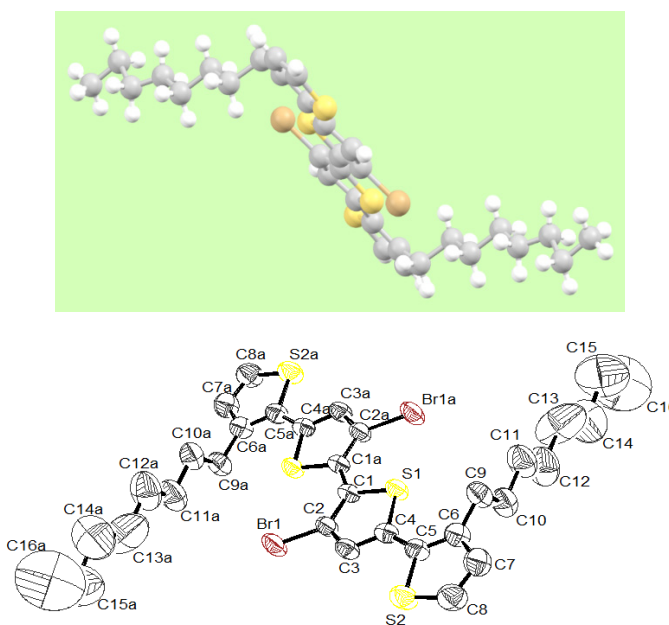
However, in both cases attempts to synthesize compounds **16** and **17** under these Stille coupling conditions failed, even with increased amounts of stannic derivative or catalyst or with longer reaction time. This absence of coupling may be due to the steric hindrance to coplanarity of the entering thiophene ring with the main conjugated system.

As a next step, we have tried a fourfold Stille coupling reaction using 2-trimethylstannyl-3-octyl-thiophene (**13**) and compound **1**. However, only the product of a two-fold coupling (**18**) was obtained in 20 % yield in this case (Scheme 12).



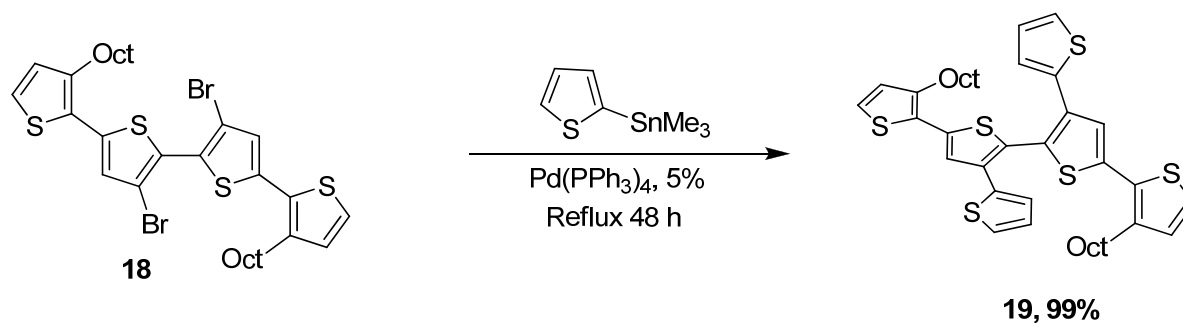
Scheme 12

The crystallographic structure of compound **18** is presented in Figure 4. The planar conformation adopted by compound **18** with short S-Br (3.16 Å) distances, suggests non-bonding S-Br interactions which contribute to the self-rigidification of the molecule.⁴³ These interactions could persist in solution and hence contribute to reduce the reactivity of the bromo-compound with the bulky octyl-thiophene, thus explaining the lack of formation of the tetra-coupling product.

Fig. 3. Side view using Mercury Program (up) and ORTEP Diagram (bottom) for compound **18**

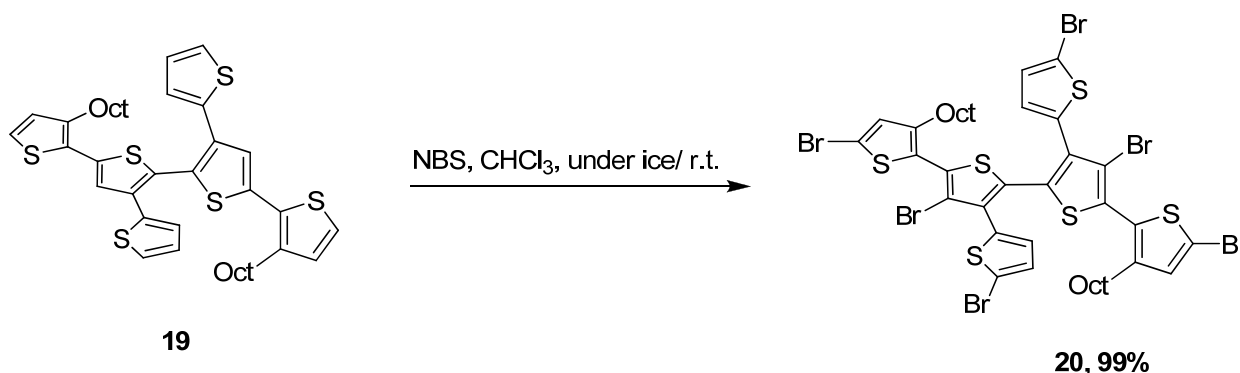
⁴³ Hergue, N.; Leriche, P.; Blanchard, P.; Allain, M.; Planas-Gallego, N.; Frere, P.; Roncali, J. *New. J. Chem.* **2008**, 932-936

To avoid this problem, we have performed the Stille coupling of compound **18** with the less hindered 2-trimethylstannylthiophene. This reaction afforded compound **19** in quantitative yield (Scheme 13). This result thus strongly supports the predominant effect of steric interactions as the major cause of the impossibility to obtain the tetra-substituted compound.



Scheme 13

The bromination results of the unsubstituted compound **10** prompted us to choose to brominate compound **19** with NBS at low temperature. The bromination reaction was, at last, achieved only at room temperature with the formation of a hexabromo-derivative **20** (Scheme 14).



Scheme 14

Monitoring the reaction (from low to room temperature) by ¹H-NMR spectroscopy we observed the formation of a mixture of bromo-derivatives which was gradually evolved into the main product **20**. Fixation of an alkyl chain at the β -positions of two of the terminal thiophene ring, prevents bromination, but reaction at the central bithiophenic core still occurs. We can conclude that the free positions of the bithiophenic core are very reactive and this reaction cannot be controlled or suppressed.

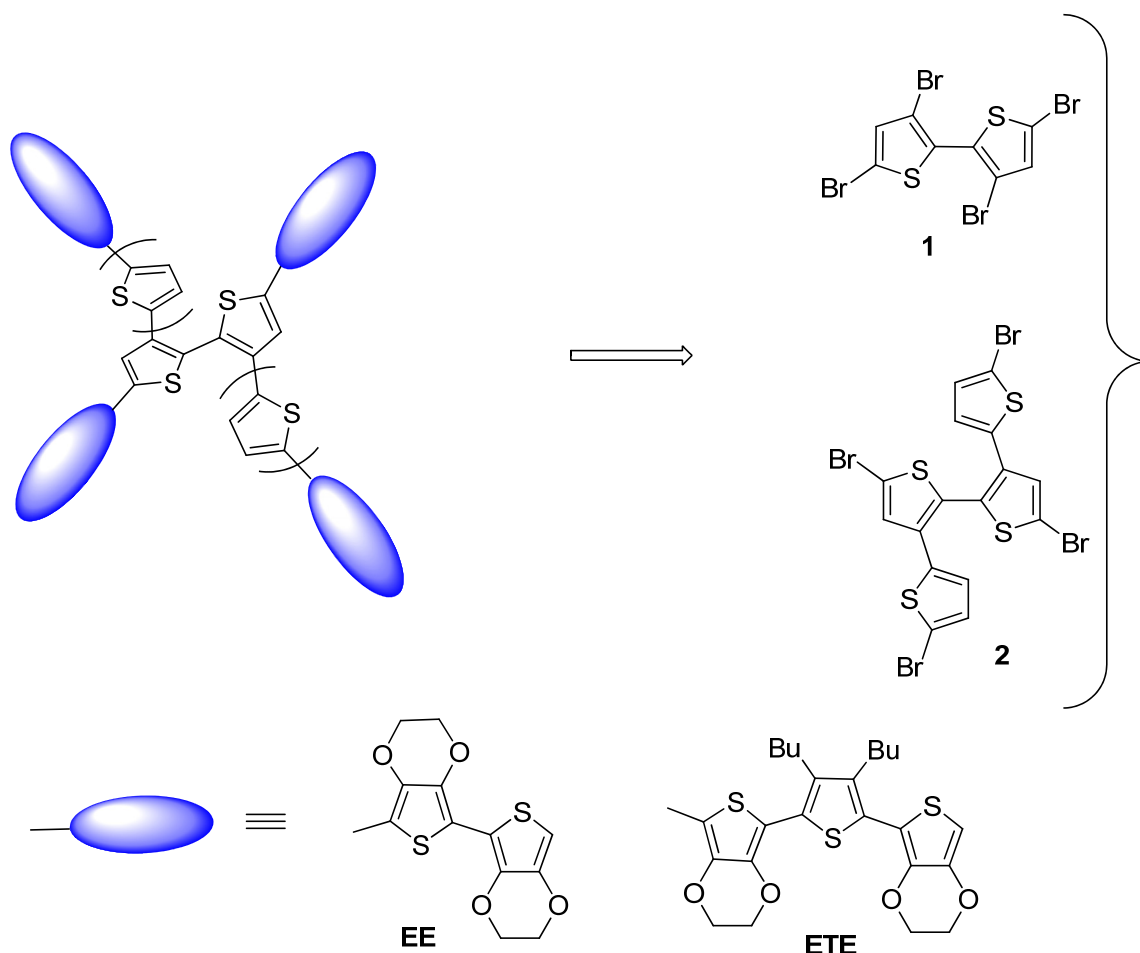
Thinking about the possibility to introduce different types of thiophenes and alkyl substituted thiophenes onto the main bithiophenic core, and the bromine in some of the

thiophene free sites, we can envisage to use these multi-bromo- compounds in the synthesis of some spider-like oligothiophenes with 6 conjugated branches instead of 4.⁴⁴

4.2.3. 3D-conjugated systems containing 3,4-ethylenedioxythiophene (EDOT) blocks

A different approach towards the synthesis of extended 3D conjugated systems involves the direct attachment of some longer hybrid conjugated oligomers such as EDOT-EDOT (**EE**) or EDOT-Thiophene-EDOT (**ETE**) onto the central bithiophenic core. This alternative route offers several advantages such as fewer synthetic steps, elimination of the bromination step and elimination of the problems associated with the selectivity of the coupling reaction.

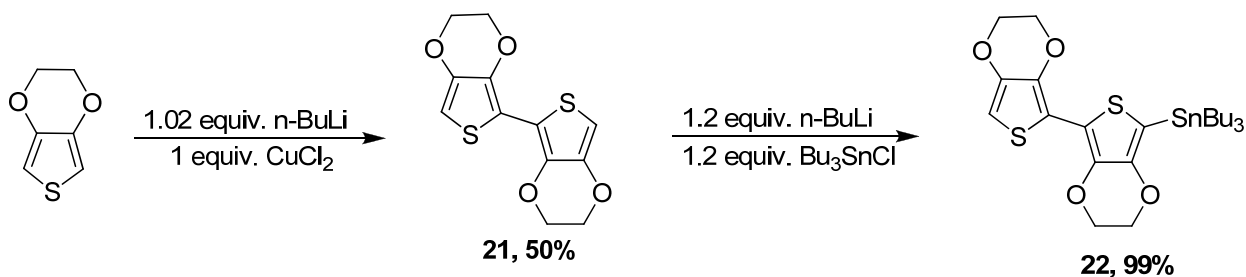
Thus **EE** and **ETE** oligomers were grafted on 3,3',5,5'-tetrabromo-2,2'-bithiophene (**1**) and tetrabromo-3,3'-bis(2-thienyl)-2,2'-bithiophene (**2**) (Scheme 15).



Scheme 15

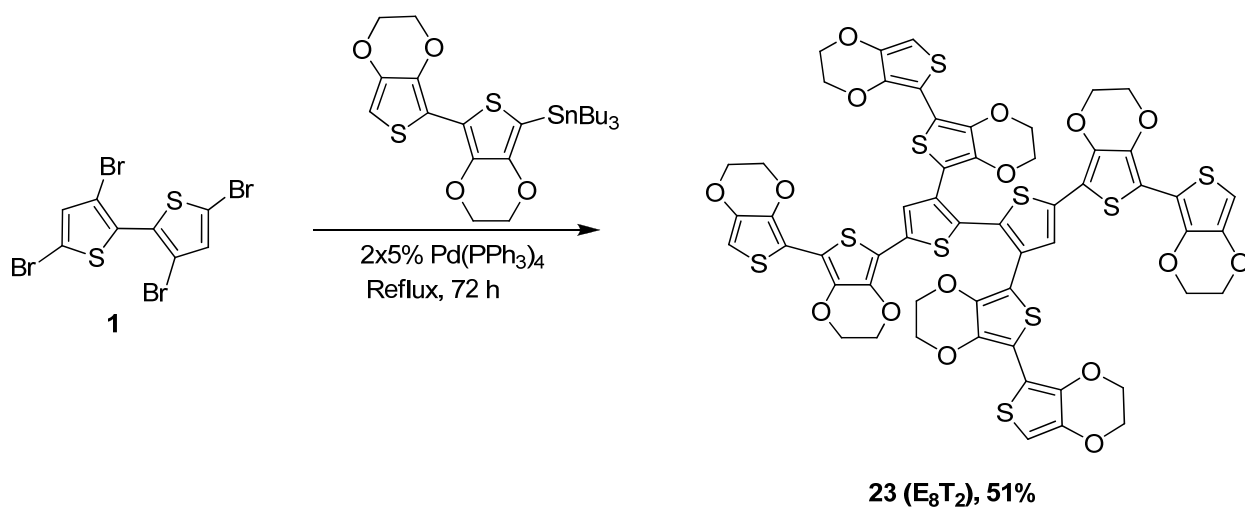
⁴⁴ Benincori, T.; Capaccio, M.; De Angelis, F.; Falciola, L.; Muccini, M.; Mussini, P.; Ponti, A.; Toffanin, S.; Traldi, P.; Sannicò, F. *Chem. Eur. J.* **2008**, *14*, 459-471

Bis-EDOT (**EE**) was synthesized in 50% yield from commercially available EDOT by oxidative coupling with copper chloride⁴⁵ and the corresponding tributylstannyl-**EE** **22**, in quantitative yield, following a procedure described in the literature (Scheme 17).¹⁵



Scheme 16

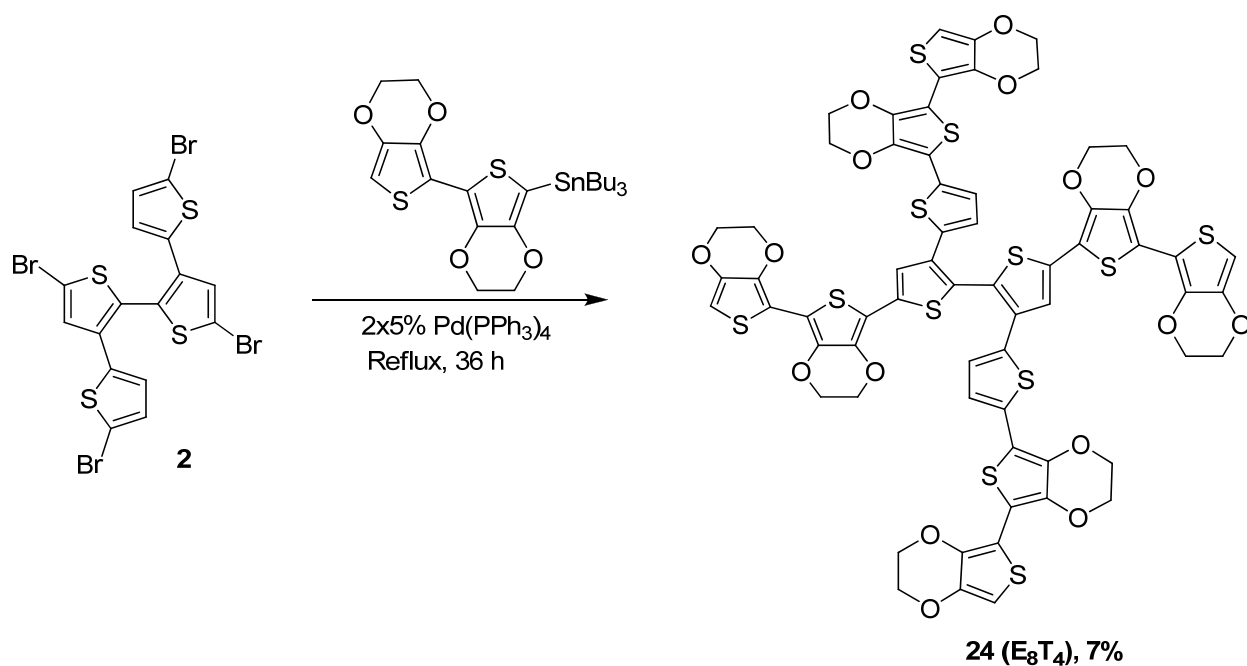
Compound **23** (**E₈T₂**) was obtained in moderate yield via the direct Stille coupling of 3,3',5,5'-tetrabromo-2,2'-bithiophene (**1**) and tributylstannyl-**EE** (**22**) (Scheme 17). A clean orange sample of compound **23** was obtained after purification by column chromatography using dichloromethane as eluent followed by precipitation from a mixture of dichloromethane and hexane.



Scheme 17

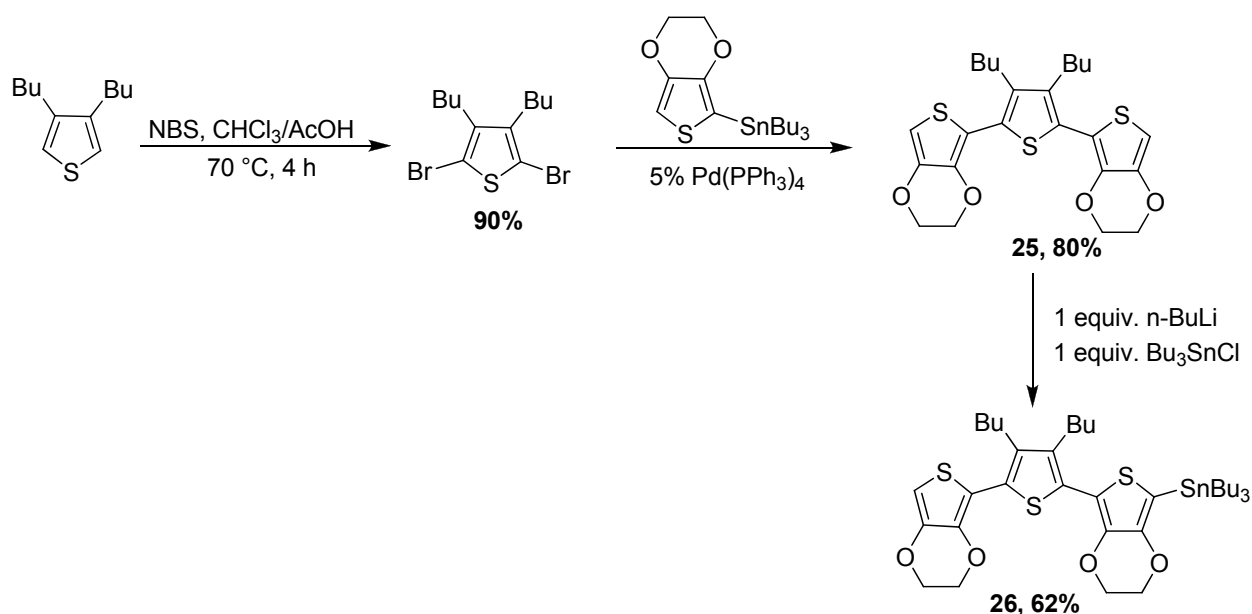
A similar route was followed in the case of compound **24** (**E₈T₄**) by coupling tetrabromo-3,3'-dithienyl-2,2'-bithiophene (**2**) with the tributylstannyl-EDOT (Scheme 18). Purifications by column chromatography using diethyl ether followed by dichloromethane and then precipitation from a mixture of dichloromethane and hexane afforded compound **24** in 7% yield.

⁴⁵ Kagan, J.; Arora, S.K. *Heterocycles* **1983**, *20*, 1937



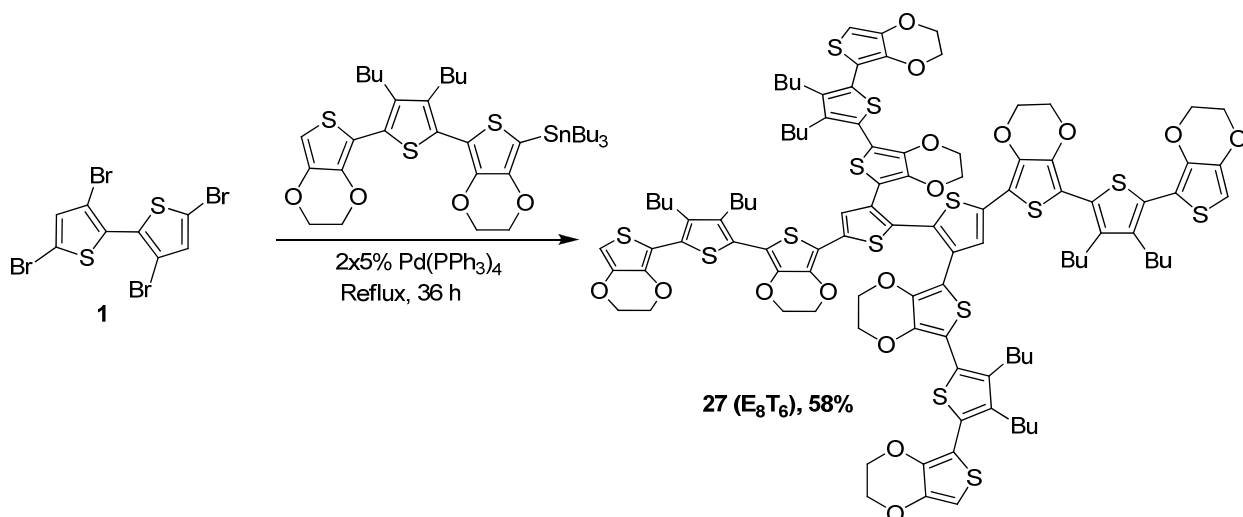
Scheme 18

Compound **26** was obtained in three steps from 3,4-dibutylthiophene. Bromination of the 2,5 positions of this compound, followed by coupling with two equivalents of 2-tributylstannyl-(3,4-ethylenedioxythiophene) gave the tricyclic compound **25** in 80% yield. Treatment of this latter compound with *n*-BuLi and Bu₃SnCl at low temperature gave the stannylated derivative **26** in 62% yield (Scheme 19).



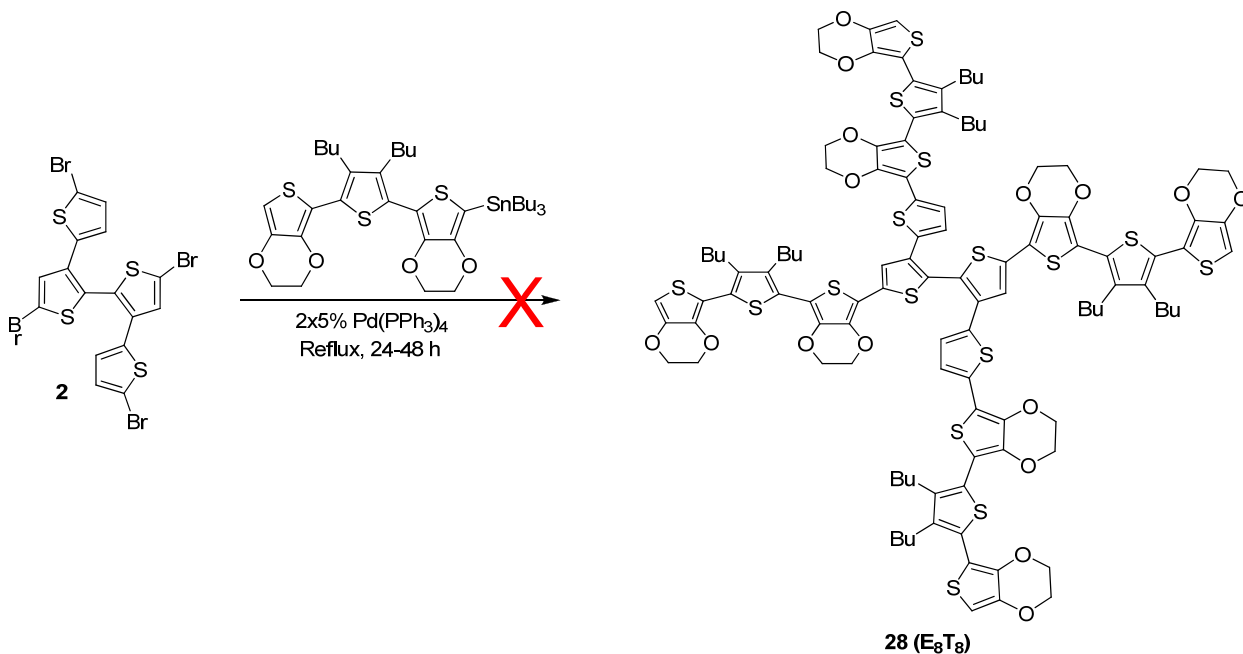
Scheme 19

Compound **27** (E₈T₆) was obtained in good yields (58%) by a fourfold Stille coupling between the stannic derivative **26** and 3,3',5,5'-tetrabromo-2,2'-bithiophene (**1**) (Scheme 20).



Scheme 20

Attempts to perform a fourfold Stille coupling using the **ETE** stannic derivative (**26**) and tetrabromo-3,3'-dithienyl-2,2'-bithiophene (**2**) remained unsuccessful. Synthesis of compound **28** failed when applying the conditions previously used for other terms (Scheme 21). This result can be attributed to the insufficient accessibility of the reactive sites of the tetrabromo compound **2** already evidenced by the low yield obtained for the synthesis of compound E_8T_4 (**24**).



Scheme 21

4.3. Electronic properties of 3D π -conjugated systems based on twisted 2,2'-bithiophene

4.3.1. Optical properties of the 3D precursors

UV-Vis absorption spectra of compounds **3** (E_4T_2) and **4** (E_4T_4) recorded in methylene chloride show two maxima, at 310 nm and a shoulder at 370 nm for E_4T_2 and at 300 nm and 370 nm for and E_4T_4 , respectively (Fig. 4). These two maxima are consistent with the coexistence of two different conjugation lengths in the twisted structures. In comparison with the absorption maximum of EDOT-thiophene-thiophene-EDOT (**ETTE**) ($\lambda_{\max} = 424$ nm), which corresponds to the main conjugated segment in E_4T_2 and E_4T_4 ,¹⁵ we observe a considerable hypsochromic shift, in agreement with the larger torsion angle at the bithiophenic core.

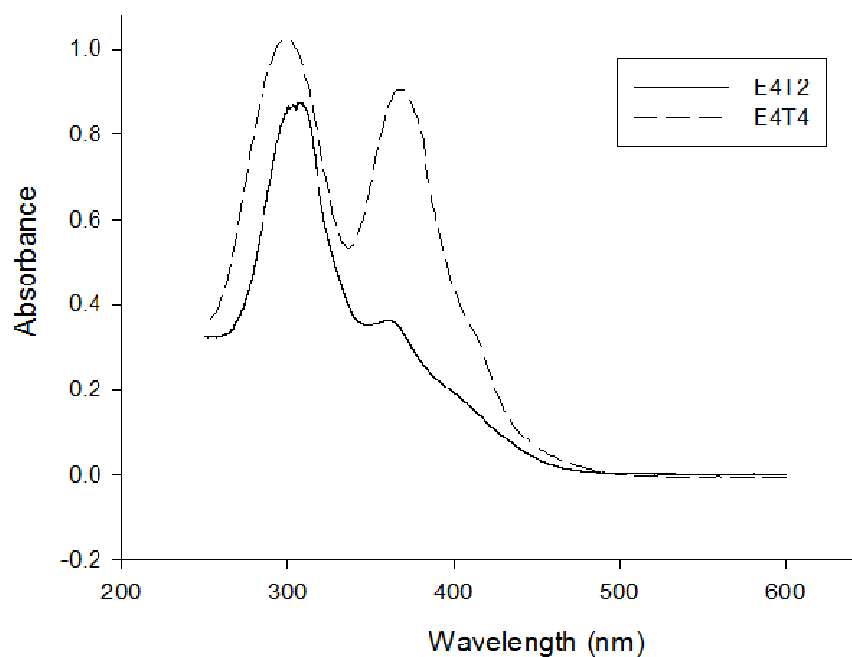


Fig. 4. UV-Vis absorption spectra of E_4T_2 and E_4T_4 in methylene chloride

Table 1 lists the UV-Vis spectroscopic data for thiophene-EDOT 3D systems recorded in methylene chloride solutions. The type of branches of each structure is indicated for better comparison.

Table 1. Absorption maxima for 3D precursors

Compound	Branches	$\lambda_{max.}(nm)$
E₄T₂ (3)	4-E	310, 370
E₄T₄ (4)	2-E, 2-TE	300, 370
E₈T₂ (23)	4-EE	390
E₈T₄ (24)	2-EE, 2-TEE	416
E₈T₆ (27)	4-ETE	390

Figure 5 and 6 present the spectra and the structures of **E₈T₂ (23)/E₄T₂ (3)** and **E₈T₄ (24)/E₄T₄ (4)** respectively.

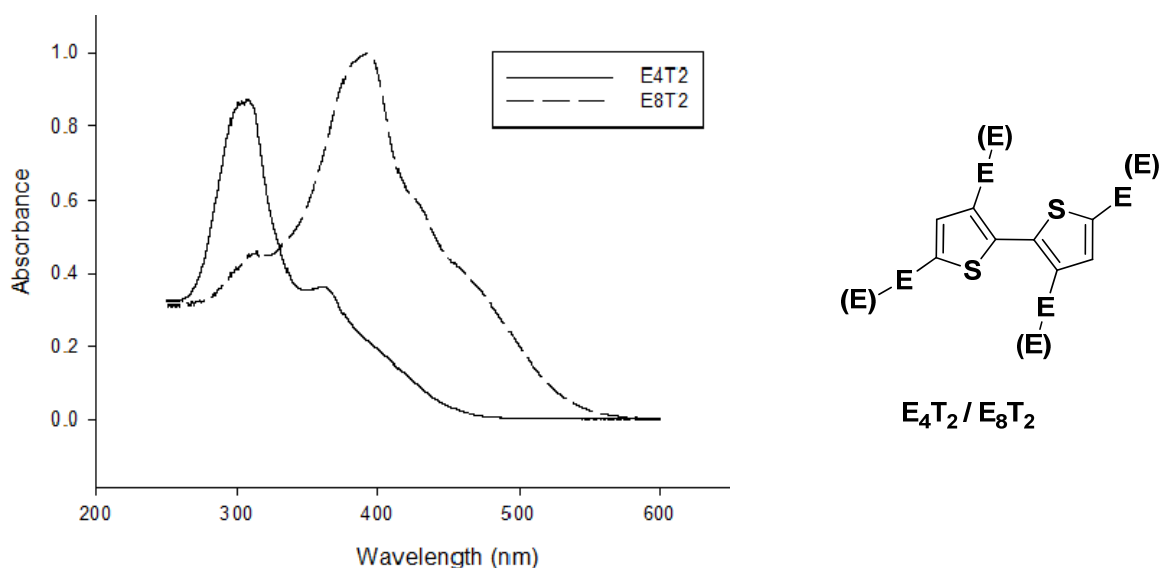


Fig. 5. UV-Vis absorption spectra of **E₈T₂** and **E₄T₂** in methylene chloride

All compounds present a complex UV-Vis spectrum in which at least two main features can be distinguished. The spectrum of **E₄T₂** shows a maximum at 310 nm and a weak absorption band at 370 nm with a long absorption tail. For **E₈T₂**, the spectrum exhibits a maximum at 390 nm while a weak absorption is still visible at 300 nm as well as two shoulders at 420 and 480 nm (Fig. 5). While the bathochromic shift of the absorption maximum of **E₈T₂** compared to **E₄T₂** can be attributed to the extension of the conjugation length of the main conjugated segment, namely the α - α linked six rings system twisted in its middle, a detailed attribution of the various spectral features is clearly not possible due to the presence of conjugated segments of different lengths connected via various twisted angles.

A similar effect is observed for the 3D systems built around the twisted quaterthiophene 3,3'-di(2-thienyl)-2,2'-bithiophene, namely **E₄T₄** and **E₈T₄** (Fig. 6). In this case a 116 nm of λ_{max}

is observed which suggests that compared to the previous series E_4T_2 and E_8T_2 , replacement of EDOT by the less bulky thiophene at the 3 and 3' positions of the bithiophene core allows a decrease of the value of the dihedral angle in the middle of the bithiophene core.³⁴

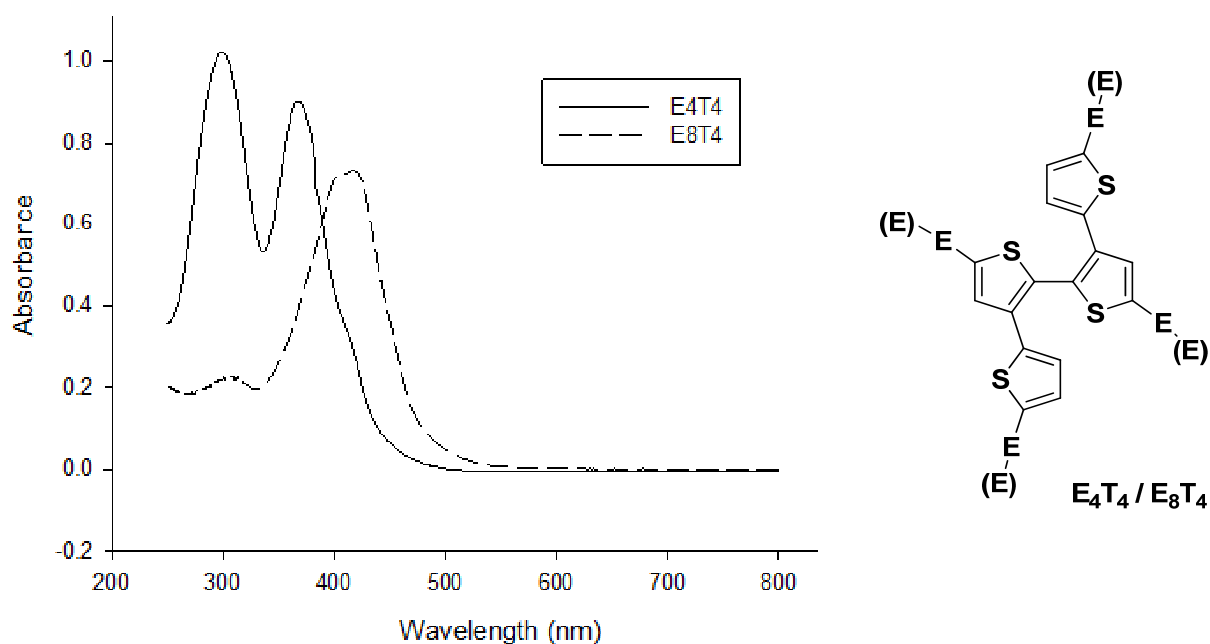


Fig. 6. UV-Vis absorption spectra of **24** (E_8T_4) and E_4T_4 in methylene chloride

The UV-Vis absorption spectrum of E_8T_6 (**27**) shows a λ_{max} at 390 nm comparable to that of its analogue with EDOT units in the 3,3' positions of the bithiophene core (E_8T_2). However, comparison of the spectrum of E_8T_4 which poses an additional thiophene unit in lateral chains reveals a 26 nm blue shift of λ_{max} (Fig. 7, Table 1). This effect can be attributed to a loss of conjugation caused by an increase of the median twisting angle due to steric interactions imposed by the two 3,4-dibutyl thiophene rings.

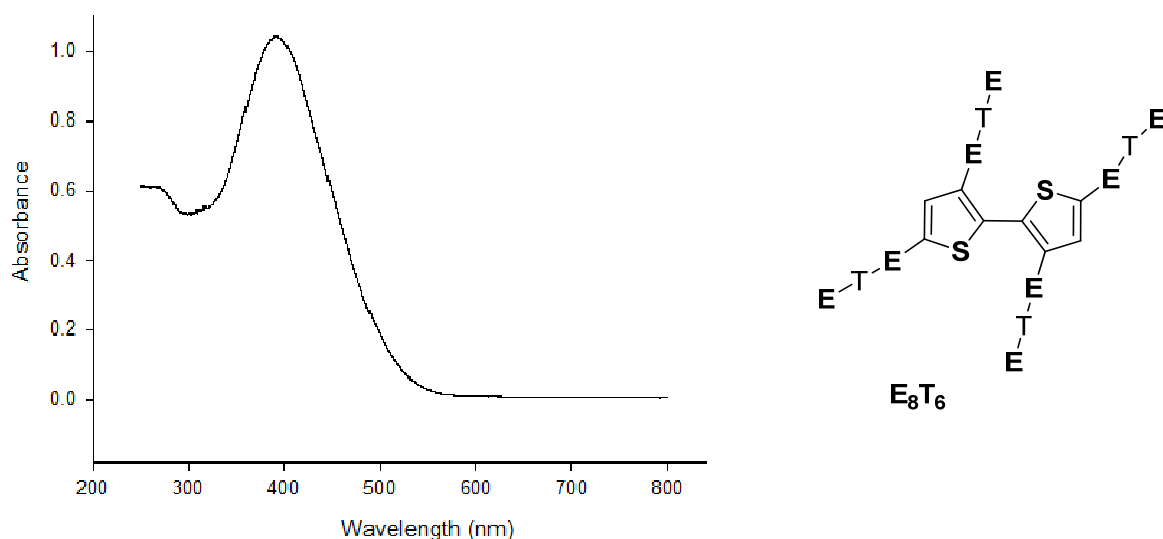


Fig. 7. UV-Vis absorption spectrum of E_8T_6 (**27**) in methylene chloride

4.3.2. Electrochemical properties of the monomers

The electrochemical properties of the monomers have been analyzed by cyclic voltammetry in acetonitrile, dichloromethane or a mixture of the two solvents, in the presence of 0.10 M tetrabutylammonium hexafluorophosphate as supporting electrolyte and the results are presented in Table 2.

Application of a single potential scan to a millimolar solution shows a first anodic peak potential (E_{pa}) which can be attributed to the oxidation of the longest conjugated segment of the system. Due to the twist angle created in the middle of the bithiophene core (θ) and thus of the molecule by steric interactions, one can consider that the minimal length of the longest conjugated segment present in the structure corresponds to that defined by a complete interruption of conjugation in the middle of the conjugated chain when $\theta = 90^\circ$ (Fig. 8).

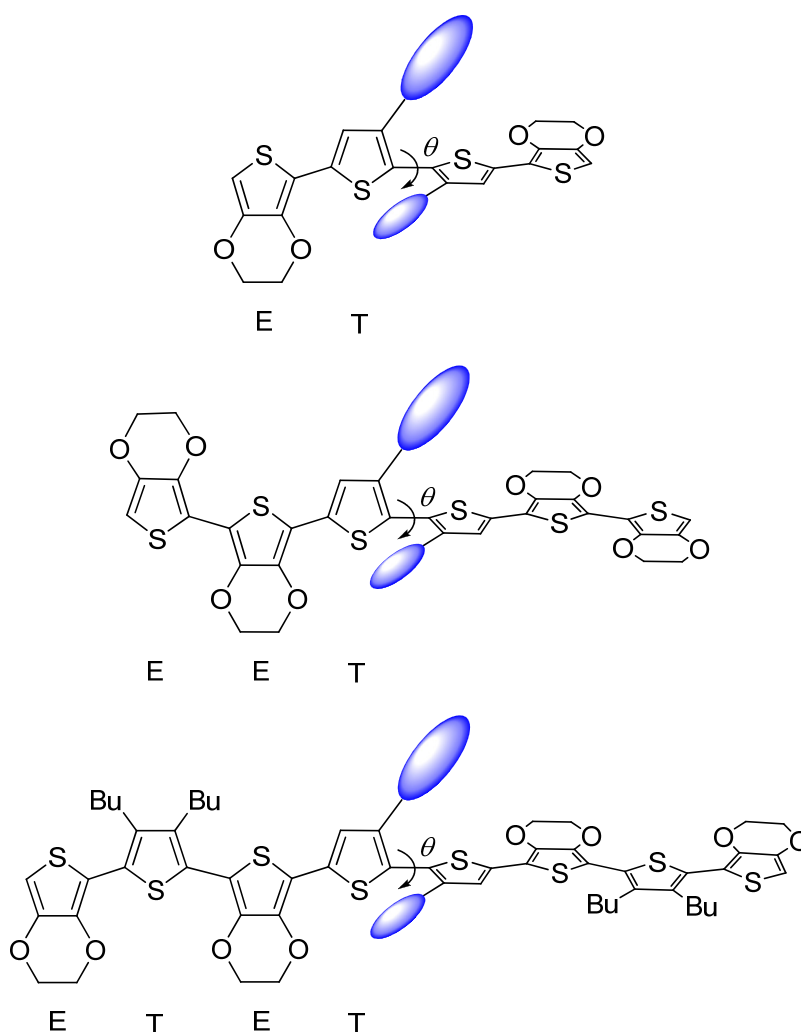


Fig. 8. Different conjugation segments in the molecules

This minimal length corresponds to an EDOT-thiophene (ET) block in the case of $\mathbf{E}_4\mathbf{T}_2$ and $\mathbf{E}_4\mathbf{T}_4$, EET for $\mathbf{E}_8\mathbf{T}_2$ and ETET for $\mathbf{E}_8\mathbf{T}_6$. Of course this is only a rough estimation since the value of θ can be inferior to 90° thus leading to an increase of conjugation which roughly follows a cosine law.⁴⁶

Examination of the data in Table 2 and of the cyclic voltammograms (CV) in Figure 9 shows that the values of E_{pa} agree well with that conclusion. In fact $\mathbf{E}_4\mathbf{T}_2$ and $\mathbf{E}_4\mathbf{T}_4$ present very similar E_{pa} values at 0.85 and 0.87 V respectively. The CV of $\mathbf{E}_8\mathbf{T}_2$ shows a similar E_{pa} value however the shape of the anodic wave clearly indicates that the onset for oxidation is much lower than for the previous compounds. This lesser defined CV suggests that various conjugated segments coexist due to the increasing number of possible molecular conformations. Nevertheless, the much lower onset for oxidation compared to the $\mathbf{E}_4\mathbf{T}_2$ and $\mathbf{E}_4\mathbf{T}_4$ suggest the presence of longer conjugated segments. On the other hand, the fact that the oxidation process presents some reversibility is consistent with a stabilization of the cation-radical state expected for a more extended conjugated system. However, it should be underlined that in the case of $\mathbf{E}_8\mathbf{T}_2$ the low solubility contributes to make a direct comparison more difficult.

Finally, $\mathbf{E}_8\mathbf{T}_6$ presents the lowest E_{pa} value of 0.65 V which is consistent with the longest conjugated main segment (TETE). Furthermore, the oxidation process becomes clearly reversible whereas a second oxidation process can be discerned around 1.00 V and which can be tentatively assigned to the dication state of the TETE chain. These data are in good agreement with previous results and in particular with the E_{pa} values of 0.56 and 0.90 V reported for the TETE oligomer.¹⁵ However, in spite of this agreement, the possibility that the second anodic wave corresponds to the oxidation of a shorter conjugated branch to the cation radical state cannot be *a priori* excluded. Further detailed ESR investigations would be required to discriminate between these two possible situations.

Table 2. Oxidation potential of the monomers
(details, conditions in Fig. 10)

Compd	E_{pa} (V)
$\mathbf{E}_4\mathbf{T}_2$	0.85
$\mathbf{E}_4\mathbf{T}_4$	0.87
$\mathbf{E}_8\mathbf{T}_2$	0.86
$\mathbf{E}_8\mathbf{T}_6$	0.65

⁴⁶ Brédas, J. L.; Street, G. B.; Thémans, B.; André, J. M. *J. Chem. Phys.* **1985**, *83*, 1323-1326

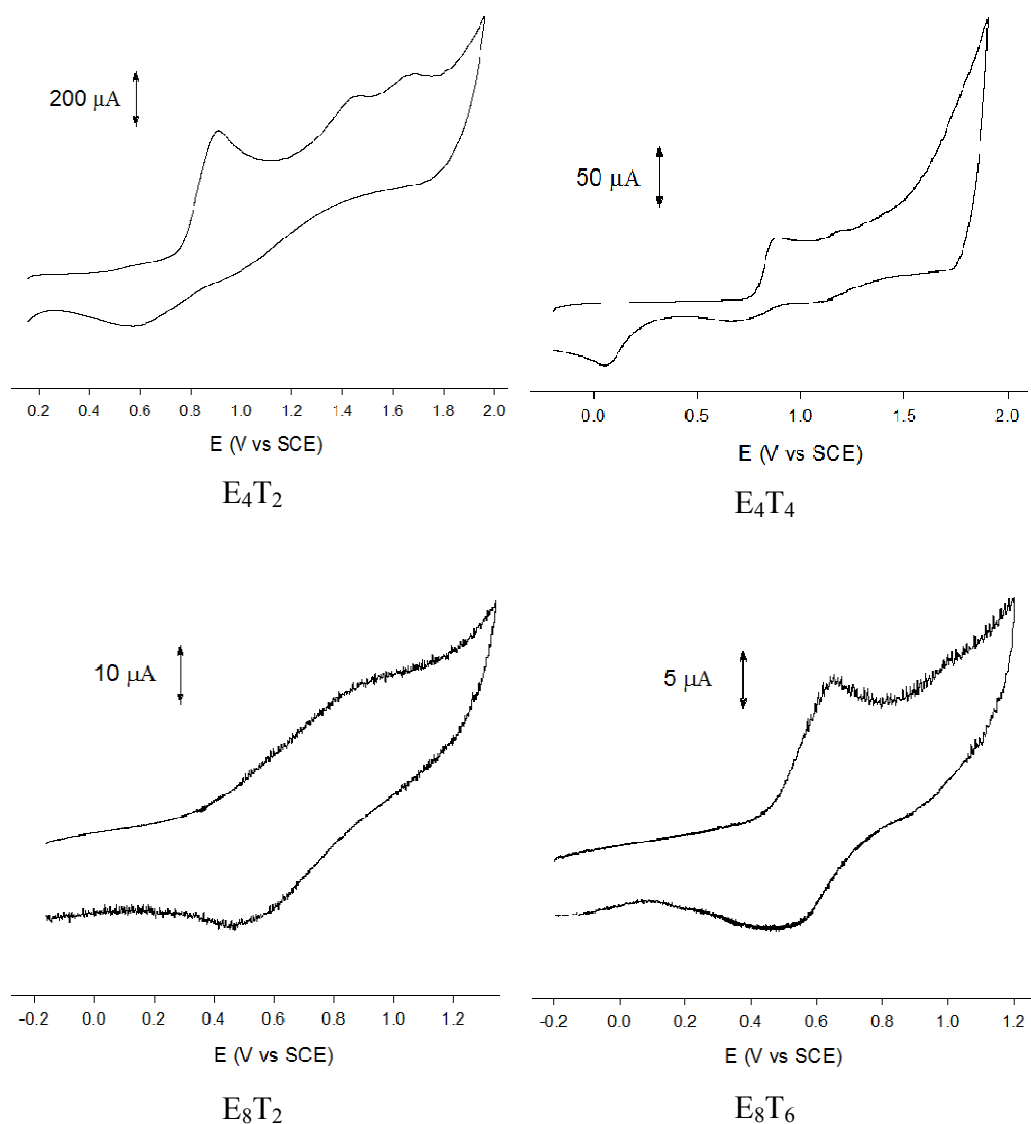


Fig. 9. Cyclic voltammograms of EDOT containing 3D conjugated systems, *ca* 10 mM in 0.10 M Bu₄NPF₆ in CH₃CN for E₄T₂, *ca* 10 mM in 0.10 M Bu₄NPF₆ in 1:1 CH₃CN/CH₂Cl₂ for E₄T₄, *ca* 1 mM in 0.10 M Bu₄NPF₆ in CH₂Cl₂ for E₈T₂ and E₈T₆, scan rate 200 mV s⁻¹.

4.3.3. Electropolymerization of the 3D precursors

Electropolymerization of the four compounds was achieved in both potentiostatic and potentiodynamic conditions. Upon application of repetitive potential scans to a solution containing 10 or 1 mM of precursor in acetonitrile, dichloromethane or a mixture of the two, a broad redox system typical of the electrodeposition of an electroactive material progressively emerges in the potential region that precede the oxidation wave of the precursor namely 0.20-0.30 to 0.80 V (Fig. 10). This new redox system is essentially structureless except for $\mathbf{E}_8\mathbf{T}_2$ for which two sub-components can be distinguished at ca 0.50 and 0.80 V.

Despite the sterically twisted structure of the precursors electropolymerization proceeds straightforwardly. This result confirms that the α -positions of the peripheral EDOT units are highly reactive and thus allow efficient coupling.⁴⁷

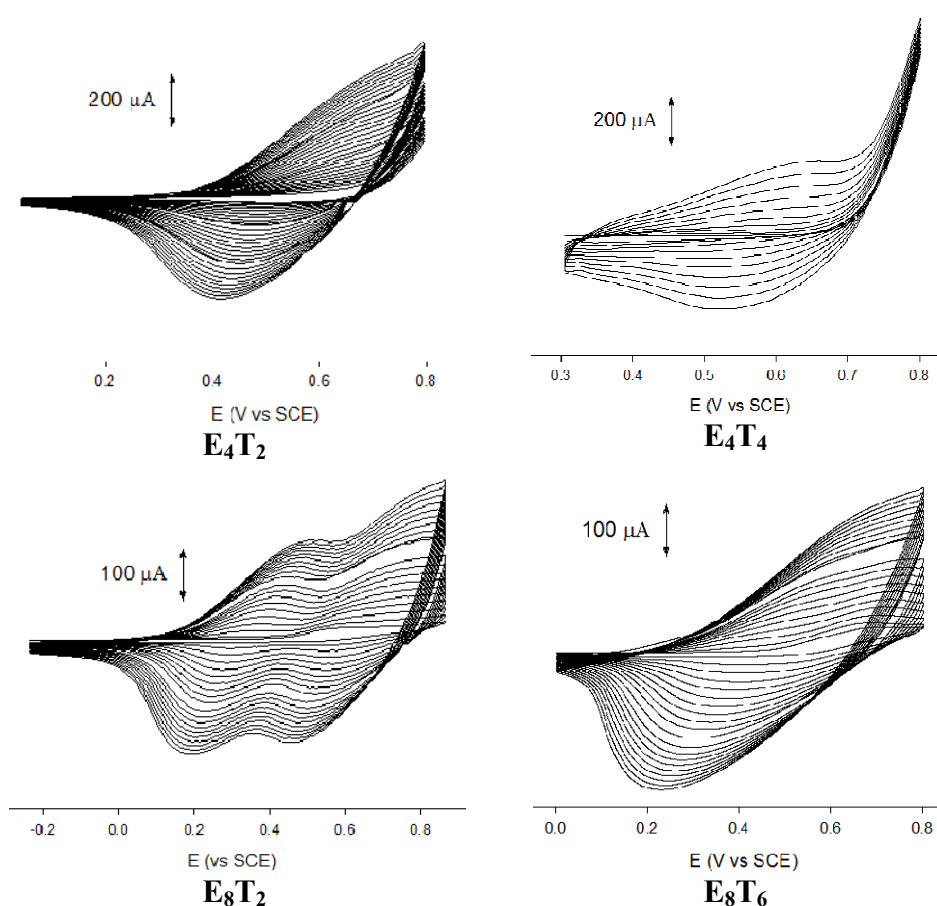


Fig. 10. Potentiodynamic deposition of EDOT containing 3D conjugated systems, ca 10 mM in 0.10 M Bu_4NPF_6 in CH_3CN for $\mathbf{E}_4\mathbf{T}_2$, ca 10 mM in 0.10 M Bu_4NPF_6 in 1:1 $\text{CH}_3\text{CN}/\text{CH}_2\text{Cl}_2$ for $\mathbf{E}_4\mathbf{T}_4$, ca 1 mM in 0.10 M Bu_4NPF_6 in CH_2Cl_2 for $\mathbf{E}_8\mathbf{T}_2$ and $\mathbf{E}_8\mathbf{T}_6$, scan rate 100 mV s^{-1} .

⁴⁷ Leriche, P.; Piron, F.; Ripaud, E.; Frere, P.; Allain, M.; Roncali, J. *Tetrahedron Letters* **2009**, *50*, 5673-5676

Table 3. Cyclic voltammetric data for the 3D precursors and the corresponding polymers

Compd	E_{pa} (V)	E_{appl} (V)	$E_{pa\ pol}$ (V)	Qd (mC cm ⁻²)	Qr/Qd
E₄T₂	0.85	0.95	0.65	33	0.336
E₄T₄	0.87	1.00	0.69	20	0.225
E₈T₂	0.86	0.90	0.50, 0.75	13	0.667
E₈T₆	0.65	0.80	0.62	16	0.684
PEDOT		1.32	0.04	132	0.08

Electropolymerization in potentiostatic conditions was performed at an applied potential slightly higher than the anodic peak potential determined by single scan CV (Table 3). This slight overpotential was found necessary to obtain stable and homogeneous deposited films. Poly(**EDOT**) films were deposited at an applied potential of 1.32 V for comparison.

Examination of the ratio of the charge reversibly exchanged upon redox cycling of the polymers (Q_r) to the electrodeposition charge (Q_d) shows that Q_r/Q_d is approximately four times larger for **E₄T₂** than for poly(**EDOT**) and *ca* eight times larger for the **E₈T₂** and **E₈T₆**, in agreement with the expected larger amount of electroactive material produced with a given Q_d for poly(**E_nT_m**).

Figure 11 shows the CV of the four polymers recorded in acetonitrile in the presence of 0.10 M B₄NPF₆ as supporting electrolyte, while the corresponding electrochemical data are listed in Table 3.

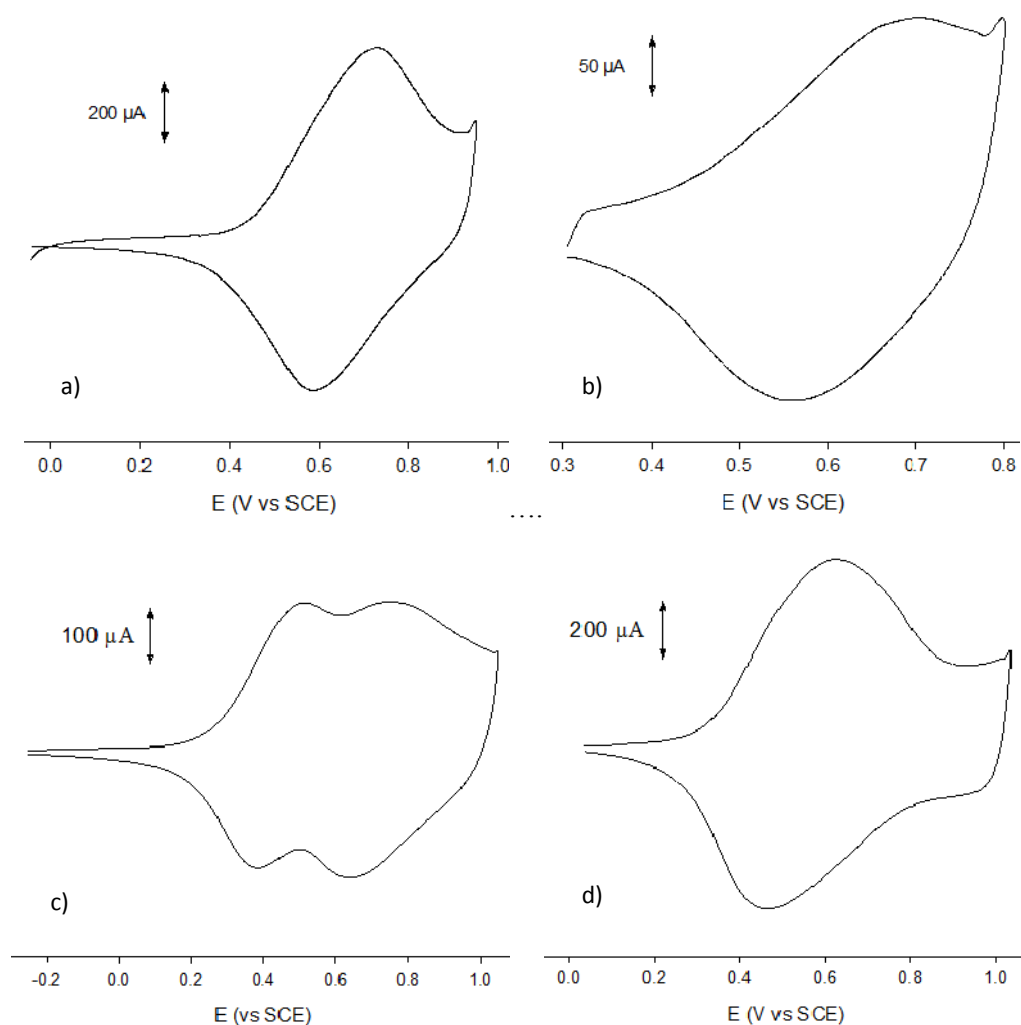


Fig. 11. Cyclic voltammograms recorded in 0.10M $\text{Bu}_4\text{NPF}_6/\text{CH}_3\text{CN}$, scan rate 100 mV s^{-1} . a) poly(E_4T_2), b) poly(E_4T_4), c) poly(E_8T_2), d) poly(E_8T_6); The polymers were deposited in potentiostatic conditions using deposition charges listed in Table 3.

The electropolymerization of 3D precursors possessing terminal EDOT groups is expected to produce 3D conjugated networks by linkage of the terminal EDOT units. However, because of the large median dihedral twisted angle the main conjugated chain can be considered as divided into two independent conjugated segments. Similarly, due to the combined effects of the non coplanarity with the conjugated segments and of the 2-3' linkage, the thiophene or EDOT groups attached at the 3 and 3' position of the bithiophene core are interact weakly with the main conjugated system and can also be roughly considered as independent. Consequently, it may be considered that the polymer produced by coupling of the terminal EDOT units contains in fact discrete conjugated segments, resulting from the duplication of the elemental starting segments namely the “horizontal” elemental segments resulting from the median torsion of the

bithiophene core and the “vertical” ones corresponding to the side chain attached at the 3,3’ position of the bithiophenic core.

Examination of the various possibilities of coupling in the case of E_4T_2 shows that the coupling of the **TE** horizontal branch leads to a **TEET** sequence which represents the maximum possible conjugated segment. A homo-coupling of two “vertical” **E** branches leads to an **EE** segment since the thiophene connected by their 3-position are not conjugated with the formed **EE** segment and finally a hetero-coupling between a “horizontal” and a “vertical branch will generate an **EET** segment (Fig. 12). Similar considerations show that for E_4T_4 all kind of coupling will lead to a **TEET** sequence, while for E_8T_2 and E_8T_6 the longest possible sequences are **TEEEET** and **TETEETET** respectively.

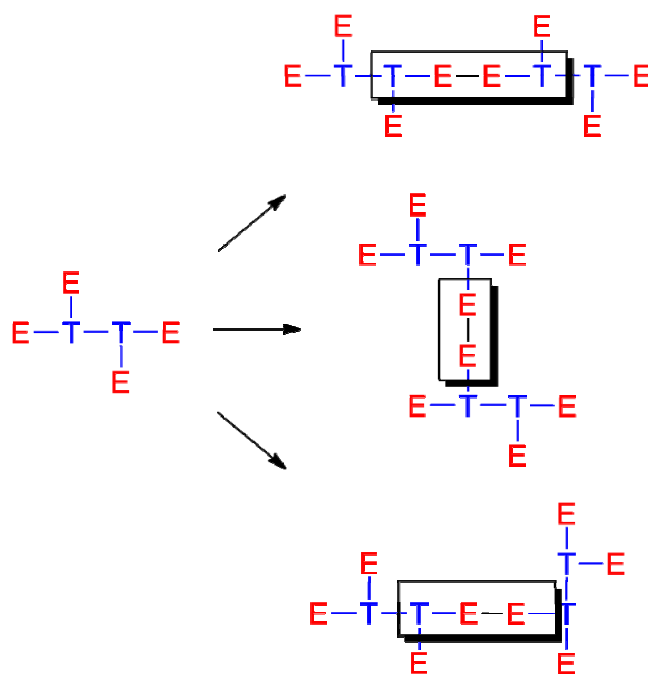


Fig. 12. Coupling possibilities of the E_4T_2 monomer

Examination of the E_{pa} values for the various polymers shows a good agreement with the trend expected on the basis of the above analysis (Table 4). Thus, as expected, polymers derived from E_4T_2 and E_4T_4 show close E_{pa} values of 0.65 and 0.69 V. A slightly lower value is found for poly(E_8T_6), which contains longer conjugated sequence but for which the effective conjugation length is limited by the distortions imposed by the two 3,4-dibutylthiophene units. Finally, the low E_{pa} value and the presence of two redox systems in the CV of poly(E_8T_2) can be explained by the formation of the **EEEE** sequence which combines the strong donor effect of EDOT units with the self-rigidification associated with intramolecular sulfur-oxygen interactions.¹⁶

Table 4. Maximum conjugated sequence in electrogenerated polymers and E_{pa} values^a of the polymers and of defined oligomers.

Polymer^a	Longest conjugated sequence	E_{pa} (V)
poly(E₄T₂)	TEET	0.65
poly(E₄T₄)	TEET	0.69
poly(E₈T₂)	TEEEET	0.50, 0.75
poly(E₈T₆)	TETEETET	0.62
Oligomer^b	TEET ^b	0.48
	TETET ^b	0.50
	TEEET ^b	0.37

^a in V vs SCE, ^b in V vs AgCl/Ag, from reference 15.

On the other hand, it is worth noting that the E_{pa} values of the polymers are consistent with what could be expected on the basis of the electrochemical data of well-defined hybrid EDOT-thiophene linear oligomers. For example the lowest E_{pa} value is found for poly(E₈T₂) which contains adjacent EDOT units like for example TEEET (0.37 V vs Ag/AgCl) while poly(E₈T₆) which contains alternate EDOT and thiophene units like the TETEET system oxidizes at a higher potential.

Although the above results have clearly shown that all precursors can be straightforwardly electropolymerized, a major point is to confirm that all EDOT groups are effectively involved in the electropolymerization process, thus providing an indirect support to the formation of electroactive 3D conjugated networks.

Previous work on the electropolymerization of oligothiophenes has demonstrated that because of the low reactivity of compounds like terthiophene, their electropolymerization leads to the electrodeposition of materials that contain significant amounts of short chain oligomers and of unreacted starting material.⁴⁸ This phenomenon can be evidenced by extraction of the deposited material,⁴⁹ or by simple electrochemical experiment which consists in the application of increasingly positive potentials to an electrodeposited film and analyzing the changes produced in the electrochemical,⁵⁰ optical or electrical⁵¹ properties of the material.

Thus, in the case of some poly(terthiophenes), application of this procedure produces a negative shift of the oxidation wave and a bathochromic shift of the absorption maximum due to

⁴⁸ Zotti, G.; Schiavon, G. *Synth. Met.* **1990**, *39*, 183-190

⁴⁹ Roncali, J.; Garnier, F.; Lemaire, M.; Garreau, R. *Synth. Met.* **1986**, *15*, 323-331

⁵⁰ Roncali, J. *Chem. Mater.* **1993**, *5*, 1456-1464

⁵¹ Roncali, J.; Lemaire, M.; Garreau, R.; Garnier, F. *Synth. Met.* **1987**, *18*, 139-144

increase of the mean conjugation length resulting from the coupling of short-chain oligomers trapped in the material.⁴⁹ Other studies have demonstrated that these modifications are accompanied by a significant increase of the conductivity of the material.⁴⁷

Figure 13 shows the CVs of the four polymers when subjected to continuous redox cycling with application of a progressively increasing positive potential limit. As shown by these CVs, the application of this procedure does not produce any change in the CV of the polymer until the potential reaches a value where the polymer begins to degrade (*ca* 1.30 V). This absence of modification of the shape and potential of the oxidation wave provides a strong support to the conclusion that all EDOT groups have been oxidized and coupled during the initial electropolymerization process.

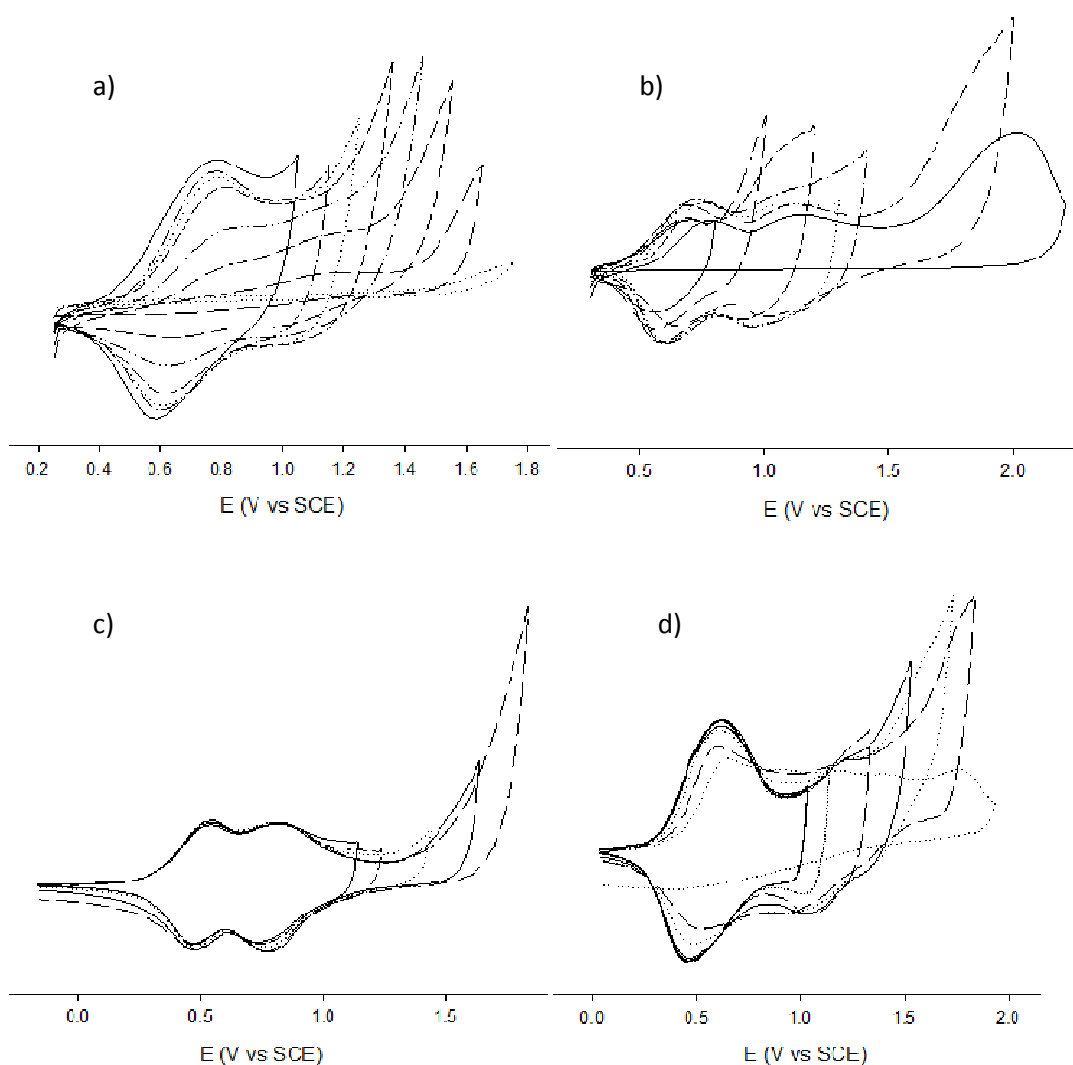


Fig. 13. CV recorded over wider potential range (0 to +2 V) for a) poly(E_4T_2), b) poly(E_4T_4), c) poly(E_8T_2), d) poly(E_8T_6).

A porosity study of the deposited materials on the electrode surface was made. Depositions of different thickness of the poly(E_4T_2) and poly(E_4T_4) were made and their response was recorded in a solution of electrolyte in the presence of 2,3-dichloronaphthoquinone (DCINQ). Poly($EDOT$) was analyzed in the same conditions for comparison purposes.

We would expect that in the case of a porous polymer the acceptor (DCINQ) will enter the polymer pores and the thicker will be the polymer the more intense will be the signal of the acceptor. In the case of a compact polymer, electronic exchanges will occur only at the surface and thus increasing the thickness of the polymer will not affect the redox signal of the acceptor.

Poly(E_4T_2) was obtained by electropolymerization in potentiostatic conditions at an applied potential of 1 V vs SCE. CV of the polymer was recorded in tetrabutylammonium hexafluorophosphate and 2,3-dichloronaphthoquinone (DCINQ). We have compared signals intensities of the DCINQ and poly(E_4T_2) recorded at 100 mV/s at each 5 minutes. The CVs show an intensity decrease in the case of DCINQ with constancy in the case of poly(E_4T_2) (Fig. 14).

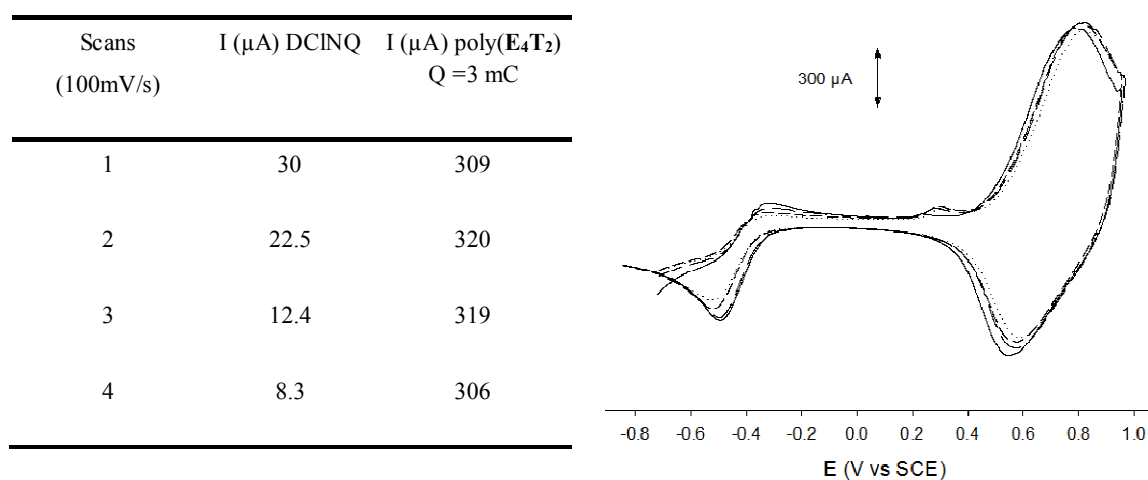


Fig. 14. Cyclic voltammogram of poly(E_4T_2) (in 0.10 M Bu_4NPF_6/CH_3CN and DCINQ, scan rate 100 mV s^{-1}) and table data.

In the case of poly(E_4T_4) the intensity of DCINQ increases as expected in the presence of a porous material at the electrode surface. This result is consistent with the penetration of the DCINQ molecules in the network pores. On the other hand, the decrease of the intensity of the polymer oxidation wave could suggest the occurrence of a charge transfer between the neutral polymer and DCINQ, further investigations are required to elucidate this point (Fig. 15).

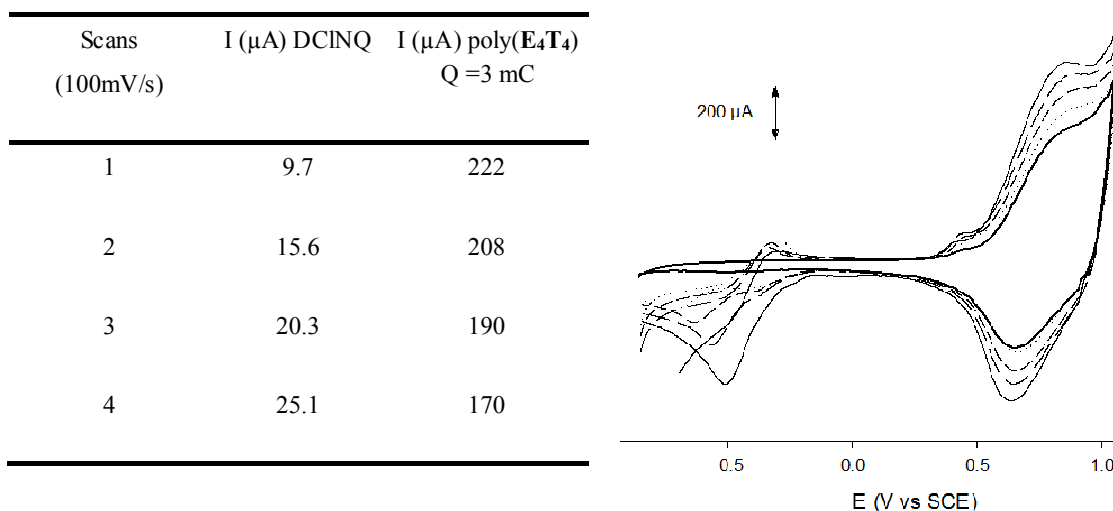


Fig. 15. Cyclic voltammogram of poly(**E₄T₄**) (in 0.10 M Bu₄NPF₆/CH₃CN and DCINQ, scan rate 100 mV s⁻¹) and table data.

The same study was made in the case of poly(**EDOT**) where, as expected, no significant modifications were observed either in the intensities of DCINQ or in that of polymer (Table 5). In the case of poly(**EDOT**) the formed material is compact and thus molecule cannot enter the polymer structure compared with the 3D networks previously presented.

Table 5. Intensities of the polyEDOT and 2,3-dichloronaphthoquinone (DCINQ)

Scans (100mV/s)	I (μA) DCINQ	I (μA) polyEDOT Q = 17 mC
1	79	70
2	81	68
3	81	66
4	83	61

These results suggests that the shorter system poly(**E₄T₂**) looks too dense to accept the guest molecule, while the second one poly(**E₄T₄**) appears more porous.

4.3.4. Electrochemical and optical properties of the polymers

The optical properties of the polymers have been analyzed on thin film electrodeposited on ITO-coated glass electrodes. Figure 16 shows the UV-Vis-NIR spectra of polymers recorded at various values of the applied potential.

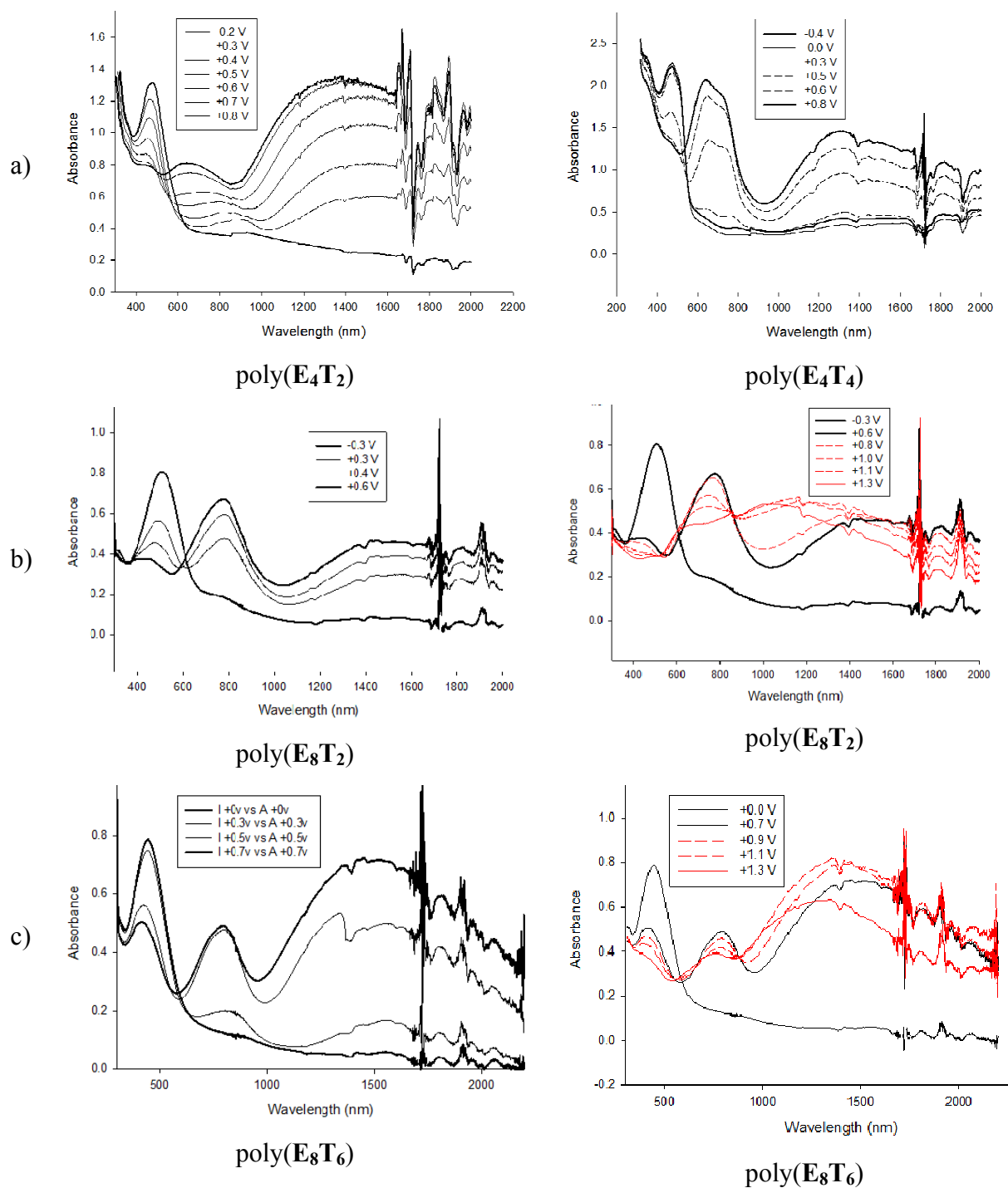


Fig. 16. Spectroelectrochemistry of the polymers on ITO at various applied potentials a) poly(E_4T_2) (left) and poly(E_4T_4) (right), initial -0.40 V final +0.80 V; b) poly(E_8T_2) left from -0.30 V to +0.60 V and right -0.3 V to +1.3 V; c) poly(E_8T_6) left from 0.00 V to +0.70 V and right 0.00 V to +1.3 V. Electrolytic medium 0.10 M Bu_4NPF_6/CH_3CN , reference SCE.

The spectrum of the fully undoped poly($\mathbf{E}_4\mathbf{T}_2$) shows an absorption maximum at 480 nm with an absorption onset at 600 nm corresponding to a band gap of 2.05-2.10 eV (Fig. 16a). The small width of the absorption band suggests a relatively narrow distribution of conjugated segments, a conclusion in accordance with the conclusions drawn from electrochemical results. Application of increasing positive potentials produces the beaching of the visible absorption band together with the concomitant development of two broad absorption bands with maxima around 600 and 1300 nm corresponding to the two transitions associated with the polaronic state of the polymer. The neutral polymer appears red and turns gradually blue upon oxidation. Interestingly, upon application of more positive potentials (up to 1.80 V) the two bands never merge into the single transition corresponding to the bipolaron state. This result is consistent with the fact that the longest effective conjugation length in the polymer network is too short to accommodate a bipolaron state, a conclusion in agreement with the formation of discrete conjugated segments with effective conjugation length determined by the mode of connection and the twist angles in the 3D polymeric network.

The UV-Vis-NIR spectra of poly($\mathbf{E}_4\mathbf{T}_4$) recorded under the same conditions shows qualitatively the same behavior. The spectrum of the fully undoped polymer shows a maximum at 470 nm with an absorption onset at 640 nm corresponding to a band gap of 1.9-2.0 eV (Fig. 16a). Application of increasing positive potentials produces the bleaching of the visible absorption band and the concomitant development of two broad absorption bands with maxima around 640 and 1300 nm. Similarly to poly($\mathbf{E}_4\mathbf{T}_2$) the neutral polymer appears red and turns gradually to blue upon oxidation. As in the previous case the spectral signature of the most charged species corresponds to that of a polaronic state a result consistent with discrete TEET segments.

For poly($\mathbf{E}_8\mathbf{T}_6$) the spectrum of the neutral polymers presents a λ_{max} at 446 nm, this relatively short wavelength can be explained by the distortion imposed to the conjugated systems by the steric effects of the butyl chains (Fig. 16c). Upon application of more positive potential the intensity of this and decreases the concomitant development of two absorption bands at *ca* 750 nm and 1500 nm. Upon application of potential more positive than 0.70 V, the intensity of these two bands progressively decreases and for an applied potential of 1.30 V, they merge into a single broad band with a maximum around 1000 nm which suggests the formation of a bipolaronic state. The spectrum of neutral poly($\mathbf{E}_8\mathbf{T}_2$) is bathochromically shifted compared to the previous ones with an absorption maximum at 510 nm (Fig. 16b). This value agrees well with the larger effective conjugation suggested by electrochemical data. Application of more positive potentials produces the progressive appearance of the two transitions of the polaron state

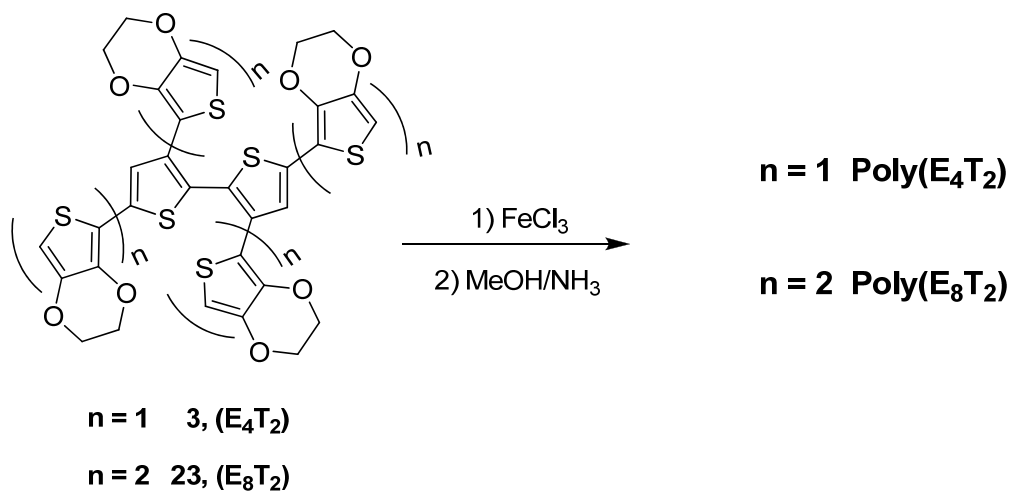
around 750 and 1500 nm while the intensity of these bands begins to decrease for potential values above 0.60 V with an evolution towards a single bipolaronic transition.

4.3.5. Chemical polymerization of 3D systems

The oxidative polymerization of the 3D-oligothiophenes was achieved in the presence of iron (III) chloride FeCl_3 . This type of polymerization is easy to handle experimentally and can lead to high molecular weight polymers. This method was initially applied for the synthesis of irregular polymers⁵² but it was proved that it can be also used for the synthesis of regioregular polymers by inverting the order of the reagents.⁵³

Recently, this procedure has been employed for the synthesis of conjugated microporous poly(thienylenearylene)⁵⁴ networks.

A solution of 3,3',5,5'-tetra-(E and EE)-2,2'-bithiophene and FeCl_3 in dry chloroform was stirred at room temperature over weekend following the classical method for this type of polymerization (Scheme 22).



Scheme 22

The oxidized polymer was precipitated by addition of methanol to the solution, reduced by addition of a mixture of methanol/ammonia = 5/1 and then filtered and washed with methanol to give a black solid. Purification and separation of the material was achieved by successive Soxhlet extractions using hexane, chloroform, tetrahydrofuran and chlorobenzene as solvents.

⁵² a) Sugimoto, R.; Takeda, S.; Gu, H. B.; Yoshino, K. *Chem. Express* **1986**, *1*, 635; b) Leclerc, M.; Martinez Diaz, F.; Wegner, G. *Makromol. Chem.* **1989**, *190*, 3105-3116 Leclerc, M.; Martinez Diaz, F.; Wegner, G. *Makromol. Chem.*, **1989**, *190*, 3105-3116

⁵³ Andersson, M.R.; Selse, D.; Berggren, M.; Jaervinen, H.; Hjertberg, T.; Inganäs, O.; Wennerström, O.; Österholm J.-E. *Macromolecules*, **1994**, *27*, 6503-650

⁵⁴ Schmidt, J.; Weber, J.; Epping, J.D.; Antonietti, M.; Thomas, A. *Adv. Mater.* **2009**, *21*, 702-705

Traces of starting material were recovered in the chloroform fraction in the case of poly(E_4T_2). The polymers were totally insoluble in all solvents tested, thus could not be further analyzed and were used as obtained for the determination of the porosity of the materials.

Previous work on microporous conjugated polymers derived from 3D precursors has shown that the nature and the size of the precursor determine the formation of a 3D-network with different effective conjugation length in the chain and different porosities. In particular it has been shown that the pore structure of these networks can be tuned by controlling the length of the connecting units.²³

In a first attempt to measure the porosity of this polymer, a sample was sent to Dr. Frank Millange, laboratory of the Lavoisier Institute, University of Versailles. The porosity of the poly(E_4T_2) network was investigated by N_2 gas adsorption of the guest-free material.

Thus poly(E_4T_2) was degassed at 100 and 150°C. A weight loss of 36.5%, attributed to water was observed upon heating at 100°C with no further modification up to 150°C. However, no evidence for porosity larger than that the inter-grannular one could be observed by nitrogen adsorption on the activated material. Similar experiments have been carried out on poly(E_8T_2) and gave similar results.

Two explanations can be envisaged for this behaviour. A first possibility could be that the size of the entrance of the pores is too small to allow the ingress of the nitrogen molecules. Indeed compared to already reported systems based on the interconnection of terminal thiophene units, the presence of the ethylenedioxy groups can exert a crowding effect and strongly reduce the size of the pores. Another possibility could involve an excessive flexibility of the 3D structure. Consequently, when submitted to a gas pressure, such a flexible structure undergoes a contraction instead of absorbing gas. In fact these two explanations are not independent since an insufficient size of the pores will also contribute to the collapse of the 3D structure. In fact, the microporous conjugated polymers reported until now are based on rather rigid structures.³⁰

At this stage this project can be developed into two directions. First it is necessary to evaluate the higher terms of this series in order to determine whether systems with longer branches can eventually present a larger porosity. On the other hand, one can envision to rigidify the structure of the precursor introduction of more rigid linkages like for example acetylenic bridges in the branches. Such an approach could contribute at the same time to provide a more rigid structure and to enlarge the size of the pores.

4.4. 3D-conjugated systems containing 2-(ethylhexyl)-carbazole units

Prior to being used as precursors of electrogenerated conjugated networks, 3D conjugated systems have been initially developed in Angers as elemental units of organic semiconductors possessing isotropic optical and charge transport properties.³³⁻³⁵ In this context, we have been interested in a first exploration of the use of carbazole as building block for the synthesis of 3D conjugated systems that could be potentially used as active material in organic devices.

Carbazole and its derivatives have been previously used as flexible building blocks for material construction⁵⁵ due to their electron-donating nature, distinct photoconductivity and nonlinear optical property.⁵⁶ Consequently they have been intensively used for the synthesis of some donor-acceptor alternating conjugated copolymers with applications in organic photovoltaic cells⁵⁷ thin film transistors,⁵⁸ electroluminescent materials,⁵⁹ dyes⁶⁰ and light emitting devices.⁶¹

In order to graft the carbazole moiety on compounds **1** and **2**, the boronic ester of carbazole was synthesized in a three step procedure.

First 3-bromo-carbazole (**29**) was obtained from commercially available carbazole using bromine in dimethylformamide at low temperature.⁶² In order to increase the solubility of this derivative, the active proton from the carbazole NH group was alkylated with 2-ethylhexyl bromide before the lithiation was carried out. The corresponding 3-bromo-9-(2-ethylhexyl)carbazole (**30**)³³ and 9-(2-ethylhexyl)-3-(4,4,5,5-tetramethyl[1,3,2]dioxaborolan-2-yl)-carbazole (**31**)⁶³ were prepared in good yields (Scheme 23). The boronic ester of carbazole was prepared from the corresponding bromo-derivative by successive treatment with *n*-BuLi and 2-isopropoxy-4,4,5,5-tetramethyl-1,3,2-dioxaborolane.

⁵⁵ Blouin, N.; Leclerc, M. *Acc. Chem. Res.* **2008**, *41*, 1110-1119

⁵⁶ Shi, J.; Huang, M.; Xin, Y.; Chen, Z.; Gong, Q.; Xu, S.; Cao, S. *Materials Letters* **2005**, *59*, 2199-2203

⁵⁷ Tsai, J.H.; Chueh, M.H.; Lai, M.H.; Wang, C.F.; Chen, W.C.; Ko, B.T., Ting, C. *Macromolecules* **2009**, *46*, 1897-1905

⁵⁸ Sonntag, M.; Kreger, K.; Hanft, D.; Strohrriegl, P.; Setayesh, S.; Leeuw, D. *Chem. Mater.* **2005**, *17*(11), 3031-3039

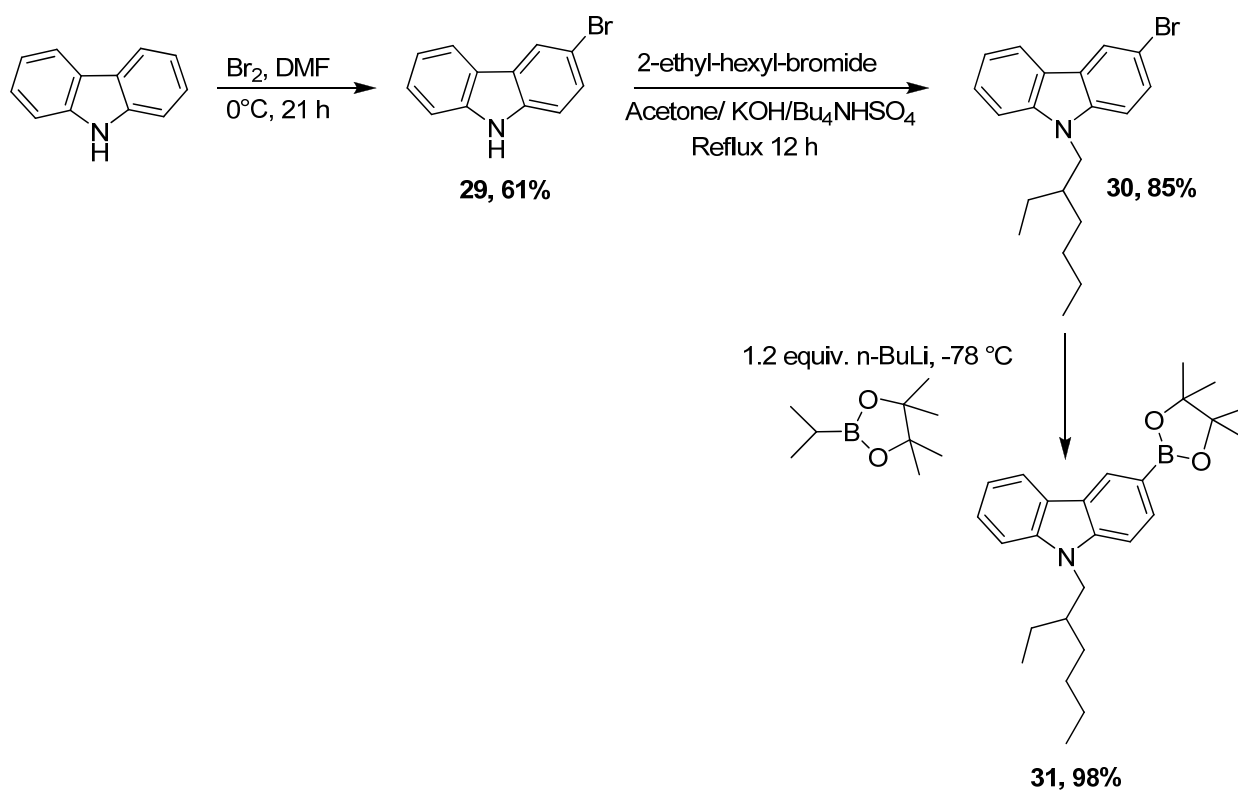
⁵⁹ Shin, M.-H.; Wong, F.F.; Lin, C.-M.; Chen, W.-Y.; Yeh, M.-Y. *Heteroatom Chemistry* **2006**, *17*, 160-165

⁶⁰ Mishra, A.K.; Jacob, J.; Mullen, K. *Dyes and Pigments* **2007**, *75*, 1-10

⁶¹ Zhu, Y.; Rabindranath, R.; Beyerlein, T.; Tieke, B. *Macromolecules* **2007**, *40*, 6981-6989

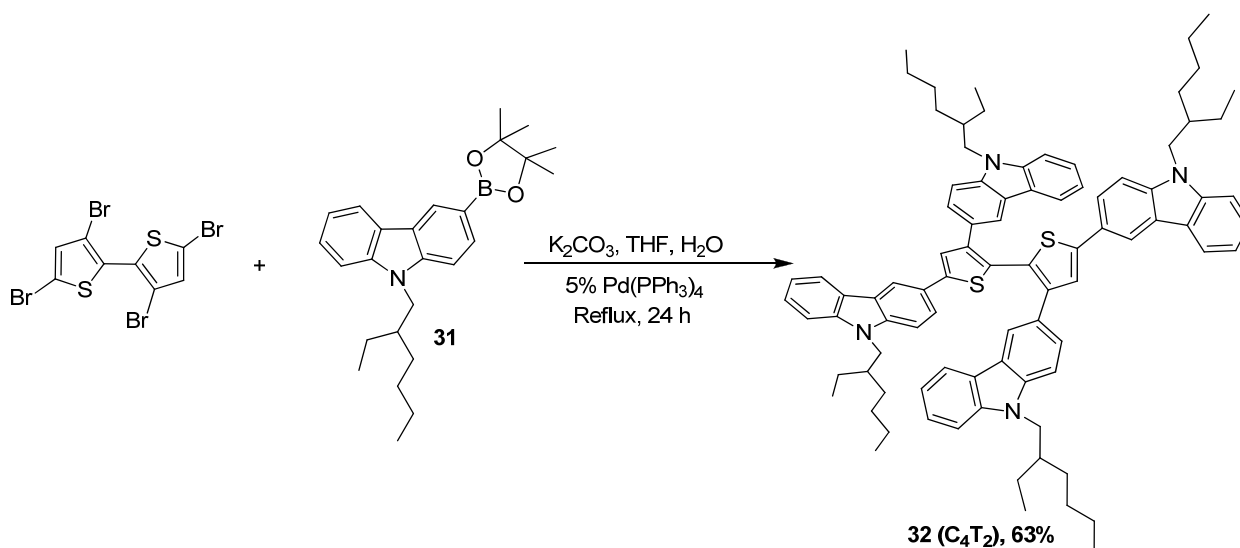
⁶² Tavasli, M.; Bettington, S.; Bryce, M.R.; Batsanov, A.S.; Monkman, A.P. *Synthesis* **2005**, *10*, 1619-1624

⁶³ Sonntag, M.; Strohrriegl, P. *Chem. Mater.* **2004**, *16*, 4736-4742



Scheme 23

The tetracarbazole 3D structure **32** was synthesized by Suzuki coupling reaction. Boronic ester **31** was used together with 3,3',5,5'-tetrabromo-2,2'-bithiophene to give 3,3',5,5'-tetra(2-ethylhexyl-carbazole)-bithiophene (**32**) in 70 % yield (Scheme 24).



Scheme 24

The UV-Vis absorption spectrum of **32** recorded in acetonitrile solution is shown in Figure 17. The spectrum shows two absorption maxima at 240, 303 nm and a shoulder at 360

nm. As in the previous systems, this complex optical spectrum reveals the coexistence of different conjugated segments in the structure.

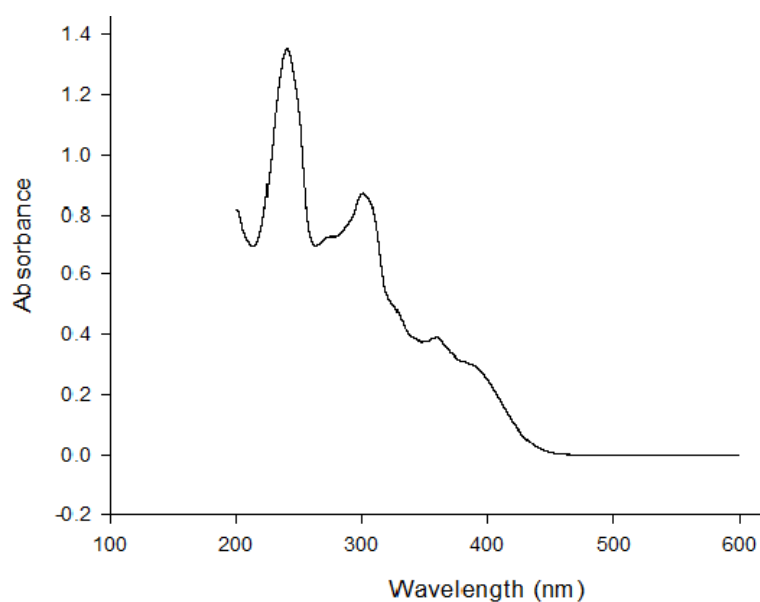


Fig. 17. UV-Vis absorption spectrum of **32** in acetonitrile

In a first attempt to evaluate the potentialities of this type of material, compound **32** has been used as donor in a bulk heterojunction solar cells using a soluble C60 derivative (PCBM) as acceptor.

Under simulated solar irradiation a 100 mW cm^{-2} , the cell delivered a short circuit density of 3.0 mA cm^{-2} , an open-circuit voltage of 0.47 V and a power conversion efficiency of 0.33% . Although modest, these results must be considered with regard to those obtained on the parent system (**33**) (Fig. 18).

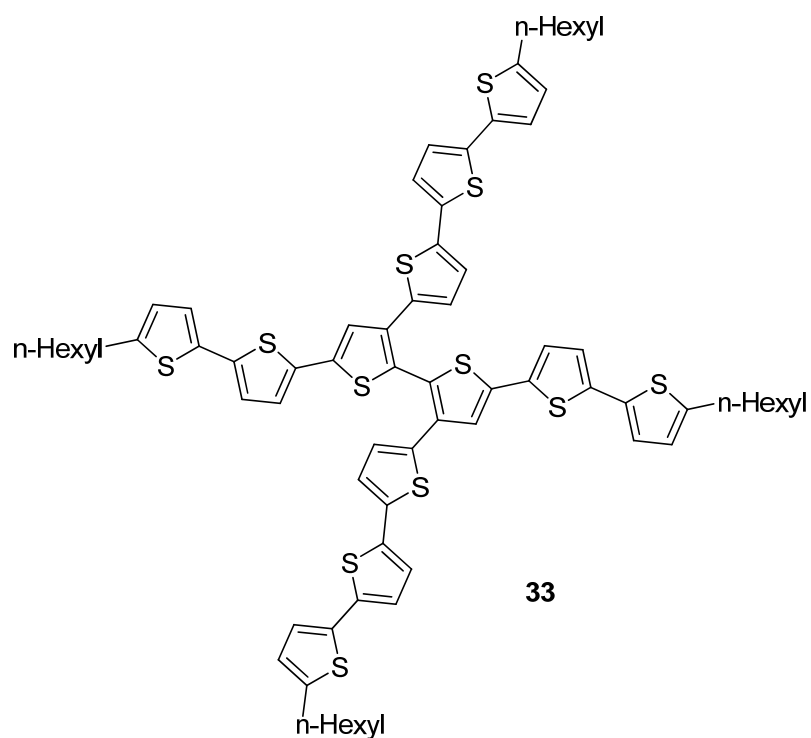


Fig. 18

This compound which absorbs at a longer wavelength than **32** (400 nm) gave only 1.3 mA cm⁻² under the same conditions. The fact that compound **32** can produce a current density more than twice larger current in spite of its limited light harvesting properties clearly indicate that the use of the carbazole block for the construction of 3D systems can significantly contribute to improve the charge transport properties.

4.5. Conclusions

A new series of twisted systems based on a twisted 2,2'-bithiophenic node derivatized with conjugated branches containing terminal EDOT units has been synthesized. By modifying the size and composition of the conjugated branches it is possible to synthesize 3D conjugated architectures of different sizes and electronic properties.

Four new precursors with terminal EDOT units and one with carbazole unit have been synthesized by Stille and Suzuki coupling reactions. Their electronic properties were studied by electrochemistry and optical spectroscopy.

All EDOT containing compounds have been successfully electropolymerized and lead to electroactive materials consisting of 3D conjugated networks. Their voltamperometric and spectroscopic properties were correlated with the size and the nature of the conjugated branches linked on the central node.

Attempts have been made to analyse the porosity study of the electrodeposited materials by electrochemical experiments. Although some indications suggesting that the materials are indeed porous, the obtained results are complex and difficult to interpret due to the intrication of mechanical effects and redox processes. On the other hand, the first attempt to measure the active area of two of these materials by nitrogen sorption remained unsuccessful and no porosity larger than that the inter-grannular one could be evidenced. Future work should now focus of a more detailed evaluation of the larger terms of the series as well as on the design and synthesis of new precursors with more rigid structure.

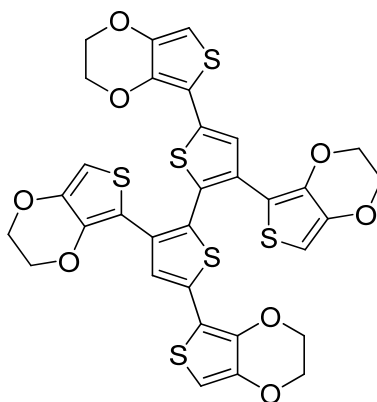
4.6. Experimental Part

4.6.1. General remarks

^1H NMR and ^{13}C NMR spectra were recorded on a Bruker AVANCE DRX 500 spectrometer operating at 500.13 and 125.7 MHz and Bruker AVANCE 300 spectrometer operating at 300 and 75 MHz; δ are given in ppm (relative to TMS) and coupling constants (J) in Hz. Mass spectra were recorded under EI mode on a VG-Autospec mass spectrometer or under MALDI-TOF mode on a MALDI-TOF-MS BIFLEX III Bruker Daltonics spectrometer. UV-visible optical data were recorded with a Perkin-Elmer lambda 19 and lambda 950 spectrophotometers. Melting points were obtained from a Reichert-Jung Thermovar hot-stage microscope apparatus and are uncorrected. Column chromatography purifications were carried out on Merck silica gel Si 60 (40-63 μm).

Electrochemical experiments were performed with an EG&G 273 potentiostat in a standard three-electrode cell using platinum electrodes and a saturated calomel reference electrode (SCE). The solutions were degassed by argon bubbling and experiments were carried under an argon blanket. The working electrode was a 2 mm diameter Pt disk sealed in glass. Tetrabutylammonium hexafluorophosphate (Fluka puriss) was used as received.

4.6.2. Synthesis and characterization of compounds

3,3',5,5'-tetra(3,4-ethylenedioxythiophene)-2,2'-bithiophene (**3**)**3** (E_4T_2)

3,3',5,5'-tetrabromo-2,2'-bithiophene (0.964g, 2 mmol), 2-(tributylstannyl)-3,4-(ethylenedioxy) thiophene (6.899 g, 16 mmol), and Pd(PPh₃)₄ catalyst (0.924 g, 0.8 mmol, 5%) were mixed in 100 mL of dry toluene and refluxed for 8 h under nitrogen. A second portion of catalyst (1%) was added and the mixture was refluxed for another 24 h period. The mixture was washed with water, extracted with toluene (20 ml), filtered over celite and dried under vacuum. The residue was purified by column chromatography (diethyl ether) to generate 1.0 g of a yellow-orange solid. Yield: 69%, mp 215°C.

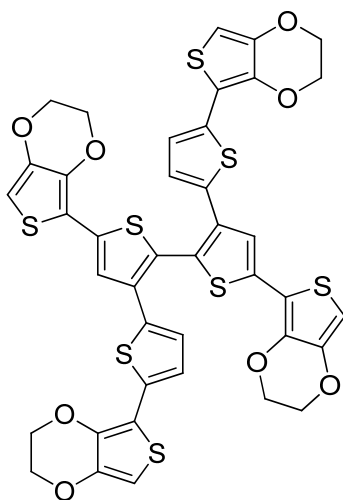
¹H NMR (500 MHz, CDCl₃) δ ppm: 7.58 (s, 2H), 6.24 (s, 2H), 6.13 (s, 2H), 4.32-4.33 (m, 4H), 4.23-4.25 (m, 4H), 4.17-4.18 (m, 4H), 4.14-4.15 (m, 4H).

¹³C NMR (125 MHz, CDCl₃) δ ppm: 114.78, 140.97, 137.95, 137.78, 135.55, 133.10, 126.23, 122.39, 112.29, 111.94, 99.13, 97.20, 64.98, 64.63, 64.57, 64.39.

MS (MALDI-TOF): found 725.95, calculated for C₃₂H₂₂O₈S₆ 725.96.

ESI-MS⁺: found 726.970 [M+H]⁺, 748.952 [M+Na]⁺ calculated for C₃₂H₂₂O₈S₆ 725.960.

2,2',5,5'-tetra(3,4-ethylenedioxythiophene)-3,3'-dithienyl-2,2'-bithiophene (4)



4 (E₄T₄)

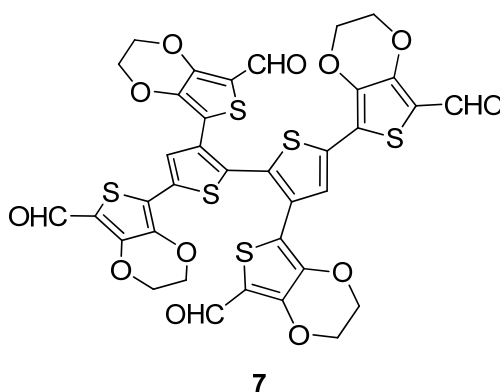
Tetrabromo-3,3'-dithienyl-2,2'-bithiophene (0.210g, 0.325 mmol), 2-(tributylstannyl)-3,4-(ethylenedioxy)thiophene (1.121 g, 2.6 mmol), and Pd(PPh₃)₄ catalyst (150 g, 0.13 mmol, 5%) were mixed in 25 mL of dry toluene and refluxed for 8 h under nitrogen. A second portion of catalyst (1%) was added and the mixture was refluxed for another 48 h period. The mixture was washed with water, extracted with toluene (20 ml), filtered over celite and dried under vacuum. The residue was purified by column chromatography (diethyl ether) to generate 90 mg of a yellow-orange solid. Yield: 31%, mp decomposition after 142°C.

¹H NMR (500 MHz, CDCl₃) δ ppm: 7.40 (s, 2H), 6.98 (d, 2H), 6.88 (d, 2H), 6.27 (s, 2H), 6.15 (s, 2H), 4.33-4.35 (m, 4H), 4.24-4.27 (m, 4H), 4.19-4.20 (m, 4H).

¹³C NMR (125 MHz, CDCl₃) δ ppm: 141.81, 141.74, 138.20, 137.40, 136.29, 135.77, 135.45, 134.32, 125.37, 125.01, 123.29, 122.41, 112.28, 111.51, 97.54, 96.80, 65.02, 64.85, 64.55 (2C).

MS (MALDI-TOF): found 889.7, calculated for C₄₀H₂₆O₈S₈ 889.94.

ESI-MS⁺: found 890.945 [M+H]⁺, 912.926 [M+Na]⁺ calculated for C₄₀H₂₆O₈S₈ 889.94.

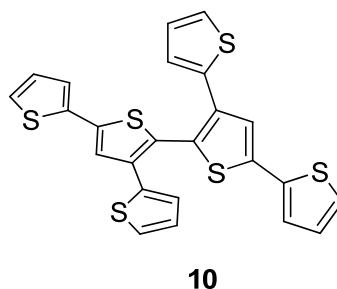
3,3',5,5'-tetra(3,4-ethylenedioxythiophene-5-carboxyaldehyde)-2,2'-bithiophene (7)

To a solution of 3,3',5,5'-tetra(3,4-ethylenedioxythiophene)-2,2'-bithiophene (3.63 g, 5 mmol) in 150 ml of dichloroethane, dimethylformamide (2.7 ml, 35 mmol) and POCl₃ (3.26 ml, 35 mmol) were added and the mixture was refluxed for 24 hours under nitrogen atmosphere. Hydrolysis was made with sodium acetate, followed by dichloromethane extraction. The crude was purified on chromatography using diethylether/dichloromethane 1/1 as eluent, affording 1.2 g of **7**. Yield: 29%, mp decomposition >200°C.

¹H NMR (500 MHz, CDCl₃) δ ppm: 9.95 (s, 1H), 9.81 (s, 1H), 7.89 (s, 1H), 4.44 (m, 4H), 4.35-4.29 (m, 4H).

¹³C NMR (125 MHz, CDCl₃) δ ppm: 179.90, 179.67, 148.40, 148.25, 138.23, 137.90, 135.54, 132.83, 130.18, 126.37, 122.00, 121.68, 177.19, 115.72, 65.43, 65.11, 65.03, 64.65.

HRMS: 838.9509, calculated for C₃₆H₂₂O₁₂S₆ 838.94.

3,3',5,5'-tetra(2-thienyl)-2,2'-bithiophene (10)

3,3',5,5'-tetrabromo-2,2'-bithiophene (2g, 4.15 mmol), 2-(tributylstannyl)thiophene (6.81 g, 18.26 mmol), and Pd(PPh₃)₄ catalyst (1.05 g, 0.91 mmol, 5%) were mixed in 50 mL of dry toluene and refluxed for 12 h under nitrogen. The mixture was washed with water, extracted with toluene (20 ml), filtered over celite and dried under vacuum. The residue was purified by column

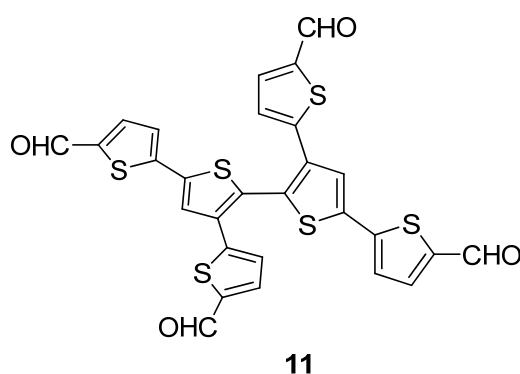
chromatography (petroleum spirits/diethyl ether = 2/1) to generate 400 mg of a white solid. Yield: 20%.

¹H NMR (500 MHz, CDCl₃) δ ppm: 7.42 (s, 2H), 7.28 (d, 2H), 7.24 (d, 2H), 7.14 (d, 2H), 7.08 (d, 2H), 7.04-7.05 (dd, 2H), 6.90-6.92 (dd, 2H).

¹³C NMR (125 MHz, CDCl₃) δ ppm: 139.00, 137.12, 136.72, 136.42, 127.95, 127.03, 125.60, 125.30, 125.13, 124.44, 123.79.

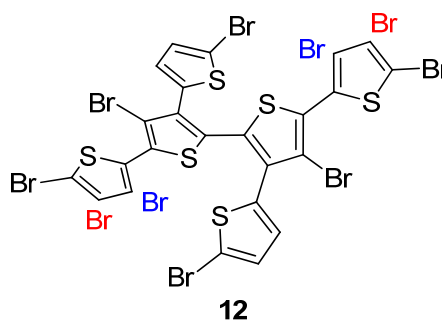
MS (EI) 493.85, calculated for C₂₄H₁₄S₆ 493.94.

3,3',5,5'-tetra(2-thienyl-5-carboxyaldehyde)-2,2'-bithiophene (11)



To a solution of 3,3',5,5'-tetra(thiophene)-2,2'-bithiophene (50 mg, 0.1 mmol) in 10 ml of dichloroethane, dimethylformamide (0.054 ml, 0.7 mmol) and POCl₃ (0.065 ml, 0.7 mmol) were added and the mixture was refluxed for 24 hours under nitrogen atmosphere. Sodium acetate was added to the mixture and extraction was made with dichloromethane. The organic layer was washed several times with water and after concentration was purified on chromatography using as eluent dichloromethane/ethylacetate 95/5, affording 20 mg of white solid. Yield: 33%.

¹H NMR (500 MHz, CDCl₃) δ ppm: 9.92 (s, 1H), 9.80 (s, 1H), 7.74 (d, 1H), 7.61 (s, 1H), 7.60 (d, 1H), 7.36 (d, 1H), 7.19 (d, 1H).

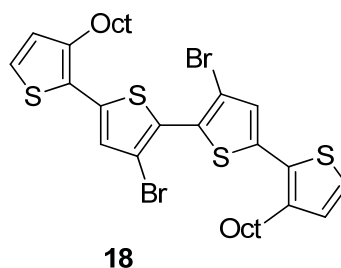
Octabromo-3,3',5,5'-tetra(2-thienyl)-2,2'-bithiophene (12)

To a solution of **4** (0.25 g, 0.5 mmol) in 40 mL CHCl_3 under nitrogen atmosphere, was added dropwise a solution of 0.11 mL Br_2 in 10 mL of CHCl_3 . The mixture was stirred at room temperature for 15 minutes and the reaction was quenched with 20 mL of NaHCO_3 solution. Extraction was made with dichloromethane. The organic layer was washed with NaHCO_3 and brine solutions, giving 400 mg yellow solid. Yield: 98%.

$^1\text{H NMR}$ (500 MHz, CDCl_3) δ ppm: 7.06 (s, 2H), 7.03 (d, 2H), 6.75 (d, 2H).

$^{13}\text{C NMR}$ (125 MHz, CDCl_3) δ ppm: 135.40, 133.64, 133.58, 133.05, 130.36, 130.07, 129.84, 129.68, 115.53, 115.04, 114.91, 112.17.

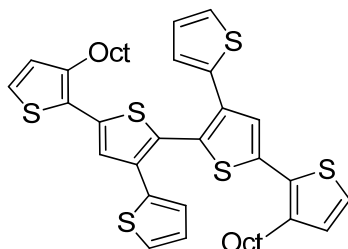
MS (MALDI-TOF): found 1125.85, calculated for $\text{C}_{24}\text{H}_6\text{Br}_8\text{S}_6$ 1117.23 (exact mass), 1125.93 (molecular weight).

3,3'-dibromo-5,5'-di(2-thienyl-3-octyl)-2,2'-bithiophene (18)

3,3',5,5'-tetrabromo-2,2'-bithiophene (402 mg, 0.84 mmol), 2-(trimethylstannyl)-3-octylthiophene (1.5 g, 4.17 mmol), and $\text{Pd}(\text{PPh}_3)_4$ catalyst (242 mg, 0.21 mmol, 5%) were mixed in 30 mL of toluene and refluxed for 24 h under nitrogen. A second portion of catalyst (1%) was added and the mixture was refluxed for another 24 h period. The mixture was washed with water, extracted with toluene (20 ml), filtered over celite and dried under vacuum. The residue was purified by column chromatography (petroleum spirits) to generate 112 mg of a yellow-green solid. Yield: 20%. $^1\text{H NMR}$ (500 MHz, CDCl_3) δ ppm: 7.23 (d, $J = 5.19$ Hz, 1H), 7.08 (s, 1H), 6.96 (d, $J = 5.20$ Hz, 1H), 2.77 (t, 2H), 1.66-1.25 (m, 10H), 0.87 (t, 2H).

MS (EI) 712.05, calculated for C₁₆H₆Br₂S₄ 710.04 (exact mass), 712.13 (molecular weight).

3,3'-di(2-thienyl)-5,5'-di(2-thienyl-3-octyl)-2,2'-bithiophene (19)

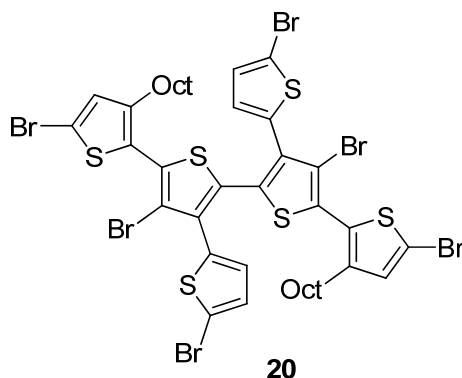


19

Compound **7** (112 mg, 0.157 mmol), 2-(tributylstannyl)-thiophene (234.35 mg, 0.628 mmol), and Pd(PPh₃)₄ catalyst (50 mg, 5%) were mixed in 10 mL of toluene and refluxed for 24 h under nitrogen. A second portion of catalyst (1%) was added and the mixture was refluxed for another 24 h period. The mixture was washed with water, extracted with toluene (20 ml), filtered over celite and dried under vacuum. The residue was purified by column chromatography (petroleum spirits) to generate 119 mg of a yellow-green oily liquid. Yield: 99%.

¹H NMR (500 MHz, CDCl₃) δ ppm: 7.43 (s, 1H), 7.24 (d, *J* = 5 Hz, 1H), 7.16 (d, *J* = 5 Hz, 1H), 7.12 (d, *J* = 3.5 Hz, 1H), 6.99 (d, *J* = 5 Hz, 1H), 6.96-6.93 (dd, ³*J* = 5 Hz, ⁴*J* = 4 Hz, 1H).

Hexabromo-3,3'-di(2-thienyl)-5,5'-di(2-thienyl-3-octyl)-2,2'-bithiophene (20)

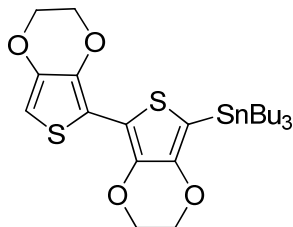


20

To a solution of **8** (50 mg, 0.07 mmol) in 10 mL CHCl₃ under nitrogen atmosphere was added NBS (49.84 mg, 0.28 mmol) at 0°C. This mixture was stirred at 0°C for 2 hours and after usually work-up NMR spectroscopy was performed. ¹H-NMR of the crude shows a mixture of several bromo-derivatives unable to separate on chromatography. Thus this mixture was solved in 10 ml of chloroform and another portion of NBS was added. The mixture was stirred at room temperature for 1 hour affording the hexa-bromoderivative **20** in quantitative yield.

$^1\text{H NMR}$ (500 MHz, CDCl_3): δ ppm: 7.00 (d, $J = 4$ Hz, 1H), 6.95 (s, 1H), 6.74 (d, $J = 4$ Hz, 1H).

5-tributylstannyl-2,2'-bis-(3,4-ethylenedioxythiophene) (22)

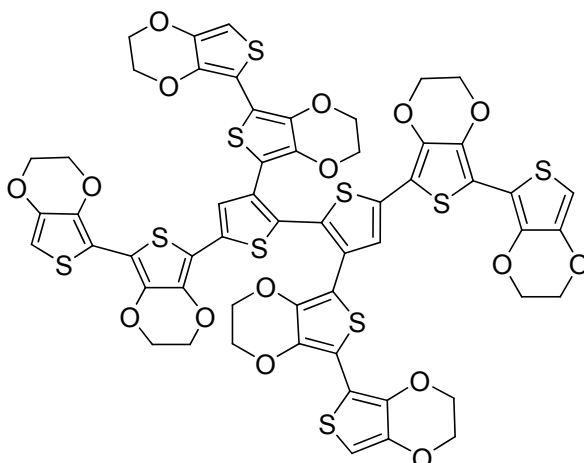


22

To a solution of 2,2'-bis(ethylene3,4-dioxy)-thiophene (2.82 g, 10 mmol) in 200 ml of dry THF, $n\text{-BuLi}$ 1.6 M (7.5 ml, 12 mmol) was added at -78°C under nitrogen and stirred for 1 hour. Tributylstannyl chloride (3.2 ml, 12 mmol) was added dropwise at -40°C and the mixture was stirred overnight while affording to warm to room temperature. Solvent was removed, extraction was made with ethyl acetate and the organic layer was washed several times with sodium fluoride saturated solution. After drying over magnesium sulfate, solvent was removed affording 6.4 g of colorless liquid. Yield: 99%.

$^1\text{H NMR}$ (500 MHz, CDCl_3) δ ppm: 6.24 (s, 1H), 4.34-4.32 (m, 2H), 4.30-4.28 (m, 2H), 4.24-4.22 (m, 2H), 4.18-4.17 (m, 2H), 1.57-1.52 (m, 6H), 1.36-1.29 (m, 6H), 1.12-1.10 (m, 6H), 0.91-0.86 (t, 9H).

3,3',5,5'-tetra[bis(3,4-ethylenedioxythiophene)]-2,2'-bithiophene (23)



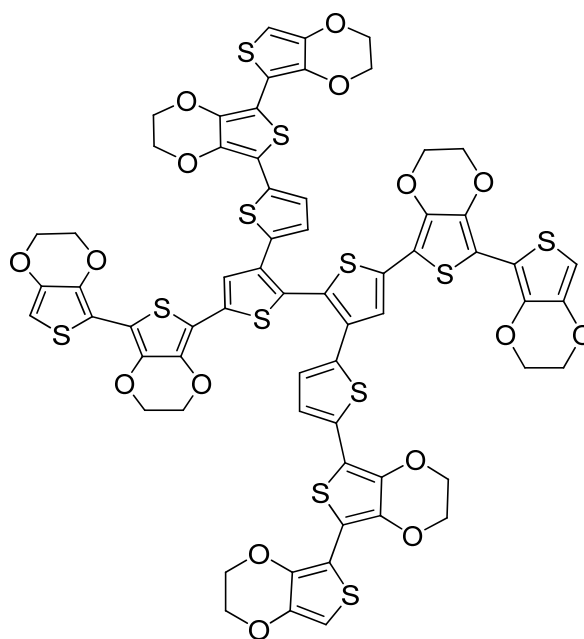
23 (E₈T₂)

3,3',5,5'-tetrabromo-2,2'-bithiophene (240.92 mg, 0.5 mmol), 5-(tributylstannyl)-2,2'-bis(3,4-(ethylenedioxy) thiophene) (1.71 g, 3 mmol), and Pd(PPh₃)₄ catalyst (150 mg, 5%) were mixed in 50 mL of dry toluene and refluxed for 12 h under nitrogen. A second portion of catalyst (1%) and stannic were added and the mixture was refluxed for another 12 h period. The mixture was filtered over a pad of silica and celite, washed with toluene, diethylether, dichloromethane and acetone. Toluene fraction contains mostly 2,2'-bis(3,4-ethylenedioxythiophene), in dichloromethane fraction we isolated the desired product **23 (E₈T₂)**, and acetone fraction contains triphenylphosphine. After solvent evaporation, compound was purified by column chromatography (dichloromethane) and precipitated using a mixture of dichloromethane and hexane, to generate 330 mg of an orange solid. Yield: 51%.

¹H NMR (500 MHz, CDCl₃) δ ppm: 7.34 (s, 1H), 6.29 (s, 1H), 6.18 (s, 1H), 4.37-4.35 (m, 6H), 4.27-4.24 (m, 2H), 4.15-4.16 (m, 6H), 4.03-4.01 (m, 2H).

¹³C NMR (125 MHz, CDCl₃) δ ppm: 141.37 (1C), 141.33 (1C), 137.49 (1C), 137.32 (1C), 137.21 (1C), 137.12 (1C), 136.91 (1C), 136.66 (1C), 134.75 (1C), 131.70 (1C), 128.54 (1C), 124.20 (1C), 110.30 (1C), 110.24 (1C), 109.91 (2C), 109.66 (1C), 107.90 (1C), 98.09 (1C), 96.97 (1C), 65.18 (1C), 65.03 (2C), 64.80 (1C), 64.73 (1C), 64.68 (2C), 64.47 (1C).

HRMS: 1285.9404, calculated for C₅₆H₃₈O₁₆S₁₀ 1285.94.

2,2',5,5'-tetra[bis(3,4-ethylenedioxythiophene)]-3,3'-dithienyl-2,2'-bithiophene (4)**24 (E₈T₄)**

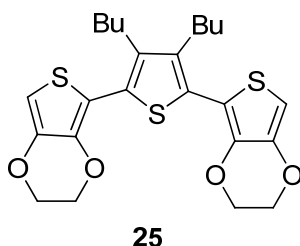
Tetrabromo-3,3'-dithienyl-2,2'-bithiophene (323.04 mg, 0.5 mmol), 5-(tributylstannyl)-2,2'-bis(3,4-ethylenedioxythiophene) (1.71 g, 3 mmol), and Pd(PPh₃)₄ catalyst (150 mg, 5%) were mixed in 50 mL of dry toluene and refluxed for 12 h under nitrogen. A second portion of catalyst (1%) and stannic were added and the mixture was refluxed for another 24 h period. The mixture was filtered over a pad of silica and celite, washed with toluene, diethylether, dichloromethane and acetone. Toluene fraction contains mostly 2,2'-bis(3,4-ethylenedioxythiophene), dichloromethane and acetone fractions have the desired product **24 (E₈T₄)**. After solvent evaporation, compound was purified by column chromatography (diethylether followed by dichloromethane) and precipitated using a mixture of dichloromethane and hexane, to generate 50 mg of an orange solid. Yield: 7%.

¹H NMR (500 MHz, CDCl₃) δ ppm: 7.42 (s, 1H), 6.99 (d, 1H), 6.90 (d, 1H), 6.31 (s, 1H), 6.25 (d, 1H), 4.38 (m, 6H), 4.26 (m, 6H), 4.23 (m, 1H), 4.20 (m, 1H).

¹³C NMR (125 MHz, CDCl₃) δ ppm: 141.34 (1C), 141.28 (1C), 137.86 (1C), 137.29 (2C), 137.09 (1C), 137.02 (2C), 136.96 (1C), 135.76 (1C), 135.48 (1C), 134.32 (1C), 125.61 (1C), 123.09 (1C), 110.26 (1C), 109.92 (1C), 109.81 (1C), 109.28 (1C), 108.43 (1C), 107.64 (1C), 98.23 (1C), 97.83 (1C), 65.20 (1C), 65.11 (2C), 65.02 (2C), 64.92 (1C), 64.70 (2C).

HRMS: 1449.9128, calculated for C₆₄H₄₂O₁₆S₁₂ 1449.91.

2,5-di(3,4-ethylenedioxythiophene)-3,4-dibutylthiophene (25)

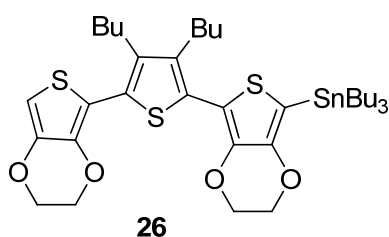


2,5-dibromo-3,4-dibutyl-thiophene (6.15 g, 17.4 mmol), 5-(tributylstannyl)- 2,2'-bis(3,4-ethylenedioxythiophene) (22.5 g, 52.2 mmol), and Pd(PPh₃)₄ catalyst (3 g, 5%) were mixed in 500 mL of dry toluene and refluxed for 12 h under nitrogen. A second portion of catalyst (1%) was added and the mixture was refluxed for another 12 h period. The mixture was filtered over silica and celite, washed with toluene and dichloromethane. Solvents were evaporated and the residuum was purify on chromatography (petroleum spirit/dichloromethane 2/1) affording 6.7 g of oily liquid. Yield: 80%.

¹H NMR (500 MHz, CDCl₃) δ ppm: 6.36 (s, 1H), 4.26-4.24 (m, 2H), 4.23-4.20 (m, 2H), 2.67-2.64 (m, 2H), 1.53-1.49 (m, 2H), 1.40-1.36 (m, 2H), 0.93-0.90 (t, 3H).

¹³C NMR (125 MHz, CDCl₃) δ ppm: 141.25, 140.74, 138.06, 127.47, 110.41, 98.80, 64.69, 64.40, 32.59, 27.80, 22.94, 13.80.

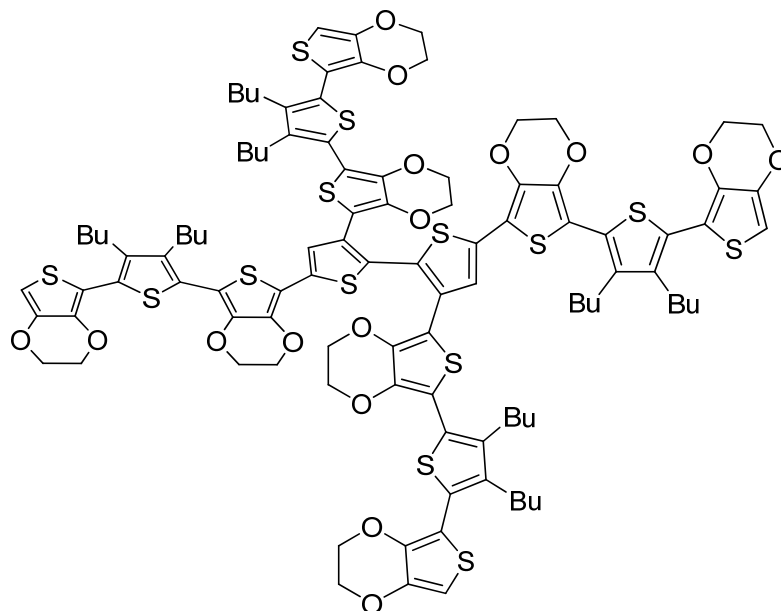
2-(2-tributylstannyl-3,4-ethylenedioxythiophene)-5-(3,4-ethylenedioxythiophene)-3,4-dibutyl-thiophene (25)



To a solution of 2,5-bis(3,4-ethylenedioxy-thiophene)-3,4-dibutyl-thiophene (3.35 g, 7 mmol) in 300 ml of dry THF, n-BuLi (4.4 ml, 7 mmol) was added at -78°C under nitrogen and stirred for 1 hour. Tributylstannyl chloride (1.9 ml, 7 mmol) was added dropwise at -40°C and the mixture was stirred overnight while affording to warm to room temperature. Solvent was removed, extraction was made with ethyl acetate and the organic layer was washed several times with sodium fluoride saturated solution. After drying over magnesium sulfate, solvent was removed affording 2.7 g of brown liquid. Yield: 62%.

$^1\text{H NMR}$ (500 MHz, CDCl_3) δ ppm: 6.33 (s, 1H), 4.25-4.24 (m, 2H), 4.23-4.21 (m, 4H), 4.17-4.16 (m, 2H), 2.68-2.62 (m, 4H), 1.58-1.55 (m, 10H), 1.39-1.30 (m, 10H), 1.13-1.09 (m, 6H), 0.92-0.88 (m, 15H).

2,2',3,3'-tetra[2,5-bis(3,4-ethylenedioxythiophene)-3,4-dibutylthiophene]bithiophene



27 (E₈T₆)

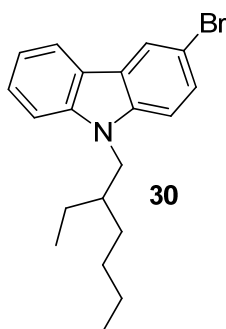
3,3',5,5'-tetrabromo-2,2'-bithiophene (200 mg, 0.41 mmol), compound **26** (1.9 g, 2.5 mmol), and $\text{Pd}(\text{PPh}_3)_4$ catalyst (150 g, 5%) were mixed in 100 mL of dry toluene and refluxed for 12 h under nitrogen. A second portion of catalyst (1%) and stannic were added and the mixture was refluxed for another 24 h period. The mixture was filtered over a pad of silica and celite, washed with toluene, diethylether, dichloromethane and acetone. After solvent evaporation, compound was purified by column chromatography (diethyl ether first, followed by dichloromethane). A second chromatography was made using toluene as eluent, to generate 500 mg of a red-brown solid. Yield: 58%.

$^1\text{H NMR}$ (500 MHz, CDCl_3) δ ppm: 7.67 (s, 1H), 6.36 (s, 1H), 6.31 (s, 1H), 4.36-4.19 (m, 16H), 2.59-2.52 (m, 4H), 2.74-2.64 (m, 4H), 1.56-1.19 (m, 16H), 0.96-0.77 (m, 12H).

$^{13}\text{C NMR}$ (125 MHz, CDCl_3) δ ppm: 141.34, 141.28, 137.86, 137.29, 137.09, 137.02, 136.96, 135.76, 125.61, 123.09, 109.92, 109.81, 108.43, 98.23, 97.83, 65.20, 65.11, 65.02, 64.92, 64.70.

MS (MALDI-TOF): found 2062.295, calculated for $\text{C}_{204}\text{H}_{110}\text{O}_{16}\text{S}_{14}$ 2062.3884.

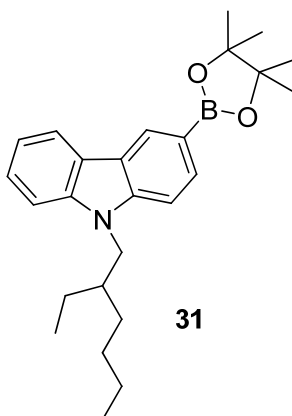
3-bromo-9-(2-ethylhexyl)carbazole (**30**)



To a solution of 3-bromocarbazole (4.5 g, 18.28 mmol) in 50 mL of acetone, KOH powder (2.05 g, 36.6 mmol), 2-ethylhexylbromide (6.5 ml, 36.6 mmol), and tetrabutylammonium hydrogen sulfate (0.3 g) as phase-transfer catalyst were added. The reaction mixture was heated to reflux for 18 h before the solvent was evaporated. The residue was poured into water and extracted with diethyl ether. The organic layer was washed with water and dried over MgSO_4 before the solvent was evaporated. The crude product was purified by column chromatography on silica gel with petroleum spirit as eluent, yielding 5.5 g of 3-bromo-9-(2-ethylhexyl)carbazole (**30**) as a colorless oil. Yield: 85%.

$^1\text{H NMR}$ (500 MHz, CDCl_3) δ ppm: 8.21 (s, 1H), 8.05 (d, 1H), 7.55-7.48 (m, 2H), 7.39 (d, 2H), 7.27-7.24 (m, 2H), 4.11 (m, 2H), 2.04 (m, 1H), 1.37-1.26 (m, 8H), 0.94-0.88 (m, 6H).

9-(2-ethylhexyl)-3-(4,4,5,5-tetramethyl[1,3,2]dioxaborolan-2-yl)-carbazole (**31**)

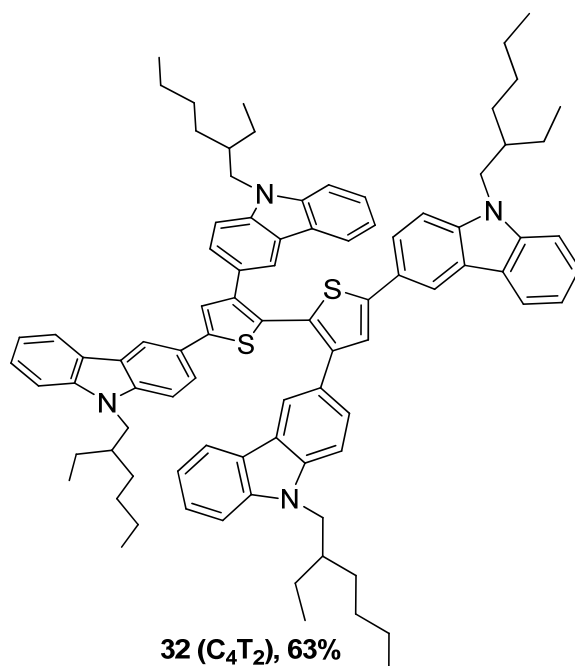


3-bromo-9-(2-ethylhexyl)carbazole (**30**) (2.7 g, 7.53 mmol) were dissolved in 100 mL of absolute THF under nitrogen. The solution was cooled to $-78\text{ }^\circ\text{C}$ before *n* BuLi (1.6 M solution in hexane, 5.65 ml, 9.04 mmol) was added dropwise. The reaction mixture was stirred for 20 min before of 2-isopropoxy-4,4,5,5-tetramethyl-1,3,2-dioxaborolane (2.06 ml, 9.8 mmol) was added. The reaction mixture was allowed to warm to room temperature and stirred for another 12 h before it was poured into ice water. The solution was extracted with diethyl ether, and the

organic phase washed with brine and dried with MgSO_4 before the solvent was evaporated. Purification was carried out by column chromatography on silica gel (hexane and 5% ethyl acetate) giving 3 g of 9-(2-Ethylhexyl)-3-(4,4,5,5-tetramethyl[1,3,2]dioxaborolan-2-yl)-carbazole (**31**). Yield: 98%.

$^1\text{H NMR}$ (500 MHz, CDCl_3) δ ppm: 8.59 (s, 1H), 8.13 (d, 1H), 7.91 (dd, $J = 8.24$, 1H), 7.47-7.43 (m, 1H), 7.38-7.37 (m, 2H), 7.25-7.22 (m, 1H), 4.18-4.15 (m, 2H), 2.07-2.04 (m, 1H), 1.39 (s, 1H), 1.36-1.20 (m, 8H), 0.90-0.88 (t, 3H), 0.86-0.83 (t, 3H).

3,3',5,5'-tetra[9-(2-ethylhexyl)carbazole]-2,2'-bithiophene (**32**)

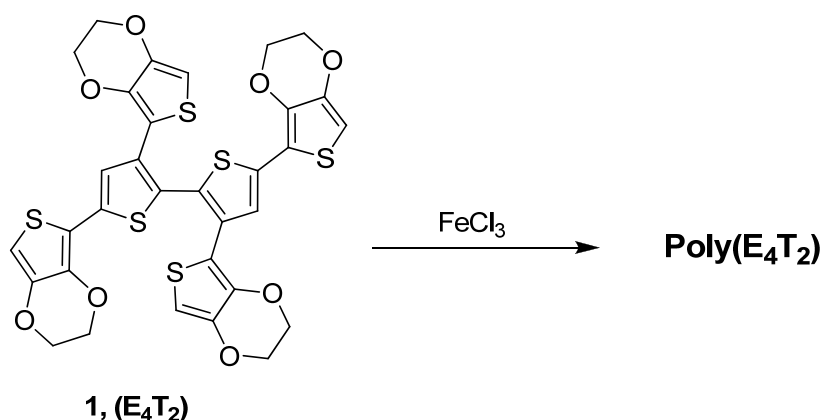


3,3',5,5'-tetrabromo-2,2'-bithiophene (228.8 mg, 0.47 mmol) were dissolved in 20 ml of tetrahydrofuran, and this solution was degassed by nitrogen bubbling. Compound **31** (1.14 g, 2.82 mmol), K_2CO_3 (276 mg, 2 mmol), $\text{Pd}(\text{PPh}_3)_4$ (150 mg, 5%) and 10 ml of water were added to the solution and the mixture was refluxed for 12 h. the solution was extracted with dichloromethane, and the organic layer was washed with water, dried over MgSO_4 and evaporated. Purification was carried out by chromatography on silica gel (petroleum spirit/diethyl ether 9/1) affording 440 mg of mixture which was further purify in chromatography using petroleum spirit first, followed by petroleum spirit with 1% of diethyl ether giving 380 mg of light green product. Yield: 63%.

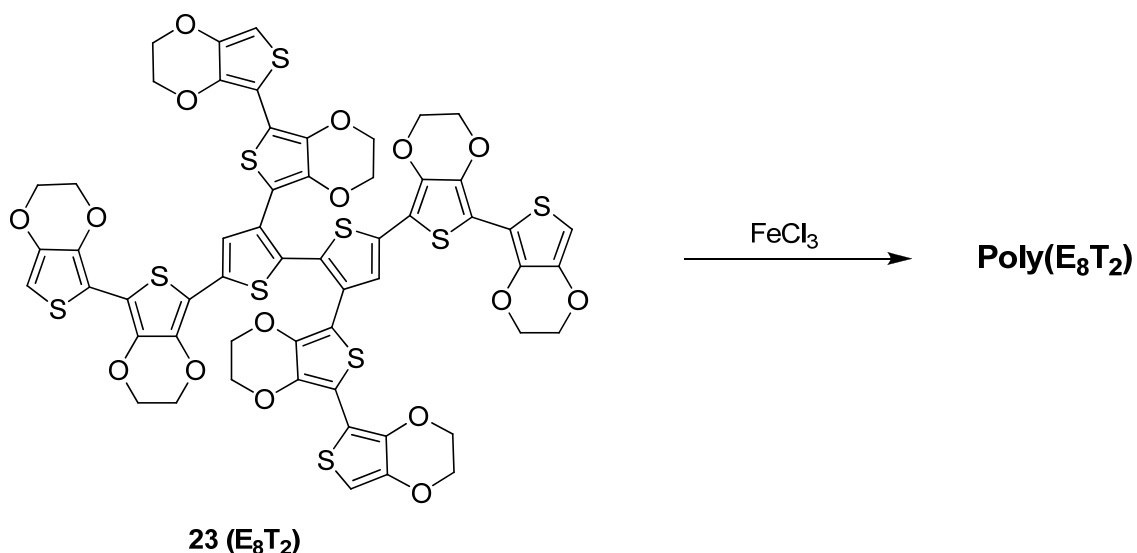
$^1\text{H NMR}$ (300 MHz, CDCl_3) δ ppm: 8.41 (s, 1H), 8.16 (d, $J = 7.72$ Hz, 1H), 7.80 (dd, $J = 8.52$, 1.44 Hz, 1H), 7.73 (d, $J = 7.65$ Hz, 1H), 7.67 (s, 1H), 7.51-7.35 (m, 7H), 7.13 (t, $J = 7.40$, 7.40 Hz, 1H), 6.96 (d, $J = 8.48$ Hz, 1H), 4.19 (d, $J = 6.84$ Hz, 2H), 3.81 (d, $J = 7.10$ Hz, 2H), 2.17-2.04 (m, 1H), 2.03-1.89 (m, 1H), 1.49-1.20 (m, 16H), 1.01-0.82 (m, 12H).

^{13}C NMR (125 MHz, CDCl_3) δ ppm: 144.76 (1C), 142.33 (1C), 141.36 (1C), 14.95 (1C), 140.55 (1C), 139.71 (1C), 128.06 (1C), 127.47 (1C), 126.34 (1C), 125.86 (1C), 125.43 (1C), 125.13 (1C), 124.91 (1C), 123.85 (1C), 123.24 (1C), 122.81 (1C), 122.76 (1C), 122.44 (1C), 120.51 (1C), 120.16 (1C), 119.96 (1C), 118.99 (1C), 118.35 (1C), 117.40 (1C), 109.26 (1C), 109.14 (1C), 108.73 (1C), 108.13 (1C), 47.54 (1C), 47.17 (1C), 39.42 (1C), 39.34 (1C), 29.70 (2C), 28.83 (2C), 24.41 (1C), 24.37 (1C), 23.08 (1C), 23.05 (1C), 14.05 (2C), 10.91 (2C).

ESI-MS⁺: found 1274.7204 $[\text{M}]^+$, 1275.7220 $[\text{M}+\text{H}]^+$ calculated for $\text{C}_{88}\text{H}_{98}\text{N}_4\text{S}_2$ 1274.7233.



To a suspension of FeCl_3 (324 mg, 2 mmol) in 10 mL of dry CHCl_3 , a solution of **E₄T₂** (364 mg, 0.5 mmol) in 10 mL of dry CHCl_3 was added dropwise under nitrogen atmosphere. The mixture was stirred at room temperature over week-end. The solution was poured over 100 ml of methanol to flocculate over night. The solid precipitated was filtered and then undoped using a 180 ml mixture of methanol/ammonia 5/1, by stirring at room temperature for 2 hours. The solid (200 mg) was further extracted with a Soxhlet using: methanol, hexane, chloroform, tetrahydrofuran and chlorobenzene. The solid is not soluble in the used solvents.

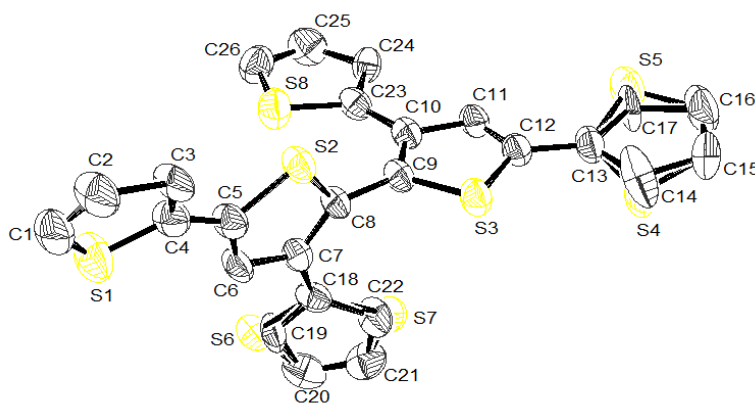


To a suspension of FeCl_3 (50.4 mg, 0.3 mmol) in 10 mL of dry CHCl_3 , a solution of **E₈T₂** (100 mg, 0.07 mmol) in 10 mL of dry CHCl_3 was added dropwise under nitrogen atmosphere. The mixture was stirred at room temperature over week-end. The solution was poured over 100 ml of methanol to flocculate over night. The solid precipitated was filtered and then undoped using a 180 ml mixture of methanol/ammonia 5/1, by stirring at room temperature for 2 hours. The solid (99 mg) was further extracted with a Soxhlet using: methanol, hexane, chloroform, and tetrahydrofuran. The solid is not soluble in the used solvents.

Annex 1

Crystal data and structure refinement for compound 10

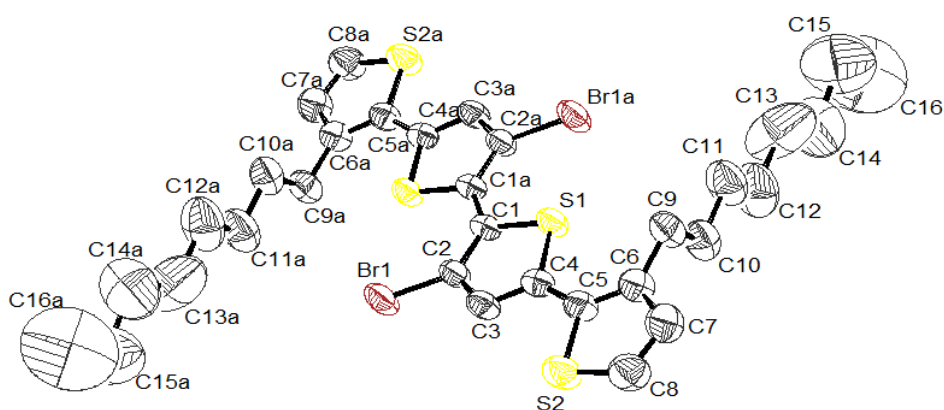
Empirical formula	C₂₄H₁₄S₆	
Formula weight	494.71	
Temperature (K)	293(2)	
Wavelength, Å	0.71073	
Crystal system	Monoclinic	
Space group	P 1 21 1	
Unit cell dimensions, Å	a = 12.010(1) b = 6.0745(4) c = 15.626(2)	$\alpha = 90^\circ$ $\beta = 104.14(1)^\circ$ $\gamma = 90^\circ$
Volume, Å ³	1105.48(18)	
Z	2	
Density (calculated) mg/m ³	1.486	
Absorption coefficient, mm ⁻¹	0.629	
F(000)	508	
Crystal size/mm	0.62 x 0.15 x 0.08	
Theta range for data collection/ (°)	1.75 to 26.04	
Index ranges	-14 ≤ h ≤ 14, -7 ≤ k ≤ 7, -19 ≤ l ≤ 19	
Reflections collected	15744 / 4289	
Independent reflections	[R(int) = 0.0745]	
Refinement method	Full-matrix least-squares on F ²	
Data/restraints/parameters	4289 / 6 / 309	
Goodness-of-method on F ²	1.022	
Final R indices [I > 2σ(I)]	R1 = 0.0462, wR2 = 0.1265	
R indices (all data)	R1 = 0.0689, wR2 = 0.1424	
Largest diff. peak and hole, eA ⁻³	0.421 and -0.434	



Annex 2

Crystal data and structure refinement for compound **18**

Empirical formula	C₃₂H₄₀Br₂S₄	
Formula weight	712.70	
Temperature (K)	293(2)	
Wavelength, Å	0.71073	
Crystal system	Triclinic	
Space group	P -1	
Unit cell dimensions, Å	a = 5.4587(6)	$\alpha = 78.74(1)^\circ$
	b = 9.321(1)	$\beta = 85.79(1)^\circ$
	c = 16.626(2)	$\gamma = 84.52(1)^\circ$
Volume, Å ³	824.6(2)	
Z	1	
Density (calculated) mg/m ³	1.435	
Absorption coefficient, mm ⁻¹	2.731	
F(000)	366	
Crystal size/mm	0.69 x 0.19 x 0.13	
Theta range for data collection/ (°)	2.24 to 25.91	
Index ranges	-6 ≤ h ≤ 6, -11 ≤ k ≤ 11, -20 ≤ l ≤ 20	
Reflections collected	9622 / 2995	
Independent reflections	[R(int) = 0.0511]	
Refinement method	Full-matrix least-squares on F ²	
Data/restraints/parameters	2995 / 3 / 173	
Goodness-of-method on F ²	0.912	
Final R indices [I > 2σ(I)]	R1 = 0.0357, wR2 = 0.0888	
R indices (all data)	R1 = 0.0563, wR2 = 0.0959	
Largest diff. peak and hole, eÅ ⁻³	0.397 and -0.378	



General conclusions

The thesis, structured in four distinct chapters, presents the contributions brought in the field of organic chemistry concerning the synthesis of some new macrocyclic derivatives, chiral tetrahalo-1,3-dienes, building blocks for solar cells and 3D monomers based on twisted bithiophene.

We have synthesized and analyzed two new series of podands which were subjected to homocoupling reactions catalyzed by copper with the obtainment of two new types of macrocyclic compounds: seven podands with cyanurate units; five podands with isocyanurate units; two cryptand closed by oxidative acetylenic dimerization; four bis-macrocycles closed by two intramolecular and one intermolecular acetylenic couplings.

The X-ray analysis of bis-macrocycle **36** possessing 1,3,5-triazine-2,4,6-trione units reveals the *trans-trans* isomer, while the dynamic NMR experiments suggest an diastereotopic equilibrium between the *cis-cis* and *trans-trans* forms.

We have performed the analysis of seven atropisomers with tetrahalo-1,3-diene core (Cl, Br, I) possessing different substituents. The enantiomers of tetrabromo- and tetraiodo-derivatives were stable enough at room temperature to be separated and to determine their rotation barriers by DHPLC experiments.

The experimental and theoretical VCD spectra of the same compounds together with theoretical calculations permitted the determination of the absolute configurations of the enantiomers. We could also conclude that the band arising from the symmetric stretching mode of the butadiene moiety in the VCD spectra has the role of a “signature band” and its sign allows the assignment of the absolute configuration.

Benzo[2,1-b:3,4-b']-dithiophene-4,5-dione was used as key unit to obtain some new building blocks for solar cells. Thus the synthesis of this dione was improved and other dithiophene blocks were obtained in order to be combined either as single monomer or as donor/acceptor alternating copolymers to produce low band gap systems.

In the last chapter the synthesis, structural analysis and electronic properties of thirteen twisted systems based on 2,2'-bithiophenic node with terminal EDOT units was presented. The monomers possessing terminal EDOTs were electropolymerized and thus electroactive 3D conjugated networks were generated.

The properties of these compounds were correlated with the size and nature of the conjugated branches. Therefore various possibilities of coupling could be formed in the case of the E_4T_2 precursors generating three types of conjugated segments: a) **TEET** which represents

the maximum conjugated segment generated by coupling the **TE** horizontal branches; b) **EE** by homo-coupling of two “vertical” **E** branches and c) **EET** by hetero-coupling between a “horizontal” and a “vertical branch. Similar considerations show that for **E₄T₄** all kind of coupling will lead to a **TEET** sequence, while for **E₈T₂** and **E₈T₆** the longest possible sequences are **TEEEET** and **TETEETET**, respectively.

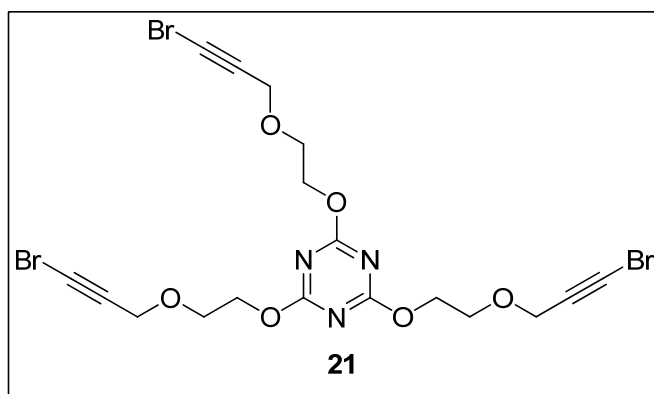
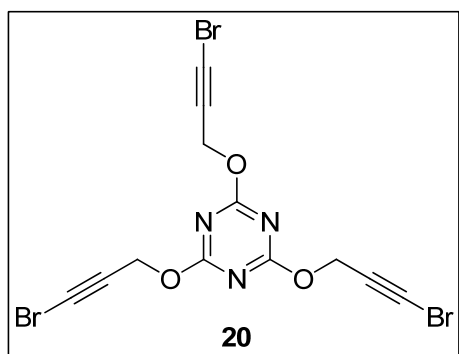
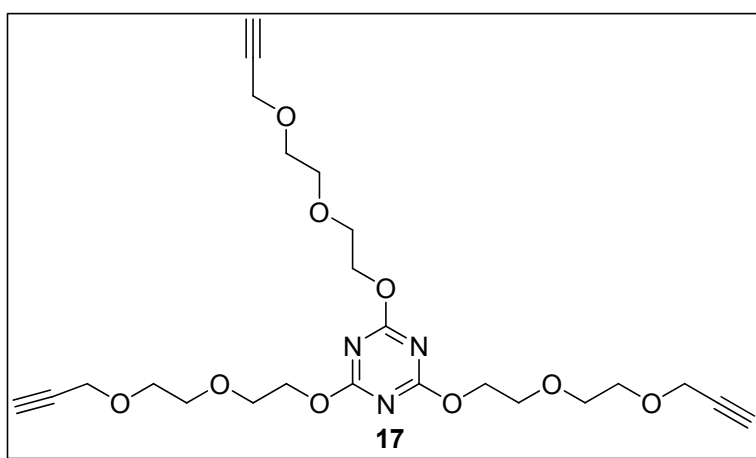
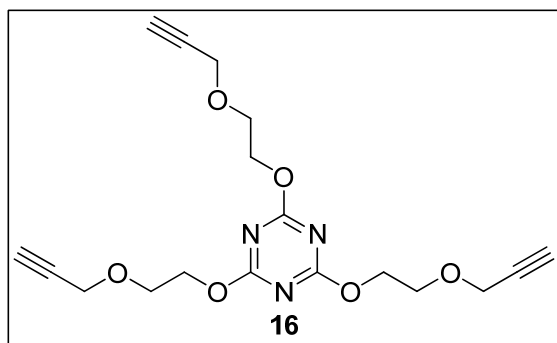
The optical properties of the polymers have been analyzed on thin film electrodeposited on ITO-coated glass electrodes. Upon application of more positive potentials (up to 1.80 V) in the case of **E₄T₂** and **E₄T₄** the two bands never merge into the single transition corresponding to the bipolaron state. This result is consistent with the fact that the longest effective conjugation length in the polymer network is too short to accommodate a bipolaron state. In the case of the larger precursors **E₈T₂** and **E₈T₆** the positive potentials produces the progressive appearance of the two transitions of the polaron state while the intensity of these bands begins to decrease for potential values above 0.60 V with an evolution towards a single bipolaronic transition.

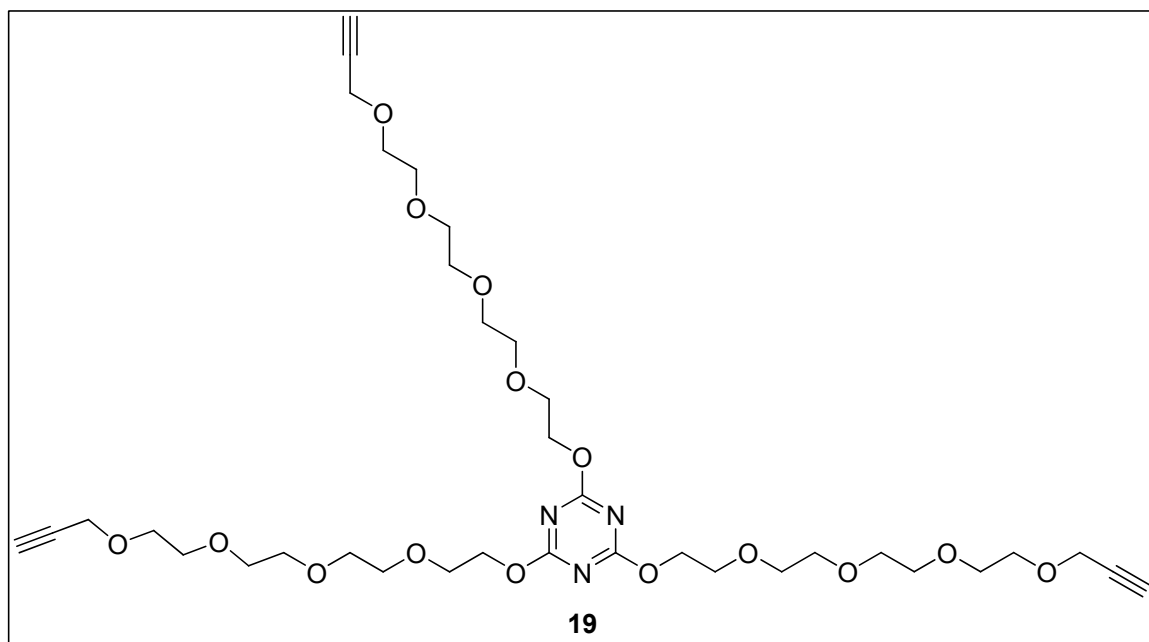
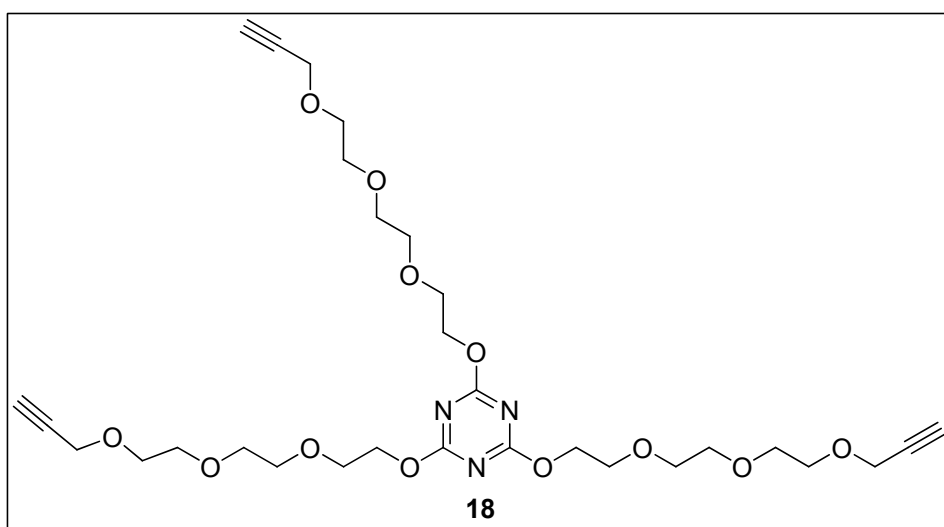
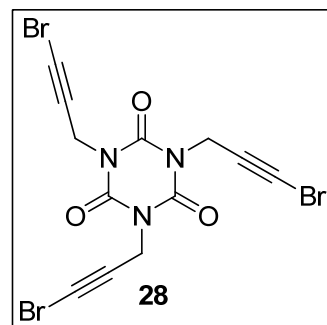
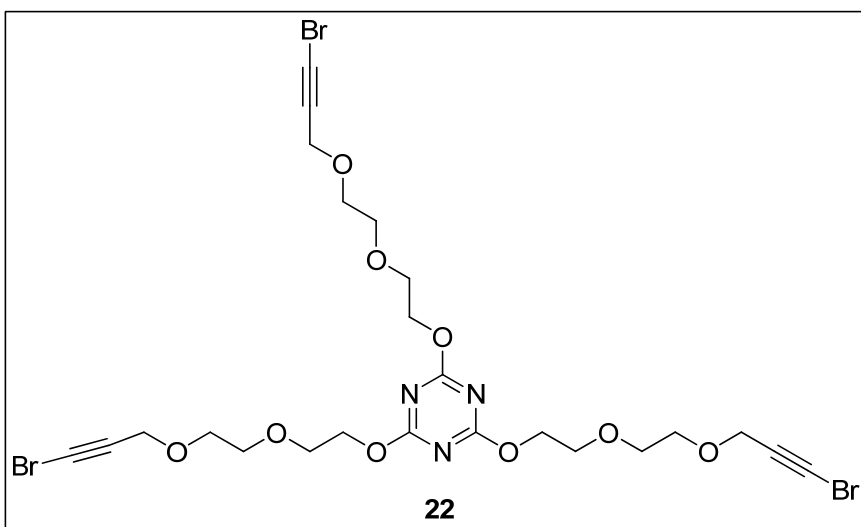
We have tried to analyse the porosity of the electrodeposited materials and first attempts to measure the active area of two of these materials by nitrogen sorption remained unsuccessful.

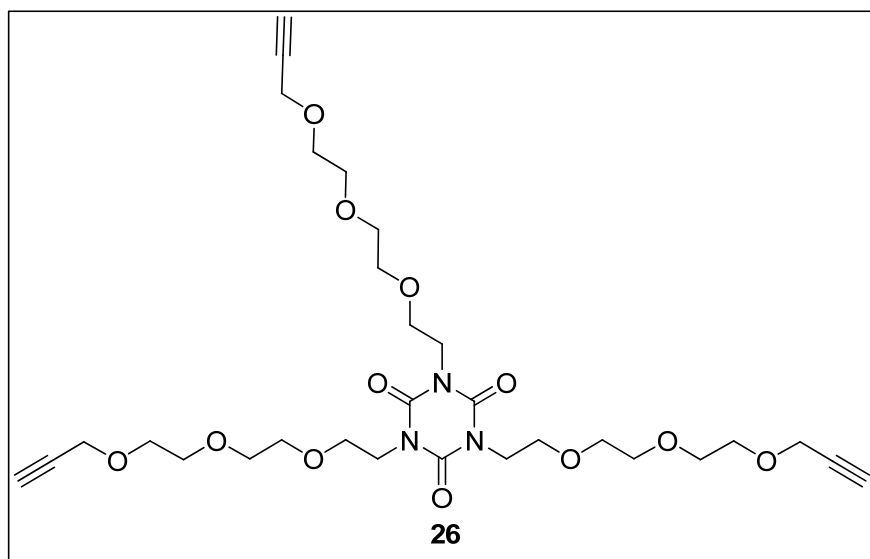
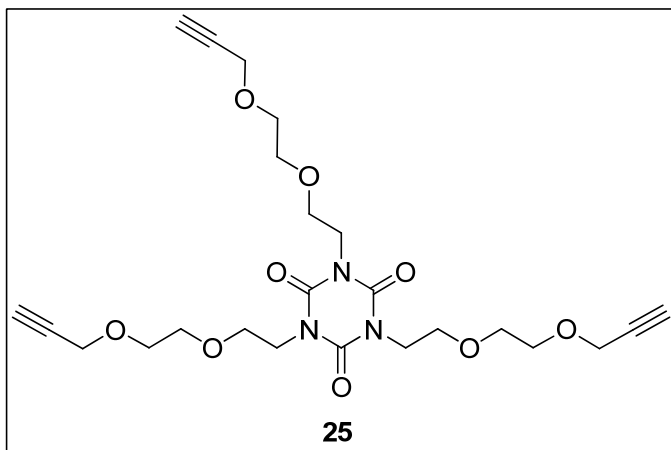
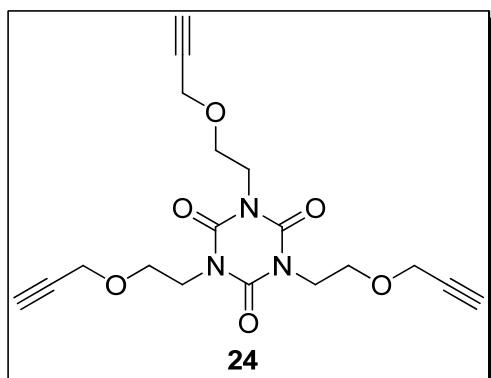
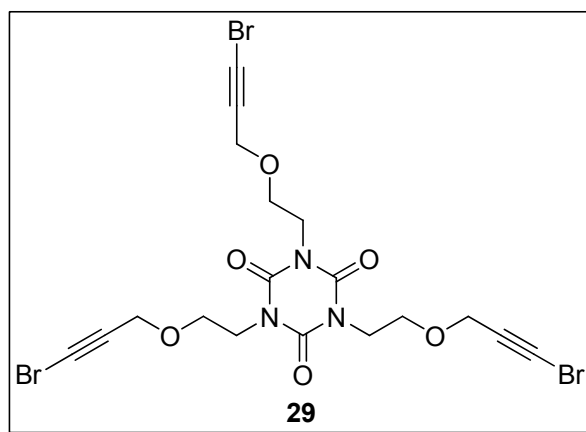
As a perspective we will focus on a more elaborate evaluation of the larger terms of the series and also on the diversification the structure of these types of precursors.

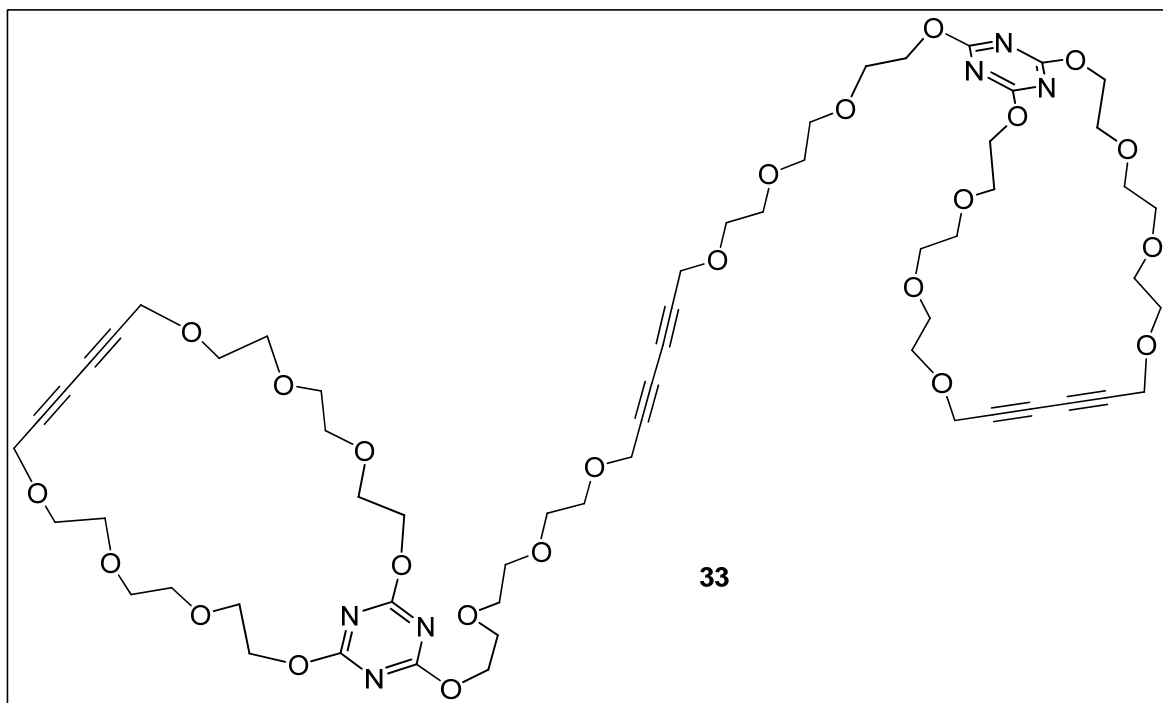
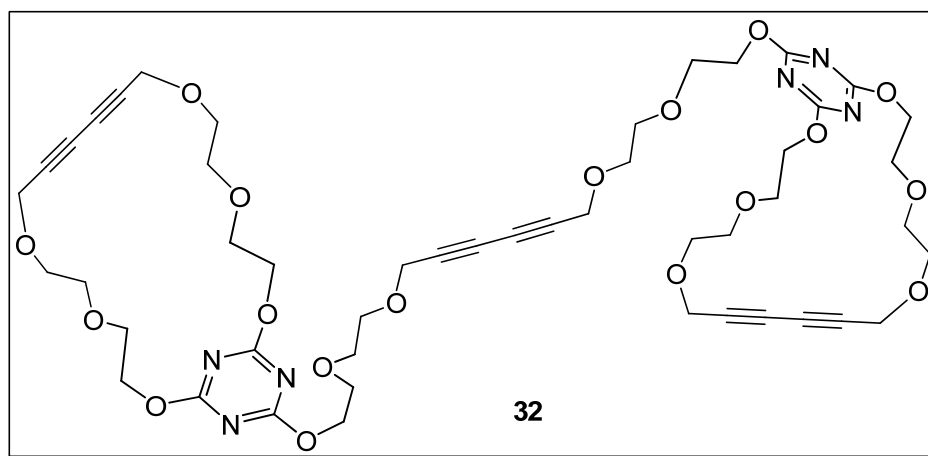
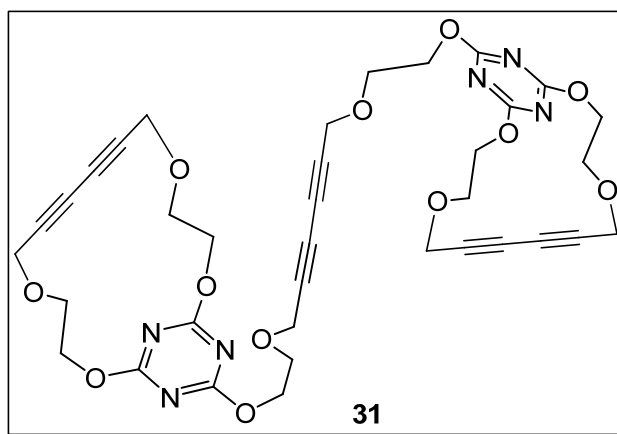
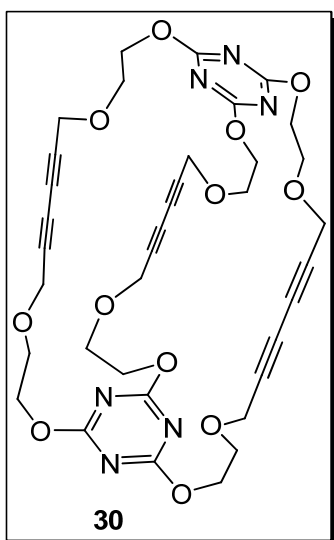
List of compounds

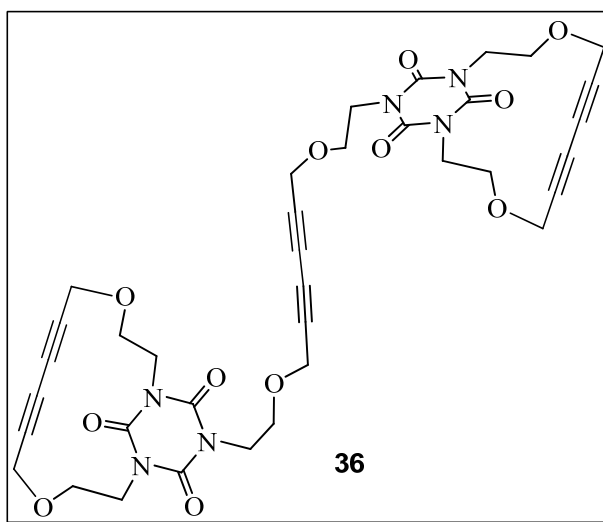
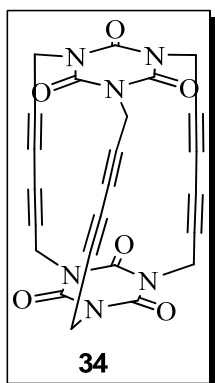
Chapter 1



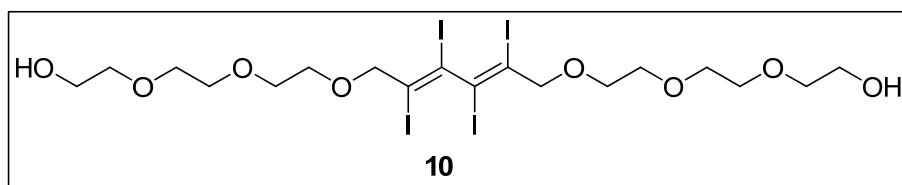
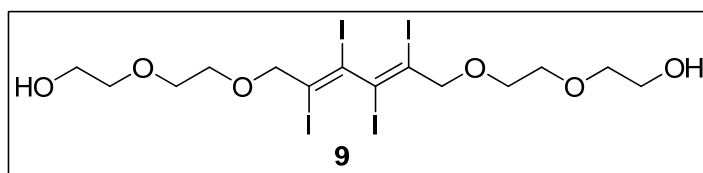
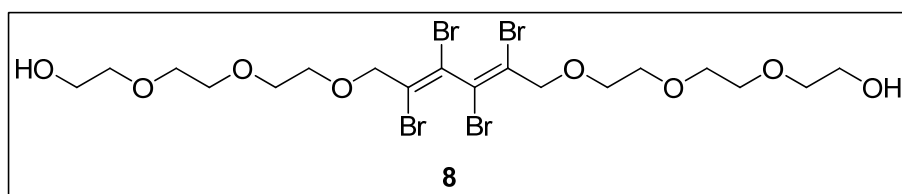
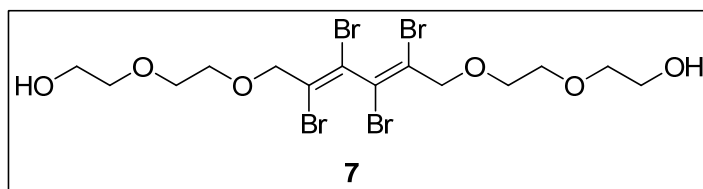
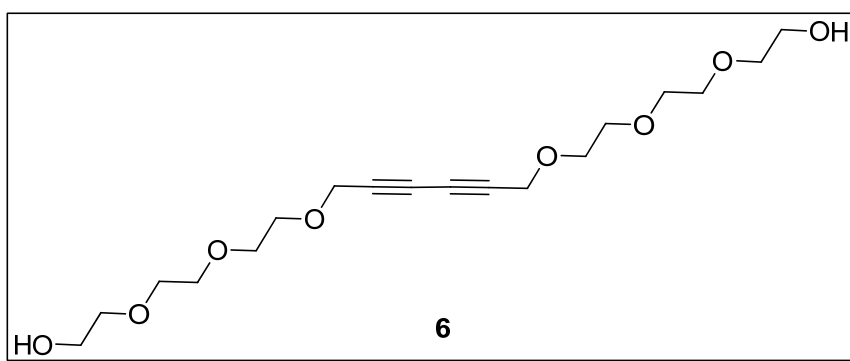
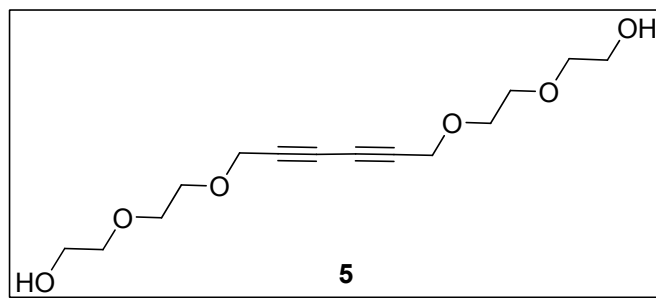
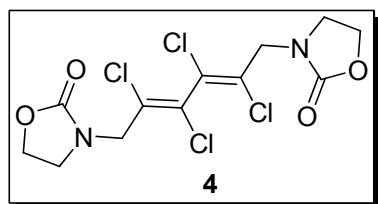
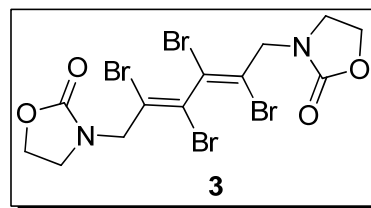
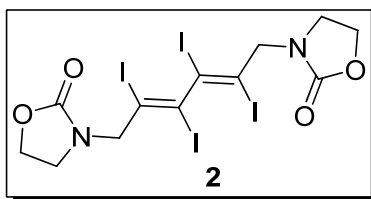
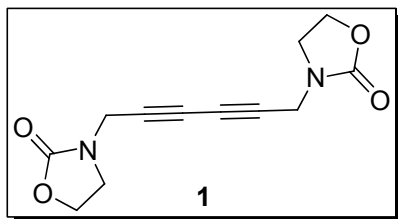




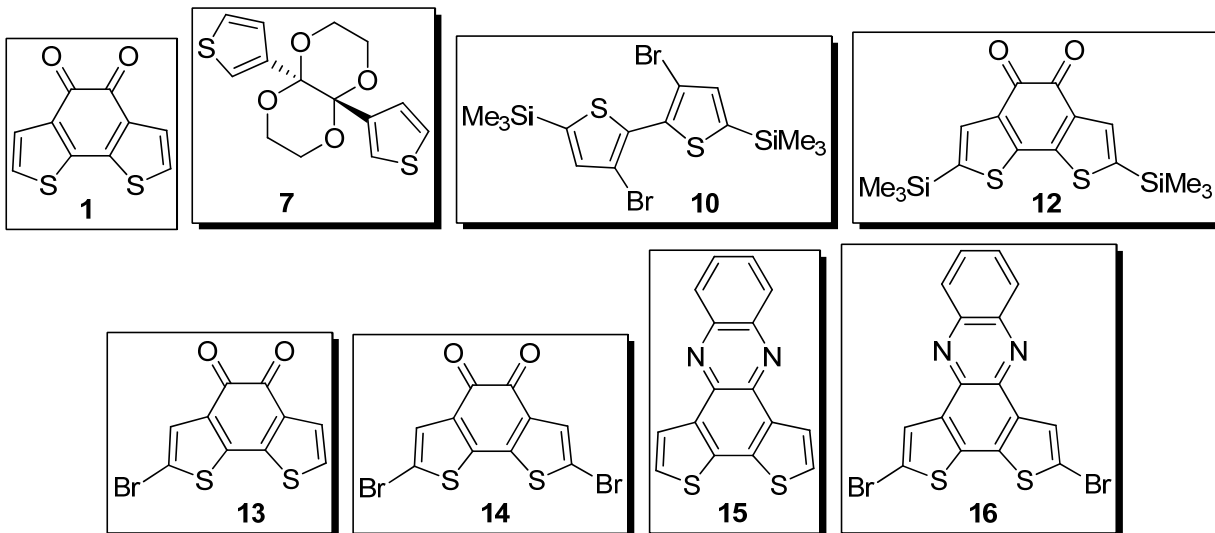




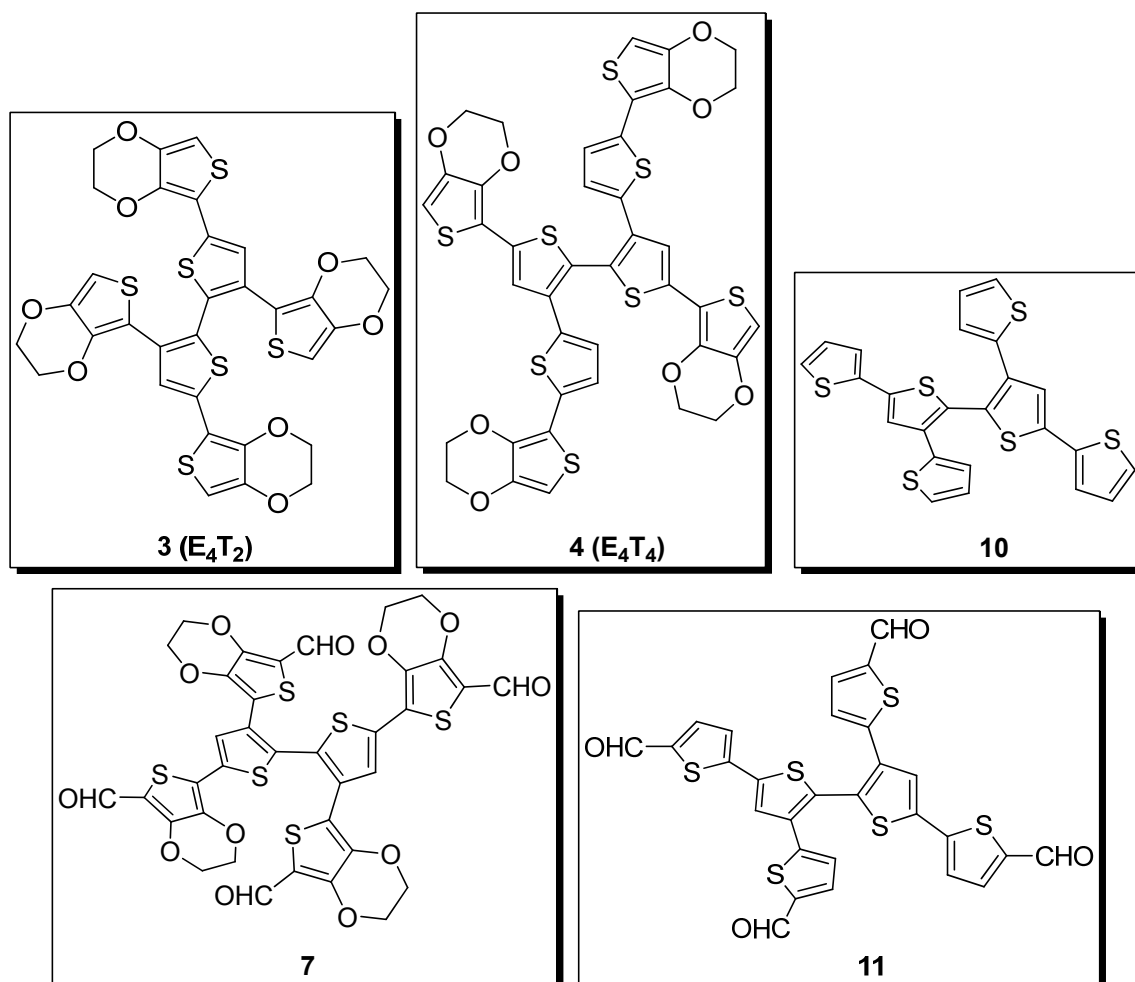
Chapter 2

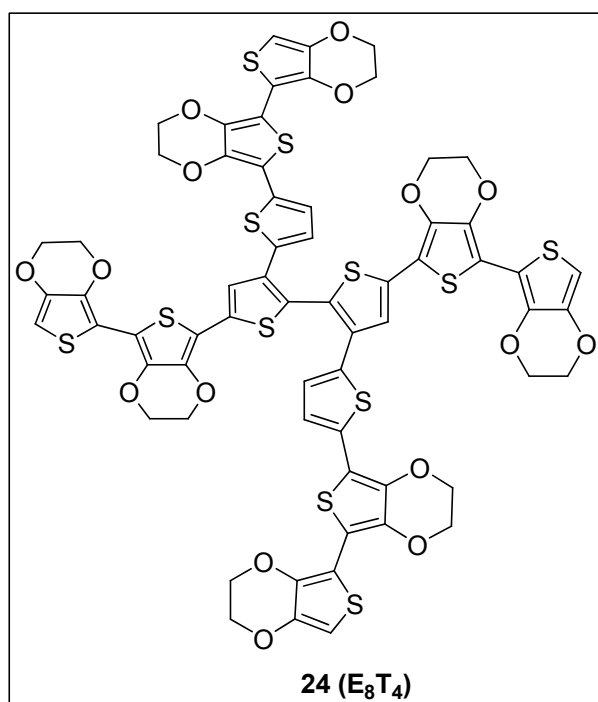
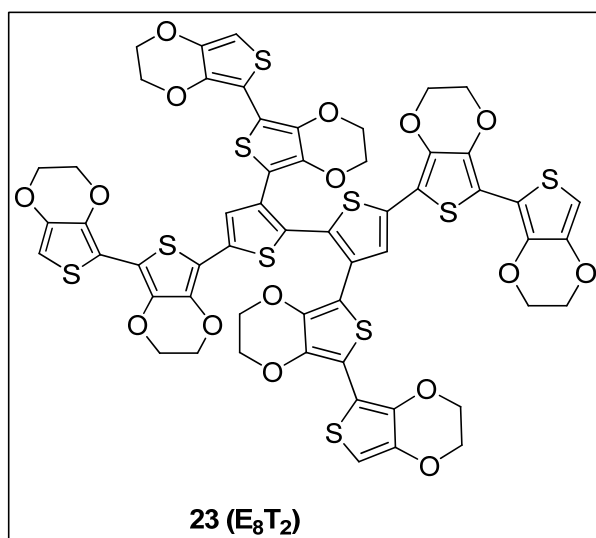
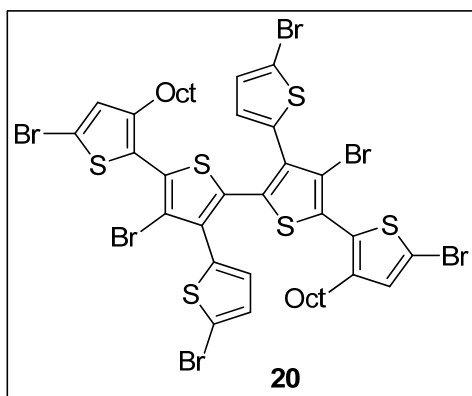
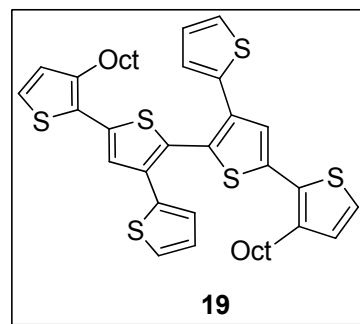
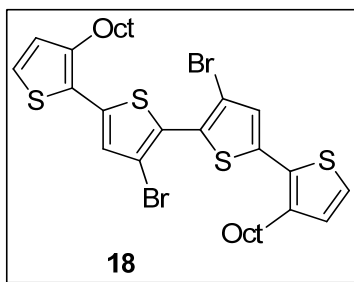
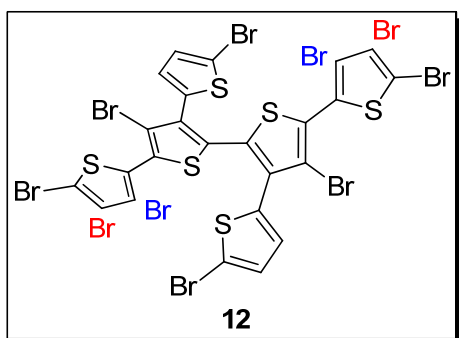


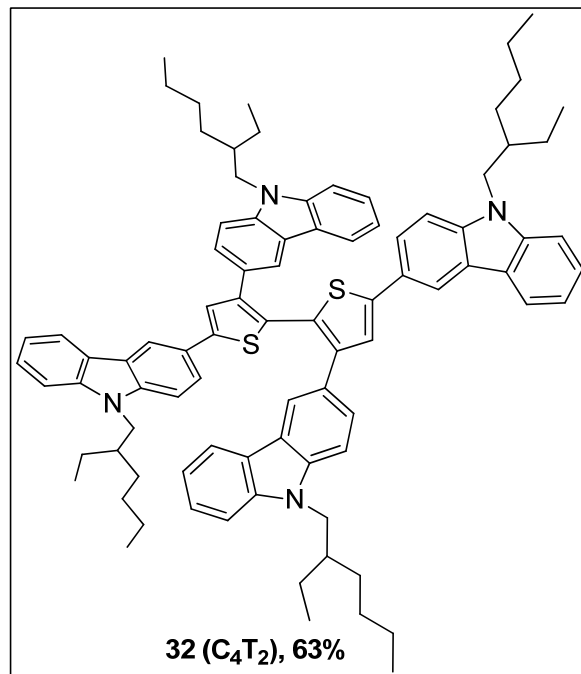
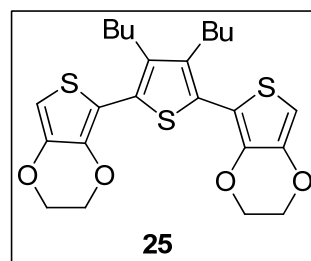
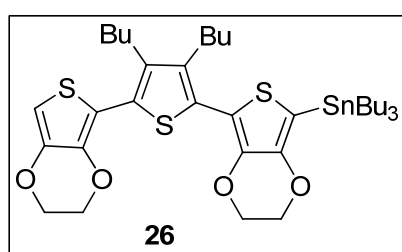
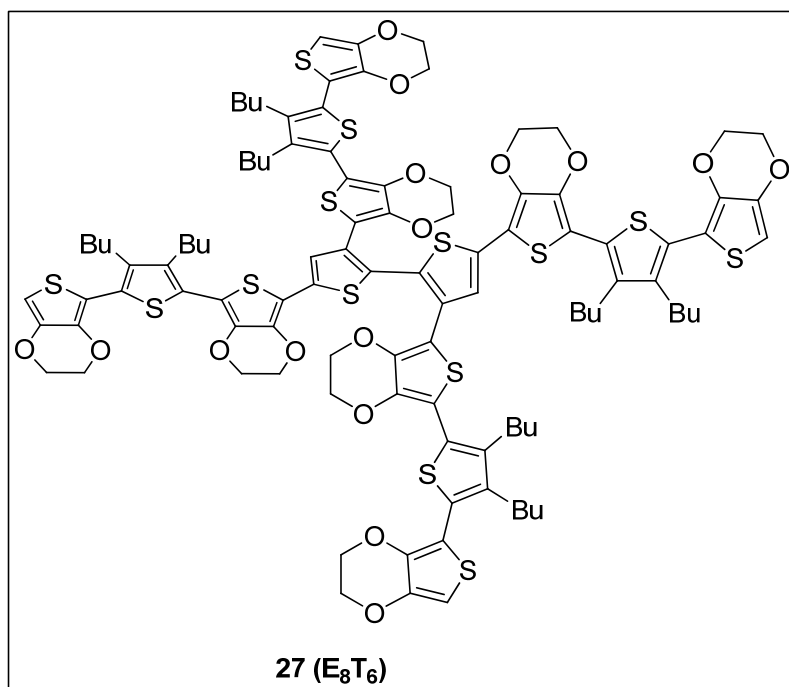
Chapter 3



Chapter 4







List of publications

1. *Electropolymerization of Three-dimensional pi-Conjugated System based on 3,4-Ethylenedioxythiophene (EDOT)*

F. Piron, P. Leriche, G. Mabon, I. Grosu, J. Roncali*

Electrochemistry Communications **2008**, *10*, 1427-1430

2. Cryptands by One-Pot Homoacetylenic Cu-Catalyzed Coupling –Synthesis, Structure and Properties

Flavia Piron, Crina Cismaș,* Anamaria Terec, Jean Roncali and Ion Grosu*

Mini-Reviews in Organic Chemistry 2008, *6(2)*, 78-85

3. *Star-shaped Triazine-thiophene pi-conjugated systems*

P. Leriche,* F. Piron, E. Ripaud, P. Frère, M. Allain, J. Roncali

Tetrahedron Letters **2009**, *50*, 5673-5676

4. *Synthesis, Structural Analysis and Chiral Investigations of Some Atropisomers with EE-Tetrahalogeno-1,3-Butadiene Core*

Flavia Piron, Nicolas Vanthuyne, Bérangeère Joulin, Jean-Valère Naubron, Crina Cismaș, Anamaria Terec, Richard Attila Varga, Christian Roussel,* Jean Roncali and Ion Grosu*

Journal of Organic Chemistry, **2009**, *74 (23)*, 9062-9070

5. *Synthesis and structural analysis of some new sterically hindered dienes*

Flavia Piron, Elena Bogdan, Crina Cismaș, Anamaria Terec, Ion Grosu*

Studia Univ. “Babes-Bolyai”, Chemia, submitted manuscript

Abstract:

Thesis entitled “*New Functional Architectures for Molecular Recognition, Low Band Gap Conjugated Systems and Advanced Electrode Material*” is structured in four chapters dealing with new a) supramolecular structures such as cryptands and bis-macrocycles; b) chiral sterically hindered tetrahalo-1,3-dienes; c) blocks for the synthesis of low band gap conjugated polymers and d) 3D conjugated architectures based on twisted bithiophene with terminal EDOTs.

In the first chapter two new series of tripodal macrocycle precursors possessing C_3 symmetry built up from 1,3,5-triazine with reactive functional groups at the ends of the pendant arms are presented. Supramolecular structures obtained by Cu-catalyzed acetylenic coupling reactions are also reported. Cryptands were closed by intermolecular dimerization and bis-macrocycles were formed by intramolecular couplings followed by intermolecular dimerization.

The second chapter deals with the investigations of some new atropisomers with *E,E*-tetrahalo-1,3-butadiene core including separation of the enantiomers, determination of their rotation barriers and absolute configuration.

The third chapter includes the synthesis of benzo[2,1-*b*:3,4-*b'*]-dithiophene-4,5-dione based blocks used for low band gap conjugated polymers as active materials for organic solar cells.

In the last chapter synthesis and electronic properties of various new types of 3D conjugated architectures based upon twisted bithiophene with terminal EDOTs are reported in view of the electrochemical generation of electroactive microporous conjugated networks. The different size, surface areas and electronic properties depend on the block used for the construction of lateral branches.

Key words: cryptand, bis-macrocycle, atropenantiomers, low band gap blocks, twisted bithiophene, electroactive networks.

Resumé:

La thèse intitulée « *New Functional Architectures for Molecular Recognition, Low Band Gap Conjugated Systems and Advanced Electrode Material* » est structurée en quatre chapitres traitant de a) structures supramoléculaires tels que cryptands et bis-macrocycles; b) tetrahalo-1,3-diènes chiraux stériquement encombrés; c) blocs pour la synthèse de polymères faible gap conjugués d) architectures 3D conjugués à base de bithiophènes portant des EDOTs terminaux.

Dans le premier chapitre, on présente deux nouvelles séries de précurseurs macrocycliques *tripodaux* possédant une symétrie C_3 construites à partir de 1,3,5-triazine avec des groupes fonctionnels réactifs aux extrémités des bras. Les structures supramoléculaires obtenues par des réactions de couplage acétylénique catalysées par Cu sont également présentées. Les cryptands ont été fermés par dimérisation intermoléculaire et les bis-macrocycles ont été formés par des couplages intramoléculaires suivis par dimérisation intermoléculaire.

Le deuxième chapitre présente l'étude de nouveaux atropisomères à base d'*EE*-tetrahalo-1,3-butadiène y compris la séparation des énantiomères, la détermination des barrières de rotation et des configurations absolues.

Le troisième chapitre a été consacré à la synthèse des blocs à base de benzo [2,1-*b*:3,4-*b'*]-dithiophène-4,5-dione utilisés pour obtenir des polymères conjugués à faible gap pouvant fonctionner comme matériau actif dans des cellules solaires organiques.

Dans le dernier chapitre on décrit la synthèse et les propriétés électroniques de différents types de nouvelles architectures 3D conjuguées à base de bithiophène comportant des unités EDOTs terminales, en vue de la génération électrochimique de réseaux microporeux électroactifs conjugués. Il est montré que la taille, la surface active et les propriétés électroniques dépendent de la nature des blocs utilisés pour la construction des bras latéraux.

Mots clés: cryptand, bis-macrocycle, atropenantiomère, bande interdite, oligothiophènes 3D, réseaux électroactifs.



Electropolymerization of three-dimensional π -conjugated system based on 3,4-ethylenedioxythiophene (EDOT)

Flavia Piron^{a,b}, Philippe Leriche^a, Gilles Mabon^a, Ion Grosu^b, Jean Roncali^{a,*}

^a University of Angers, CNRS, CIMA, Group Linear Conjugated Systems, 2 Bd Lavoisier F-49045, Angers, France

^b Organic Chemistry Department and CCOCCAN, "Babes-Bolyai" University, 11 Arany Janos Street, 400028, Cluj-Napoca, Romania, France

ARTICLE INFO

Article history:

Received 20 June 2008

Received in revised form 2 July 2008

Accepted 8 July 2008

Available online 16 July 2008

Keywords:

Electropolymerization

Polythiophenes

Conjugated network

3D-conjugated network

Nanoporous materials

ABSTRACT

A 3D π -conjugated system obtained by grafting 3,4-ethylenedioxythiophene (EDOT) on a twisted bithiophene core has been synthesized and used as precursor for electropolymerization. Preliminary investigations of its electrochemical properties shows that it can be straightforwardly electropolymerized into an electroactive conjugated material.

© 2008 Elsevier B.V. All rights reserved.

1. Introduction

Electrogenerated functional poly(thiophenes) (PTs) possessing specific electrochemical properties have been a focus of sustained interest for more than two decades [1,2]. These materials have been developed for a large variety of applications including energy storage, electrocatalysis or electrochemical or bioelectrochemical sensors [1,2].

For all of these applications, the active area of the electroactive material is a crucial parameter as it determines important factors such as the charge storage capacity, the rate of charge/discharge processes in energy storage systems or the contacting area between the analyte and the electroactive sensing surface for sensors. The development of electrodes exhibiting a high surface-to-volume ratio implies the design and synthesis of new materials combining high nano- or mesoscopic porosity and electroactivity.

Until now, the vast majority of electrogenerated functional conducting polymers have been synthesized by electropolymerization of a precursor, generally a monomer or a short-chain oligomer, derivatized with functional groups endowed with specific properties such as hydrophilicity, molecular recognition, catalysis etc. [1–3]. We have shown already that the use of precursor containing multiple polymerizable groups leads to electrode materi-

als with improved stability due to the crosslinking of the polymer chains [1]. However, examples of precursors able to create a 3D conjugated network by connecting electropolymerizable groups attached at the periphery of a 3D structure remain scarce [1–4].

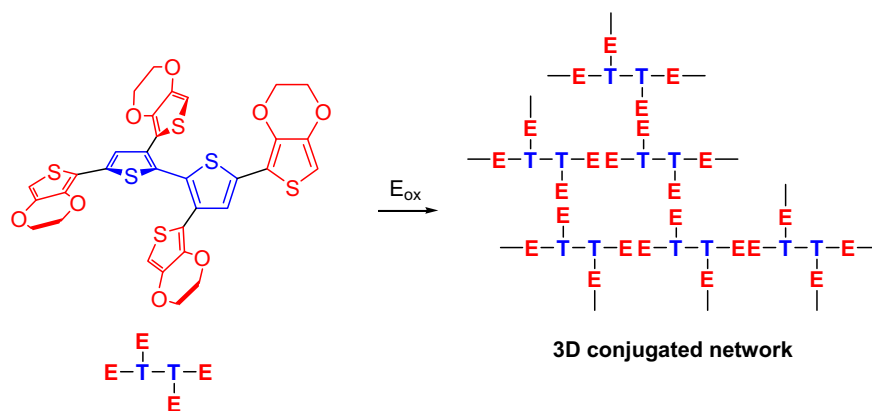
We have initially reported the electropolymerization of tetrahedral structures involving four terthiophenes branches attached onto a silicon atom [4a]. Although clear evidences for electropolymerization were obtained, the relatively labile thiophene-silicon bond can represent an obstacle for the development of this approach. Recently, we have shown that bithiophenic structures twisted by means of steric interactions constitute interesting starting nodes to construct 3D π -conjugated architectures that can be used as donor material in organic solar cells [5].

On the basis of these results, we now report a first example of electropolymerizable 3D conjugated structure designed according to the same principles. To this end, four EDOT groups have been attached at the relevant positions of a bithiophenic structure in order to generate a 3D basic unit (E_4T_2 , Scheme 1) which combines the 3D structure of the twisted bithiophene core with the high polymerizability of EDOT [6]. It was anticipated that electropolymerization of this type of precursor can produce an electroactive 3D π -conjugated network (Scheme 1).

We describe here the synthesis of the E_4T_2 precursor as well as preliminary results on its electropolymerization behaviour and on the electronic properties of the resulting electrogenerated electroactive material.

* Corresponding author. Fax: +33 2 41 735405.

E-mail address: Jean.roncali@univ-angers.fr (J. Roncali).



Scheme 1. Generation of a 3D conjugated network by electropolymerization of a pseudo-tetrahedral precursor.

2. Experimental

Electrochemical experiments were performed with a EG&G 273 potentiostat in a standard three-electrode cell using platinum electrodes and a saturated calomel reference electrode (SCE). The solutions were degassed by argon bubbling and experiments were carried under an argon blanket. The working electrode was a 2 mm diameter Pt disk sealed in glass. Tetrabutylammonium hexafluorophosphate (Fluka puriss) was used as received.

E₄T₂: 3,3',5,5'-tetrabromo-2,2'-bithiophene (0.964 g, 2 mmol), 2-(tributylstannyl)-3,4-(ethylenedioxy)thiophene (6.899 g, 16 mmol), and Pd(PPh₃)₄ as catalyst (0.924 g, 0.8 mmol, 5%) were mixed in 100 mL of dry degassed toluene and refluxed for 8 h under nitrogen. A second portion of catalyst (1%) was added and the mixture was refluxed for another 24 h period. The mixture was washed with water, extracted with toluene, filtered over Celite and dried under vacuum. The residue was purified by column chromatography (diethyl ether) to generate 1.0 g of a yellow-orange solid. Yield: 69%, mp 215 °C. ¹H NMR (500 MHz, CDCl₃): δ (ppm) 7.58 (s, 2H), 6.24 (s, 2H), 6.13 (s, 2H), 4.32–4.33 (m, 4H), 4.23–4.25 (m, 4H), 4.17–4.18 (m, 4H), 4.14–4.15 (m, 4H). ¹³C NMR (125 MHz, CDCl₃): δ (ppm) 114.78, 140.97, 137.95, 137.78, 135.55, 133.10, 126.23, 122.39, 112.29, 111.94, 99.13, 97.20, 64.98, 64.63, 64.57, 64.39. MS (MALDI): found 725.95, calculated for C₃₂H₂₂O₈S₆ 725.964.

3. Results and discussion

The UV–Vis absorption spectrum of **E₄T₂** recorded in methylene chloride solution shows an absorption maximum at 310 nm and a shoulder at 370 nm (Fig. 1). These two maxima are consistent with the expected presence of two different conjugation lengths in the twisted structure. Compared to the absorption maximum of EDOT-thiophene-thiophene-EDOT oligomer (ETTE) which corresponds to the main conjugated segment in **E₄T₂** ($\lambda_{max} = 424$ nm), [7] these data reveal a considerable hypsochromic shift, in agreement with the large torsion angle in the middle of the conjugated chain. Indeed crystallographic data of the parent system containing only thiophene units have evidenced a dihedral angle of 90° between the two inner thiophene rings [5].

On the basis of this result and taking into account the fact that the steric hindrance of EDOT is at least equal to that of thiophene, it seems reasonable to assume that in **E₄T₂**, the two inner thiophene rings also form a dihedral angle close to 90°, an hypothesis consistent with the presence of two maxima in the UV–Vis spectrum and with the result of a cursory geometry optimization.

The electrochemical properties of **E₄T₂** have been analyzed in acetonitrile in the presence of 0.10 M tetrabutylammonium hexafluorophosphate as supporting electrolyte. Application of a single potential scan to a millimolar solution shows an irreversible anodic peak at a potential E_{pa} of 0.85 V which can be ascribed to the oxidation of the peripheral EDOT groups in conjugation with the bithiophene core. In fact, examination of the structure shows that **E₄T₂** contains two crossing ETTE segments in which two EDOT units are connected through the α - α' or β - β' -positions of the bithiophene core.

As already reported, a linear ETTE system shows an oxidation potential at 0.57 V vs. Ag/AgCl [7]. On this basis, the higher E_{pa} value found for **E₄T₂** is consistent with a restricted effective conjugation length in the two kinds of ETTE systems due to the distortion imposed to the structure by steric interactions.

Fig. 2 shows the cyclic voltammograms (CV) resulting from the application of recurrent potential scans to a 10 mmol solution of **E₄T₂**. The positive potential limit (0.80 V) was set at the foot of the oxidation wave of the precursor. Application of repetitive potential scans leads to the progressive development of a broad redox system in the 0.30 to 0.80 V region corresponding to the electrodeposition of an electroactive material on the electrode surface. In spite of the sterically twisted structure of **E₄T₂** electropolymerization proceeds straightforwardly. This result thus confirms that the α -position of the peripheral EDOT units are highly reactive and lead to efficient coupling. Similar activation effects have been

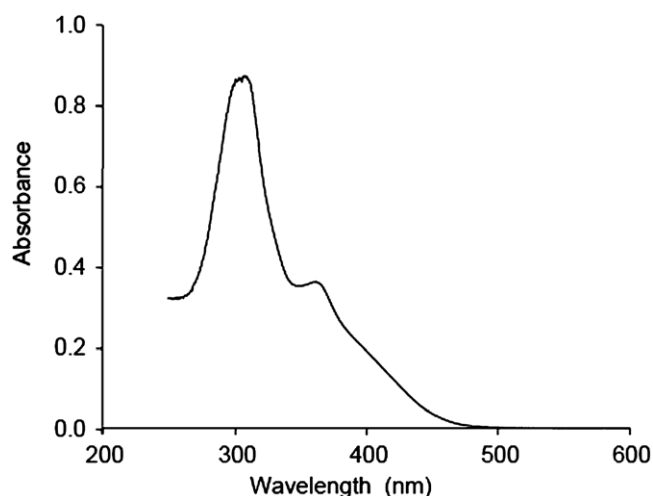


Fig. 1. UV–Vis absorption spectrum of **E₄T₂** in methylene chloride.

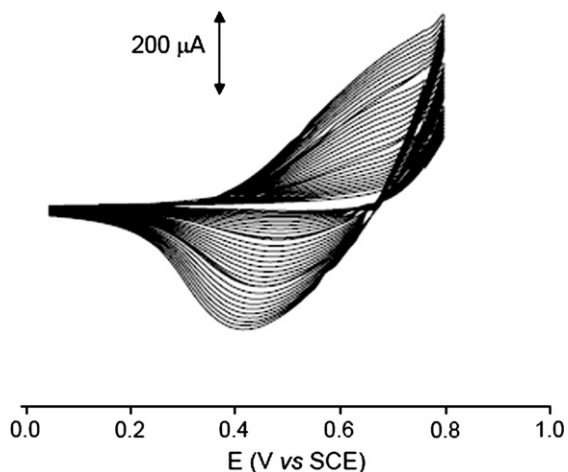


Fig. 2. Potentiodynamic electropolymerization of E_4T_2 , 10 mM in 0.10 M $Bu_4NPF_6/MeCN$, scan rate 100 mV s^{-1} .

observed when electron-donating methoxy or sulfide groups are present at the external β -positions of oligothiophenes [8].

E_4T_2 was also electropolymerized in potentiostatic conditions at an applied potential of 0.95 V vs. SCE. Poly(EDOT) films were deposited at an applied potential of 1.32 V for comparison. Examination of the ratio of the charge reversibly exchanged upon redox cycling of the polymers (Q_r) to the electrodeposition charge (Q_d) shows that Q_r/Q_d is ca four to five times larger for E_4T_2 than for poly(EDOT), in agreement with the expected larger amount of electroactive material produced with a given Q_d for poly(E_4T_2).

The CV of poly(E_4T_2) shows a reversible broad oxidation wave with an anodic current peak (E_{pa}) at 0.65 V (Fig. 3). The current peak scales linearly with scan rate, as expected for a surface-confined reaction.

Electropolymerization of E_4T_2 is expected to produce a 3D conjugated network in which the EDOT groups of the precursor connect to form different types of conjugated TEET segments (Scheme 1) containing $\alpha-\alpha'$ and $\alpha-\beta'$ linked thiophene and EDOT units. These different modes of coupling and the distortions imposed to the conjugated chains by steric interactions determine different effective conjugation lengths. Based on these considerations, a E_{pa} value of poly(E_4T_2) at 0.65 V agrees well with expectations when one considers the oxidation potential of the planar

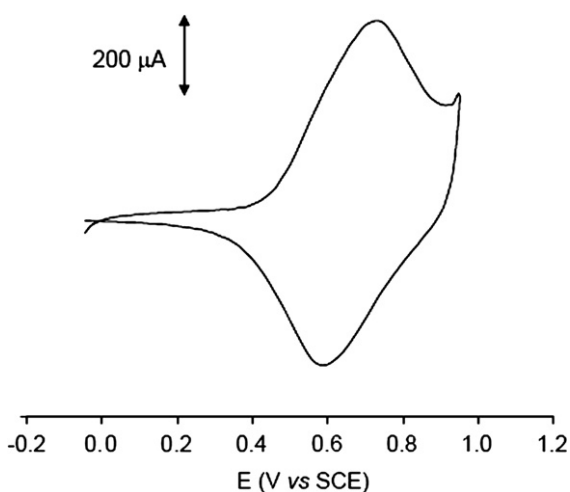


Fig. 3. Cyclic voltammogram of poly(E_4T_2) in 0.10 M $Bu_4NPF_6/MeCN$, scan rate 100 mV s^{-1} , deposition charge 33 mC cm^{-2} .

structures representing the two extreme limiting situations namely TEET (0.48 V) [7] and di-EDOT (0.84 V) [10].

In order to confirm that all EDOT groups are effectively involved in the electropolymerization process, a film of poly(E_4T_2) has been subjected to continuous redox cycling with application of a progressively increasing positive potential limit. As shown by previous work, when a polymer film contains unreacted precursor, application such a procedure produces to major changes in the shape of the CV with a negative shift of E_{pa} and an increase of the conductivity of the material due to the coupling of the unreacted precursor molecules trapped in the film [9]. The fact that this procedure does not produce any change in the CV of poly(E_4T_2) until the potential reaches a value where the polymer begins to degrade (1.20–1.30 V), is a clear indication that all EDOT groups have been oxidized and coupled.

The optical properties of poly(E_4T_2) have been analyzed by spectroelectrochemistry on thin films electrodeposited on ITO-coated glass electrodes. Fig. 4 shows the UV–Vis–NIR spectra recorded at various values of the applied potential.

The spectrum of the fully undoped polymer shows a λ_{max} at 480 nm with an absorption onset at 600 nm corresponding to a band gap of $\sim 2.10\text{ eV}$. The small width of the absorption band is consistent with the expected relatively narrow distribution of conjugated segments (see Scheme 1). Application of increasingly positive potentials produces the bleaching of the visible absorption band together with the concomitant development of two broad absorption bands with maxima around 600 and 1300 nm corresponding to the two transitions associated with the polaronic state of the polymer. The neutral polymer appears red and turns gradually blue upon oxidation. Interestingly, upon application of more positive potentials (up to 1.80 V) these two bands never merge into the single transition corresponding to the bipolaron state. This result is consistent with an average effective conjugation length in the polymer network too short to accommodate a bipolaron state. This results thus provides a further support to the formation of discrete conjugated segments with effective conjugation length determined by the mode of connection and the twist angles between monomer units in the 3D polymeric network.

To summarize a 3D π -conjugated system involving four EDOT units attached on a twisted bithiophene core has been synthesized and used as precursor for electropolymerization. The electrochemical and optical properties of the resulting polymer are consistent with the formation of an electroactive conjugated network containing discrete and relatively well defined conjugated segments.

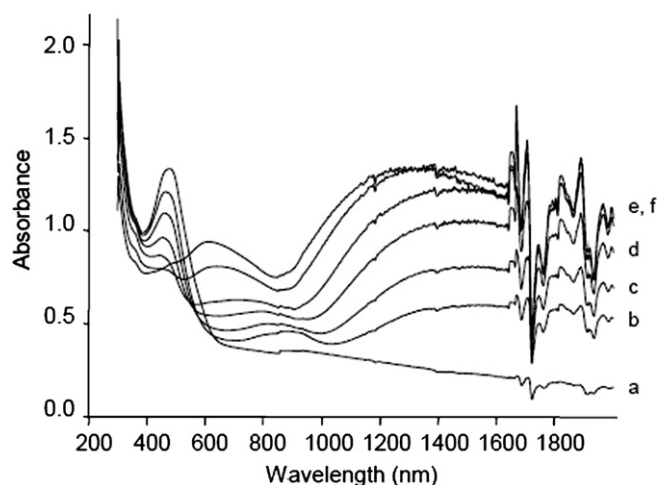


Fig. 4. Spectroelectrochemistry of poly(E_4T_2) on ITO at various applied potentials. (a) -0.20 V , (b) 0.3 V , (c) 0.4 V , (d) 0.5 V , (e) 0.6 V , (f) 0.7 V , and (g) 0.8 V .

Based on the straightforward electropolymerization of this precursor, these preliminary results open interesting perspectives for the development of electrogenerated nanoporous electroactive materials with potential applications in energy storage, sensors or catalysis.

Work aiming at the design and synthesis of other members of this new class of electrode materials is now underway and will be reported in future publications.

References

- [1] J. Roncali, *J. Mater. Chem.* 9 (1999) 1875.
- [2] D.T. McQuade, A.E. Pullen, T.M. Swager, *Chem. Rev.* 100 (2000) 2537.
- [3] A. Deronzier, J.C. Moutet, *Coord. Chem. Rev.* 147 (1996) 339.
- [4] (a) J. Roncali, C. Thobie-Gautier, H. Brisset, J.F. Favard, A. Guy, *J. Electroanal. Chem.* 381 (1995) 257;
(b) R.M. Sebastian, A.M. Caminade, J.P. Majoral, L. Huchet, E. Levillain, J. Roncali, *Chem. Commun.* (2000) 507;
(c) J.H. Bauer, P. Espindola, P. Sonar, J. Heinze, K. Müllen, *Angew. Chem. Int. Ed.* 44 (2005) 2447.
- [5] S. Karpe, A. Cravino, P. Frère, M. Allain, G. Mabon, J. Roncali, *Adv. Funct. Mater.* 17 (2007) 1163.
- [6] (a) J. Roncali, P. Blanchard, P. Frère, *J. Mater. Chem.* 15 (2005) 1589;
(b) S. Kirchmeyer, K. Reuter, *J. Mater. Chem.* 15 (2005) 2077.
- [7] M. Turbiez, P. Frère, M. Allain, C. Videlot, J. Ackerman, J. Roncali, *Chem. Eur. J.* 11 (2005) 3742.
- [8] A. Smie, A. Synowczyk, J. Heinze, R. Alle, P. Tschuncky, G. Götz, P. Bäuerle, *J. Electroanal. Chem.* 452 (1998) 87.
- [9] (a) G. Zotti, G. Schiavon, *Synth. Met.* 39 (1990) 39. 183;
(b) J. Roncali, A. Gorgues, M. Jubault, *Chem. Mater.* 5 (1993) 1456.
- [10] S. Akoudad, J. Roncali, *Synth. Met.* 93 (1998) 111.

Volume 6, Number 2, May 2009

ISSN: 1570-193X

Mini-Reviews in Organic Chemistry

TIB/UB Hannover



ZL 3122
2009/6/2

Impact Factor: 0.6



**BENTHAM
SCIENCE
PUBLISHERS LTD.**

Cryptands by One-Pot Homoacetylenic Cu-Catalyzed Coupling – Synthesis, Structure and Properties

Flavia Piron,^{a,b} Crina Cismaș,^{a*} Anamaria Terec,^a Jean Roncali,^b and Ion Grosu^{a*}

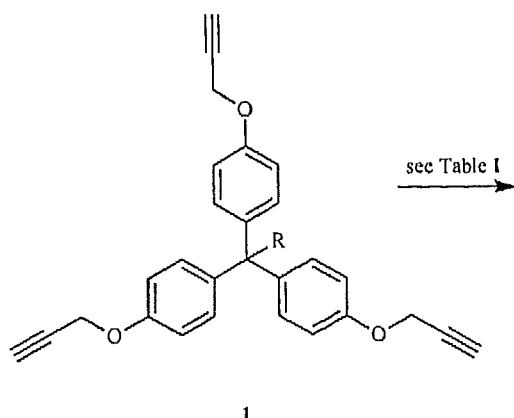
^aOrganic Chemistry Department and CCOCCAN, Babes-Bolyai University, Cluj-Napoca, 11 Arany Janos Str., 400028, Cluj-Napoca, Romania

^bUniversity of Angers, CNRS, CIMA, Group Linear Conjugated Systems, 2 Bd Lavoisier, 49045, Angers, France

Abstract: This review presents the synthesis of macrobicyclic compounds built from triphenylmethane, triphenylphosphine oxide units and other three-dimensional molecules with an aromatic core, as well as some fullerene precursors and buta-1,3-diyne diyl spacers. The dependence of the coupling yield on the solvent, catalysts (Cu⁺ and/or Cu²⁺) and presence of oxygen is also addressed. The formation of inclusion complexes of these cage molecules with appropriately sized neutral guests such as solvent molecules (acetonitrile, benzene, dichloromethane, chloroform), cubane, benzyl cyanide and structural information of the host derivatives are also reviewed.

1. INTRODUCTION

The synthesis of three-dimensional cage-like molecules is of continuous interest in the field of supramolecular chemistry [1]. Among them, molecules with a well-defined cavity are particularly appealing for their potential binding properties [2]. We became interested to obtain such macrocyclic derivatives, starting from pre-organized half-cages with terminal triple bonds, by a one-pot three-fold oxidative homoacetylenic coupling and therefore it was considered of interest to review them.



Scheme 1. Synthesis of derivatives 2 – 4.

2. GENERAL REMARKS ON CU-CATALYZED ACETYLENIC COUPLING

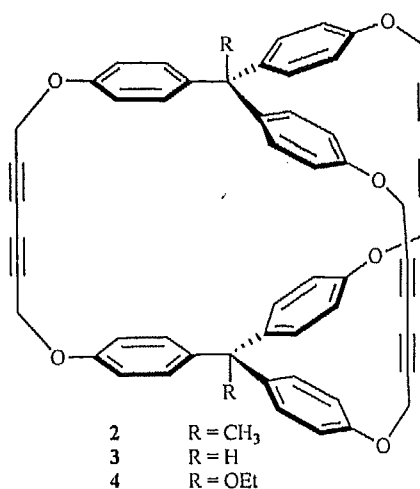
Acetylenic homocoupling represents an interesting tool for molecular construction and has been extensively used and diversified since Glaser's discovery of oxidative coupling of copper alkynylbenzene [3]. The most important and successful modifications of the initial Glaser coupling technique were reported by Eglinton [4] (the Eglinton-Galbraith method: excess Cu(OAc)₂ in pyridine, 20–40 % yield) and Hay [5] [the Glaser-Hay coupling: CuCl, *N,N,N',N'*-tetramethylethylenediamine (TMEDA), solvent, up to 97 % yield]. Despite the wide range of applications of alkyne coupling [6], from natural products to pharmaceuticals and macrocyclic de-

rivatives [7], the mechanism of this reaction has not yet been elucidated. In the present review, we are summarizing the modified coupling procedures that have been used to afford cage compounds by one-pot cyclization reactions.

3. CRYPTANDS WITH AROMATIC UNITS

a. Triphenylmethane Units

The formation of three-dimensional macrobicyclic receptors with triphenylmethane units containing three buta-1,3-diyne diyl



spacers, by a one-pot triple-coupling reaction of two tris-ethynyl substituted half cages, has been first reported by Breslow and co-workers [8]. They have obtained the 1,1,1-triphenylethane derivative 2 by performing the triple oxidative dimerization in *dry oxygen-free pyridine* in the presence of both anhydrous Cu(I) and Cu(II) salts (Scheme 1, Table 1). Despite their report on complete failure when employing standard coupling conditions [Cu(II)-pyridine or Cu(I)-TMEDA-O₂], Voegtle and co-workers have later obtained compound 2 in similar yields, by using Cu(OAc)₂ in pyridine or acetonitrile [9].

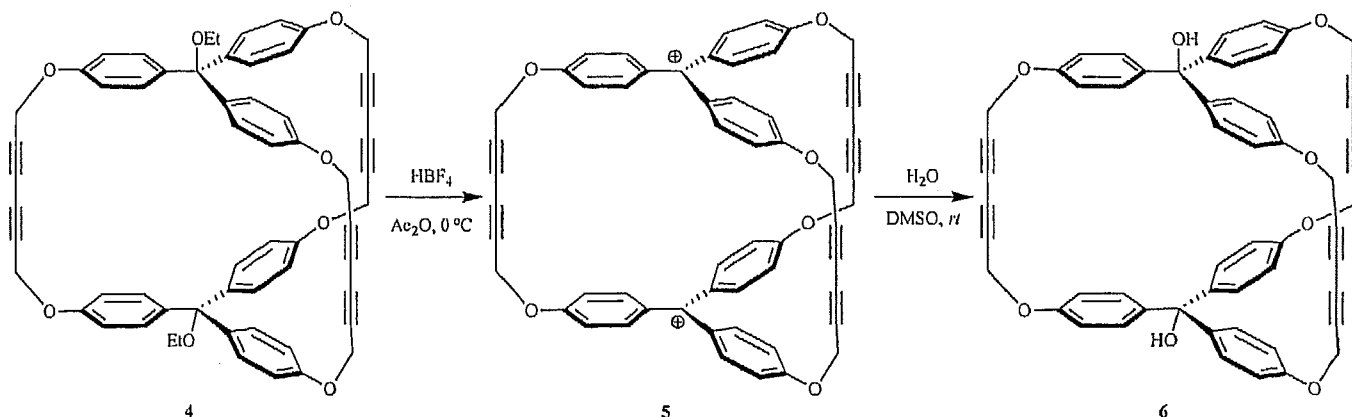
Breslow's macrocyclization reaction was also employed for the synthesis of macrobicyclic compound 3 [10] in 35 % yields (Scheme 1, Table 1). The dimeric cage molecule 3 has also been synthesized following Eglinton coupling procedure with copper(II) acetate monohydrate in pyridine or acetonitrile [10b].

Voegtle and co-workers have reported on the first synthesis of a new type of concave dyestuff [11] bearing a relatively large cavity

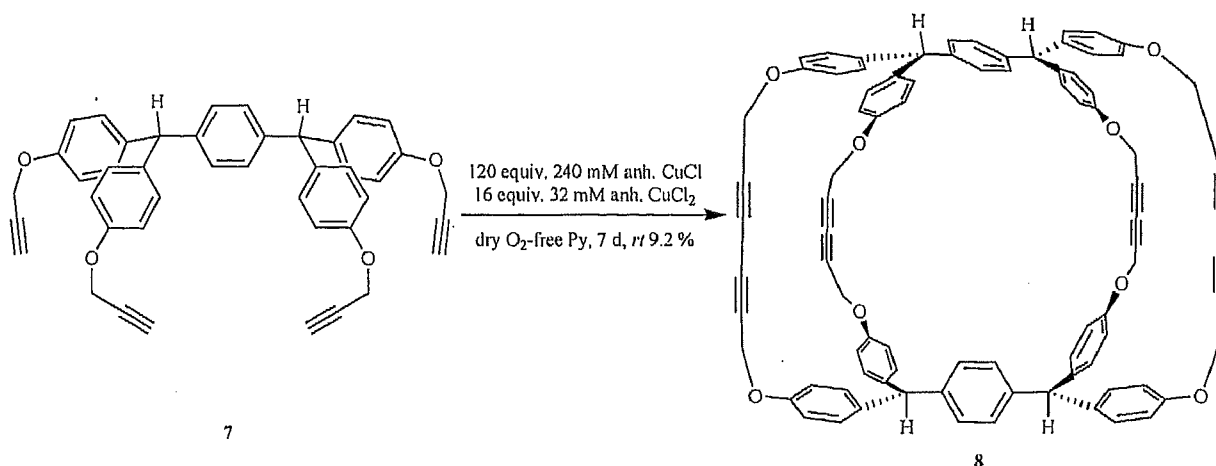
*Address correspondence to these authors at the Organic Chemistry Department and CCOCCAN, Babes-Bolyai University, Cluj-Napoca, 11 Arany Janos Str., 400028, Cluj-Napoca, Romania; Tel: 0040264593833; Fax: 0040264590818; E-mail: igrosu@chem.ubbcluj.ro; crinacismas@yahoo.com

Table 1. Reaction Conditions for Cu-catalyzed Acetylenic Coupling for the Formation of Derivatives 2 – 4

Compd.	Reaction Conditions	Yield (%)	Ref.
2	100 equiv. 100 mM anh. CuCl/ 12.2 equiv. 12.2 mM anh. CuCl ₂ , dry O ₂ -free Py, 48 h, 0 °C	35	[8]
	Cu(OAc) ₂ in Py or AcCN	17-21	[9]
3	100 equiv. 200 mM anh. CuCl/ 12 equiv. 24 mM anh. CuCl ₂ , dry O ₂ -free Py, 7 d, rt	35	[10]
4	10 equiv. 112 mM Cu(OAc) ₂ in AcCN, 1 h, 60 °C	32	[11]



Scheme 2. Synthesis of derivatives 5 and 6.



Scheme 3. Synthesis of derivative 8.

formed from two tritylium cation units (5, Scheme 2). The precursor is the diethoxy protected derivative 4, obtained by oxidative cyclodimerization with Cu(II) in acetonitrile. The use of acetonitrile instead of pyridine had led to a considerable yield improvement, from 18 % to 32 %, probably due to a template effect of the first.

An interesting example is compound 8 (Scheme 3), an analogue of derivative 3, with a larger cavity formed by triphenylmethane units. Performing the four-fold oxidative Cu(I)/Cu(II)-catalyzed acetylenic coupling, a significant decrease in yield was observed when compared to the three-fold bridging (3) (9.2 % vs. 35 %).

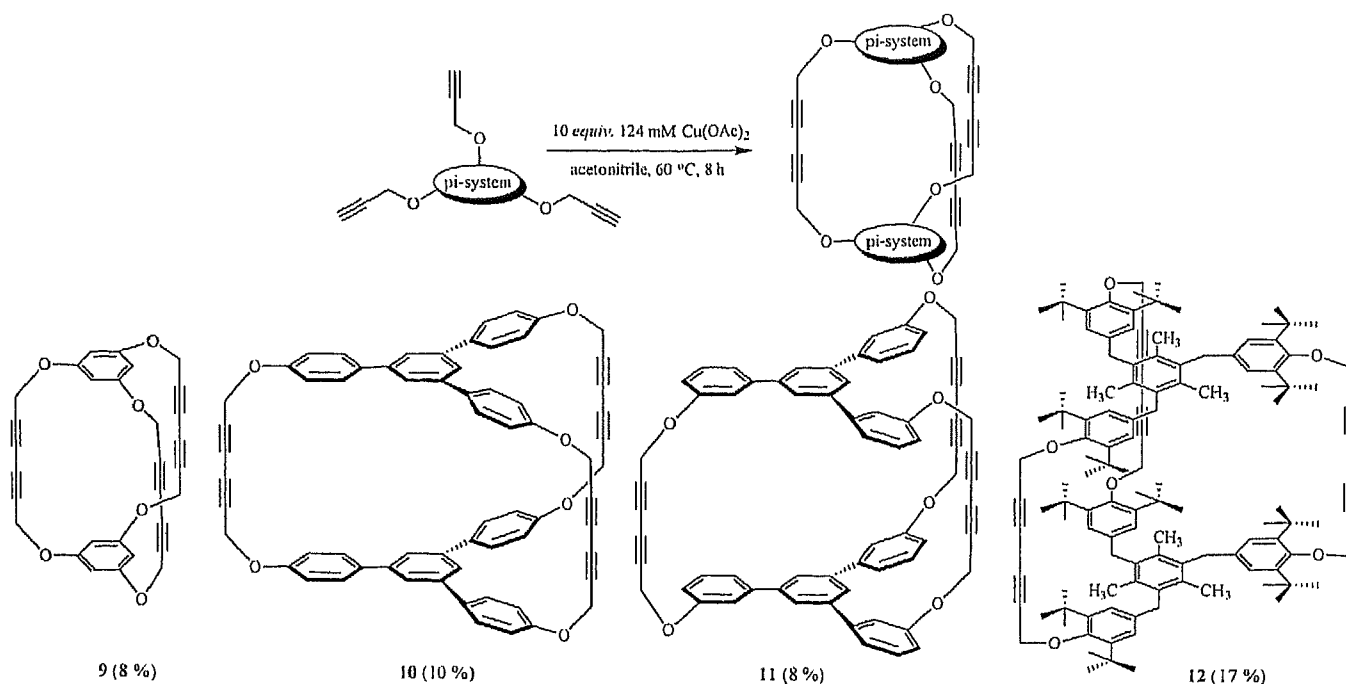
b. Other Aromatic Units

An example of a smaller macrobicyclic cavity for the inclusion of acetonitrile was described by the same authors [12]. Derivative 9 (Scheme 4) was synthesized in 8 % yields using Cu(OAc)₂·H₂O in pyridine under air. The larger cage compounds 10 – 12 were ob-

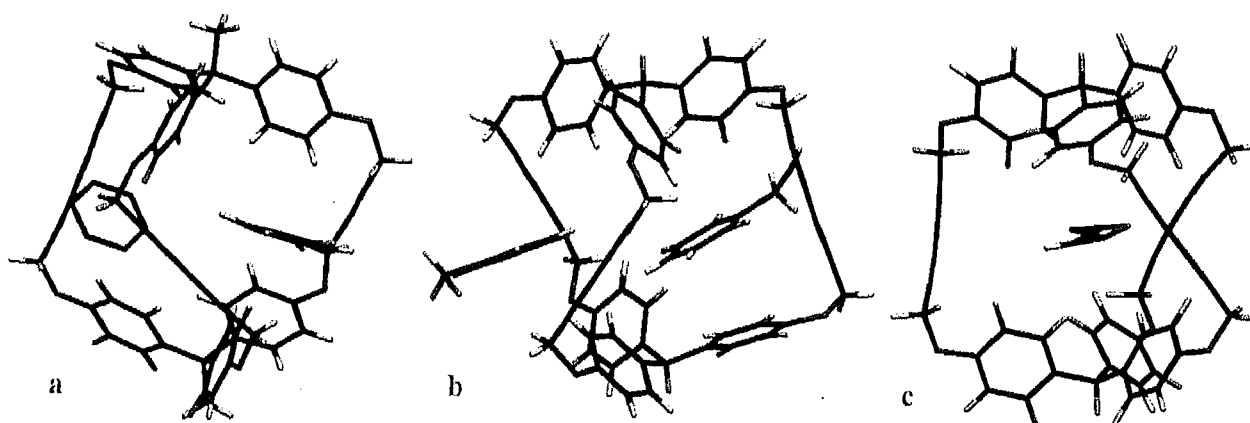
tained in low yields by performing the mild, modified Eglinton acetylenic coupling in acetonitrile [13].

Structure and Properties. The multiple hexa-2,4-diyne bridges in combination with the above described aromatic units are forming cavities able to include neutral organic guests, mainly solvent molecules. The conjugated alkyne units do not show interactions for the inclusion process with the guest molecules.

The macrobicyclic 3 was crystallized from acetonitrile as a 1:1 adduct and from phenylacetonitrile as a 1:3 adduct (Fig. 1). A comparison with the complex of 2 with benzene (2x5C₆H₆) shows that hosts 2 and 3 have similar torsion angles along their *pseudo* C₃ axis (26 – 36°) and similar cavity sizes (Fig. 1). These guests are not located in the center of the cavity and it was assumed that flat aromatic compounds are not sterically suitable for a spherical shaped host. This assumption has been proved later by the single-crystal X-ray structure of the inclusion complex of 2 with acetone



Scheme 4. Synthesis of derivatives 9 – 12.

Fig. (1). X-ray structures for inclusion complexes: a. 2x5 C₆H₆, b. 3x3BnCN and c. 3xMeCN.

(Fig. 2a). Acetone was located in the center of the cavity and held by multiple σ - π interactions between the methyl groups of the guest and the aromatic rings of the host.

Further evidence of the importance of topological complementarities between the shape of the host and the bonded guest has been provided by the inclusion complex of DMSO in the cavity of compound 6 (Scheme 2). The guest molecule is situated, as acetone in 2, in the middle of the cavity (Fig. 2b).

The geometry of the complex formed by the smaller host 9 with acetonitrile turned out to be completely different from 3 with respect to the orientation of acetonitrile (Fig. 3). The host phenylene rings in 3xMeCN (Fig. 1c) interact with the nitrile group, while in 9xMeCN there is an interaction between the methyl group of acetonitrile and the host phenyl rings. The two aromatic rings approach each other to 7.12 Å and a torsion angle along its *pseudo* C₃ axis of 13° was measured.

The larger host 10 did not show any endocavitary complexation with flat aromatic guests, possibly because the distance between the aromatic units (8.09 Å) is far from the ideal distance for the inclusion of aromatic guests by π - π interactions (6.84 Å) [14].

Cram and co-workers [15] have reported the synthesis of chiral [1.1.1]orthocyclophane carcerand 14 by oxidative Eglinton coupling of acetylene 13 (Scheme 5). They performed the most detailed study published so far on the employed conditions and concluded that *anaerobic conditions, even with excess Cu(II) salt gave no desired product*, while increasing the reaction temperature to 85 °C led to the formation of traces of intramolecularly coupled product 15.

Structure and Properties. The configurations of the two diastereoisomers have been assigned by single crystal X-ray structure determinations. The crystal structure of (\pm)-14 (from CH₂Cl₂) shows a compact structure with an almost spherical cavity and D₃ symmetry (Fig. 4a). In contrast, *meso*-14 presents a larger cavity with an approximately ellipsoidal shape (Fig. 4b).

In order to assess the complexation properties of the diastereoisomeric carcerands 14, ¹H NMR studies in hexachloroacetone were performed. The results demonstrated that (\pm)-14 is strongly binding small neutral organic molecules with complementary shape and appropriate size. The association constants for complexing CHCl₃,

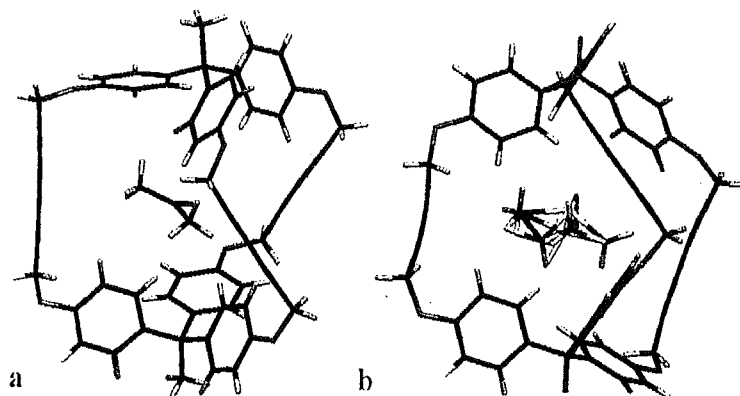


Fig. (2). X-ray structures for inclusion complexes: a. 2xacetone and b. 6xDMSO.

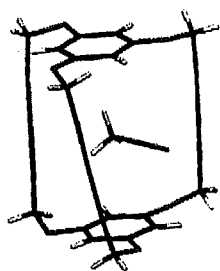
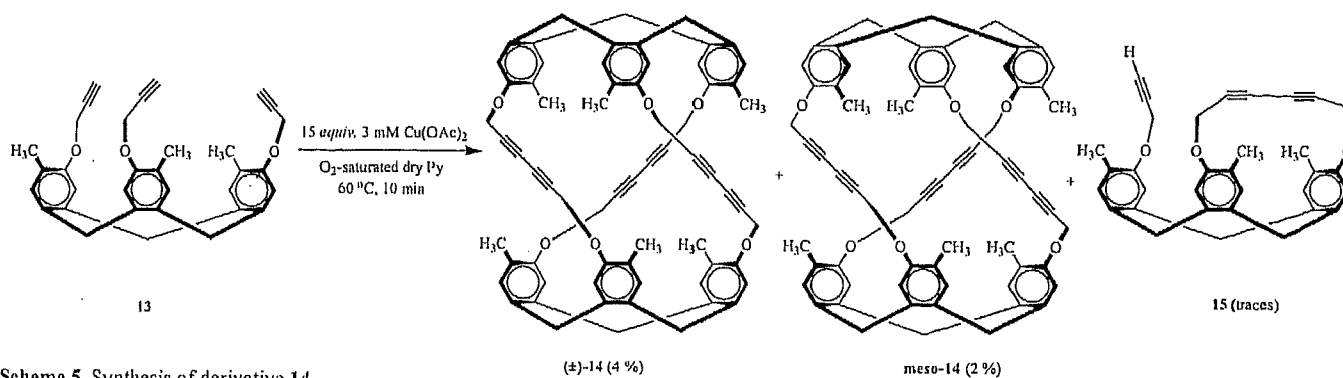


Fig. (3). X-ray structures for inclusion complex 9xMeCN.

assumed to be due to the fact that solvent binds better to the *meso* diastereoisomer than it binds to the (\pm) one.

4. CRYPTANDS WITH TRIPHENYLPHOSPHINE UNITS

As phosphine oxides can serve as hydrogen-bond acceptors, Whitlock and Friedrichsen [16, 17] have considered this moiety for the synthesis of this type of well defined three-dimensional host molecules. Treatment of **16** in pyridine at 60 °C with Cu(OAc)₂·H₂O provided a mixture of isomeric diyne-bridged bis-phosphoryl macrocycles **17** (*exo-exo*) and **18** (*endo-exo*) in 14 % and 7 % yield, respectively (Scheme 6).



Scheme 5. Synthesis of derivative **14**.

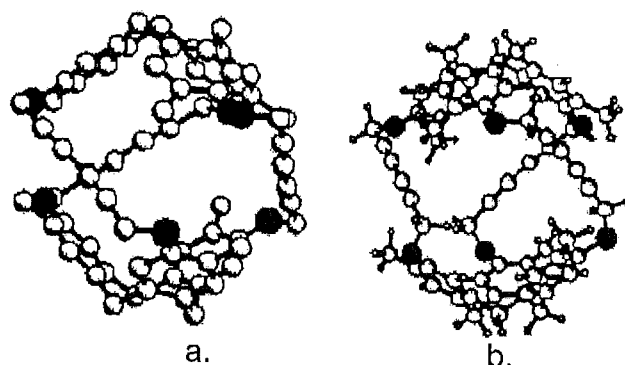
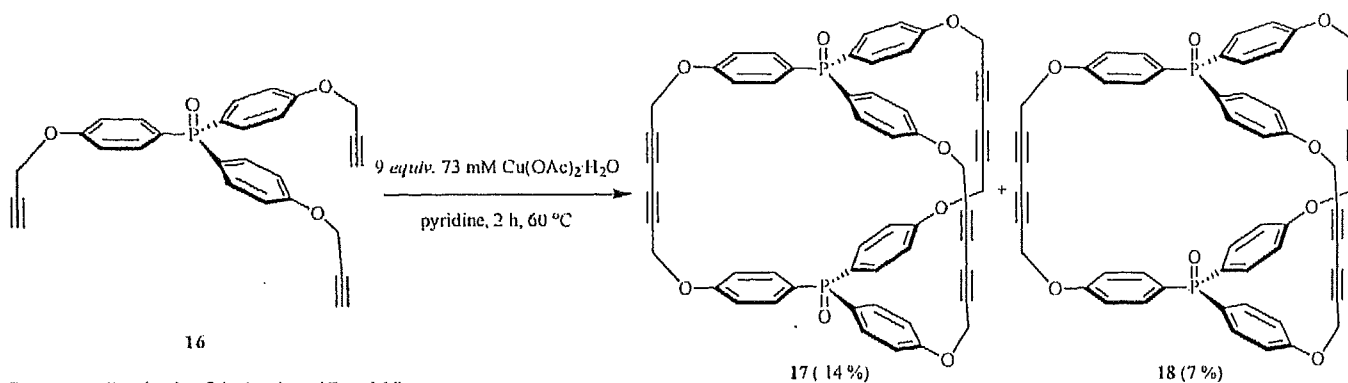


Fig. (4). X-ray structures for the free diastereomeric carcerands: a. (\pm)-**14** and b. *meso*-**14** (Permission to reprint is granted by the American Chemical Society).

(CH₃)₂COH, CH₂Cl₂, cubane, propylene oxide and benzene were determined in (CCl₃)₂CO at -20 °C.

The ¹H NMR spectra of *meso*-**14** in (CCl₃)₂CO showed no signs of complexation with any of the guests, from -20 to -40 °C. It was

Structure and Properties. The X-ray structures of compound **17** (from chloroform, Fig. 5a) and **18** (from anisole, Fig. 5b) showed the orientation of the phosphoryl groups and the helical nature of both species. Complete ¹H and ³¹P NMR studies were



Scheme 6. Synthesis of derivatives 17 and 18.

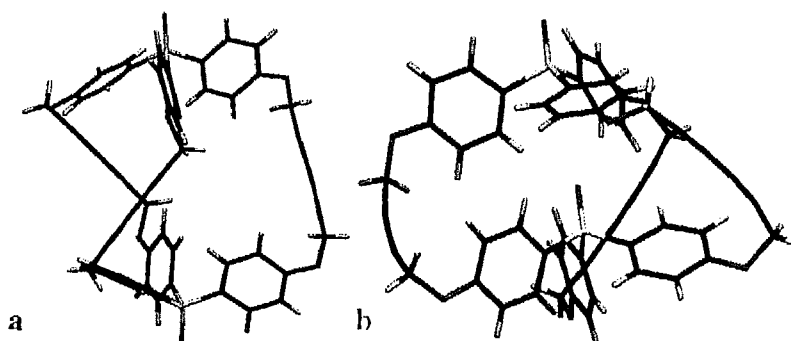
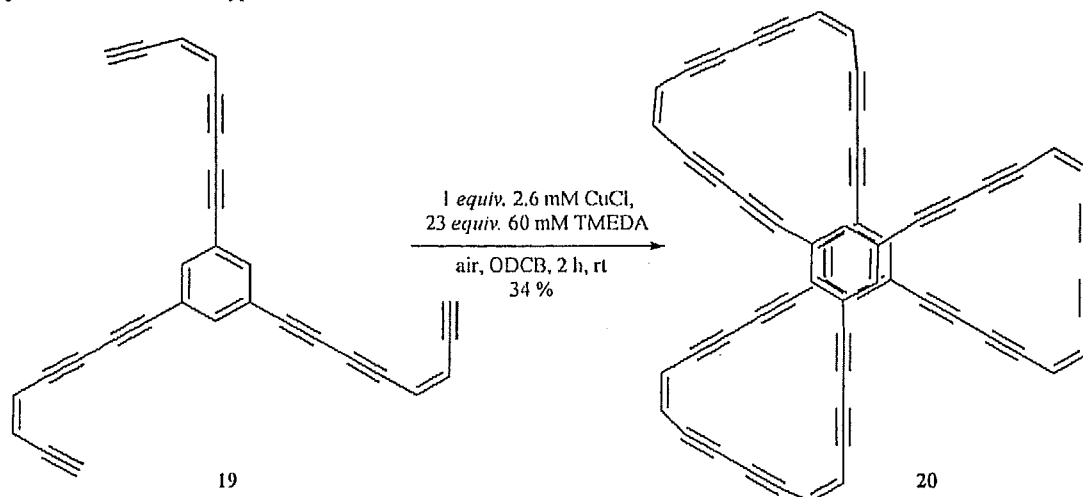


Fig. (5). X-ray structures for the free cryptands: a. 17 and b. 18.



Scheme 7. Synthesis of derivative 20.

undertaken and proved that *exo-exo* host 17 forms only extracavity complexes, while *endo-exo* host 18 allows also intracavity complexation.

The 1:2 complexation mechanism of 18 with a variety of guests has been studied by ^1H NMR spectroscopy. The calculated chemical shifts for the 1:1 and 1:2 complexes have evidenced the initial *endo* complexation of most of the guests. The association constants were modest and range from 18 M^{-1} (for phenol) to 354 M^{-1} (for *p*-nitrophenol) for the formation of the 1:1 complex with mono- and unsubstituted phenols, while the association constants for 1:2 complexes range from 1 M^{-1} to 320 M^{-1} . Surprisingly, even larger hosts such as 4-[(*p*-nitrophenyl)-azo]phenol and 6-nitro-2-naphthol showed preference for the initial *endo* complexation. The exception from this mechanism was proved for pentafluorophenol, which prefers to complex with 18 by initial *exo* pathway. No complexation

was observed for 2,4-dinitrophenol, 4-nitrothiophenol, benzoic acid and pyridine hydrochloride.

The ^{31}P NMR studies allowed calculation of the association constants for the *exocavit* complexes of 17 and brought further information regarding the complexation of 18. It has been shown that 2,6-dimethyl-4-nitrophenol, acetic acid and pentafluorophenol prefer initial *exo* complexation with the *endo-exo* phosphine oxide moieties.

5. FULLERENE PRECURSORS

The first approach to the unconventional synthesis of buckminsterfullerene (C_{60}) and heterofullerenes from polyalkynyl precursors was reported by Rubin [18]. Cyclization of 19 under Hay conditions, in *o*-dichlorobenzene at 25°C , afforded the corresponding macrocyclic cyclophane 20 in 34% yield (Scheme 7).

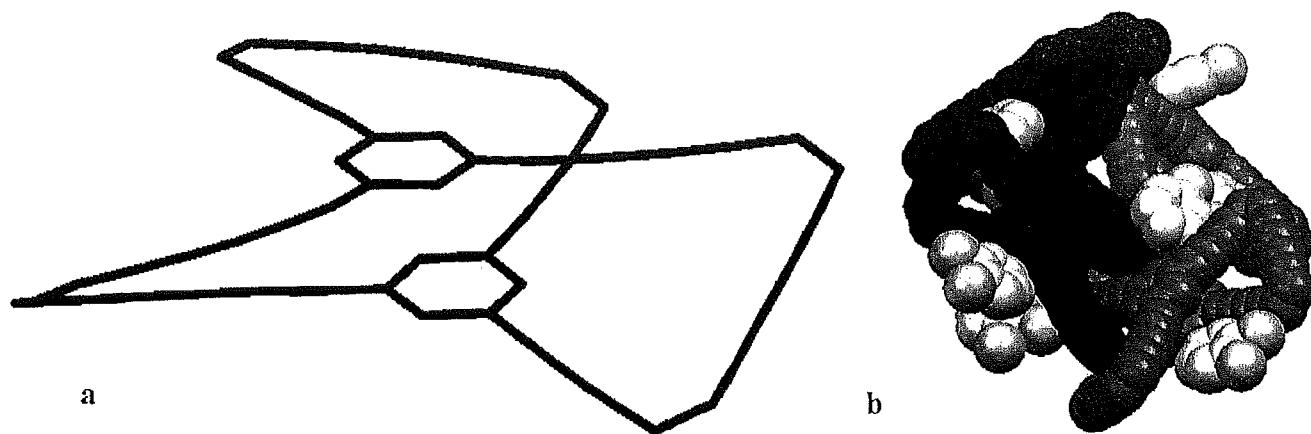
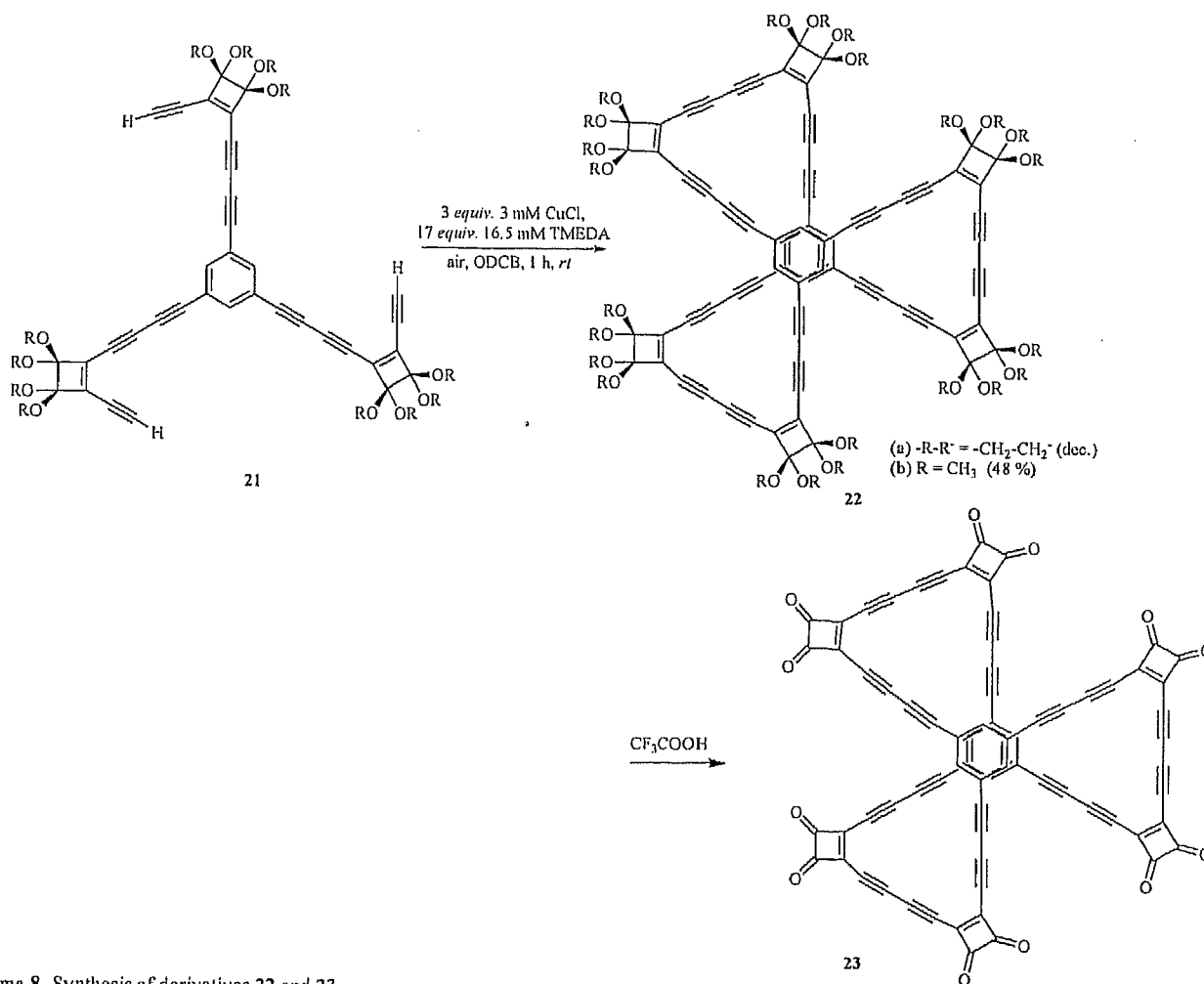


Fig. (6). X-ray structure (a) and crystal packing (b) for the free cage 20.



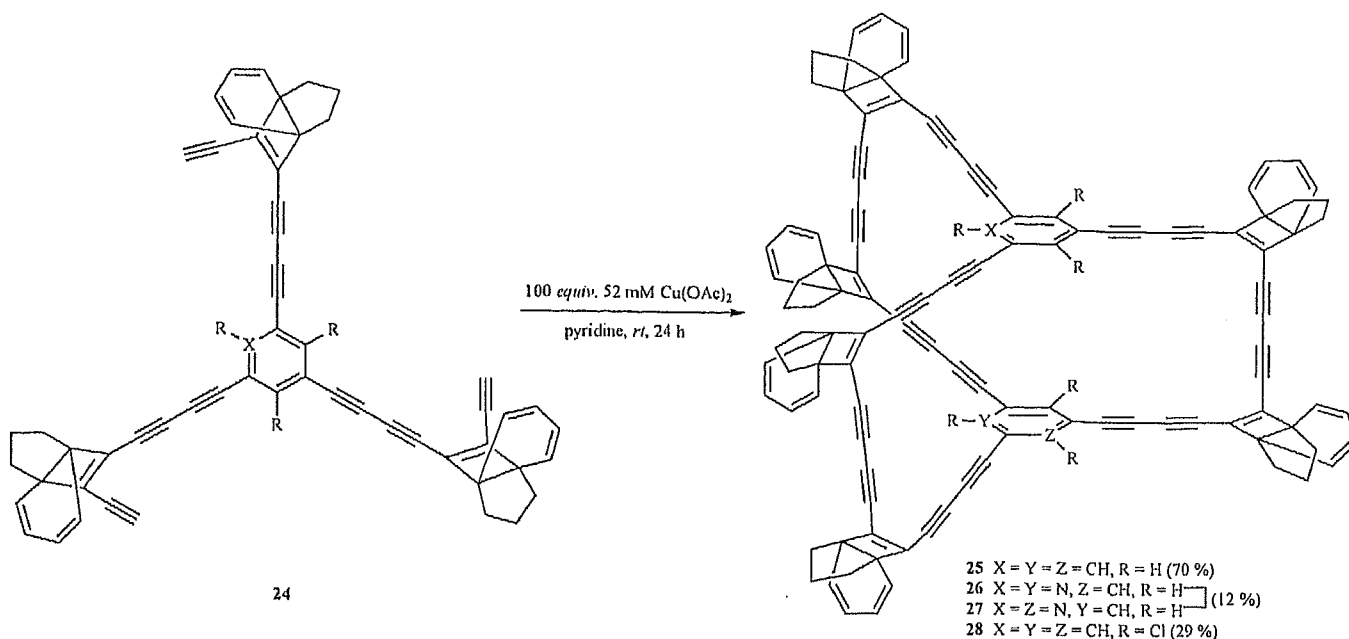
Scheme 8. Synthesis of derivatives 22 and 23.

Structure. The single crystal X-ray structure of macrobicyclic compound 20, together with the partial packing diagram is showing the helical chirality of the structure (Fig. 6). The only solvent that resulted in well defined crystals was *o*-dichlorobenzene, forming co-crystals with the cyclophane by separating the right handed helices from the opposite-handed partner.

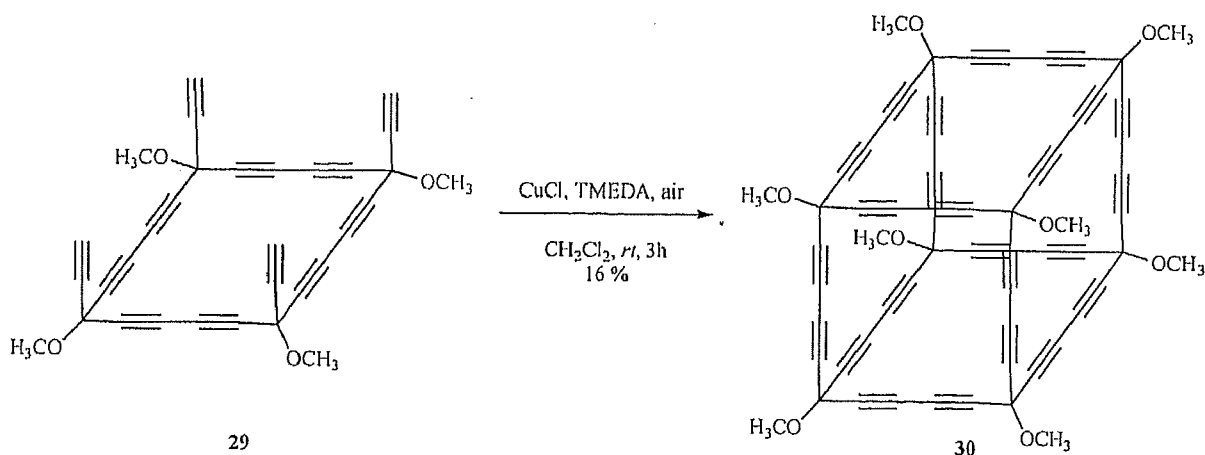
Thermochemical studies on macrocycle 20 have shown an unexpected stability of the parent molecular ion ($C_{60}H_{18}$). Therefore, Rubin and co-workers have synthesized the cyclobutanedione 23

(Scheme 8) that would rearrange to the more highly unsaturated precursor $C_{60}H_6$ and generates C_{60} ions in mass spectrometric experiments. Cyclization of dimethoxyacetal alkyne 21 [19] ($R = CH_3$) by a modified Hay procedure (Scheme 8) has led to the formation of macrocycle 22 as a solid in a very good yield (48 %).

A different approach in the formation of fullerenes was reported by Tobe and co-workers [20-22]. Cage molecule 25 was synthesized in an impressive 70 % yield by oxidative homoacetylenic coupling under high dilution modified Eglinton conditions (Scheme



Scheme 9. Synthesis of derivatives 25 – 28.



Scheme 10. Synthesis of derivative 30.

9). The analogue tris(propellane)trichloro-substituted benzene macrocyclic derivative **28** was obtained in only 29 % yield, probably due to its increased instability.

The same dimerization conditions were followed for the synthesis of macrocyclic polyynes $\text{C}_{58}\text{H}_4\text{N}_2$ (**26** and **27**) as precursors to diazafullerene [23]. The nitrogen substitution of one carbon atom in the benzene ring has led to the formation of a mixture of both regioisomers in a rather low yield (12 %).

Diederich and co-workers [24] have successfully applied Hay's acetylenic homocoupling conditions for the synthesis of expanded cubane **30** (Scheme 10). The four-fold oxidative coupling cyclization afforded **30** in a quite low yield (16 %), reasonable when considering its instability.

CONCLUSIONS

The procedures for the one-pot formation of cage molecules by Cu-catalyzed acetylenic coupling uses both Cu (I) and Cu (II) catalysts and acetonitrile, dichlorobenzene, pyridine or dichloromethane as solvents. The yields of these reactions vary from fair to good in

agreement with the preorganization and the steric complementarities of the reacting molecules, but the mechanism of this coupling reaction is not yet elucidated. The target cryptands successfully bind neutral molecules such as solvents and aromatic compounds. The host guest interactions are ensured by the participation of the aromatic core of the cryptands and no evidence of the participation of the diyne bridges to this process was revealed. Some of the target molecules were used for the synthesis of fullerenes and heterofullerenes.

ACKNOWLEDGEMENTS

We acknowledge the financial support of this work by UE-FISCSU (projects PD-8/2006, ID-570/2007 and Td-82/2007).

REFERENCES

- [1] Atwood, J. L., Steed, J. W. *Encyclopedia of Supramolecular Chemistry*, by Marcel Dekker, Inc., 2004
- [2] Han, T., Chen, C.-F. Selective templated complexation of a cylindrical macrotricyclic host with neutral guests: three cation-controlled switchable processes. *J. Org. Chem.*, 2007, 72, 7287.

- [3] Glaser, C. Beitrage zur kenntniss des acetylenbenzols. *Ber. Dtsch. Chem. Ges.*, 1869, 2, 422.
- [4] Eglinton, G., Galbraith, A. R. Cyclic diynes. *Chem. Ind., (London)* 1956, 737.
- [5] Hay, A. S. Oxidative coupling of acetylenes. *J. Org. Chem.*, 1962, 27, 3320.
- [6] Siemsen, P., Livingston, R. C., Diederich, F. Acetylenic coupling: a powerful tool in molecular construction. *Angew. Chem., Int. Ed. Engl.*, 2000, 39, 2634.
- [7] (a) Breitenbach, J., Boosfeld, J., Voegtle, F. In *Comprehensive Supramolecular Chemistry*; Voegtle, F., Ed.; Pergamon, Oxford, 1996, vol. 2 p. 29. (b) Whitlock, B. J., Whitlock, H. W. *ibid.*, p. 309.
- [8] O'Krongly, D., Denmeade, S. R., Chiand, M. Y., Breslow, R. Efficient triple coupling reaction to produce a self-adjusting molecular cage. *J. Am. Chem. Soc.*, 1985, 107, 5544.
- [9] Berscheid, R., Nieger, M., Voegtle, F. Konkave farbstoffmoleküle vom triphenylmethan-ty. *Chem. Ber.*, 1992, 125, 2539.
- [10] (a) Voegtle, F., Berscheid, R., Schnick, W. Inclusion of acetonitrile in a macrobicyclic host molecule. *J. Chem. Soc. Chem. Commun.*, 1991, 414. (b) Berscheid, R., Nieger, M., Voegtle, F. Mehrfach verbrückte triphenylmethane. *Chem. Ber.*, 1992, 125, 1687.
- [11] Berscheid, R., Voegtle, F. Concave dyestuffs: a triple bridged triphenylmethyl dication. *Synthesis*, 1992, 58.
- [12] Berscheid, R., Nieger, M., Voegtle, F. Orientational selectivity for the inclusion of acetonitrile in tailor-made macrobicyclic host molecules. *J. Chem. Soc., Chem. Commun.*, 1991, 1364.
- [13] Voegtle, F., Michel, I., Berscheid, R., Nieger, M., Rissanen, K., Kotila, S., Airola, K., Armarolli, N., Maestri, M., Balzani, V. Concave macrobicycles: absorption spectra, luminescence properties, and endocavitational complexation of neutral organic guests. *Liebigs Ann.*, 1996, 1697.
- [14] Whitlock, B. J., Whitlock, H. W. Effect of cavity size on supramolecular stability. *J. Am. Chem. Soc.*, 1994, 116, 2301.
- [15] Cram, D. J., Tanner, M. E., Keipert, S. J., Knobler, C. B. Two chiral [1.1.1] jorthocyclophane units bridged by three biacetylene units as a host which binds medium-sized organic guests. *J. Am. Chem. Soc.*, 1991, 113, 8909.
- [16] Friedrichsen, B. P., Whitlock, H. W. Concave functionality: intracavity phosphine oxide as a locus of complexation. *J. Am. Chem. Soc.*, 1989, 111, 9132.
- [17] Friedrichsen, B. P., Powell, D. R., Whitlock, H. W. Sterically encumbered functional groups: an investigation of endo versus exo phosphoryl complexation using ^1H and ^{31}P NMR. *J. Am. Chem. Soc.*, 1990, 112, 8931.
- [18] Rubin, Y., Parker, T. C., Khan, S. I., Holliman, C. L., McElvany, S. W. Precursors to endohedral metal fullerene complexes: synthesis and x-ray structure of a flexible acetylenic cyclophane $\text{C}_{60}\text{H}_{18}$. *J. Am. Chem. Soc.*, 1996, 118, 5308.
- [19] Rubin, Y., Parker, T. C., Pastor, S. J., Jalisatgi, S., Boule, C., Wilkins, C. L. Acetylenic cyclophanes as fullerene precursors: formation of C_{60}H_6 and C_{60} by laser desorption mass spectrometry of $\text{C}_{60}\text{H}_6(\text{CO})_{12}$. *Angew. Chem. Int. Ed.*, 1998, 37, 1226.
- [20] Tobe, Y., Nakagawa, N., Naemura, K., Wakabayashi, T., Shida, T., Achiba, Y. [16.16.16](1,3,5)cyclophanetetraosayne (C_{60}H_6): A precursor to C_{60} fullerene. *J. Am. Chem. Soc.*, 1998, 120, 4544.
- [21] Tobe, Y., Nakagawa, N., Kishi, J., Sonoda, M., Naemura, K., Wakabayashi, T., Shida, T., Achiba, Y. Polyyne cyclization to form carbon cages: [16.16.16](1,3,5)cyclophanetetraosayne derivatives C_{60}H_6 and $\text{C}_{60}\text{C}_{16}$ as precursors to C_{60} fullerene. *Tetrahedron*, 2001, 57, 3629.
- [22] Tobe, Y., Umeda, R., Sonoda, M., Wakabayashi, T. Size-selective formation of C_{78} fullerene from a three dimensional polyyne precursor. *Chem. Eur. J.*, 2005, 11, 1603.
- [23] Tobe, Y., Nakanishi, H., Sonoda, M., Wakabayashi, T., Achiba, Y. Pyridine analogue of macrocyclic polyyne $\text{C}_{58}\text{H}_4\text{N}_2$ as a precursor to diazafullerene C_{58}N_2 . *Chem. Commun.*, 1999, 1625.
- [24] Manini, P., Amrein, W., Gramlich, V., Diederich, F. Expanded cubane: synthesis of a cage compound with a C_{36} core by acetylenic scaffolding and gas-phase transformations into fullerenes. *Angew. Chem. Int. Ed. Engl.*, 2002, 41, 4339.

Received: May 06, 2008

Revised: September 15, 2008

Accepted: September 15, 2008

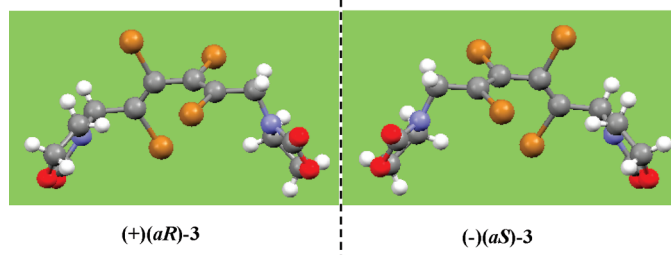
Synthesis, Structural Analysis, and Chiral Investigations of Some Atropisomers with *EE*-Tetrahalogeno-1,3-butadiene Core

Flavia Piron,^{†,‡} Nicolas Vanthuyne,[§] Bérangère Joulin,[§] Jean-Valère Naubron,[§]
Crina Cismaș,[†] Anamaria Terec,[†] Richard Attila Varga,[†] Christian Roussel,^{*,§}
Jean Roncali,[‡] and Ion Grosu^{*,†}

[†]Faculty of Chemistry and Chemical Engineering, Babes-Bolyai University, Cluj-Napoca, 11 Arany Janos str., 400028, Cluj-Napoca, Romania, [‡]University of Angers, CNRS, CIMA, Group Linear Conjugated Systems, 2 Bd Lavoisier, 49045, Angers, France, and [§]University Paul Cézanne-Aix-Marseille III, ISM2, Chirosciences, 13397 Marseille CEDEX 20, France

christian.roussel@univ-cezanne.fr; igrosu@chem.ubbcluj.ro

Received August 26, 2009



The atropenantiomers of stable 1,2,3,4-tetrahalo-1,3-butadiene derivatives (where halogeno stands for bromine or iodine) were separated with use of chiral HPLC. The barriers for the enantiomerization process were determined on-line by dynamic HPLC (DHPLC) or off-line by classical kinetic measurements. In the case of the tetrachloro compound, the barrier was too low for DHPLC and its value was obtained by dynamic NMR experiments. The obtained barriers for chloro, bromo, and iodo derivatives correlate with the van der Waals radii of the halogens. The absolute configuration of the isolated enantiomers of the tetraiodo and tetrabromo compounds was assigned by comparison of the experimental and conformations averaged calculated VCD spectra. The identification of a signature band of the absolute configuration of the butadiene core, the sign and location of which are independent from the different conformations and substituents, allowing the safe assignment of the absolute configuration of the enantiomers of chiral 1,3-butadienes, is also reported.

Introduction

Starting with the first resolution of the atropisomeric enantiomers of 6,6'-dinitro-2,2'-diphenic acid (Christie and Kenner in 1922)¹ the investigation of various compounds exhibiting atropenantiomers became an important target in organic chemistry.^{2a-c}

Many axial chiral biphenyls [e.g., (*R*)-(+)-2,2'-bis-(diphenylphosphino)-6,6'-dimethoxy-1,1'-biphenyl (MeO-BIPHEP)],³ binaphthyls [e.g., 2,2'-bis(diphenylphosphino)-1,1'-binaphthyl (BINAP)^{4a} or 2,2'-dihydroxy-1,1'-dinaphthyl (BINOL)^{4b}], naphthylisoquinoline alkaloids,^{4c-e} and [2.2]cyclophanes with planar chirality [e.g., (*R*)-(-)-4,

*To whom correspondence should be addressed. Fax: 33 (0)4 91 28 91 46 and 40-264-590818.

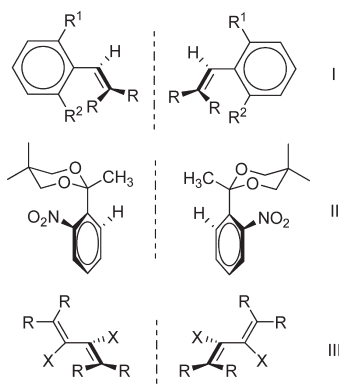
(1) Christie, G. H.; Kenner, J. H. *J. Chem. Soc.* **1922**, 121, 614–620.
(2) (a) Eliel, E. L.; Wilen, S. H. *Stereochemistry of Organic Compounds*; Wiley: New York, 1994; p 1142. (b) Roussel, C.; Vanthuyne, N.; Bouchekara, M.; Djaffi, A.; Elguero, J.; Alkorta, I. *J. Org. Chem.* **2008**, 73, 403–411. (c) Vanthuyne, N.; Andreoli, F.; Fernandez, S.; Roman, M.; Roussel, C. *Lett. Org. Chem.* **2005**, 2, 433–443. (d) Roussel, C.; Popescu, C. *Chirality* **1994**, 6, 251–260. (e) Roussel, C.; Stein, J. L.; Beauvais, F. *New J. Chem.* **1990**, 14, 169–173.

(3) Schmid, R.; Foricher, J.; Cereghetti, M.; Schonholzer, P. *Helv. Chim. Acta* **1991**, 74, 370–389.

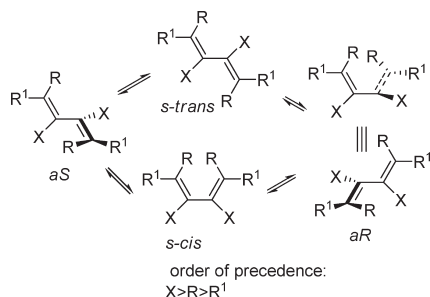
(4) (a) Cai, D. W.; Payack, J. F.; Bender, D. R.; Hughes, D. L.; Verhoeven, T. R.; Reider, P. J. *Org. Synth.* **1999**, 76, 6–11. (b) Brunel, J. M. *Chem. Rev.* **2005**, 105, 857–897. (c) Bringmann, G.; Hamm, A.; Schraut, M. *Org. Lett.* **2003**, 5, 2805–2808. (d) Bungard, C. J.; Morris, J. C. *Org. Lett.* **2002**, 4, 631–633. (e) Bungard, C. J.; Morris, J. C. *J. Org. Chem.* **2006**, 71, 7354–7363.

(5) Pye, P. J.; Rossen, K.; Reamer, R. A.; Tsou, N. N.; Volante, R. P.; Reider, P. J. *J. Am. Chem. Soc.* **1997**, 119, 6207–6208.

SCHEME 1



SCHEME 2



12-bis(diphenylphosphino)[2.2]paracyclophane (Phanephos)⁵ are commercially available as chiral auxiliaries or are biologically active compounds. Besides these well-known atropenantiomeric compounds, atropisomerism and the axial chirality was evidenced for many other unexpected cases (e.g., vinylbenzenes I,⁶ 2-aryl,2-methyl-1,3-dioxanes II,⁷ 1,3-butadienes III;⁸ Scheme 1).

The atropisomers of 1,3-butadienes are due to the hindered rotation around the central bond C²–C³. These compounds prefer the conformation with perpendicular arrangement of the double bonds, which ensure the longest distance between the large substituents at positions 2 and 3 (X, Scheme 2).

The racemization of the atropenantiomers (*aR* ⇌ *aS*) occurs by rotation around the C²–C³ bond, via either the *s-trans* isomer (*transoid*) or the *s-cis* structure (*cisoid*) of the 1,3-butadiene core.

The dynamic experiments and the molecular modeling indicate a considerably higher barrier of the inversion through the *cisoid* form,⁹ thus the further discussion is focused on the interactions in the ground state (with perpendicular double bonds) and in the

SCHEME 3

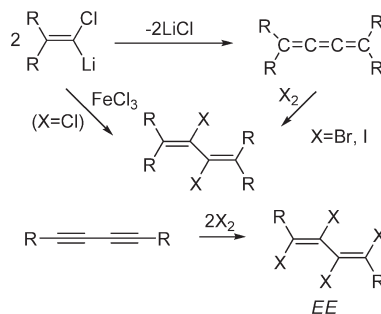
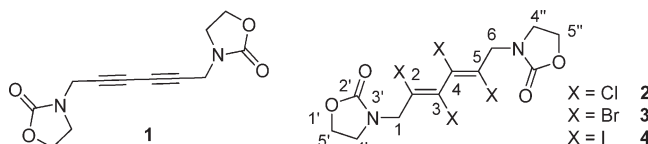
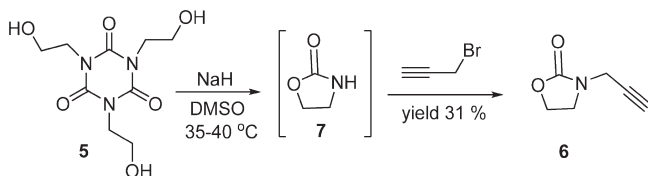


CHART 1



SCHEME 4



transoid isomer (with coplanar double bonds) which are mainly involved in the conformational equilibria of chiral 1,3-dienes.

The values of the barriers of racemization are strongly correlated with X and R groups (named internal substituents). In several cases when these internal substituents are not very large (e.g., R, X = Cl, Cl; Cl, CH₂C₆H₅; Ph (CH₃), COOC_nH_{2n+1}); according to Scheme 2) the barriers could be estimated by dynamic NMR experiments.^{8a–d,10} For few other compounds (e.g., R = X = Br, CH₃) the barriers could be determined using polarimetry measurements. In these cases a previous resolution of the racemates either by derivatization with CDAs (chiral derivatizing agent) or by chiral chromatography (triacytcellulose as the chiral stationary phase) was required.^{11a,b}

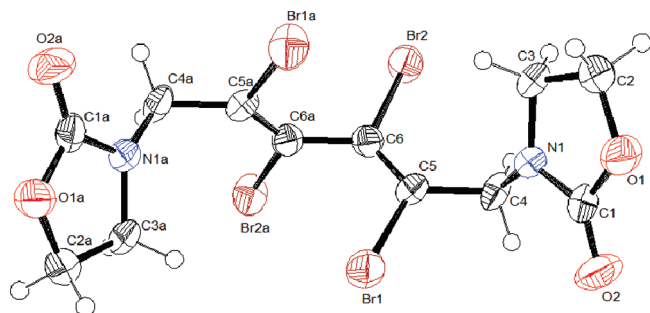
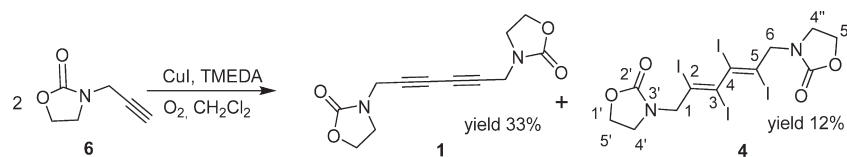
The majority of the compounds were obtained and were investigated in *EE* configuration, but for some cases, when the syntheses were not stereoselective and all isomers were obtained, the two other isomers (*EZ* and *ZZ*) were also separated and investigated. An increase of the rotation barrier in the series *ZZ* < *EZ* < *EE* was observed.^{8d,10}

The R¹ groups (named external substituents) are not involved directly in the hindrance of the rotation around the C²–C³ bonds, but if they are large they increase the barrier of rotation by the *buttressing* effect.^{8a,b,c,f} The sensitivity to the *buttressing* effect of the external substituents depends on the actual size of the buttressed substituents.^{12a,b}

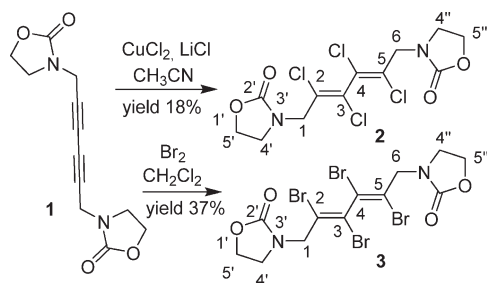
(6) Fang, Y. Q.; Lautens, M. *Org. Lett.* **2005**, *7*, 3549–3552.
 (7) Grosu, I.; Plé, G.; Mager, S.; Mesáros, E.; Dulau, A.; Gego, C. *Tetrahedron* **1998**, *54*, 2905–2916.
 (8) (a) Wolf, C. *Dynamic Stereochemistry of Chiral Compounds*; RCS Publishing: Cambridge, UK, 2008; p 98. (b) Köbrich, G.; Mannschreck, A.; Misra, R. A.; Rissmann, G.; Rösner, M.; Zündorf, W. *Chem. Ber.* **1972**, *105*, 3794–3806. (c) Köbrich, G.; Kolb, B.; Mannschreck, A.; Misra, R. A. *Chem. Ber.* **1973**, *106*, 1601–1611. (d) Elbe, H.-L.; Köbrich, G. *Chem. Ber.* **1974**, *107*, 1654–1666. (e) Rösner, M.; Köbrich, G. *Angew. Chem., Int. Ed.* **1974**, *13*, 741–743. (f) Bödecker, H.-O.; Jonas, V.; Kolb, B.; Mannschreck, A.; Köbrich, G. *Chem. Ber.* **1975**, *108*, 3497–3508. (g) Rösner, M.; Köbrich, G. *Angew. Chem.* **1975**, *87*, 715–717.
 (9) (a) Devaquet, A. J. P.; Townshend, R. E.; Hehre, W. J. *J. Am. Chem. Soc.* **1976**, *98*, 4068–4076. (b) Bachrach, S. M.; Liu, M. *J. Am. Chem. Soc.* **1991**, *113*, 7929–7937. (c) Squillacote, M. E.; Liang, F. *J. Org. Chem.* **2005**, *70*, 6564–6573. (d) Hansen, A. E.; Bak, K. L. *J. Phys. Chem. A* **2000**, *104*, 11362–11370.

(10) Becher, G.; Mannschreck, A. *Chem. Ber.* **1983**, *116*, 264–272.
 (11) (a) Mannschreck, A.; Mintas, M.; Becher, G.; Stühler, G. *Angew. Chem.* **1980**, *92*, 490–491. (b) Becher, G.; Mannschreck, A. *Chem. Ber.* **1981**, *114*, 2365–2368.
 (12) (a) Berg, U.; Liljefors, T.; Roussel, C.; Sandström, J. *Acc. Chem. Res.* **1985**, *18*, 80–86. (b) Gallo, R.; Roussel, C.; Berg, U. *Adv. Heterocycl. Chem.* **1988**, *43*, 173–299.

SCHEME 5

FIGURE 1. ORTEP diagram for compound **3**.

SCHEME 6



Chiral halogenodienes were obtained either by oxidative coupling reactions of vinyl derivatives or by halogen addition reactions to diynes or cumulenes (Scheme 3).^{8a–d,f}

We considered it of interest to revisit and to develop the investigations in the field of chiral dienes with modern tools and to obtain starting from diyne **1** new chiral tetrahalo-2,4-hexadienes **2–4** (Chart 1), to determine their structure, to separate the enantiomers, to measure the barriers of racemization, and to determine the absolute configuration of the resolved enantiomers.

Results and Discussions

The strategy for the synthesis of target diyne **1** and then of the corresponding chiral tetrahalo-diene compounds **2–4** was based on obtaining *N*-propargyl-1,3-oxazolidine-2-one **6** by the reaction of the commercially available 1,3,5-tris(2'-hydroxyethyl)cyanuric acid **5** with propargyl bromide (Scheme 4). In the process the in situ transposition of **5** to the 1,3-oxazolidine-2-one **7** occurs. This transposition reaction was first achieved by Frazier et al. in vacuum pyrolysis.¹³

Diyne **1** was obtained by the Hay's coupling reaction (Scheme 5).¹⁴ In the process, a part of the diyne **1** was transformed into the *EE*-tetraiodo-2,4-hexadiene **4** (Scheme 5; the **1**:**4** ratio \approx 3).

(13) Frazier, T. C.; Little, E. D.; Lloyd, B. E. *J. Org. Chem.* **1960**, *15*, 1944–1946.

(14) Hamilton, D. G.; Prodi, L.; Feeder, N.; Sanders, J. K. M. *J. Chem. Soc., Perkin Trans. 1* **1999**, 1057–1065.

TABLE 1. Values of Some Selected Bond Angles (the numbering corresponds to ORTEP diagrams; Figure 1 and Supporting Information)^a

compd	bond angles (deg)		d [distances (Å)]	
	$\text{X}^1\text{--C}^5\text{--C}^6$; $\text{X}^{1a}\text{--C}^{5a}\text{--C}^{6a}$	$\text{C}^{6a}\text{--C}^6\text{--X}^2$; $\text{C}^6\text{--C}^{6a}\text{--X}^{2a}$	$\text{X}^2\text{--H}(\text{C}^3)$; $\text{X}^{2a}\text{--H}(\text{C}^{3a})$	$\Delta d = d(r_X + r_H)^b$
2	117.86	113.39	2.691	−0.149
3	116.27	112.00	2.784	−0.156
4 (A)	118.01;	110.89;	2.782;	−0.288;
	118.30	112.72	2.830	−0.240
4 (B)	118.04;	110.49;	2.903;	−0.167;
	119.18	111.56	2.836	−0.234

^aFor **4** the crystal exhibits two type of molecules denoted with A and B (see Supporting Information). ^b r_X and r_H are the vdW radii of X and H: $r_H = 1.09$ Å; $r_{\text{Cl}} = 1.75$ Å; $r_{\text{Br}} = 1.85$ Å; $r_{\text{I}} = 1.98$ Å.¹⁶

Tetrachloro and tetrabromo 2,4-hexadienes **2** and **3** were synthesized as single *EE* isomers by direct halogenation of the corresponding diyne (**1**) using specific procedures (Scheme 6) reported for similar reactions on different substrates.^{8b,e,15}

Solid State Structural Investigations of 2–4. The single crystal molecular structures for **2–4** (Figure 1 and the Supporting Information) were obtained by X-ray diffractometry, using suitable crystals obtained from double layered CHCl_3 /hexane solutions. The crystals contain both enantiomers. The crystal of **4** due to the packing effects contains two different types of molecules (with slightly different interatomic distances and bond and torsion angles (Supporting Information). The molecular structures reveal the perpendicular orientation of the planes of the double bonds (torsion angles vary in the range 88.33–91.13°) and the ground state strain induced by the (1',3'-oxazolidine-2'-one-3'-yl)methyl groups. This effect determines a diminishing (correlated with the increasing of the values of the van der Waals radii of the halogen atoms) of the bond angles $\text{X}^1\text{--C}^5\text{--C}^6$ ($\text{X}^{1a}\text{--C}^{5a}\text{--C}^{6a}$) and $\text{C}^{6a}\text{--C}^6\text{--X}^2$ ($\text{C}^6\text{--C}^{6a}\text{--X}^{2a}$) (Table 1). The values of the bond angles $\text{X}^1\text{--C}^5\text{--C}^6$ ($\text{X}^{1a}\text{--C}^{5a}\text{--C}^{6a}$) for **4** are somewhat higher than expected, probably due to intramolecular halogen–hydrogen interactions [$\text{X}^2\text{--H}(\text{C}^3)$; $\text{X}^{2a}\text{--H}(\text{C}^{3a})$] which can be appreciated by the amplitude of the differences between the sum of the van der Waals radii of hydrogen and halogen atoms and the corresponding measured distance in the X-ray structure (Table 1).

The lattice of **4** shows many supramolecular interactions (Supporting Information): halogen–halogen ($d_{\text{I–I}} = 3.784$

(15) Uemura, S.; Okazaki, H.; Onoe, A.; Okano, M. *J. Chem. Soc., Perkin Trans. 1* **1977**, 676–680.

(16) (a) Bondi, A. *J. Phys. Chem.* **1964**, *68*, 441–452. (b) Rowland, R. S.; Taylor, R. *J. Phys. Chem.* **1996**, *100*, 7384–7391.

(17) Bui, T. T. T.; Dahaoui, S.; Lecomte, C.; Desiraju, G. R.; Espinosa, E. *Angew. Chem., Int. Ed.* **2009**, *48*, 3838–3841.

(18) (a) Metrangolo, P.; Resnati, G.; Arman, H. D. *Halogen Bonding: Fundamentals and Applications*; Springer-Verlag: Berlin, Germany, 2008. (b) Metrangolo, P.; Meyer, F.; Pilati, T.; Resnati, G.; Terraneo, G. *Angew. Chem., Int. Ed.* **2008**, *47*, 6114–6127. (c) Zou, W. S.; Han, J.; Jin, W. *J. Phys. Chem. A* **2009**, *113*, 10125–10132.

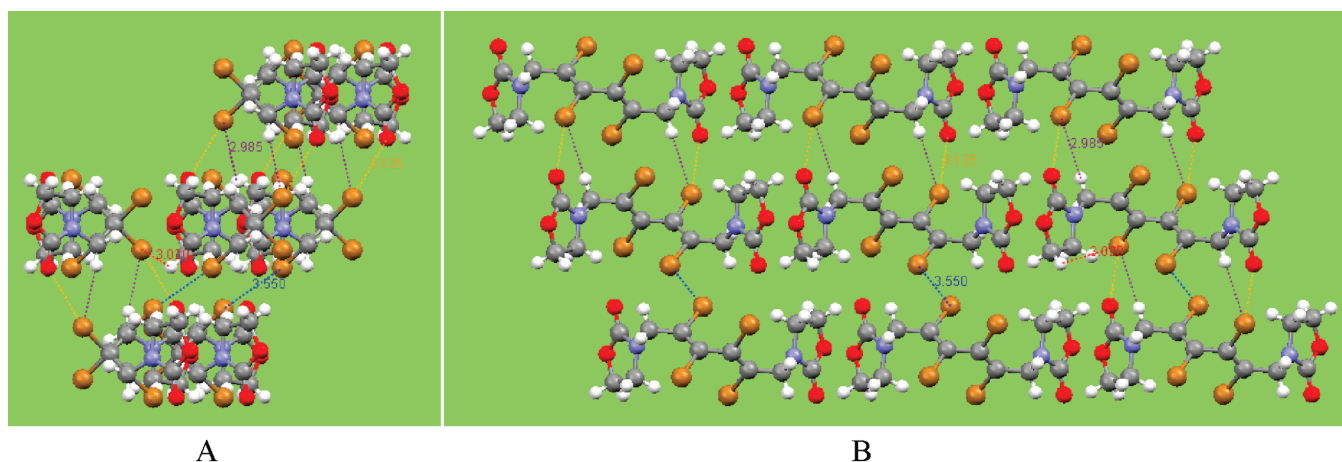


FIGURE 2. Views (A along the axis *a* and B along the axis *b*) of the lattice of **3** obtained with the Mercury program.

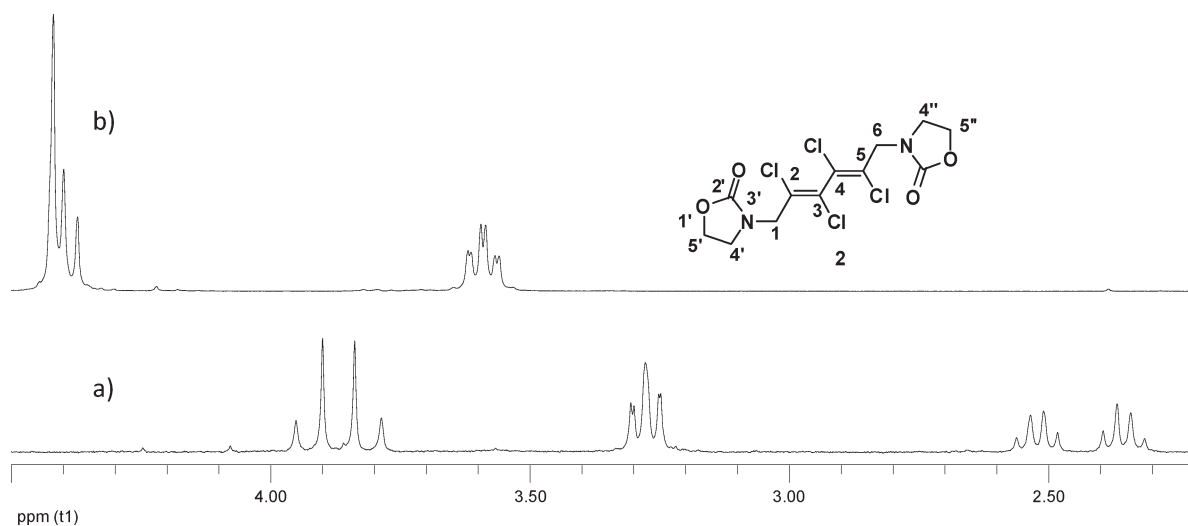


FIGURE 3. ^1H NMR (300 MHz) of compound **2** at room temperature in C_6D_6 (a) and CDCl_3 (b).

Å ; type I interactions¹⁷), $\text{C}^{4(4a)}\text{---H---I}$ ($d_{\text{H---I}} = 3.101, 3.148 \text{ Å}$), $\text{C}^{2(2a),3(3a)}\text{---H---O}^{2(2a)}\text{=C}^{2(2a)}$ ($d_{\text{H---O}} = 2.704$ and 2.594 Å , respectively), and halogen bondings¹⁸ (X bondings; $\text{X---O}^{2(2a)}\text{=C}^{2(2a)}$; $d_{\text{I---O}} = 2.982, 3.069, 3.143, 3.154, 3.360 \text{ Å}$) which can also influence the values of the bonds angles (Table 1) in the X-ray molecular structure of this compound.

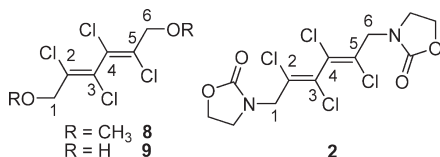
The inspection of the associations of the molecules in the lattices revealed for **2** and **3** layered structures (Figure 2 and the Supporting Information) in which the $\text{C}^{4(4a)}\text{---X}$ bonds of different molecules exhibit antiparallel orientations generating favorable dipole–dipole interactions ($d_{\text{C}^{4(4a)}\text{---X}}$ of neighboring molecules are 3.943 Å for $\text{X} = \text{Br}$ and 3.743 Å for $\text{X} = \text{Cl}$, respectively). In addition halogen–halogen interactions ($d_{\text{Cl---Cl}} = 3.454 \text{ Å}$; $d_{\text{Br---Br}} = 3.550 \text{ Å}$; type I interactions¹⁷), $\text{C}^{4(4a)}\text{---H---X}$ ($d_{\text{H---Br}} = 2.985, 3.020 \text{ Å}$ and $d_{\text{H---Cl}} = 2.946 \text{ Å}$), $\text{C}^{2(2a),3(3a)}\text{---H---O}^{2(2a)}\text{=C}^{2(2a)}$ interactions ($d_{\text{H---O}}(\mathbf{2}) = 2.652, 2.639 \text{ Å}$), and halogen bonding supramolecular interactions ($\text{X---O}^{2(2a)}\text{=C}^{2(2a)}$; $d_{\text{Cl---O}} = 3.225 \text{ Å}$; and $d_{\text{Br---O}} = 3.125 \text{ Å}$) were observed.^{18,19}

This underlines the increase of the X bondings in the series $\text{Cl} < \text{Br} < \text{I}$ suggested by the dramatic decrease of the $\text{X---O}=\text{C}$ distances ($d_{\text{Cl---O}} = 3.225 \text{ Å}$, $d_{\text{Br---O}} = 3.125 \text{ Å}$, and $d_{\text{I---O}} = 2.982$) in a reversed relation with the values of the van der Waals radii of the halogens.

Structural Investigations in Solution of 2–4: Enantiomerization Barriers. Compounds **2–4** have large internal substituents and exhibit anancomeric structures (stable atropisomers at the NMR scale) and therefore their ^1H NMR spectra (C_6D_6) show at rt different signals for the protons of the prochiral centers (CH_2 groups) of the molecules (these protons are diastereotopic). As an example, the ^1H NMR spectrum of **2** (Figure 3) exhibits an AB system ($\delta_{1,6} = 3.92$, $\delta'_{1,6} = 3.81 \text{ ppm}$; $J = 15.4 \text{ Hz}$) for the protons of the CH_2 groups connected to the diene units and two overlapped doublets of doublets of doublets ($\delta_{5',5''} = 3.275 \text{ ppm}$, $\delta'_{5',5''} = 3.272 \text{ ppm}$; $J = J' = 8.1 \text{ Hz}$; $J'' \approx 0 \text{ Hz}$) and two doublets of doublets of doublets ($\delta_{4',4''} = 2.51 \text{ ppm}$, $\delta'_{4',4''} = 2.35 \text{ ppm}$; $J = 15.7 \text{ Hz}$, $J' = 8.1 \text{ Hz}$; $J'' \approx 0 \text{ Hz}$) for the protons at positions $5'$ ($5''$) and $4'$ ($4''$), respectively. The spectra of **2–4** run in CDCl_3 cannot differentiate the diastereotopic protons at positions 1 (6) and $5'$ ($5''$) and these display unique signals (Figure 3 and the Supporting Information). Similar situations were recorded for some

(19) Csoregh, I.; Brehmer, T.; Bombicz, P.; Weber, E. *Cryst. Eng.* **2001**, *4*, 343–357.

SCHEME 7



chiral N-substituted 1,3-oxazolidinone derivatives bearing $-\text{CH}_2-\text{R}^*$ groups (R^* is a chiral substituent).²⁰ These experiments reveal important ASIS (Aromatic Solvent Induced Shifts)²¹ effects for the NMR spectra of **2–4**. To determine the barriers induced by the hindered rotation of the molecules around C^3-C^4 bonds we carried out variable-temperature NMR experiments by increasing the temperature. For compounds **3** and **4** the spectra run in C_6D_6 and $\text{DMSO}-d_6$ at higher temperatures (until 343 and 400 K, respectively) did not show significant modifications in comparison with the spectra recorded at rt, indicating that the barrier is too high to be determined by this method. Similar variable-temperature NMR experiments run with **2** using C_6D_6 as solvent gave relevant results. The coalescence of the signals was obtained at 333 K and the barrier (calculated from two sets of signals) was found to be $\Delta G^\ddagger = 69.57 \pm 0.62$ kJ/mol, in excellent agreement with the data reported for other similar compounds.^{8b,f}

The barrier for the 2,3,4,5-tetrachloro-1,6-dimethoxy-2,4-hexadiene **8** (Scheme 7: $\text{R} = \text{Me}$) was 70.3 kJ/mol by DNMR at 54 °C in decalin and the barrier for the diol analogue **9** (Scheme 7, $\text{R} = \text{H}$) was 68.8 kJ/mol by DNMR at 53 °C in toluene- d_8 . The resulting mean value of the barriers obtained by DNMR in decalin, benzene, or toluene for three butadienes having in common the tetrachloro-diene core and differing by the substituent on the terminal methylene groups is 69.55 ± 0.95 kJ/mol. This value constitutes a good estimate of the barrier arising from the interaction in the tetrachloro core in the presence of substituted methyl groups. A buttressing effect was observed in the case of secondary or tertiary substituents in the place of the substituted methyl.^{8f}

Compounds **2–4** were submitted to a screening on various chiral stationary phases. Chiralpak IC, a recently marketed column from Daicel composed of cellulose tris(3,5-dichlorophenylcarbamate) immobilized on silica, afforded baseline separation of the enantiomers of **3** and **4** at 25 °C. It is worth recalling that previous attempts of separation of compound **3** analogues by chromatography on chiral support lasted from the pioneering period of chiral chromatography on microcrystalline cellulose triacetate (MCTA). On MCTA no baseline separation was achieved and a recycling technique with peak shaving was used by Mannschreck's group in Germany to obtain enriched samples in one enantiomer.^{11a,b} As known from DNMR experiments, compound **2** presents a too low

barrier for a separation at room temperature and accordingly a single peak was observed. Cryogenic chromatography^{22a,b} might be helpful in that case but no attempts were performed in that direction since the barrier was already available from NMR experiments. The enantiomers of the tetrabromo **3** and tetraiodo **4** derivatives were isolated under semipreparative conditions. In both cases the enantiomer with a (–) sign was eluted first on Chiralpak IC, using various mixtures of hexane– CHCl_3 –EtOH.²³ The off-line first-order kinetic rate of racemization of the isolated enantiomers of **3** was determined in CHCl_3 at 40 °C yielding a barrier to enantiomerization ($\Delta G^\ddagger = 102.3 \pm 0.5$ kJ/mol) corresponding to a 101 min half-life. The rotation barrier is in the range of a possible observation of a plateau during chiral chromatography.^{24a–d} Indeed when running chiral chromatography at 50 °C with the same mobile phase as for room temperature separation, a very clear plateau was observed allowing an estimation of the barrier by using Trapp and Schurig equation:²⁵ $\Delta G^\ddagger = 103.6$ kJ/mol at 50 °C in the mixture ethanol/chloroform/hexane 3/3/1 (corresponding to a 43 min half-life at 50 °C). The barriers of enantiomerization of two butadienes having in common with compound **3** the core of four bromides and differing by the so-called external group $\text{CH}_2\text{R}'$ [$\text{R}' = \text{OH}$, OMe, or oxazolidinone unit ($\text{C}_3\text{H}_4\text{NO}_2$) for **3**] have been reported in the literature.^{11b} The barriers in acetone were 102.2 kJ/mol (recalculated at 53.5 °C) for $\text{R}' = \text{OH}$ and 104.5 kJ/mol (recalculated at 53.5 °C) for $\text{R}' = \text{OMe}$. The barriers for **3** (this work) are 102.3 kJ/mol in CHCl_3 at 40 °C by off-line racemization and 103.6 kJ/mol by DHPLC at 50 °C in a mobile phase composed of EtOH/ CHCl_3 /hexane (3:3:1). Differences in barriers determined by DHPLC and off-line racemization have been observed and discussed already in terms of different rates of racemization on the chiral support and in the mobile phase in the DHPLC experiments. A serious issue is a possible temperature gradient in the column, which is difficult to evaluate.²⁶

Noteworthy, the four determinations of the barriers under different solvent, temperature, and method afford a mean value of 103.15 ± 1.35 kJ/mol. Further discussion on possible entropy or solvent effect on such a small variation of the barriers is beyond the scope of this paper. The three external groups (CH_2OH , CH_2OMe , and $\text{CH}_2-\text{C}_3\text{H}_4\text{NO}_2$) all present a methylene group; in the transition state of the rotation, the bulky substituent is likely rotated away and thus the buttressing “if any” between the CH_2 and the bromines turns out to be very similar for the three compounds. Significant buttressing effects are expected if one or two of the methylene protons were substituted by a carbon.

The tetraiodo derivative **4** did not show a plateau, the off-line measured barrier of enantiomerization at 131 °C in

(20) Ng, S. S.; Ho, C. Y.; Jamison, T. F. *J. Am. Chem. Soc.* **2006**, *128*, 11513–11528.

(21) The use of C_6D_6 , toluene- d_8 , or pyridine- d_5 is a well-documented trick to enhance chemical shift difference for prochiral protons in (thio)amides, (thio)ureas, (thio)carbamates (such as in compounds **2**, **3**, and **4**), and dithiocarbamates. All these functional groups present a positive charge on the nitrogen and are very sensitive to ASIS. For other examples see: (a) Stewart, W. E.; Siddall, T. H. *Chem. Rev.* **1970**, *70*, 517–551. (b) Roussel, C.; Liden, A.; Chanon, M.; Metzger, J.; Sandstrom, J. *J. Am. Chem. Soc.* **1976**, *98*, 2847–2852. (c) Liden, A.; Roussel, C.; Liljefors, T.; Chanon, M.; Carter, R. E.; Metzger, J.; Sandstrom, J. *J. Am. Chem. Soc.* **1976**, *98*, 2853–2860. (d) Grosu, I.; Plé, G.; Mager, S.; Martinez, R.; Mesaros, C.; Camacho, B. C. *Tetrahedron* **1997**, *53*, 6215–6232. (e) Mesaros, E.; Grosu, I.; Mager, S.; Plé, G.; Farcas, S. I. *Monatsh. Chem.* **1998**, *129*, 723–733.

(22) (a) Gasparrini, F.; Grilli, S.; Leardini, R.; Lunazzi, L.; Mazzanti, A.; Nanni, D.; Pierini, M.; Pinamonti, M. *J. Org. Chem.* **2002**, *67*, 3089–3095. (b) Wolf, C.; Tumambac, G. E. *J. Phys. Chem. A* **2003**, *107*, 815–817.

(23) The reported sign was found with a Jasco on-line polarimeter and corresponds to the summation of the optical rotation between 350 and 900 nm in the mobile phase: Roussel, C.; Vanthuyne, N.; Serradeil-Albalat, M.; Vallejos, J. C. *J. Chromatogr. A* **2003**, *995*, 79–85.

(24) (a) Schurig, V. *J. Chromatogr. A* **2009**, *1216*, 1723–1736. (b) Wolf, C. *Chem. Soc. Rev.* **2005**, *34*, 595–608. (c) Trapp, O. *Anal. Chem.* **2006**, *78*, 189–198. (d) Trapp, O. *Chirality* **2006**, *18*, 489–497.

(25) Trapp, O.; Schurig, V. *Chirality* **2002**, *14*, 465–470.

(26) (a) D'Acquarica, I.; Gasparrini, F.; Pierini, M.; Villani, C.; Zappia, G. *J. Sep. Sci.* **2006**, *29*, 1508–1516. (b) Villani, C.; Gasparrini, F.; Pierini, M.; Mortera, S. L.; D'Acquarica, I.; Ciogli, A.; Zappia, G. *Chirality* **2009**, *21*, 97–103.

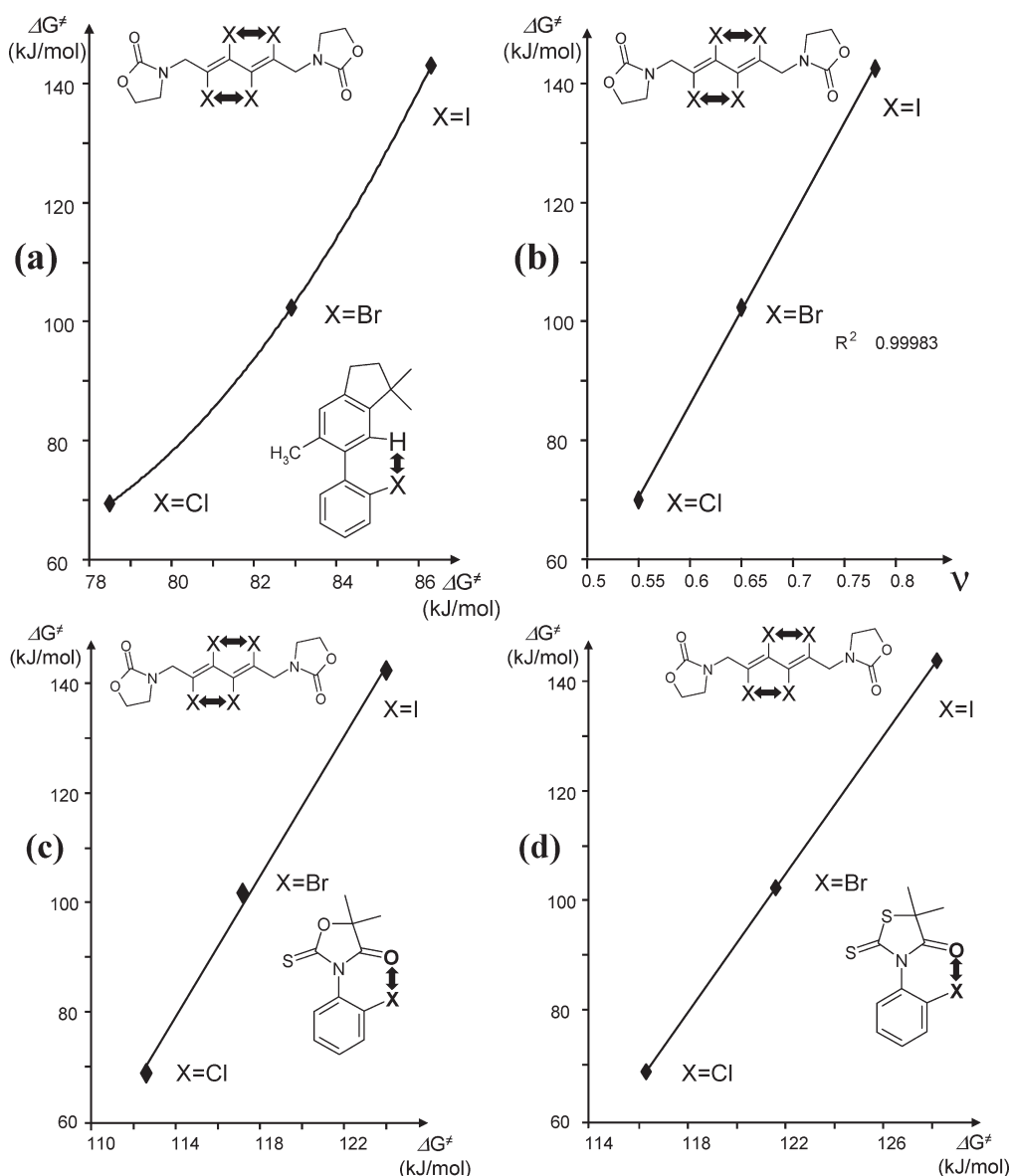


FIGURE 4. Correlations between barriers to rotation found in **2**, **3**, and **4** with barriers reported in the literature for the chloro, bromo, iodo halogen triad in different scaffolds (a, c, d). Correlation between barriers to rotation found in **2**, **3**, and **4** with v parameters derived from van der Waals radii of the halogen series (b). The table of data and references used in these correlations are given in the Supporting Information.

chlorobenzene was 143 ± 1 kJ/mol corresponding to a 1.56 day half-life at 131 °C. This is the first experimental determination of the barrier of a tetraiodobutadiene derivative.

Having in hand the complete set of barriers for the halogen triad composed of chlorine, bromine, and iodine for the tetrahalogenobutadiene framework, these barriers shall be compared to barriers disclosed in the literature for the same triad in other frameworks. In the absence of specific interaction such as buttressing effect or conformational restriction, steric barriers extracted from different models should be linearly correlated, the slope of the correlation monitoring the sensitivity to the models. This statement is particularly true for spherical groups such as the halogens. Inspection of the literature reveals that very few complete sets of data are available for the chlorine, bromine, and iodine triad. The only available barriers for a complete set of dihalogen (Cl, Br, and I) on butadiene substituted by four

benzyl groups were reported by Mannschreck and Coll.^{8b} Unfortunately DNMR study did not allow the determination of the actual barriers to rotation. An estimated barrier was given for the dichloro derivative (ca. 88 kJ/mol, $T_c = 140$ °C), and lower limits for the barriers in dibromo and diiodo compounds were guessed since coalescence in DNMR was not reached: > 92 kJ/mol at a higher temperature of 165 °C in decalin for dibromo compound and > 100 kJ/mol at a higher temperature of 195 °C in nitrobenzene for diiodo compound, respectively. Under these circumstances, references for the steric size of halogens under nonbuttressed conditions shall be taken outside the butadiene framework. The barriers in phenylindans carrying a halo and a methyl group in the ortho positions (Figure 4a) are available from a DNMR study.²⁷ In

(27) Bott, G.; Field, L. D.; Sternhell, S. *J. Am. Chem. Soc.* **1980**, *102*, 5618–5626.

TABLE 2. Conformations and Energies of (aS)-3a–d and (aS)-4a–d

conformers	energies + ZPE (au)	ΔE^{ZPE} (kJ·mol ⁻¹)	Boltzmann population (%)
3a	-928.165204	0.00	32
3b	-928.1650985	0.28	28
3c	-928.1645934	1.60	17
3d	-928.1645149	1.81	15
4a	-920.3194935	0.00	33
4b	-920.3194672	0.07	32
4c	-920.3186295	2.27	13
4d	-920.3184769	2.67	11

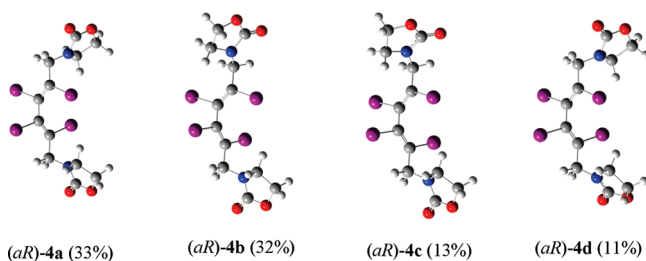


FIGURE 5. Most populated conformations for (aR)-4.

this model the barrier changes in the series chlorine, bromine, and iodine arise from the difference in interaction between a nonbutressed halogen and a C_{ar}-H whereas all other contributions to the barrier are almost unvarying.

Plotting the barriers reported in the phenylindan model against those determined for **2**, **3**, and **4** reveals a significant curvature (Figure 4a) that could have been assigned to a buttressing effect in the congested butadienes.

However, as said before the barrier in the phenylindan model results from the interaction of a halogen presenting lone pairs of electrons with a C-H group. It is probably not a good model to account for the lone pair-lone pair interaction that occurs between halogens in close contact. A more realistic model that includes lone pair-lone pair interaction in a transition state to rotation is provided by the recent study of the barriers to rotation in axially chiral *N*-(*o*-halogenophenyl)-2-thiooxazolidinone-4-one and *N*-(*o*-halogenophenyl)-2-thiothiazolidinone-4-one (Figure 4, panels c and d).²⁸

In these compounds, the nonbutressed halogen situated in the ortho position on the phenyl group interacts in the transition state to rotation with a (thio)carbonyl group presenting a lone pair of electrons. The ν steric parameters which are derived from van der Waals radii of the halogens extracted from symmetrical dihalogens provide another scale of halogen size that implicitly comprises the interaction of the lone pairs of electron in dihalogen equilibrium geometry.²⁹

Panels c, d, and b of Figure 4 report the comparison of the barriers in the series **2**, **3**, and **4** with the corresponding barriers of *N*-heteroaryl atropisomers or the ν steric parameters. In all these cases perfect linear correlations are observed between the data of tetrahalobutadienes and the reference compounds or the ν steric parameters. The sensitivity

(28) Yilmaz, E. M.; Dogan, I. *Tetrahedron: Asymmetry* **2008**, *19*, 2184–2191.

(29) Exner, O. *Correlation Analysis in Chemistry*; Plenum Press: New York, 1978; p 531 (Table 10-5).

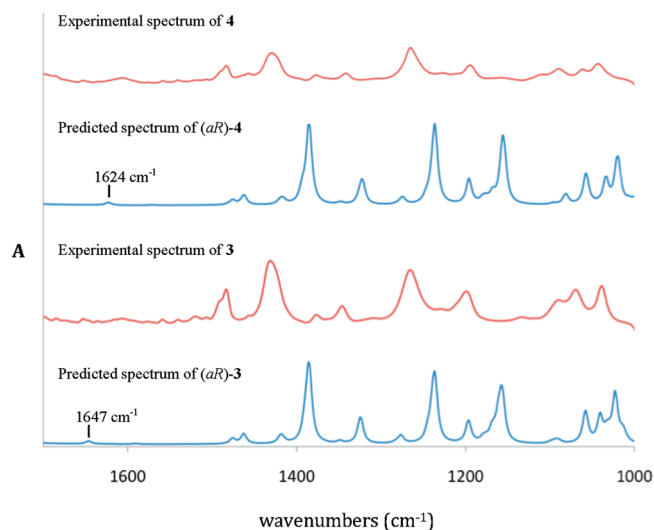


FIGURE 6. Comparison of the experimental IR spectra of **3** and **4** in CD₂Cl₂ solution (first and third traces) with the predicted IR spectrum (second and fourth traces) of the *aR* configuration of **3** and **4** obtained with the B3LYP/6-31+G(d,p) level. For predicted spectra, wavenumbers are scaled by the factor 0.96. The traces labeled “predicted” are the population-weighted spectra with populations given in Figure 5.

to the steric interactions in the butadiene framework is dramatically higher than that in the heteroaryl models as shown by the large value of the slope of the line. It turns out that no buttressing effect induced by the external substituent in **2**, **3**, and **4** can be detected or that the buttressing, if any, is linearly correlated with the size of the interacting groups.

Determination of the Absolute Configurations of **3 and **4** Enantiomers by VCD.** The absolute configuration of (+)-**3**, (–)-**3**, (+)-**4**, and (–)-**4** was determined by means of vibrational circular dichroism (VCD) by comparing experimental spectra of both enantiomers with the calculated VCD spectra of the *aR* enantiomer.³⁰ The geometry optimizations, vibrational frequencies, IR absorption, and VCD intensities were calculated by using Density Functional Theory (DFT) with B3LYP functional and a 6-31+G(d,p) basis set for H, C, N, and O atoms. For I and Br atoms, we used the Stuttgart/Dresden effective core potential (ECP), respectively MWB46 and MWB28. IR absorption and VCD spectra were constructed from calculated dipole and rotational strengths assuming Lorentzian band shape with a half-width at half-maximum of 4 cm⁻¹. All calculations were performed with the Gaussian 03 package.^{31,32} The conformational study of **4** showed that among the 20 conformations arising from the attached oxazolidinone groups, only **4**, (*aR*)-**4a–d**, have a Boltzmann population higher than 5% (Table 2 and Figure 5). Normal mode analysis confirmed that those conformations are minima on the potential energy surface since no

(30) (a) Nafie, L. A.; Keiderling, T. A.; Stephens, P. J. *J. Am. Chem. Soc.* **1976**, *98*, 2715–2723. (b) Nafie, L. A. *Annu. Rev. Phys. Chem.* **1997**, *48*, 357–386. (c) Stephens, P. J.; Devlin, F. J. *Chirality* **2000**, *117*, 172–179. (d) Freedman, T. B.; Cao, X.; Dukor, R. K.; Nafie, L. A. *Chirality* **2003**, *15*, 743–758. (e) Polavarapu, P. L.; He, J. *Anal. Chem.* **2004**, *76*, 61–67. (f) Bürgi, T.; Urakawa, U.; Behzadi, B.; Ernst, K.-H.; Baiker, A. *New J. Chem.* **2004**, *28*, 332–334. (g) Naubron, J.-V.; Giordano, L.; Fotiadu, F.; Bürgi, T.; Vanthuyne, N.; Roussel, C.; Buono, G. *J. Org. Chem.* **2006**, *71*, 5586–5593. (h) Polavarapu, P. L. *Chem. Rec.* **2007**, *7*, 125–136. (i) Polavarapu, P. L.; Petrovic, A. G.; Vick, S. E.; Wulff, W. D.; Ren, H.; Ding, Z.; Staples, R. J. *J. Org. Chem.* **2009**, *74*, 5451–5457.

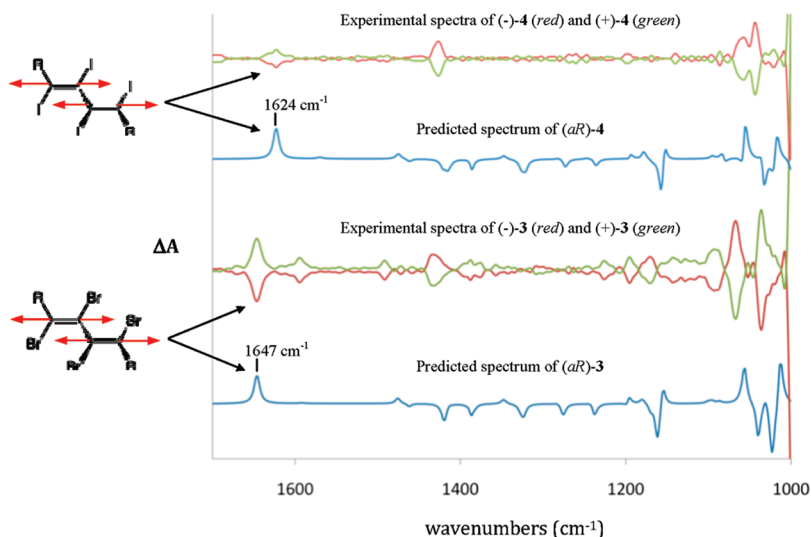


FIGURE 7. Comparison of the experimental VCD spectra of (–)-**3** (in red), (+)-**3** (in green), (–)-**4** (in red), and (+)-**4** (in green) in CD_2Cl_2 solution with predicted VCD spectrum of the *aR* configuration of **3** and **4** (in blue) obtained with the B3LYP/6-31+G(d,p) level. For predicted spectra, wavenumbers are scaled by the factor 0.96. The traces labeled “predicted” are the population-weighted spectra with populations given in Figure 5.

imaginary frequency was found. Similar results were obtained for **3** (Table 2).

As shown in Figures 6 and 7, the experimental IR absorption and VCD spectra of (+)-**3** and (+)-**4** (second eluted enantiomer on Chiralpak IC column) in CD_2Cl_2 solution are in good agreement with the predicted spectra of (*aR*)-**3** and (*aR*)-**4** which were obtained by weighting the spectrum of each conformer by its Boltzmann population. The shape and the relative intensities of the IR and VCD bands were well reproduced by the calculations. The calculated bands at 1647 cm^{-1} in **3** (experimental 1647 cm^{-1}) and 1624 cm^{-1} in **4** (experimental 1625 cm^{-1}) are particularly interesting. Both come from the symmetric stretching mode of the butadiene moiety (Figure 7) and are weakly affected by the attached groups.

The shift observed between these two bands is due to the drastic change of four iodine into four bromine atoms on the butadiene framework. For those bands, the IR absorptions are very weak and are not visible on the experimental spectra. On the other hand, the corresponding VCD bands are intense. The positive sign of those bands is an invariant in the calculated VCD spectra of each conformation of (*aR*)-**3** and (*aR*)-**4** (see Figure S14 in Supporting Information).

Further studies of that symmetric vibrational mode of a butadiene have shown that the positive sign of the corresponding VCD band can be safely associated to the (*aR*) absolute configuration, independently of the substituents of the butadiene. This work will be published elsewhere. The comparison in Figure 7 of the experimental and theoretical VCD spectra provides a high level of confidence for the assignment of the absolute configuration (*aR*) to (+)-**3** and (+)-**4**.

Conclusions

The structures of three new chiral sterically hindered tetrahalogenated dienes were investigated in the solid state by X-ray diffraction and in solution by NMR measurements. The enantiomers of the tetrabromo and tetraiodo dienes were separated by semipreparative chiral chromatography. The barrier for the rotation in the diene moiety was determined by off-line and by DHPLC for the tetrabromo compound ($\Delta G^\ddagger \approx 103\text{ kJ/mol}$), by the racemization reaction at the boiling point of chlorobenzene coupled with chiral HPLC analysis of the process for the tetraiodo derivative ($\Delta G^\ddagger = 143\text{ kJ/mol}$), and by DNMR experiments for the tetrachloro diene ($\Delta G^\ddagger = 69.6\text{ kJ/mol}$). The absolute configurations of the enantiomers of the tetrabromo and tetraiodo derivatives were determined by VCD, and the presence of a specific VCD band, which facilitates the assignment of the configurations, was revealed.

Experimental Section

1,6-Bis(1',3'-oxazolidine-2'-one-3'-yl)-2,3,4,5-tetrachlorohexane-2*E*,4*E*-diene 2. A solution of diacetylene **1** (80 mg, 0.32 mmol), CuCl_2 (174 mg, 1.29 mmol), and LiCl (22 mg, 0.512 mmol) in dry acetonitrile (7 mL) was refluxed overnight. Compound **2** was precipitated with acetone. Yield: 18% (22 mg), white crystals, mp $201\text{ }^\circ\text{C}$. Calcd for $\text{C}_{12}\text{H}_{12}\text{Cl}_4\text{N}_2\text{O}_4$: C, 36.95; H, 3.10; Cl, 36.36; N, 7.18. Found: C, 37.11; H, 3.02; Cl, 36.16; N, 7.31. $^1\text{H NMR}$ (300 MHz, CDCl_3) δ 3.59 (m, 2H, 4'-H, 4''-H), 4.39 (m, 2H, 5'-H, 5''-H), 4.41 (s, 2H, 1-H, 6-H); $^1\text{H NMR}$

(31) Frisch, M. J.; Trucks, G. W.; Schlegel, H. B.; Scuseria, G. E.; Robb, M. A.; Cheeseman, J. R.; Montgomery, J. A., Jr.; Vreven, T.; Kudin, K. N.; Burant, J. C.; Millam, J. M.; Iyengar, S. S.; Tomasi, J.; Barone, V.; Mennucci, B.; Cossi, M.; Scalmani, G.; Rega, N.; Petersson, G. A.; Nakatsuji, H.; Hada, M.; Ehara, M.; Toyota, K.; Fukuda, R.; Hasegawa, J.; Ishida, M.; Nakajima, T.; Honda, Y.; Kitao, O.; Nakai, H.; Klene, M.; Li, X.; Knox, J. E.; Hratchian, H. P.; Cross, J. B.; Bakken, V.; Adamo, C.; Jaramillo, J.; Gomperts, R.; Stratmann, R. E.; Yazyev, O.; Austin, A. J.; Cammi, R.; Pomelli, C.; Ochterski, J. W.; Ayala, P. Y.; Morokuma, K.; Voth, G. A.; Salvador, P.; Dannenberg, J. J.; Zakrzewski, V. G.; Dapprich, S.; Daniels, A. D.; Strain, M. C.; Farkas, O.; Malick, D. K.; Rabuck, A. D.; Raghavachari, K.; Foresman, J. B.; Ortiz, J. V.; Cui, Q.; Baboul, A. G.; Clifford, S.; Cioslowski, J.; Stefanov, B. B.; Liu, G.; Liashenko, A.; Piskorz, P.; Komaromi, I.; Martin, R. L.; Fox, D. J.; Keith, T.; Al-Laham, M. A.; Peng, C. Y.; Nanayakkara, A.; Challacombe, M.; Gill, P. M. W.; Johnson, B.; Chen, W.; Wong, M. W.; Gonzalez, C.; Pople, J. A. *Gaussian 03*, Revision C.02; Gaussian, Inc., Wallingford, CT, 2004.

(32) Walsh, J. G.; Furlong, P. J.; Byrne, L. A.; Gilheany, D. G. *Tetrahedron* **1999**, *55*, 11519–11536.

(300 MHz, C_6D_6) δ 2.35 (2H, dd, $J = 15.7, 8.1$ Hz, 4'-H, 4''-H), 2.51 (2H, dd, $J = 15.7, 8.1$ Hz, 4'-H', 4''-H'), 3.27 (m, 4H, 5'-H, 5''-H), 3.81 (2H, d, $J = 15.4$ Hz, 1-H, 6-H), 3.92 (2H, d, $J = 15.4$ Hz, 1-H', 6-H'); ^{13}C NMR (75 MHz, $CDCl_3$) δ 43.88 (4'-C, 4''-C), 46.59 (1-C, 6-C), 61.92 (5'-C, 5''-C), 125.41 (2-C, 5-C), 131.49 (3-C, 4-C), 158.14 (2'-C, 2''-C). EI-MS m/z (%) 354 (7.5%, $[M^+ - Cl]$), 308 (23%), 264 (42%), 216 (65%), (literature data for similar cases 0.1% M^+ , and 100% $[M^+ - Cl]$)²⁶. Chiral HPLC: Chiralpak IC, 25 °C, ethanol/ $CHCl_3$ /hexane 3/3/1, 1 mL/min, one peak at 7.50 min, $k = 1.42$.

1,6-Bis(1',3'-oxazolidine-2'-one-3'-yl)-2,3,4,5-tetrabromohexane-2E,4E-diene 3. To a solution of diacetylene **1** (125 mg, 0.5 mmol) in dichloromethane (50 mL) was added bromine (1 mmol, 160 mg dissolved in 1 mL of dichloromethane) dropwise. The mixture was stirred at room temperature overnight, and at the end the organic phase was washed with a solution of sodium sulfite and then with water. After drying over sodium sulfate, the solvent was removed and the crude product was purified by chromatography. R_f 0.35 (silica gel, toluene/acetone 4/1). Yield: 37% (106 mg), yellow solid, mp 215 °C dec. Calcd for $C_{12}H_{12}Br_4N_2O_4$: C, 25.38; H, 2.13; Br, 56.29; N, 4.93. Found: C, 25.49; H, 2.28; Br, 56.11; N, 4.77. 1H NMR (300 MHz, $CDCl_3$) δ 3.60 (m, 4H, 4'-H, 4''-H), 4.39 (m, 4H, 5'-H, 5''-H), 4.47 (s, 4H, 1-H, 6-H); 1H NMR (300 MHz, C_6D_6) δ 2.41 (2H, dd, $J = 15.4, 8.1$ Hz, 4'-H, 4''-H), 2.60 (2H, dd, $J = 15.4, 8.1$ Hz, 4'-H', 4''-H'), 3.31 (m, 4H, 5'-H, 5''-H), 3.88 (d, 2H, $J = 15.4$ Hz, 1-H, 6-H), 3.99 (d, 2H, $J = 15.4$ Hz, 1-H', 6-H'). ^{13}C NMR (75 MHz, $CDCl_3$) δ 43.82 (4'-C, 4''-C), 50.43 (1-C, 6-C), 61.97 (5'-C, 5''-C), 118.07 (2-C, 5-C), 122.53 (3-C, 4-C), 158.05 (2'-C, 2''-C). ESI-MS m/z 564.7 $[M + H]^+$, 586.7 $[M + Na]^+$. Chiral HPLC: Chiralpak IC, 25 °C, ethanol/ $CHCl_3$ /hexane 3/3/1, 1 mL/min, $R_{t1} = 7.92$ min (-), $R_{t2} = 9.32$ min (+), $k_1 = 1.56$, $k_2 = 2.01$, $\alpha = 1.29$, and $R_s = 2.88$.

1,6-Bis(1',3'-oxazolidine-2'-one-3'-yl)-2,3,4,5-tetraiodohexane-2E,4E-diene 4. CuI (6.07 g, 95.4 mmol) was added to a solution of *N*-propargyl-1,3-oxazolidine-2-one (0.2 g, 1.59 mmol) in dry dichloromethane (100 mL) containing dry TMEDA (7.37 g, 190.8 mmol). The reaction mixture was stirred for 1 h in dry air. The mixture was then diluted with dichloromethane (50 mL) transferred into a separating funnel, and washed with 2 M HCl

(2 \times 50 mL) and then several times with water until the aqueous layer remains colorless. The organic layer was then separated, dried over Na_2SO_4 , and evaporated. The final product was then purified by column chromatography. R_f 0.21 (silica gel, toluene/acetone 4/1). Yield: 12% (72 mg), yellow solid, mp 190 °C dec. Calculated for $C_{12}H_{12}I_4N_2O_4$: C, 19.07; H, 1.60; I, 67.16; N, 3.71. Found: C, 18.89; H, 1.51; I, 66.97; N, 3.88. 1H NMR (300 MHz, $CDCl_3$) δ 3.61 (m, 4H, 4'-H, 4''-H), 4.36 (s, 4H, 1-H, 6-H), 4.40 (m, 4H, 5'-H, 5''-H). 1H NMR (300 MHz, C_6D_6) δ 2.47 (dd, 2H, $J = 15.6, 8.1$ Hz, 4'-H, 4''-H), 2.69 (dd, 2H, $J = 15.6, 8.1$ Hz, 4'-H', 4''-H'), 3.36 (m, 4H, 5'-H, 5''-H), 3.83 (d, 2H, $J = 15.4$ Hz, 1-H, 6-H), 3.93 (d, 2H, $J = 15.4$ Hz, 1-H', 6-H'). ^{13}C NMR (75 MHz, $CDCl_3$) δ 44.18 (4'-C, 4''-C), 59.19 (1-C, 6-C), 62.06 (5'-C, 5''-C), 102.64 (2-C, 5-C), 105.58 (3-C, 4-C), 158.01 (2'-C, 2''-C). ESI-MS m/z 756.7 $[M + H]^+$, 778.6 $[M + Na]^+$. Chiral HPLC: Chiralpak IC, 25 °C, ethanol/ $CHCl_3$ /hexane 3/3/1, 1 mL/min, $R_{t1} = 8.20$ min (-), $R_{t2} = 9.63$ min (+), $k_1 = 1.65$, $k_2 = 2.11$, $\alpha = 1.28$, and $R_s = 2.68$.

Acknowledgment. We dedicate this work to Professor Albrecht Mannschreck on the occasion of his 75th birthday to acknowledge his outstanding contribution in the field of butadiene stereochemistry. We acknowledge the financial support of this work by the PNCDDI II program (UEFISCSU; projects IDEAS 515 and 2358). We thank the referees for stimulating comments. We thank the CRCMM and the "Spectropôle Marseille" for computer time and the VCD facility, respectively.

Supporting Information Available: Procedures and characterization of **1**, CIF files, ORTEP diagrams for **2** and **4**, views of the lattices for **2–4**, table of the parameters for the crystallographic determinations, DNMR experiment run with **2**, details of the chiral chromatography carried out with **3** and **4**, determination of the barriers of rotation for **2–4**, VCD spectra and the assignment of the absolute configuration of the enantiomers, and copies of 1H and ^{13}C NMR spectra for **1–4**. This material is available free of charge via the Internet at <http://pubs.acs.org>.

Abstract:

Thesis entitled “*New Functional Architectures for Molecular Recognition, Low Band Gap Conjugated Systems and Advanced Electrode Material*” is structured in four chapters dealing with new a) supramolecular structures such as cryptands and bis-macrocycles; b) chiral sterically hindered tetrahalo-1,3-dienes; c) blocks for the synthesis of low band gap conjugated polymers and d) 3D conjugated architectures based on twisted bithiophene with terminal EDOTs.

In the first chapter two new series of tripodal macrocycle precursors possessing C_3 symmetry built up from 1,3,5-triazine with reactive functional groups at the ends of the pendant arms are presented. Supramolecular structures obtained by Cu-catalyzed acetylenic coupling reactions are also reported. Cryptands were closed by intermolecular dimerization and bis-macrocycles were formed by intramolecular couplings followed by intermolecular dimerization.

The second chapter deals with the investigations of some new atropisomers with *E,E*-tetrahalo-1,3-butadiene core including separation of the enantiomers, determination of their rotation barriers and absolute configuration.

The third chapter includes the synthesis of benzo[2,1-*b*:3,4-*b'*]-dithiophene-4,5-dione based blocks used for low band gap conjugated polymers as active materials for organic solar cells.

In the last chapter synthesis and electronic properties of various new types of 3D conjugated architectures based upon twisted bithiophene with terminal EDOTs are reported in view of the electrochemical generation of electroactive microporous conjugated networks. The different size, surface areas and electronic properties depend on the block used for the construction of lateral branches.

Key words: cryptand, bis-macrocycle, atropenantiomers, low band gap blocks, twisted bithiophene, electroactive networks.

Resumé:

La thèse intitulée « *New Functional Architectures for Molecular Recognition, Low Band Gap Conjugated Systems and Advanced Electrode Material* » est structurée en quatre chapitres traitant de a) structures supramoléculaires tels que cryptands et bis-macrocycles; b) tetrahalo-1,3-diènes chiraux stériquement encombrés; c) blocs pour la synthèse de polymères faible gap conjugués d) architectures 3D conjugués à base de bithiophènes portant des EDOTs terminaux.

Dans le premier chapitre, on présente deux nouvelles séries de précurseurs macrocycliques *tripodaux* possédant une symétrie C_3 construites à partir de 1,3,5-triazine avec des groupes fonctionnels réactifs aux extrémités des bras. Les structures supramoléculaires obtenues par des réactions de couplage acétylénique catalysées par Cu sont également présentées. Les cryptands ont été fermés par dimérisation intermoléculaire et les bis-macrocycles ont été formés par des couplages intramoléculaires suivis par dimérisation intermoléculaire.

Le deuxième chapitre présente l'étude de nouveaux atropisomères à base d'*EE*-tetrahalo-1,3-butadiène y compris la séparation des énantiomères, la détermination des barrières de rotation et des configurations absolues.

Le troisième chapitre a été consacré à la synthèse des blocs à base de benzo [2,1-*b*:3,4-*b'*]-dithiophène-4,5-dione utilisés pour obtenir des polymères conjugués à faible gap pouvant fonctionner comme matériau actif dans des cellules solaires organiques.

Dans le dernier chapitre on décrit la synthèse et les propriétés électroniques de différents types de nouvelles architectures 3D conjuguées à base de bithiophène comportant des unités EDOTs terminales, en vue de la génération électrochimique de réseaux microporeux électroactifs conjugués. Il est montré que la taille, la surface active et les propriétés électroniques dépendent de la nature des blocs utilisés pour la construction des bras latéraux.

Mots clés: cryptand, bis-macrocycle, atropenantiomère, bande interdite, oligothiophènes 3D, réseaux électroactifs.